Elucidating the importance of programmed cell death -1 in modulating innate lymphoid cells within the tumour microenvironment.

Grace Evelyn Mallett

A thesis submitted for the degree of Doctor of Philosophy

Institute of Translational and Clinical Research

Newcastle University

July 2021

Declaration

I declare that no work presented in this thesis has been submitted elsewhere for the award of any other degrees or qualifications. Work presented here has been carried out by myself unless otherwise stated and all sources of information have been acknowledged by reference.

Grace E Mallett

Summary

Programmed cell death – 1 receptor (PD-1) is an inhibitory co-receptor which is critical for immune regulation and tolerance. Following engagement with its ligands, Programmed cell death ligand (PDL)- 1 and -2, PD-1 inhibits cellular proliferation and cytokine production. Although literature has focused on T cells, emerging literature has identified PD-1 as a negative regulator of innate lymphoid cells (ILCs). ILCs are a tissue resident subset of the innate immune system which are divided into 3 groups; namely group 1 (including NK cells and ILC1s), group 2 and group 3 (including Lymphoid Tissue Inducers; LTi cells). We have demonstrated that PD-1 regulates ILC2s, whereby inhibition of PD-1 results in increased cell proliferation and cytokine production (Taylor et al., 2017). In human, all ILC subsets are capable of expressing PD-1 within the tumour (Salimi et al., 2018) though the regulation of these cells within the tumour microenvironment (TME) remains undetermined. Murine cancer models identified a unique ILC1 subset, namely $Tbet^{+}Nkp46^{+}ROR\gamma t^{-}$ ILC1s, that were found to upregulate PD-1 expression in the TME ($p=0.01$) and were significantly increased in the absence of PD-1 ($p=0.02$). Absence of PD-1 also led to the increase in cellular proliferation and cytokine production. Data indicated PD-1 may modulate the metabolic profile of ILC1 subset $Tbet^{+}NKp46^{+}ROR\gamma t^{-}$ ILC1s. Human data confirmed observations in mice, whereby human ILCs were capable of upregulating PD-1 in the presence of tumour cells and PD-1 negatively regulated cellular proliferation. Specifically, an equivalent $PD\text{-}1^{+}$ subset was identified within human cutaneous squamous cell carcinoma (cSCC) tumours which was absent in patient peripheral blood mononuclear cells (PBMCs). In conclusion, PD-1 signalling specifically dampens $Tbet^{+}Nkp46^{+}ROR\gamma t^{-}$ILCs activity within the TME highlighting a potential therapeutic target which could enhance patient responses.

Acknowledgements

I would primarily like to thank Dr Shoba Amarnath for her continued academic and pastoral support, patience and guidance throughout the project. I would also like to thank Professor Mark Birch-Machin for his support and encouragement.

I would like to acknowledge and thank all the members of the Amarnath research group from the last 4 years with all of their help and support, particularly with their assistance in large *in vivo* experimental harvests. I am grateful for the help and support of Dr Stephanie Laba, particularly during the last year of my PhD; it has been very much appreciated.

I would like to give thanks to all the staff in the Comparative Biology Centre at Newcastle University for their continued support and assistance. In particular, I wish to thank Mr Chris Huggins and Ms Brigid Griffin and Ms Demi Minhinnett for their assistance, particular for their assistance in performing intravenous injections. I would like to thank them for their continued patience in my training. The project would not have been possible without their help. I would like to extend thanks to Dr Johnathon Scott from Professor John Simpson's research group for processing and providing healthy donor samples for human experiments. I would additionally like to thank the staff of the Flow Cytometry Core Facility for their help and assistance.

I would like to acknowledge the contribution of Dr Chester Lai and Professor Eugene Healy, University of Southampton for the collaboration on the work with the Squamous Cell Carcinoma patients. I would like to thank Dr Lai for acquiring and analysing patient samples for this project. I would also like to thank Mr Michael Alexander and Professor Penny Lovat for providing human cancer cell lines and their help.

My work has been supported by the Medical Research Council Discovery Medicine North (DiMeN) Doctoral Training partnership and thank them for the opportunity.

Last but by no means least, I would like to thank my partner, my family and my friends for the last 4 years. I would like to thank them for their help, understanding and support throughout.

Table of Contents

Table of Figures

List of Tables

Abbreviations

Ab	Antibody
Ahr	Aryl hydrocarbon receptor
APC	Antigen Presenting Cell
AOM	Azoxymethane
BSA	Bovine Serum Albumin
CD	Cluster of Differentiation
CHILP	Common Helper Innate Lymphoid Progenitor
CLP	Common Lymphoid Progenitor
cSCC	cutaneous Squamous Cell Carcinoma
CTLA-4	Cytotoxic T-Lymphocyte associated protein – 4
CXCR	C-X-C chemokine receptor
CCR	Chemokine Receptor
DC	Dendritic Cell
DMEM	Dulbecco's Modified Eagle Media
DMSO	Dimethyl Sulfoxide
DR3	Death Receptor 3
DSS	Dextran Sodium Sulphate
EDTA	Ethylenediaminetetraacetic acid
EOMES	Eomesodermin
ETP	Early T cell progenitor
FBS	Fetal Bovine Serum
FACs	Fluorescence-activated cell sorting
FMO	Fluorescence minus one
FoxP3	Forkhead box P3
FSC	Forward Scatter
GM-CSF	Granulocyte-Macrophage Colony Stimulating Factor
GvHD	Graft versus Host Disease
HSC	Haematopoietic Stem Cell
ICOS	Inducible T cell Co-stimulator
Id2	Inhibitor of DNA binding - 2
IFN	Interferon
IL-	Interleukin

ILC	Innate Lymphoid Cell
ILCp	Innate Lymphoid Cell progenitor
ITSM	Immune-receptor Tyrosin Switch Motif
i.p.	Intraperitoneal
IPF	Idiopathic Pulmonary Fibrosis
KLRG1	Killer cell Lectin-like Receptor subfamily G
KO	Knockout
LCMV	Lymphocytic Choriomeningitis Virus
LP	Lymphoid Progenitor
LSM	Lymphocyte Separation Media
MadCAM-1	Mucosal vascular addressin cell adhesion molecular 1
MDSC	Myeloid-Derived Suppressor Cells
MHC	Major Histocompatibility Complex
MLN	Mesenteric Lymph Node
mTOR	mechanistic target of rapamycin
Nfil3	Nuclear factor interleukin -3
NFκB	Nuclear factor kappa B
NK cell	Natural Killer cell
PAMPs	Pathogen-associated molecular patterns
PMA	Phorbol 12-myristate 13-acetate
PBMCs	Peripheral Blood Mononuclear Cells
PBS	Phosphate-Buffered Saline
PI3K	Phosphoinostide-3-kinase
PIP3	Phosphatidylinositol (3,4,5) - trisphosphate
PD-1	Programmed Cell Death-1
PDL-1	Programmed Cell Death Ligand-1
PDL-2	Programmed Cell Death Ligand-2
PRR	Pathogen Recognition Receptors
Rag	Recombinase activating gene
RBC	Red Blood Cell
RORγt	RAR-related orphan receptor gamma
RunX3	Runt-related transcription factor 3
SMAD	Suppressor of Mothers Against Decapentaplegic
SSC	Side Scatter
STAT	Signal Transducer and Activator of Transcription

S1P	Sphingosine-1-phosphate
Tbet	T-box transcription factor *TBX21*
TCF1	Transcription factor T-cell factor 1
TCR	T Cell Receptor
Th	T helper cell
TLR	Toll-Like Receptors
Treg	Regulatory T cell
TDLN	Tumour Draining Lymph Node
TIL	Tumour Infiltrating Lymphocytes
TL1A	TNF-like Ligand 1-A
TME	Tumour Microenvironment
TNF	Tumour-Necrosis Factor
TOX	Thymocyte selection-associated HMG-bOX
TRAIL	TNF-Related Apoptosis-Inducing Ligand
WT	Wildtype
VAT	Visceral Adipose Tissue

Chapter 1: Introduction

The immune system is essential for providing the body with defence against an array of microorganisms including bacteria, viruses and fungi. This is divided into two arms; namely the innate immune system and the adaptive immune system. The innate immune system is the primitive branch of the immune system which is conserved between all multicellular organisms and provides the first response against immune challenge. Innate immune cells use pattern recognition receptors (PRRs) such as Toll-like receptors (TLRs) to recognise microbial components named pathogen associated recognition patterns (PAMPs) and mount an immune response (Reviewed by (Akira et al., 2006)). The adaptive immune system provides a later stage pathogen-specific response and immune memory. This system consists of cellular responses driven by T cells and humoral defence driven by B cells and the complement system.

In 2010, a novel set of innate immune cells was identified known as innate lymphoid cells (ILCs) (Neill et al., 2010, Buonocore et al., 2010). ILCs are a family of lymphocytes which are predominately tissue resident, and share many phenotypical and functional characteristics with T Cells. Since their discovery, ILCs have been shown to be present in the majority of tissues, however primarily reside within mucosal barrier tissues. ILCs play a key role in tissue homeostasis and being first immune responders. There are, however, many questions remaining regarding how ILC subsets function within specific tissues and particularly within pathological conditions such as cancer.

Cancer is one of the leading causes of death worldwide, with approximately 10 million cancer associated deaths annually (Sung et al., 2021). Immunosuppressed patients demonstrate an increased incidence of cancer development inferring that the immune system plays a critical role in tumour progression (Sung et al., 2021). The tumour microenvironment (TME) is a complex environment containing a vast number of cells including a variety of immune cells. Immune cells such as $CD8^+$ T cells are capable of directly recognising antigens expressed by tumour cells (van der Bruggen et al., 1991). Other immune cells, such as NK cells can recognise and target cancer cells and directly kill them through the production of granzyme and perforin. In contrast, presence of immunosuppressive cells such as regulatory T cells (Treg) and immunosuppressive macrophages dampen immune responses and enable tumour growth and progression. Increased infiltration of immunosuppressives cells is associated with poor clinical outcome (Gordon et al., 2017, Gao et al., 2017). Immunotherapies have been developed to target immune cells with the aim of boosting effector anti-tumour responses, however, there

has been limited success within the clinic. ILCs are a tissue resident subset of cells which are thought to reside within cancer tissue. The role of ILCs within pathology but particularly within cancer remains largely unknown. A full understanding in ILC regulation and activation is required to fully elucidate their role and assess how they may respond to immunotherapy treatment.

1.1. Innate Lymphoid Cells

1.1.1. Overview

ILCs are a tissue resident subset of the innate immune system which are first responders cell enriched at mucosal surfaces and are critical for barrier homeostasis and defence (Gil-Cruz et al., 2016, Brestoff et al., 2015, Neill et al., 2010, Sonnenberg et al., 2011, Monticelli et al., 2011). ILCs, the innate counterpart of T lymphocytes, lack recombinating activating gene (RAG)- dependent rearranged receptors so are unable to respond to antigen presentation, responding instead to environmental stimuli such as cytokines and alarmins produced in the tissue. Based on expression of transcription factors, surface protein expression and effector function, ILCs can be divided into 3 main subsets; Group 1 ILCs (including ILC1s and natural killer cells; NK cells), group 2 (ILC2) and group 3 (including ILC3s and Lymphoid Tissue Inducers; LTi) which mirror $CD4^+$ T helper cells subsets Th1, Th2 and Th17 cells respectively. ILCs respond to specific tissue microenvironment stimuli and respond with the relevant effector cytokines to elicit an appropriate response either in mounting an immune defence or boosting tissue repair. Cytokines produced by ILCs can either elicit a direct response (ILC3 production of IL-17), or can recruit other immune cells to the site of infection (e.g. IL-5 production by ILC2s recruits Th2 cells and eosinophils) (Jie et al., 2014, Walker and McKenzie, 2013).

Group 1 ILCs, broadly defined by expression of transcription factor Tbet (T-box transcription factor TBX21), are responsible for anti-viral defence and anti-tumour responses through the production of type 1 cytokines including interferon (IFN) γ and TNFα (Gao et al., 2017). NK cells are widely regarded as the innate counterpart to $CD8^+$ T cells, and have the ability to produce granzyme and perforin to mount a cytotoxic response (Loh et al., 2005). In addition to cytokines such as IL-15, NK cells can be activated by "lack of self" antigen on cells. Major histocompatibility complex class I (MHC I) expression is lost once a cell becomes infected or in tumour cells. When unable to recognise MHC I, NK cells mount an immune response (Jaeger

and Vivier, 2012). ILC1s have a helper-like pro-inflammatory phenotype, and respond to stimulation from IL-12 and IL-18 (Bernink et al., 2015). Group 2 ILCs are defined by the upregulation of GATA3 and mirror Th2 cells. ILC2s respond to helminth infection with the production of IL-5 and IL-13 (Yang et al., 2011). They also play an important role in allergy and atopic dermatitis (Salimi et al., 2013). Group 3 ILCs are sub-divided by the expression of NK receptor NKp46 (in mice) or NKp44 (in humans) but all express transcription factor RAR-related orphan receptor gamma (RORγt). NCR^+ ILC3s are positive for NKp46/NKp44 whereas NCR^- lack this expression. Under normal physiological conditions, NCR^- ILC3s are the predominant ILC3 subset present within tissue whereas NCR^+ ILC3s are upregulated during inflammatory conditions such as psoriasis (Villanova et al., 2014). On the contrary, within the intestine, NCR^+ ILC3s are the prominent. LTi cells, also regarded as a group 3 ILC subset by their expression of the transcription factor RORγt, are critical for the development of lymphoid tissue and Peyer's patches (Reviewed in (Buettner and Lochner, 2016)) (Summarised in Figure 1.2)

ILCs have a role in both immune defence and are increasingly being identified as key players in a variety of pathologies including psoriasis and atherosclerosis (Salimi et al., 2013, Newland et al., 2017). Furthermore, the role and significance of ILCs in tumour biology is an emerging area of interest. The precise mechanisms as to whether ILCs aid with tumour progression or mount anti-tumour responses remains unclear. ILC respond, almost exclusively, to the tissue environment, therefore understanding how ILCs behave within the tumour microenvironment (TME) could be extremely beneficial in order to fine tune cancer therapies within the clinic.

1.1.2. ILC Development

ILCs develop from the common lymphoid progenitor (CLP); a progenitor which also gives rise to other immune cells including T and B cells. Development occurs within the bone marrow; a process tightly regulated by a multitude of transcription factors including nuclear factor interleukin 3 (Nfil3), inhibitor of DNA binding 2 (Id2) and GATA3 (Monticelli et al., 2011, Hoyler et al., 2013) (Figure 1.1.). Immature B cells remain in the bone marrow until they develop into naïve B cells, where they enter the blood stream and elicit immune response upon activation. For T cell development, the CLP migrates to the thymus and gives rise to the early T cell progenitor (ETP) which ultimately develops into T cells through double positive $CD4^+CD8^+$ cells and through to final single positive T cells. The fate of CLP is determined by a carefully orchestrated Notch signalling. High levels of Notch signalling drive CLP

development towards T cell development, conversely B cells require low notch signalling (Koga et al., 2018). Of note, ILC2s have been shown to require high levels of Notch signalling in combination with IL-7 for development (Koga et al., 2018); whether this is exclusive to ILC2s or whether this is required for all ILC subset development remains unclear.

In addition to changes in Notch signalling, adaptive immune cells require a family of transcription factors known as E proteins. The transcription factor Id2 drives the formation of non-functional heterodimers; essentially blocking E proteins. Id2 is therefore, is critical for driving CLP development through intermediate α-lymphoid progenitor (αLP) into the common helper ILC precursor (CHILP) and preventing T and B cell development (Benezra et al., 1990, Morrow et al., 1999). Upregulation of Id2 is critical for development of all ILC subsets, and in the absence of Id2 there is a failure of any of the ILC subsets to develop (Yokota et al., 1999, Boos et al., 2007).

Id2 is the critical transcription factor for fate decisions in CLP progression into ILCs, so unsurprisingly Id2 expression in CLPs is tightly regulated by the basic leucine zipper transcription factor Nfil3. Upregulation of Nfil3 is driven by IL-7 induced signal transducer and activator of transcription (STAT) 5 phosphorylation; expression is important for all ILC subset development (Geiger et al., 2014, Seillet et al., 2016, Klose et al., 2014). Crucially, Nfil3$^{-/-}$ mice, only demonstrate a reduction in ILCs and not a complete ablation. This infers that although important, Nfil3 is not critical for development and alternative regulatory mechanisms must be in place which are not yet well described. Nfil3 is closely associated with the transcription factor Thymocyte selection-associated HMG-bOX (TOX). As with Nfil3, absence of TOX demonstrated a reduction in all 3 ILC subsets (Seehus et al., 2015). NK cell development, in particular, is impaired in the absence of TOX; a defect which is rescued upon the transduction of TOX (Aliahmad et al., 2010). A signalling cascade has been described whereby TCF-1 expression is driven by TOX. IL-7 induces Nfil3 which then binds to the TOX promoter to drive TCF-1 expression. TOX is critical for the progression of the CLP through the αLP to the CHILP. With the exception of NK cells, all ILC subsets progress to the CHILP (Figure 1.1).

Up regulation of integrin α4β7 is another indication that the cells have lost the ability to develop into adaptive immune cells and cements the development into ILCs. α4β7 is critical for lymphocyte homing and adhesion through adhesion molecule MadCAM1 (Ruegg et al., 1992).

ILC migration into the intestine is facilitated by CXCR6 as well as CCR7, which specifically regulates ILC1 and ILC3 migration into the intestine (Kim et al., 2015).

In addition to TOX and NFil3, GATA3 is another transcription factor critical to ILC development; whereby ILC 1-3 fail to develop in its absence (Serafini et al., 2014, Klose et al., 2014). This is similar requirement in the development of $CD4^+$ T cells, whereby GATA3 binds to the *Il7r* promoter region in human T cells; this was shown to inhibit NK cell development (Van de Walle et al., 2016). GATA3 is continually expressed throughout development until ILC precursor (ILCp), where subset specific induction occurs (Hoyler et al., 2013).

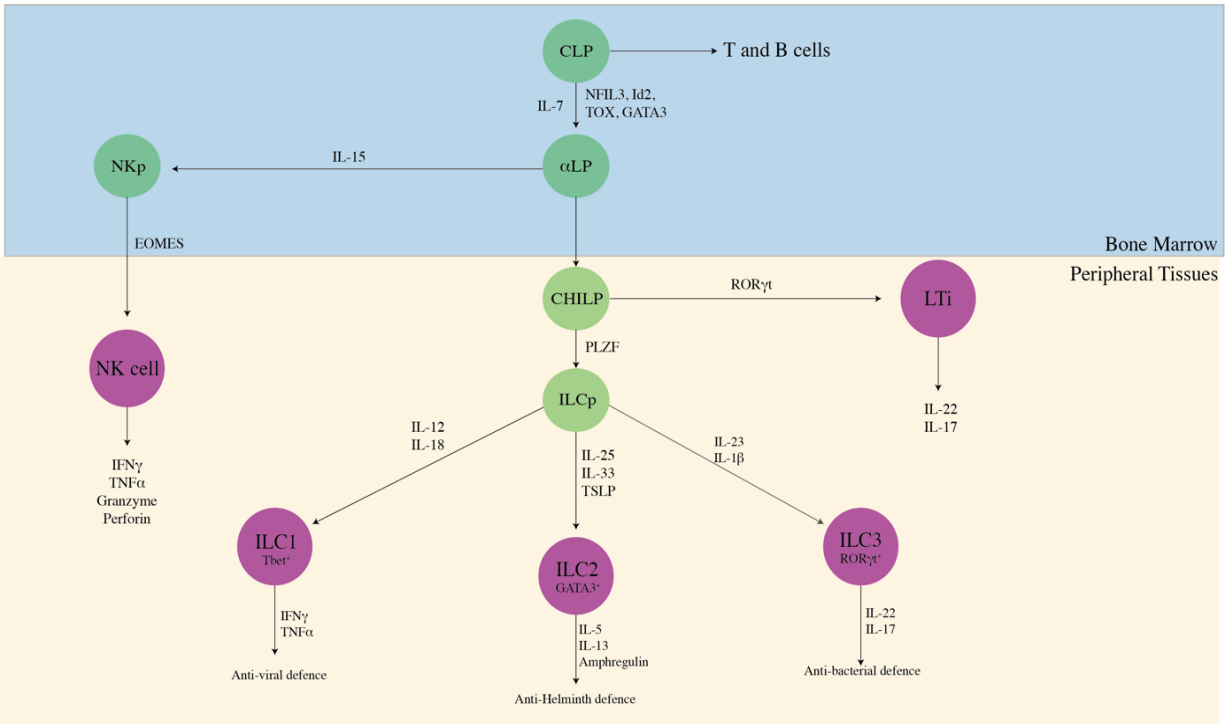

Figure 1.1. Innate Lymphoid Cell Development. Innate Lymphoid Cells (ILCs) develop from the common lymphoid progenitor (CLP) in the bone marrow. Through the upregulation of transcription factors (Nfil3, Id2, TOX and GATA3) and cytokine IL-7, CLP develop into α lymphoid progenitor (αLP). IL-15 drives the development of Natural killer cell progenitor (NKp). Upregulation of transcription factor Eomes then further drives development of NK cells within the peripheral tissue. Promyelocytic leukaemia zinc finger (PLZF) drives the development of other ILC subsets into the ILCprogenitor (ILCp) within the peripheral tissue. Individual ILC subsets develop in response to subset specific cytokines and alarmins and then provide the appropriate immune response within the tissue.

Although classified as an ILC, NK cells differ in development from the rest of the ILC subsets. IL-15 drives the progression of the αLP away from the ILCp into the NK cell precursor (NKp) (Serafini et al., 2015). Development of NKp into mature NK cells is dependent on the

upregulation of transcription factor Eomes. Although NK cells also express Tbet, unlike with ILC1s, development of NK cells is not dependent on Tbet expression (Klose et al., 2013).

CHILP develop from the αLP. Constantinides et al. demonstrated that promyelocytic leukaemia zinc finger (PLZF) is critical for the development of ILCs, but not NK cells nor LTi cells (Constantinides et al., 2014). Although lineage tracing experiments of *Zbtb16* (gene encoding PLZF) demonstrated expression in all ILCs, in the absence of PLZF only ILC1 and ILC2 subsets were reduced, whereas ILC3s remained unaffected. These contradictory findings suggest subset specific regulation of ILCs even at this early stage. Although important, PLZF did not completely eliminate ILC1 and ILC2s, it further enhances the suggestion that other regulatory pathways are underway (Constantinides et al., 2014). PLZF drives the progression of ILC development into the ILCp and α4β7 expression in CHILP and ILCp highlight the migratory tendency of these cells. CHILP, in particular, upregulate homing chemokines such as CCR7 and CCR9 in order to facility migration from the bone marrow to peripheral tissues such as the intestine (Hoyler et al., 2012). Once in the tissues, ILCps respond to environmental stimuli produced in the tissue or by other cells such as dendritic cells. These specific stimuli drive the development of individual specific subsets, induce subset specific transcription factors and drive subset specific phenotype.

The development of ILC1s and ILC3s rely on similar components including Tbet and Runt related transcription factor 3 (RunX3). Transcription factor Tbet, is essential for the development of $NKp46^+$ cells, including both ILC1s and ILC3s. This is demonstrated in the absence of Tbet, where mice lack ILC1s and NCR^+ ILC3s, however NCR^- ILC3s are still able to develop through stimulation from the Notch signalling pathway (Rankin et al., 2013, Klose et al., 2013). RunX3 is required for both subsets, however it is specifically required for the upregulation of RORγt expression in ILC3s (Ebihara et al., 2015). GATA3 is required for the development of all ILC subsets, however sustained high levels of GATA3 drives ILC2 specification and is not seen in the other subsets (Hoyler et al., 2012). Huang et al. further subdivided ILC2 subsets based on their expression of IL-33 receptor ST2 and KLRG1. $ST2^+$ or "natural" ILC2s are present under normal homeostatic conditions. ILC2s induced by IL-25, known as inflammatory ILC2s, upregulated expression of KLRG1 on activation (Huang et al., 2015). RORα is also critical for ILC2 development, as they fail to develop in its absence (Wong et al., 2012). ILC3s rely on RORγt for differentiation and for ILC3 development as in its absence, ILC3s fail to develop. There is no notable difference however, in ILC1 and NK cell subsets, again highlight subset specificity (Klose et al., 2013).

ILCs respond to alarmin and cytokine stimulation for their differentiation and proliferation. In a similar manner to T cells, dendritic cells and other antigen presenting cells (APCs) produce cytokines in response to pathogen detection in order to stimulate response. ILCs also require cytokines for development, namely IL-7 and IL-15 (Geiger et al., 2014). Although IL-7 is required for ILC development, it has been shown that ILC2 and ILC3 subsets are capable of developing independently of IL-7, as long as they receive stimulation from IL-15 (Robinette et al., 2017).

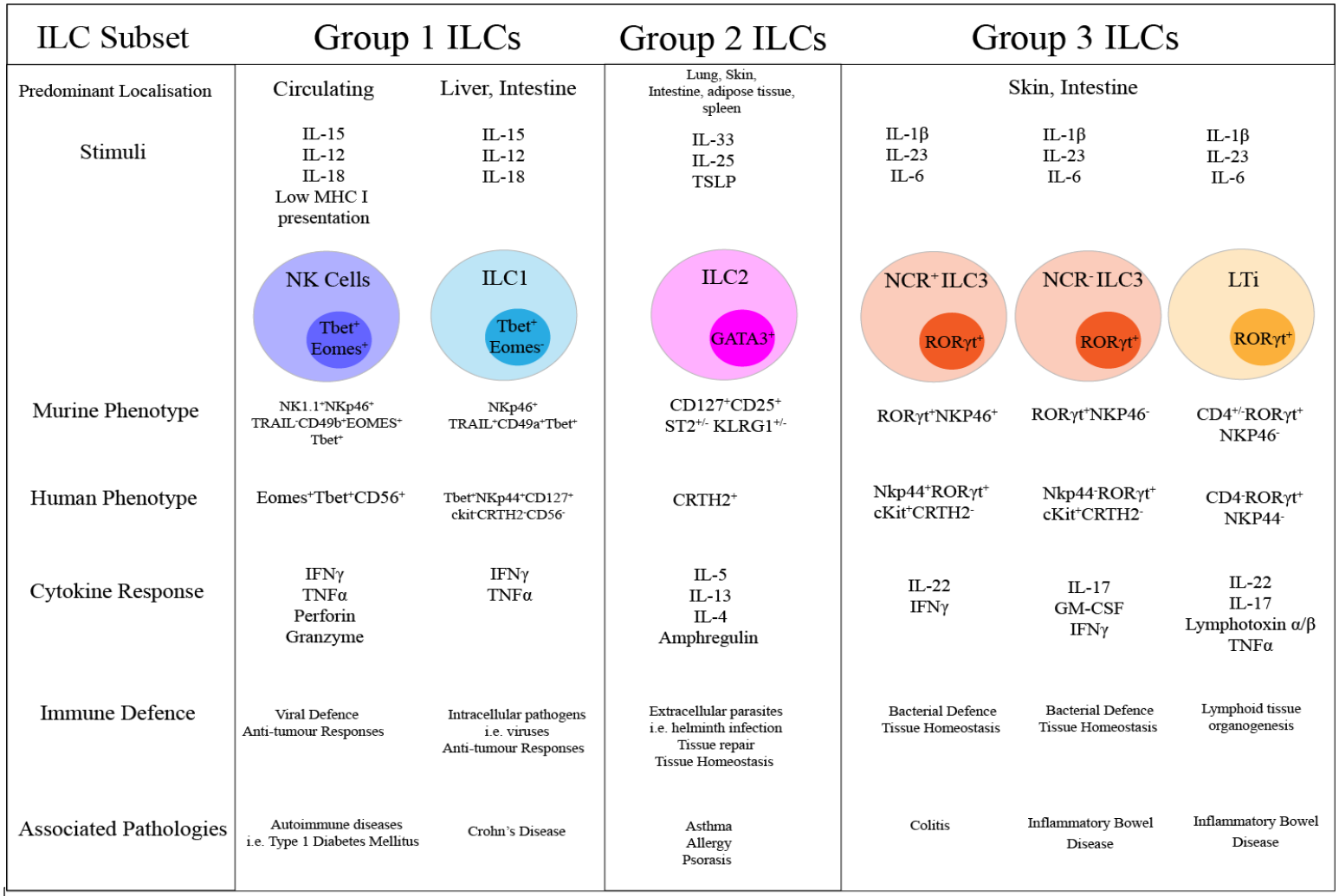

Figure 1.2. Summary of ILC subsets and function in both mouse and human. ILCs response to specific stimuli within the relevant tissue. All ILCs, in both human and mouse, are defined as being negative for lineage markers (including CD3, CD11b, Ter119), $CD45^+$ and $CD90.2^+$. In humans, all ILC subsets also express c-type lectin receptor CD161. Group 1 ILCs include NK cells and typically respond to intracellular pathogens such as viruses. Group 2 ILCs respond to parasitic infection such as helminth infection and Group 3 ILCs are responsible for intestinal tissue homeostasis and defence against bacterial infection. LTi cells, a subset of ILC3s, are required for formation of secondary lymphoid structures. Each subset produces effector molecules in order to elicit their individual immune response.

1.1.3. Group 1 Innate Lymphoid Cells

Group 1 innate lymphoid cells consist of NK cells and ILC1s and are a key component in anti-viral defence. First identified in 1975, NK cells have been well defined as a circulatory cytotoxic innate immune cell with a key role in anti-tumour responses (Kiessling et al., 1975). It is well established that NK cells respond to immunotherapies in cancer and so this project has focused on the less well recognised ILC1s. In comparison, ILC1s are poorly understood, primarily due to the lack of specific markers for identification making in particularly difficult to identify them from NK cells and other ILC populations. There are, however, some fundamental differences between NK cells and ILC1s which allows functionality between the subsets to be disseminated. NK cells are primarily circulatory cells, found within the blood and lymphoid tissues. As a result, they express circulatory marker α2 integrin subunit (CD49b). In contrast, tissue resident ILC1s primarily reside within intestinal tissue, liver, uterus and salivary glands (Filipovic et al., 2018, Fuchs, 2016). ILC1s express α-subunit of α1β1 integrin, CD49a, which retains cells in tissue by binding collagen IV and laminin within tissue (Fuchs, 2016). NK cells and ILC1s can further be distinguished based on expression of transcription factors Eomesodermin (EOMES). Although both subsets require Tbet, expression of Eomes is exclusive to NK cells; expression of which is conversely associated with the expression of TNF-related apoptosis-inducing ligand (TRAIL) (Gordon et al., 2012). Although NK cells express Tbet, unlike ILC1s, NK cells are capable of developing in the absence of this transcription factor (Daussy et al., 2014). ILC1s also express cytotoxicity receptor NKp46, absence of which reduces ILC1 expression of TRAIL. This impairs ILC1 function, and in murine cancer models, ILC1s have diminished capacity to provide anti-tumour responses (Almeida et al., 2018, Turchinovich et al., 2018). In contrast to NK cells, ILC1s lack expression of c-type lectin-like receptor Ly49 (Klose et al., 2014). Ly49 binds to MHC class I and allows NK cells to recognise infected cells, or cells lacking in expression of MHC class I; meaning ILC1s are unable to recognise lack of expression, damaged or destressed cells (Rahim et al., 2014). To distinguish the two cell types, NK cells can be defined as $Nkp46^{+}CD49a^{-}CD49b^{+}TRAIL^{-}Eomes^{+}Tbet^{+}$ in contrast to ILC1s which can be defined as $Nkp46^{+}CD49a^{+}CD49b^{-}TRAIL^{+}Eomes^{-}Tbet^{+}$.

ILC1s also express chemokine receptor CXCR6. Expression of CXCR6 was originally thought to be required for tissue homing to the liver, however, uterine ILC1s have also shown to express CXCR6 (Filipovic et al., 2018, Seillet and Belz, 2016, Wang et al., 2018). In T cells, CXCR6 is required for tissue homing, so it is likely that expression of CXCR6 on ILC1s maintains tissue

residency. It has been suggested that CXCR6 may be a marker of memory ILC1s. $CXCR6^+$ ILC1s specifically expand during second pregnancy in comparison to first suggesting a potential memory cell population in pregnancy (Filipovic et al., 2018). In response to hapten stimulation, ILC1s are capable of providing specific memory responses within the lymph nodes. In addition to expressing CXCR6, these ILC1s are also dependent on expression of IL-7Rα for the memory response (Wang et al., 2018). The exact mechanism behind the formation of memory ILCs and how they are maintained, particularly with the inability to recognise antigen presentation remains unclear. Further research would be required to determine the exact mechanism but this is an important consideration for targeting these cells.

NK cells are considered the more cytotoxic phenotype as they produce both perforin and granzyme, with the suggestion that ILC1s have a more "helper-like", immunosuppressive phenotype in the presence of TGFβ (Gao et al., 2017). Despite this, ILC1s have been shown to be pivotal in type 1 immune responses. IL-12 drives IFNγ production in both NK cells and ILC1s through the phosphorylation of STAT4 (Weizman et al., 2017). IFNγ production by ILC1s is critical to immune response to infection, tissue homeostasis and inflammatory conditions (Klose et al., 2014, Nabekura et al., 2020, O'Sullivan et al., 2016, Fuchs, 2016). ILC1s are tissue resident innate cells and so are primed to elicit early immune responses upon infection. ILC1s are the primary source of IFNγ in early *Toxoplasma gondii* and intestinal *Clostridium difficile* infections in response to IL-12 (Lopez-Yglesias et al., 2021, Abt et al., 2015, Klose et al., 2014). In first 24hour of infection with mouse cytomegalovirus (MCMV), ILC1s are the predominant source of IFNγ. Critically, Eomes-dependent NK cells were not required during this early infection phase (Weizman et al., 2017). This provides further evidence of the distinction between the two subsets and their distinct roles.

ILC1s respond to cytokines IL-12 and IL-15; both cytokines are critical for ILC1 production of IFNγ in response to infection; as in the absence of either cytokine ILC1s fail to produce sufficient IFNγ in early infection (Gil-Cruz et al., 2016). Absence of IL-15 did not, however, result in the same increase in viral load seen in the absence of IL-12, suggesting that either IL-12 is the dominant source of activation or ILC1s response to cytokine stimulation is tissue specific. Dendritic cells are the predominant source of IL-12; blockade of which through TNF inhibitor, diminishes the capacity of ILC1s to produce IFNγ (Larmonier et al., 2007).

In addition to providing viral defense, IFNγ produced by ILC1s has a key role in tissue homeostasis. In acute liver injury, IFNγ production specifically increases from activated ILC1s and not NK cells. This leads to the upregulation of anti-apoptotic protein Bcl-XL which increases survival of hepatocytes. IFNγ production from ILC1s alone is sufficient to protect against liver damage (Nabekura et al., 2020).

IFNγ is an inflammatory cytokine, therefore, dysregulation of ILC1s drives inflammatory disorders including obesity and Crohn's disease (Fuchs, 2016, Boulenouar et al., 2017). Regulation of ILCs, particularly ILC1s is poorly understood, however key correlations between ILC1 presence and disease state has been noted. In the lamina propria, ILC1s were increased in patients with Crohn's disease, a phenomenon also observed within a murine model of colitis (Fuchs et al). ILC1s are a tissue resident subset of cells and respond exclusively to the tissue microenvironment. It remains unclear at this stage whether this is in response to changes in stimuli in the tissue microenvironment in disease state, or whether the ILC1s are initiating and driving pathology. ILC1s are present in adipose tissue under steady state yet during obesity adipose associated ILC1s are significantly increased (Boulenouar et al., 2017). In obesity, IL-12 driven IFNγ produced by ILC1s drive macrophage polarization to M1 pro-inflammatory phenotype. Increase in inflammation within the adipose tissue drives obesity-associated insulin resistance in mice (O'Sullivan et al., 2016).

ILC1s are widely considered tissue resident subset set of cells, being one of the main defining features between them and NK cells. There is a suggestion, however, that ILC1s may have migratory capacity to and from the lymph nodes and liver. This has been shown to be dependent on chemokine receptor CXCR3 (Wang et al., 2018). It is yet to be determined whether this is true of all ILC1s or whether this is specific for memory ILC responses. Either way, if ILC1s are capable of migrating, this could have significant consequence for their presence within tumour tissue. It is too early to determine whether ILC1s would be able to initiate a memory response in a relapsing cancer setting and whether migration of these cells to the tumour site would be possible.

The understanding function of ILC1s has remained limited due to the lack of specific markers and limited cell number. There is evidence suggests that ILC1s primarily elicit their response through the production of IFNγ and drive inflammatory responses. Further assessment would be required in order to fully understand the role of ILC1s in health and disease.

1.1.4. Group 2 Innate Lymphoid Cells

ILC2s were one of the first ILC subsets to be described, originally termed "nuocytes" (Neill et al., 2010). Neill et al. first described ILC2s in $Rag^{-/-}$. $Rag^{-/-}$ mice lack a mature adaptive immune system but were shown to still be capable of responding to IL-25 stimulation by producing type 2 cytokines IL-5, IL-13 and immunosuppressive cytokine IL-10 (Neill et al., 2010, Bando et al., 2020). As a result of their clear expression of transcription factor GATA3 and surface markers IL-2 receptor α CD25 and IL-7 receptor CD127, along with their relatively high abundance in tissue, ILC2s are one of the most studied of the ILC subsets. ILC2s are predominantly associated with lung, skin and small intestinal tissue. ILC2s can be sub-divided into 3 subsets namely "natural" ILC2s (nILC2s; $ST2^{+}$), "inflammatory" ILC2s (iILC2s; $KLRG1^{+}$) and "mature" ILC2s (mILC2s; $ST2^{+}KLRG1^{+}$) (Huang et al., 2015). nILC2s reside within the tissues such as lung and adipose tissue under homeostatic conditions and primarily respond to IL-33 stimulation. iILC2s are difficult to detect under normal homeostatic conditions, however, rapidly expand in response to IL-25 stimulation. iILC2s increased rapidly in response to helminth infection within the lung, in contrast, increase in nILC2s is delayed and not observed until day 8-12 post infection (Huang et al., 2015). iILC2s have also shown to be capable of expressing RORγt, and in response to *Candida albicans* infection are capable of expressing Il-17, providing type 3 responses (Huang et al., 2015). This is in contrast with findings reported by Sawa et al, who suggested that IL-25 can inhibit ILC3 responses (Sawa et al., 2011). It is likely that, as with ILC1s, ILC2 response to stimulation is specific to the tissue microenvironment and it is possible that other stimuli may enhance type 3 response in ILC2s. It is well documented that ILCs, particularly ILC2s have high plasticity between subsets. This will be addressed in subsequent sections. ILC2s are widely distributed throughout barrier surfaces, unsurprisingly they are associated with driving many pathological conditions including psoriasis and asthma (Salimi et al., 2018, Wohlfahrt et al., 2016).

ILC2s primarily respond to IL-25, IL-33 and TSLP production by the tissue microenvironment and respond to parasitic infection such as helminth. Tuft cells within the intestine respond to infection by the production of IL-25. This drives the induction of iILC2s which in response produce IL-5 and IL-13 which induce immune cell responses and directly stimulate pathogen excretion. IL-5 recruits eosinophils to the site of infections whilst IL-13 stimulates mucus production in order to eliminate pathogen (Neill et al., 2010, Moro et al., 2010, Hams et al., 2013, Monticelli et al., 2015, Klose et al., 2017). ILC2s also produce amphiregulin which, as well as IL-13, which is critical for tissue repair post infection. Amphregulin production is

significantly increased within the lung following influenza infection in mice where it promotes tissue repair (Monticelli et al., 2011).

IL-33 is also a key stimulator of ILC2s. IL-33 drives cytokine production in ILC2s through the phosphorylation of STAT5. This directly leads to increased cellular proliferation and cytokine production and expulsion of helminth infection (Taylor et al., 2017). Thymic stromal lymphopoietin (TSLP), unlike IL-33 and IL-25, is not sufficient to activate ILC2s alone, however enhances ILC2 activation by IL-33 (Salimi et al., 2018). As well as cytokines, ILC2s are also stimulated by a number of other factors including neuropeptides and adhesion molecules. Neuropeptide neuomediun U (NMU) is critical for optimal ILC2 activation. Deficiency in NMU, renders mice unable to reduce worm burden following helminth infection as a direct result of diminished production of both IL-5 and IL-13 (Klose et al., 2017, Cardoso et al., 2017). Intercellular cell adhesion molecule-1 (ICAM-1) is exclusively critical for ILC2 development; it is not required for the development of any other ILC subset. In its absence, there is a significant reduction of ILC2s and they are rendered unable to respond to IL-33 stimulation with the production of IL-5 and IL-13. ILC2s, in the absence of ICAM-1 are unable to induce lung inflammation in mice (Lei et al., 2018).

ILC2s are critical in the protection in several tissues including lung and adipose tissue. ILC2s play a key role in metabolic homeostasis and are particularly important for the development of white adipose tissue (Moro et al., 2010). In both human and murine studies ILC2s are a key player in obesity. IL-33 has shown to play an important role in the beiging of white adipose tissue (Brestoff et al., 2015, Molofsky et al., 2013, Moro et al., 2010). IL-33 drives type 2 responses, where the contribution of Th2 cells has been excluded in experiments carried out in adoptive transfer of ILC2s in $Rag^{-/-}\gamma c^{-/-}$ mice, where ILC2s rescued exacerbated obesity phenotype (Hams et al., 2013). Both IL-13 and IL-5 contribute ILC2 protection from obesity. Absence of IL-13 leads to an increase in weight gain, coupled with increase glucose uptake in mice fed a high fat diet (Hams et al., 2013). ILC2s are also the primary source of IL-5 within adipose tissue and drives eosinophil recruitment. Eosinophils are critical for the maintenance of adipose tissue and preventing obesity associated inflammation driven by pro-inflammatory cells such as neutrophils and macrophages. In lean visceral adipose tissue, eosinophils maintain immunosuppressive alternatively activated macrophages which maintains tissue homeostasis and promotes insulin sensitivity. ILC2s are critical for the recruitment of eosinophils and tissue homeostasis within this model (Molofsky et al., 2013).

ILC2s have shown a key role in protection against atherosclerosis whereby IL-5 and IL-13 derived from ILC2s is critical for protection against plaque development. Furthermore, mice fed a high fat diet were not only more susceptible to developing atherosclerotic plaques, but this was also coupled with diminished ILC2 frequency in associated lymph nodes (Newland et al., 2017).

In a similar manner to ILC1 subsets, there is evidence emerging to suggest memory capacity of ILC2 subsets. It has been proposed that the "memory" ILC2s, which have previously been exposed to specific stimuli are capable of inducing higher levels of cytokine and inducing Th2 responses with greater efficiency (Wang et al., 2019). ILC2s, although having a similar transcriptional profile to memory T cells, do not generate specific memory responses but instead can respond to unrelated allergen challenge with greater efficacy to differentiate Th2s than naïve ILC2s (Martinez-Gonzalez et al., 2016). This may translate to having important implications in disease settings such as in allergy where patients maybe sensitive to multiple allergens. Unlike with memory ILC1s, there is no evidence currently to suggest migratory capacity of memory ILC2s or the formation and regulation of these cells. It does, however, highlight the critical implication ILC2s could have in allergic diseases.

ILCs are widely described as a tissue resident innate immune cell. However, Huang et al described ILC2s as having an ability to migrate to inflammatory tissue in response to IL-25 stimulation through lymphatic vessels within 72 hours. This migration was shown to be solely dependent on sphingosine-1-phosphate (S1P) mediate chemotaxis which was shown to be particularly critical in murine response to helminth infection (Huang et al., 2018). Thus far, this has only been demonstrated in ILC2 subsets.

In humans, ILC2s are identified by expression of prostaglandin D_2 receptor 2 (CRTH2), but phenotype and activity between mouse and human is conserved with human ILC2s responding IL33 and IL-25 stimulation (Salimi et al., 2013). Although very similar, murine ILC2s and human ILC2s pose significant differences in tissue localisation. Humans demonstrate notable frequency of circulatory ILC2s within peripheral blood, which is not observed within mouse. A reduction in ILC2s within the gut and lung is noted in healthy adult tissue compared with fetal tissue, although frequencies are restored in response inflammation (Mjosberg 2011), highlighting the implications of human development on ILC distribution and the considerations which should be made when translating observations in murine models.

ILC2s are negatively regulated in human skin through the interaction of adhesion molecular e-cadherin with KLRG1. Natural cytotoxicity receptor NKp30 is expressed by human ILC2s. B7H6 is the NKp30 receptor, which is constitutively expressed by keratinocytes, however it is only capable of being activated during inflammatory conditions such as atopic dermatitis and is not activated under normal homeostasis (Salimi et al., 2018). ILC2 activation is further regulated by aryl hydrocarbon receptor (Ahr) which inhibits ILC2s response to helminth infection. ILC2s are one of the most well studied of the ILC subsets in mouse, however differences in human tissue still remain relatively unexplored.

Overall, ILC2s respond with a type 2 response to IL-33 and IL-25 stimulation. ILC2s demonstrate immune defence, tissue homeostasis and a role in pathological conditions such as allergy. ILC2s can upregulate production of cytokines including type 3 cytokines. This highlights tissue specific regulation of these cells and the importance of studying ILC2s in the context of specific tissues and pathologies. As ILC2s elicit type 2 immune responses, it suggests that they are likely to suppress type 1 anti-tumour response and be detrimental in cancer however this is yet to be fully explored.

1.1.5. Group 3 Innate Lymphoid Cells

Defined by the transcription factor RORγt, ILC3s are divided into NCR^+ and NCR^- cells based on expression of NKp46. LTi, discovered in 1997, are also regarded as ILC3s and have been shown to be critical for the development of lymphoid tissue in fetal development (Mebius et al., 1997). ILC3s are predominantly associated with intestinal tissue and are the innate counterpart of Th17 cells. ILC3 placement in the intestinal tissue occurs during embryogenesis, primarily with NCR^- ILC3s, which then become NCR^+ ILC3s predominantly within the small intestinal tissue. In addition to RORγt, human ILC3s express CD117 (c-kit). NCR^- cells are the "non-inflammatory" cells and are responsible for intestinal homeostasis. Upon activation, NCR^- ILC3s transfer to NCR^+ ILC3s following stimulation by IL-1β and IL-23 (Teunissen et al., 2014) through the expression of NKp46 (Nkp44 in human) and account for around 70% of intestinal ILC3s (Li et al., 2019). In response to stimulation, ILC3s produce IL-17 and IL-22 (Diefenbach et al., 2014). NCR^- cells are the predominant source of IL-17, particularly in response to viral infection (Jie et al., 2014). IL-17 can act independently or can act synergistically with IL-22, as shown in a murine model of *Candia albicans* (Diefenbach et al., 2014). IL-22 is produced by both ILC3 subsets, but predominantly by NCR^+ and is critical for ILC3 response to bacterial infection with *Citrobacter rodentium* and prevents murine recovery

(Zheng et al., 2008). As seen with ILC2s and ILC1s, ILC3 cytokine production is also driven by STAT phosphorylation. IL-22 is produced as a result of STAT3 phosphorylation and is essential for bacterial defence by stimulating goblet cells to produce mucus, and to induce the release of anti-microbial peptides such as RegIIIγ (Sugimoto et al., 2008, Zheng et al., 2008).In mice, NCR^+ ILC3s are also capable of producing IFNγ, however stimulation of human cells has not replicated this. ILC3s are also the major source of IL-22 in the lung. Infection with *Streptococcus pneumoniae* drives ILC3 production of type 3 cytokines which then helps to eliminate the pathogen (Van Maele et al 2014).

Both human and mice ILC3s produce granulocyte-macrophage colony-stimulator factor (GM-CSF). Intestinal and lung macrophages release IL-1β which in turn stimulates ILC3s (Mortha et al., 2014, Kim et al., 2014). In the intestine, ILC3s are the major source for GM-CSF (Mortha et al., 2014). GM-CSF induces macrophage production of immunosuppressive cytokine IL-10. IL-10 increases frequency of Treg. In doing so, this prevents intestinal inflammation and drives immune tolerance. ILC3s are further responsible for immune tolerance within the oral mucosa, however the mechanism behind this remains unclear.

Tbet is also a key regulator of ILC3 development, particularly NCR^+ ILC3s which rely on Tbet to function (Sonnenberg and Artis, 2015). Unsurprisingly, there are similarities between ILC3s and ILC1s, as such they are both required for Th17 stability and promoting T cell infiltration in a murine model of autoimmune encephalomyelitis (EAE) (Kwong et al., 2017). As a key player in intestinal inflammation, ILC3s also have a key role in metabolite sensing, and express Ahr, a ligand dependent transcription factor, which senses dietary metabolites such as tryptophan and mediate effects of environmental toxins. Ahr maintains cell survival by limiting cell apoptosis. IL-22 production by ILC3s is dependent on Ahr, and is essential for protection against *C.rodentium* infection (Qui et al 2011; Lee et al 2011).

In addition to bacteria response, ILC3s also play an important role in tissue homeostasis. ILC3s are particularly important for defence against graft versus host disease (GvHD) where, in mice, IL-22 drives intestinal stem cell recovery following intestinal damage in GvHD and promotes cellular regeneration (Lindemans et al 2015). Whether this is the case in human, is still to be determined, however it is likely as an increase ILC3 frequency is observed in patients who do not develop graft versus host disease (GvHD) following haemopoietic stem cell transplant (HSCT) (Munneke et al., 2014, Sugimoto et al., 2008).

In addition to being critical in intestinal homeostasis, as with all ILC subsets, ILC3s are also capable of driving pathologies. ILC3 production of IL-17 are associated with both allergic lung inflammation and inflammatory bowel disease (Geremia et al., 2011, Schnyder-Candrian et al., 2006). ILC3s have been described to play a key role in obesity related asthma. Patients with severe asthma have elevated frequency of ILC3s within the lung. Furthermore, in the lung of obsese mice there is a significant increase in IL-1β production from inflammatory macrophages. This drives ILC3 production of IL-17 and instigates airway hyperreactivity. Asthma patients have elevated levels of IL-22, suggesting that activation of ILC3s drives disease in humans (Kim et al., 2014). IL-1 blockade in obese mice prevented the development of airway hyperreactivity in mice; whether this is directly translational to patients remains to be determined.

The role of ILCs and driving the adaptive immune system predominantly relies on cytokine and chemokine production. ILC3s, however, have shown to be capable of expression MHC II on their surface and interacting directly with T cells. As ILCs do not also provide a co-receptor stimulation, activation through antigen presentation renders T cells, specifically commensal bacterial- specific $CD4^+$ T cells, anergic and drives the induction of cell death. Increased ILC3s drove a decrease in Th17 numbers, suggesting that ILC3s help to regulate intestinal inflammation by limiting T cell responses. Dysregulation of MHC II presentation in ILC3s is associated with paediatric patients with Crohn's disease, further confirming the ILC3s protect against intestinal inflammation (Hepworth et al., 2015) . Of note, the capacity of NCR^-ILC3s to stimulate $CD4^+$ T cells through MHC II expression is dependent on the tissue of origin, and is downregulated in the small intestine in comparison with splenic cells (Lehmann et al., 2020). This evidence further suggests that ILCs, particularly ILC3s phenotype is depicted by the tissue microenvironment, which is critical understanding when assessing the role of these cells within pathological conditions.

1.1.6. Regulatory Innate lymphoid cells

Tregs are critical for maintaining immune tolerance and immune suppression. As ILC subsets mirror all the T help cell subsets and $CD8^+$ T cell subsets it was sought to determine whether ILCs also had a regulator subset. ILCregs were identified in 2017 as $Lin^-CD45^+CD127^+IL\text{-}10^+$ however had no specific markers (Wang et al., 2017). Unlike other ILC subsets which share transcription factor expression with their adaptive counterparts, ILCregs do not express forkhead box P3 (FoxP3) nor any other T cell related transcription factors. ILCregs were shown

to be activated by autocrine TGFβ which was critical for cellular expansion (Wang et al., 2017). IL-10 produced by ILCregs inhibited ILC1 and ILC3 function through inhibiting ILC cytokine protection and were shown to protect mice against intestinal inflammation (Wang et al., 2017). In contrast, in the naïve intestine, Bando et al were unable to identify $Lin^{-}CD45^{+}CD127^{+}IL\text{-}10^{+}$ in the absence of stimulation. Furthermore, they found no evidence of ILCregs during intestinal inflammation in mice (Bando et al., 2020). ILC2s, in this study, were identified as the primary source of IL-10, however, they were shown to express specific ILC2 makers and IL-10 production was diminished in the presence of TGFβ (Bando et al., 2020). As these cells expressed specific ILC2 markers, it is unlikely that ILCregs were mis-identified for ILC2s and are in fact a separate subset. There is limited further information regarding the function of ILCregs and how they might regulate ILC subset function in other tissues remains unknown. More investigation is required in order to determine the true nature of these cells.

1.1.7. Innate Lymphoid Cell Plasticity

ILC subsets are distinct in function and phenotype however there is mounting evidence to show that these subsets are not committed and rather, as seen in T cells, ILCs have the ability to convert between subsets (Gao et al., 2017, Bernink et al., 2015, Cuff et al., 2019); a phenomenon which is driven by tissue derived cytokines. It is important to understand these conversions as it can significantly impact how tissues respond under pathological conditions and respond to treatment.

Although within the same group, ILC1 and NK cells are two distinct subsets. NK cells are associated with a more cytotoxic phenotype. In obese mice, liver resident NK cells acquire an ILC1 phenotype showing increased expression of CD49a and decreased expression of Eomes. This alteration in phenotype is driven by TGFβ which decreased degranulation in NK cells and cytotoxic activity (Cuff et al., 2019). This was also replicated within the TME whereby TGFβ drove conversion of cytotoxic NK cells to non-cytotoxic ILC1 phenotype (Gao et al., 2017). This TFGβ driven conversion is dependent on SMAD4 which is required for NK cells stability, whereby in its absence, NK cells numbers decrease and ILC1s are concomitantly increased (Cortez et al., 2017).

In 2015, Bernink et al demonstrated that there is a strong plasticity between ILC1s and ILC3s. When ILC3s were cultured in the presence of the type 1 stimulation cytokine IL-12, ILC3s had diminished production of IL-22 and instead increased production of type 1 cytokine IFNγ. The

same was shown to be true in reverse, whereby ILC1s were able to upregulate the expression of RORγt and production of IL-22 in response to IL-23 stimulation. This demonstrates that ILC subsets are not fixed within their subset and phenotype and instead this is strongly driven by environmental stimulation. This is particularly important to note when considering the potential contribution of ILC subsets to disease and is a compounding factor when considering ILC targeted therapies (Bernink et al., 2015).

Plasticity between ILC2 and ILC1 has also been noted. ILC2 plasticity is induced by IL-12, whereby when ILC2s were cultured with IL-12, they gained a type 1 phenotype and increased production of IFNγ (Lim et al., 2016). Furthermore, in Crohn's disease patients deficient in IL-12Rβ1, ILC2s were unable to exhibit the sample plasticity suggesting that IL-12 is essential for the plasticity of ILC2s. As *IL12RB1* is also required for IL-23 signalling, ILC2s demonstrated an inability to express IL-23R so it is likely to have an impact on ILC2 plasticity (Lim et al., 2016).

1.2.Co-receptors

Co-receptors are cell surface receptors found on immune cells which, once activated, initiate biological signalling cascade and modulate immune cell function. Co-receptors can broadly be divided into co-stimulatory or co-inhibitory. As the name suggests, upon activation through ligand binding, co-stimulatory receptors drive cellular processes such as proliferation and cytokine production. Co-inhibitory receptors provide a "brake" and block cell activity and in some cases can initiate apoptosis. Co-receptor signalling has been best characterised in T cells where signalling is essential for complete T cell activation. Recently, however, the requirement for co-receptor signalling in ILCs has become apparent with ILCs demonstrating expression of several co-receptor molecules as well as expression of the appropriate ligands (Schwartz et al., 2017, Halim et al., 2018, Salimi et al., 2018, Maazi et al., 2015, Dong et al., 2017). Activation of naïve T cells requires co-receptor signalling in addition to activation of the T cell receptor (TCR). TCR activation itself is insufficient in inducing T cell activation and instead renders the cells in a state of anergy (Schwartz, 2003).

For TCR activation, antigen presenting cells (APCs) present antigens to the T cell through major histocompatibility complexes (MHC). These can be divided into either MHC class I or MHC class II. Class I present antigen to $CD8^+$ T cells and present antigens which are 9 amino acids in length (Peaper and Cresswell, 2008). Conversely, $CD4^+$ T cells respond to antigens

presented by MHC class II molecules, which usually consist of more than 9 amino acids (Rudensky et al., 1991). It is this resulting MHC:TCR complex which initiates the downstream signalling pathway. It is at the point where co-receptor signalling is required in order to fully activate T cells (Mueller et al., 1989, Boise et al., 1995). Of note, T cells also require a third signal in the form of cytokine stimulation which are usually produced by innate immune cells in the tissue microenvironment. This third signal is specifically required for T helper cell differentiation. For example, IL-12 produced by dendritic cells can activate $CD8^+$ cell cytotoxic responses in order to elicit anti-tumour responses (Chowdhury et al., 2011, Kerkar et al., 2010, Heufler et al., 1996). All three T cell activation signals have now been targeted within the clinic as anti-cancer therapies and for the treatment of autoimmune diseases.

CAR-T cell therapy utilises MHC:TCR activation. TCR present on T cells extracted from patient's tumours can be genetically modified in order to recognise specific tumour neoantigens. These cells can then be expanded and introduced into the patient whereby they are able to mount a specific immune response against the tumour (Reviewed by (Waldman et al., 2020). Cytokine stimulation has also been utilised therapeutically for cancer treatment by boosting T cell responses. These therapies include IFNγ, IL-2, IL-12 and GM-CSF. These have shown to be successful within the clinic, though have demonstrated highest efficacy when used in combination with anti-co-receptor treatments (Conlon et al., 2019).

CD28 was the first co-stimulatory molecule to be described in T cells which and is the most widely described. CD28 binds to its ligands either CD80 (B7-1) or CD86 (B7-2) which are expressed by APCs (Azuma et al., 1993, Koulova et al., 1991). Although CD80 is constitutively expressed by APCs, whereas CD86 is upregulated on APCs in response to T cell activation (Paine et al., 2012). Activation of CD28 leads to the activation of the mTOR (mechanistic target of rapamycin) signalling pathway and the phosphorylation of P13K. CD28 is responsible for driving T cell proliferation and cytokine production, however, the absence of CD28, although there is a reduction in proliferation, there is not complete ablation of T cell cytokine production and proliferation (Shahinian et al., 1993, Green et al., 2000) suggesting that CD28, although important, is not critical for T cell activation and that other stimulatory co-receptors may be able to compensate.

Targeting co-receptor signalling for anti-cancer therapies has shown to be particularly promising within the clinic. In particular, the blockade of negative co-receptors cytotoxic T-lymphocyte associated protein – 4 (CTLA-4) and PD-1 are now actively used in the clinic either

as monotherapies or in combination to treat several cancers including melanoma, ovarian cancer and non-small cell lung cancer.

ILC subsets mirror T helper cell subsets in immunological response and function. Similarly to T cells, ILCs have also been shown to both express and be regulated by co-receptor signalling. Many co-receptors, both stimulatory and inhibitory, have been shown to be expressed by ILCs and also more have shown to functionally modulating ILCs. Below ILC regulation by co-receptor signalling has been discussed.

1.2.1. Inducible T Cell Co-Stimulator

Inducible T cell co-stimulator (ICOS) is a stimulatory co-receptor which is a member of the CD28 family (Simpson et al., 2010). In T cells, ICOS expression is rapidly upregulated follow TCR activation and has been shown to be critical for T cell activation and immune response (McAdam et al., 2000, Dong et al., 2001). In T cells, activation of ICOS by its ligand (ICOS-L), results in the recruitment of p50α; a subunit of phosphatidylinositol (3,4,5)- trisphosphate (PIP3), and then signals through the PI3/AkT/mTOR pathway (Fos et al., 2008). ICOS-L is expressed by APCs, B cells and ILCs which is driven by TNFα (Swallow et al., 1999). Absence of ICOS signalling in T cells results in diminished T cell function, in particular ICOS deficient Th17 cells have reduced capacity to mount an immune response against bacterial infection (Kadkhoda et al., 2010).

ILC2s have been shown to have the capacity to express both ICOS and ICOS-L. ICOS signalling in ILC2s is critical for cellular proliferation and cytokine production. In $ICOS^{-/-}$ mice, ILC2s demonstrate decrease in Bcl2 expression coupled with reduced cellular viability. IL-33 activates ILC2s through STAT5 signalling to produce type 2 cytokines, a pathway that is significantly reduced in mice which lack ICOS (Maazi et al., 2015, Paclik et al., 2015). Patients with idiopathic pulmonary fibrosis (IPF) were shown to have reduced numbers of $ICOS^{+}$ILC2s, with murine models showing ICOS is required for IL-5 production and eosinophil infiltration (Hrusch et al., 2018).

1.2.2. OX40

OX40 is a co-stimulatory molecule which binds that is a member of the tumour necrosis factor receptor superfamily (TNFRSF) and is activated by its ligand OX40L which is expressed by most APCs (Aspeslagh et al., 2016). In T cells, OX40 activation signals through the Nf-κB and results in an increase Bcl, T cell activation and survival. Within T cells, OX40 not only drives cell survival but is also capable of supressing Treg activity (So and Croft, 2007) Absence of OX40 in T cells leads to an inability to proliferate and a diminished secretion of IFNγ (Kopf et al., 1999).

OX40L has been shown to be expressed by both ILC2s and ILC3s however there is no evidence showing expression of OX40. STAT5 phosphorylation, in ILC2s, drives surface expression of OX40L (Deng et al., 2020). This OX40L on ILC2s directly activates OX40 on $CD4^+$ T cells which induces T cell polarisation to a Th2 phenotype and induces production of type 2 cytokines in a murine model of airway inflammation (Halim et al., 2018).When ILC2s cultured with $CD4^+$ T cells and αOX40L, there was a significant decrease in cytokine production (Wu et al., 2019, Drake et al., 2014).This suggest that's ILC2s induce T cell cytokine production through activation of the OX40 receptor; however further investigation is required to fully establish the OX40:OX40L axis in ILCs and T cells (Drake et al., 2014, Halim et al., 2018). In a murine model of colitis, NCR^-ILC3s were the predominant source of OX40L (Deng et al., 2020).It is likely that ILC3s directly interact with intestinal Tregs, as co-localisation of both cell types was demonstrated within the cryopatches. Ultimately, ILC3 expression of OX40L was shown to be critical for intestinal Treg homeostasis, whereby in the absence of $OX40L^+$ILC3s, Tregs failed to expand and there was a significant increase in apoptotic cells (Deng et al., 2020).

1.2.3. Glucocorticoid-induced Tumour necrosis factor Receptor

Glucocorticoid-induced Tumour necrosis factor Receptor (GITR) is a co-stimulatory molecule expressed by both $CD4^+$ and $CD8^+$ T cells which stimulates T cell expansion and cytokine production (Sabharwal et al., 2018). The ligand of GITR, GITR-L, is expressed by APCs, endothelial cells and also by activated T cells (Reviewed in (Tian et al., 2020). In order to boost T cell response, GITR activation can suppress regulatory T cell function (van Olffen et al., 2009). All three ILC subsets have demonstrated the ability to express GITR however to date, only ILC1s and ILC2s have demonstrated a functional regulation by this co-receptor.

GITR expression on ILC1 drives cellular production of IFNγ and TNFα, with relatively low expression of GITR increasing ILC1 function (Vashist et al., 2018). $GITR^{hi}$ ILC1s demonstrated an exhausted phenotype and diminished cytokine production indicating that GITR could be instrumental in inducing tolerance. In activated ILC2s, GITR was shown to signal through the NFκB pathway to induce proliferation and cytokine production. Through GITR signalling, ILC2s were able to reverse diabetes in mice fed high fat diets (Galle-Treger et al., 2019). In ILCs isolated from human tonsil, both $NKp44^{+}$ and $NKp44^{-}$ ILC3s were capable of expressing GITR (Nagasawa et 2019). Conversely, Nagasawa et al, showed in their paper that ILC2s isolated from human PBMCs did not express GITR. This demonstrates the importance and need to consider the differences that may occur in non-tissue resident subsets versus tissue resident ILCs when assessing co-receptor expression. GITR expression was demonstrated in ILC2s which were isolated from visceral adipose tissue (VAT), which is a highly inflammatory tissue which could indicate that expression of GITR relies stimulation from the tissue microenvironment or may raise an interesting question as to the phenotypic differences between migratory ILCs and tissue resident ILCs.

1.2.4. Death Receptor 3

Death receptor 3 (DR3) is a co-stimulatory molecule is expressed by $CD4^{+}$ and $CD8^{+}$ T cells, NK cells and has recently been identified to be expressed in ILC subsets (Twohig et al., 2012). DR3 is activated by its ligand TNF-like 1A (TL1A), which is predominantly expressed by APCs following stimulation of TLRs (Reviewed in (Meylan et al., 2011)). In T cells, activation through DR3 promotes cellular proliferation and cytokine production (Twohig et al., 2012). Conversely, studies have also identified DR3 activation to enhance Treg expansion and thus is indicative that DR3 signalling may play a role in immunosuppression (Bittner et al., 2017).

ILC2s and ILC3s have both been identified as being regulated by DR3 signalling (Shafiei-Jahani et al., 2020, Li et al., 2019). In ILC3s, IL-23 dependent activation of DR3 by TL1A and signals through the MAPK pathway to induce cytokine production. Increased production of GM-CSF, in particular, was shown to increase eosinophil, neutrophil and myeloid cell infiltration resulting in a decrease ILC3s, providing a negative feedback loop (Li et al., 2019). This reduction in ILC3s was able to reduce intestinal inflammation in a murine model of colitis and protect against intestinal inflammation (Li et al., 2019). ILC2s were also shown to be activated by DR3 signalling which occurred in an IL-33 dependent manner (Shafiei-Jahani et al., 2020). Together this suggests that, as with the other stimulatory molecules, ILCs require

activation prior to further stimulation through DR3. In ILC2s, however this activation was shown to occur through increased expression of p52 and signalling through the NFκB pathway (Shafiei-Jahani et al., 2020). In the case of ILC2s, increased activation through DR3 lead to increased cytokine production and ultimately a protection against insulin resistance in mice fed with a high fat diet (Shafiei-Jahani et al., 2020).

1.2.5. Herpes Virus Entry Mediator

Herpes Virus Entry Mediator (HVEM) is a co-stimulatory molecule which binds to one of its four ligands; B and T lymphocyte attenuator (BTLA-4), CD160, synaptic adhesion-like molecule 5 (SALM5) and LIGHT which is a member of the TNF (tumour necrosis factor) family (Murphy and Murphy, 2010, Shui and Kronenberg, 2013). In T cells, ligand induced oligomerization of HVEM leads to the recruitment of TRAF2 (TNF receptor-associated factor 2). This then activates nuclear factor kappa b (NF-κB) which results in T cell activation (Marsters et al., 1997, Cheung et al., 2009). In ILC3s, HVEM activation by LIGHT induces production of IFNγ (Seo et al., 2018). When HVEM is specifically knocked out of RORγt$^+$ cells, there was a significant reduction in murine survival against bacterial infection and no changes were observed in CD4$^+$ T cells suggesting that HVEM:LIGHT signalling may occur exclusively in ILC3s, as opposed to RORγt$^+$ CD4$^+$ T cells. When LIGHT was absent there was a significant reduction in ILC3 production of IFNγ which was coupled with a reduction in murine survival in response to *Yersinia* infection (Seo et al., 2018).

1.2.6. Cytotoxic T-lymphocyte-associated protein 4

Inhibitory co-receptors have a critical role in immune cell regulation and restoring immune balance. Cytotoxic T-lymphocyte-associated protein 4 (CTLA-4) is an inhibitor receptor which competes with stimulatory co-receptor CD28 for binding with receptors CD80 and CD86 in order to inhibit T cell activity. This has been shown to be critical for murine survival, whereby knockout mice were shown to be unable to survive past 3 weeks of age following extensive lymphoproliferation (Tivol et al., 1995). CTLA-4 is upregulated following T cell activation, where it then binds with higher affinity to the receptor in order to suppress T cell activation and restore immune balance (Linsley et al., 1992, van der Merwe et al., 1997). This is true on all T cell subsets, with the exception of Tregs, where CTLA-4 is constitutively expressed and is critical for their function (Rudd et al., 2009, Takahashi et al., 2000). CTLA-4 blockade was first tested by Allison et al in a murine model of colon cancer and fibrosarcoma where it was able

to boost anti-tumour immunity (Leach et al., 1996) and Ipilimumab is now used in the clinic to treat melanoma and renal cell carcinoma, however due to the severity, many side effects are associated with the treatment. CTLA-4 expression on ILCs has been shown in human breast and gastrointestinal tumours, with the highest expression shown in ILC2s. Although expression is shown in ILC1 and ILC3s, within PBMCs expression is barely detectable (Salimi et al., 2018). In line with this, tumour resident ILC1s were shown to have increased CTLA-4 expression in comparison with tumour resident NK cells (Gao et al., 2017). Although no functional data has been shown to describe CTLA-4 activity in ILCs, Gao et al described the ILC1 subset as less effector more helper like phenotype which suggests that CTLA4 may play a similar inhibitory role on ILCs as it does in T cells, however this is yet to be confirmed.

1.2.7. Programmed Cell Death – 1

PD-1 is a 288 amino acid type 1 transmembrane protein with an immune-receptor tyrosin switch motif (ITSM) (Chemnitz et al., 2004). and is a member of the immunoglobulin domain co-receptors. PD-1 is not constitutively expressed on T cells rather is upregulated following stimulation. This upregulation is not rapid, and only occurs 24 hours post activation (Chemnitz et al 2004) (Ishida et al., 1992). PD-1 activation restricts T cell activity and proliferation in order to prevent excessive T cell activation (Agata et al., 1996). In contrast to T helper cells, Tregs demonstrate constitutive expression of PD-1 (Dong et al., 2017). PD-1 binds to its ligands; programme death ligand (PDL) 1 and 2. PDL-1 is widely expressed on many cells and tissues types. PDL-2 expression is restricted to APCs including dendritic cells and macrophages (Shi et al., 2014). The binding of either PDL-1 or PDL-2 to PD-1 recruits SHP2 to the ITSM tail of the PD-1 receptor (Ishida et al., 1992, Chemnitz et al., 2004, Fife et al., 2009). This results in the blockade of ZAP70, RAS and PI3K which blocks the activation of the TCR, resulting in the reduction of T cell activity. The activity of PD-1 is tightly regulated by transcription factors such as Tbet, which suppresses PD-1 during a chronic LCMV infection model in maintain a defence (Kao et al., 2011) (Figure 1.3.).

PD-1 activation results in the attenuation of T cell activity and proliferation and is important for restoring immune balance. PD-1 is important for immune tolerance, and although ablation is not as catastrophic as CTLA-4, whereby mice are incapable of surviving into adulthood, mice will develop autoimmune disorders at a later stage of life including lupus-like glomerulonephritis or cardiomyopathy; pathologies are dependent on the genetic background of the mice (Nishimura et al., 1999, Nishimura et al., 2001). Although it is a less severe

phenotype, this still highlights the importance of PD-1 for self-tolerance. In the absence of PD-1, mice are unable to response to LCMV infection leading to murine death (Youngblood et al., 2011). The absence of PD-1 also results in excessive inflammatory responses which are detrimental in viral infection and drive an accelerated onset of type 1 diabetes (Lazar-Molnar et al., 2010, Ansari et al., 2003).

PD-1 also plays an important role in T cell metabolism. T cells have specific metabolic profiles which are associated with T cell function. For example, senescent T cells with low activity favour oxidative phosphorylation which is efficient but slow. Contrary to this, highlight active effector T cells favour glycolysis which, although is less efficient is capable of providing the rapid energy required for cellular activation, cytokine production and proliferation (Reviewed by (Buck et al., 2015). PD-1 has been shown to regulate T cell metabolism. PD-1 inhibits phosphoinostide-3-kinase (PI3K) (Parry et al., 2005). Specifically, PD-1 also inhibits glucose uptake and glutamine metabolism which is driven by TCR and CD28 signalling cascade. As a result, this promotes fatty acid oxidation and favours oxidative phosphorylation resulting in a senescent cell phenotype (Patsoukis et al., 2015).

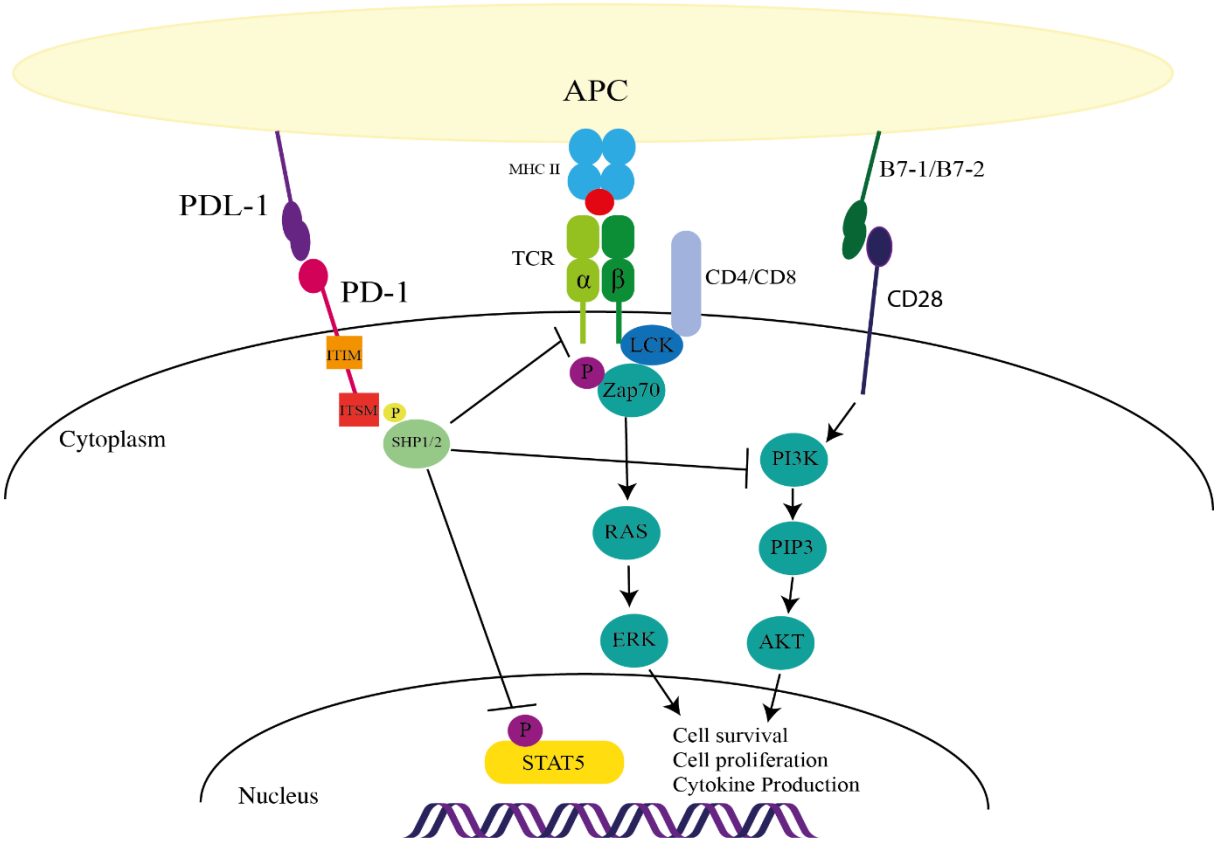

Figure 1.3 Programmed Cell Death – 1 Signalling Pathway. Upon binding to its ligands (programmed death ligand (PDL)-1 or 2), PD-1 recruits Sc homology region 2 domain containing phosphatase (SHP) ½ to the immunoreceptor tyrosine-based switch motif (ITSM) on the cytoplasmic tail. PD-1 signalling can inhibit T cell receptor (TCR) signalling and activation through CD28 signalling. In hepatises C virus (HCV) Tregs, the signalling can inhibit signal transducer and activator of transcription 5 (STAT5) phosphorylation. PD-1 inhibition is indicated by T bars; solid arrow indicate TCR and CD28 signalling pathways. Taken from Mallett et al (Mallett et al., 2019).

In order to improve patient response to therapy it is important to consider how PD-1 functions in all immune cell subsets as research has traditionally focused on PD-1 signalling in T cells, particularly $CD8^+$ T cells. PD-1 expression in tumour associated macrophages is associated with accelerated tumour development and correlated with a decreased phagocytosis (Gordon et al., 2017). Of note, in macrophages, blockade of PD-1 drives a reduction in tumour growth, suggesting that PD-1 therapy is beneficial for macrophages as well as T cells. As PD-1 has recently been described as regulating ILCs, it is important to understand how removing this inhibitor might ILC responses to tumour.

PD-1 is the first negative co-receptor to be identified on ILCs (Taylor et al., 2017)(Figure 1.4.). Of note, ILC2s have been shown to express both PD-1 and PDL-1(Schwartz et al., 2017). PD-1 was first shown to negatively regulate ILC2s in a murine model of helminth infection. In the absence of PD-1, mice demonstrated a significant increase in ILC2s within tissues following IL-33 stimulation. PD-1 was shown to regulate ILC2 cytokine stimulation through blockade of the phosphorylation of STAT5, which reduce cytokine production and proliferation. It was also demonstrated that ILC2s can be clinically targeted by αPD-1 therapy, whereby in a murine model of helminth infection, PD-1 blockade resulted in a significant increase in the ability of mice to clear worm burden and helminth infection (Taylor et al., 2017). ILC2s play a key role in metabolic distribution, and mice fed a high fat diet demonstrated a significant increase in PD-1^{+}ILC2s and diminished ILC2 function. PD-1 was shown to be driven by TNF stimulation of IL-33 (Oldenhove et al., 2018) . In T cells, PD-1 is upregulated following activation, and data suggests this could be the case within ILCs as PD-1 expression is upregulated in response to IL-33 stimulation. Recent studies have further evaluated the role of PD-1 in regulating ILC2s, whereby, in a murine model of airway inflammation, PD-1 drove changes in ILC2s metabolism by reducing cellular glycolysis and promoting fatty acid oxidation (Patsoukis et al., 2015).

Human studies have demonstrated that, in addition to ILC2s, ILC1 and ILC3s are capable of expressing PD-1. In human decidua tissue, ILC3 express PD-1 during the first trimester of pregnancy (Vacca et al., 2019). *In vitro* stimulation with IL-23 and IL-1β, demonstrated that PD-1 was able to negatively regulate decidua ILC3 IL-22 production. Notably, there was a significant decrease in PD-1 expression ILC3s during the third trimester of pregnancy (Vacca et al., 2019) suggesting that PD-1 expression maybe driven by environmental stimulation of ILCs. In human breast cancer and gastrointestinal tissue, all ILC subsets were shown to be capable of expressing PD-1 (Salimi et al., 2018) however whether PD-1 is capable of regulating all ILC subsets under these conditions remains yet to bet determined.

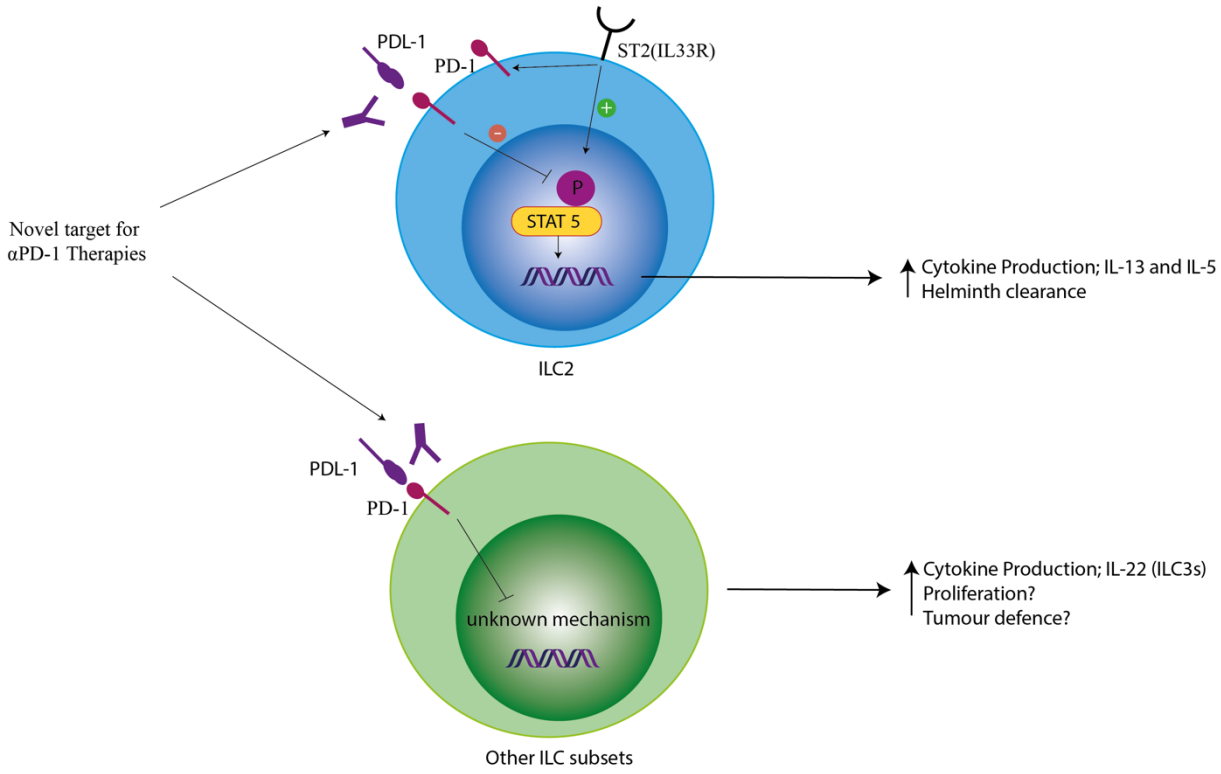

Figure 1.4.: Programmed death- 1(PD-1) signalling in innate lymphoid cells (ILCs). During immune challenges such as parasitic infections, alarmins such as IL-33 are released which activated ILC2s via ST2 (IL-33R). This activation results in the phosphorylation of signal transducer and activator of transcription (STAT) 5 and results in cellular proliferation and cytokine production. PD-1 activation inhibits the phosphorylation of STAT5 in ILC2s and thus inhibits cellular activation. PD-1 is expressed by both ILC1s and ICL3s; with evidence to show decreased IL-22 production by ILC3s upon activation in human decidua tissue. Adapted from Mallett et al 2019 In.J.Mol.Sci (Mallett et al., 2019).

1.3.Co-receptors and Cancer Therapy

The TME is the direct area surrounding tumour cells which encompasses a multitude of cells including immune cells (e.g. T and B cells, macrophages, dendritic cells and MSDCs), fibroblasts, vascular endothelial cells and the cancerous cells themselves. Interactions between these cells and the secreted factors within the TME directly influence and drive tumour progression, tumour metastasis and the ability of cancer cells to evade immune detection.

Recruitment of immune cells, such as T cells, into the TME is critical for successful responses to immunotherapies. $CD8^+$ T cells and Th1 cells are the primary adaptive immune cells which are responsible for anti-tumour responses through the production of IFNγ, granzyme and perforins. This was first demonstrated in ovarian cancer patients where the absence of intratumoural $CD3^+$ T cells significantly diminished the rate of patient survival. TMEs which

contained T cells, also had significantly increased T cell attractant cytokines compared with those which lacked T cells, which demonstrated a significant increase in vascular endothelial growth factor (VEGF; (Zhang et al., 2003). This is critical to note as VEGF not only promotes angiogenesis within the tumour, it's also a key immunosuppressive factor (Reviewed in (Yang et al., 2018)). Crucially, VEGF drives expression of $CD8^+$ T cell exhaustion markers including Tim-3, CTLA-4 and PD-1 (Voron et al., 2015). PD-1^+ B cell population has also been identified within the TME of several cancers including squamous cell carcinoma (SCC) and hepatic cell carcinoma ((Xiao et al., 2016, Mao et al., 2019)). Activation of PD-1 by its ligand PDL-1 induces production of anti-inflammatory cytokine IL-10 which diminished $CD8^+$ T cell immunity and allowed tumour progression; an observation which was reversed with αPd-1 (Xiao et al., 2016). Induction of PD-1 expression on adaptive immune cells is particularly important for patient response to αPD-1 therapy and it is important to note that PD-1 does not just play a critical role in the regulation of adaptive immune cells.

Innate immune cells, such as macrophages and dendritic cells, can destroy tumour cells through phagocytosis, inducing inflammation and recruiting adaptive immune cells. The TME, however, can drive macrophages towards a suppressive M2 phenotype which decreases ability to phagocytose and initiate an immune response (Gordon et al., 2017). PD-1 expression within the TME was demonstrated primarily on M2-like macrophages where expression was then linked with a decreased ability to phagocytose (Gordon et al., 2017). In colorectal cancer patients, PD-1^+ M2-like macrophages were associated with late-stage disease and poor prognosis. *In vivo* models demonstrated, these cells were able to be skewed towards promoting anti-tumour responses (Gordon et al., 2017). PD-1 was shown to increase on myeloid cells along with tumour progression, whereby absence of PD-1 specifically within myeloid cells was shown to significantly inhibit tumour progression within mice (Strauss et al., 2020). Dendritic cells express both PD-1 and PDL-1 in the ovarian cancer TME (Krempski et al., 2011). Anti-PD-1 therapy within mice with ovarian cancer showed reduced tumour growth as well as dendritic cell and $CD8^+$ T cell activity (Krempski et al., 2011). Dendritic cells were shown to be critical for successful use of anti PD-1 therapy (Sanchez-Paulete et al., 2016).

TME cells are able to do this through several mechanisms including upregulation of co-receptor ligands such as PDL-1 (Zou and Chen, 2008). This upregulation of PDL-1 on tumour cells can directly dampen T cell and other immune cell responses against the tumour development and allows them to evade immune detection. Expression of PDL-1 on the tumour cells can indicate patient responsiveness to therapy. Patients with metastatic melanoma showing a higher than

5% PDL-1 expression in tumour cells showed an increase survival in response to nivolumab treatment (increase from 53% to 81.5%) (Weber et al., 2015). Melanoma cells have demonstrated a sub-population of PD-1^+ tumour cells present within the TME. Conversely to immune cells, PD-1 within melanoma cells was shown to drive tumorigenesis; a mechanism which could be reversed with anti-PD-1 therapy. In patients, high expression of rpS6 (ribosomal protein S6) within tumour cells were correlated with increased survival and enhanced prognosis (Kleffel et al., 2015). Furthermore, following anti-PD-1 therapy, patients demonstrated a decrease in rpS6 expression (Kleffel et al., 2015). This highlights the relationship between PD-1 signalling pathway and mTOR signalling pathway within tumour cells. This highlights that anti-PD-1 therapy, in addition to enhancing immune cell, may directly target tumour cells in addition to immune cell subsets (Kleffel et al., 2015). Research has focused on the implications of blocking PD-1 signalling on T cell subsets, however data is clearly indicative that therapy may directly target tumour cells and further data has demonstrated that PD-1 may also target innate immune cell subsets.

Immune checkpoint inhibitors are used successfully within the clinic, in particular those which target CTLA-4 and PD-1. Therapies which target PD-1 are particularly successful within the clinic, with both pembrolizumab and nivolumab in the top 10 selling pharmaceuticals in 2020 (Urquhart, 2021). Nivolumab and other anti-PD-1 therapies are now used to target a wide variety of cancers including Hodgkin's lymphoma, melanoma and ovarian cancer (Callahan et al., 2016, Topalian et al., 2012).

Melanoma is regarded as a highly aggressive form of skin cancer which occurs from mutations within melanocytes. In early stages of disease, surgical treatment is the primary treatment option and is the preferred treatment option with survival rates exceeding 92% (Ralli et al., 2020). Survival and prognosis, however, is significantly diminished once metastasis has occurred where there is only 23% rate of survival (Ralli et al., 2020). Patients who received monotherapy treatment showed an increased survival rate (70.5% versus 60.8%) when treated with nivolumab versus ilipumab. (Weber et al., 2015). Treatments using either ipiliumab or nivolumab showed significant adverse effects within the clinic. In mice, absence of CTLA-4 has more severe consequences than absence of PD-1. Unsurprisingly, patients receiving ipiliumab had a higher incidence and severity of adverse side effects compared with treatment with nivolumab (Weber et al., 2015). Reported side effects from anti-PD-1 therapies include side effects that effect the respiratory system and can result in musculoskeletal problems (Zimmer et al., 2016). Of note, some patients still remain unresponsive to PD-1 therapies and

this highlights the lack of understanding of the exact mechanisms behind how these therapies work. Data has suggested that patient response may be dictated by immune cell infiltration, expression of co-receptors ligands such as PDL-1 and suggestions that response may be modulated through the gut microbiome (Gopalakrishnan et al., 2018). Research is now expanding from focusing on adaptive immune cells to identify the contribution of innate immune cells. Contribution of macrophages, dendritic cells and MDSCs has been discussed however the contribution of ILCs to tumour development, progression and therapeutic responses remains unclear. Furthermore, although some regulation of ILCs by PD-1 has been noted, this has not truly been investigated. If ILCs do in fact respond to PD-1 therapy it is critical to understand this regulation in order to understand patient responsiveness in the future.

1.4. Innate Lymphoid Cells in Cancer

As discussed, many cells are present within the TME, however of the immune cells present the vast majority are regulatory which results in a dampening of immune responses and an inability of an immune response to be launched against tumour development. Tumour cells themselves have evolved to protect them whereby they are able to upregulate expression of PDL-1. In doing so, tumour cells attenuate T cell activation, particularly $CD8^+$ T cells which provide the anti-tumour immune response and thus tumours are able to avoid immune responses (Juneja et al., 2017). This is partly why immunotherapies targeting PD-1 have been shown to be successful within the clinic. The success of these therapies relies on T cell infiltration within the TME therefore problems arise in solid tumours which have poor immune cell infiltration. Thus, a larger importance should be placed on the potential benefits of targeting ILCs. As ILC are tissue resident cells, there should not be a requirement of ILCs to infiltrate the TME. As PD-1 has been shown to be expressed by ILCs and importantly can be regulated by PD-1 within the tumour microenvironment it is important to understand how ILCs contribute to tumour biology. If ILCs contribute to anti-tumour responses, then boosting ILCs within the TME could be extremely beneficial as cytokines produced by ILCs can encourage T cell migration into solid tumours with poor immune infiltration. Conversely, if ILCs contribute to tumour development and progression, taking away inhibitory signalling pathways such as PD-1 signalling could be a detrimental to treatment and also provide an explanation as to why some patients are not responding to treatment. This demonstrates that understanding ILC biology is critical to fully elucidating and enhancing effective anti-cancer therapies. To add complexity to this issue, not only have all ILC subsets been shown to be present within the TME (Salimi et al., 2018), they

have also demonstrated to both promote tumour development and also to provide anti-tumour responses highlighting that ILC biology is not straight forward (Figure 1.5.)

1.4.1. Group 1 ILCs

NK cells have been well characterised in their contribution to tumour development (Melaiu et al., 2019). For example, NK cells can produce proinflammatory cytokine CCL5, which can induce tumour infiltration of dendritic cells; aiding within immune control over the tumour (Bottcher et al., 2018). There is little evidence, however, demonstrating the direct role of ILC1s in tumour development.

As there is limited research in the direct implications of ILC1 in cancer progression, to understand whether ILC1s contribute to or hinder tumour development, research into the impact of cytokines produced by ILC1s, showing potential indirect tumour responses has been critical. As previously described, ILC1s are a key producer produce IFNγ. IFNγ was shown to be beneficial in murine cancer models. By acting directly on the tumour cells, IFNγ induces major histocompatibility complex (MHC) class I expression which enhances T cell infiltration into the tumour in order to elicit anti-tumour responses. Consistent with these findings, ablation of IFNγ was shown to increase tumour angiogenesis, tumour growth and reduce immune cell infiltration into the tumour (Martini et al., 2010, Nakajima et al., 2001, Beatty and Paterson, 2001). IFNγ, in addition to TNFα, drives dendritic cell maturation and survival. In doing so, dendritic cells produce IL-12 and stimulate cytotoxic $CD8^+$ T cells which are capable of mounting sufficient immune response against tumour tissue (Pan et al., 2004). During early viral infection, ILC1s are the predominant source of IFNγ and as evidence suggests that IFNγ provides anti-tumour responses, it could be assumed that ILC1s also provide an anti-cancer response similar to what is seen in NK cells. In precancerous tissue, a significant increase in tissue resident IL-15 dependent ILC1s which capable of mounting a cytotoxic defence has been observed (Dadi et al., 2016).

There is also sufficient evidence to suggest that ILC1s may be detrimental to tumour protection. In patients with acute myeloid leukaemia, there is a significant increase dysfunctional circulating ILC1s which had a diminished capacity to produce IFNγ; an observation which was replicated in patients with chronic lymphocytic leukeamia (Trabanelli et al., 2015, de Weerdt et al., 2016). TGFβ in the TME drives the conversion of $CD49b^+$ NK cells through a

$CD49a^+CD49b^+$ intermediate to $CD49a^+$ ILC1s which downregulated expression of EOMEs and increased expression of TRAIL, confirming ILC1 phenotype. $CD49a^+$ ILC1s show an increased expression of negative co-receptors CTLA-4 and PD-1, and a reduction in the production in IFNγ production ultimately resulting in an inability to provide adequate anti-tumour defence which NK cells normally demonstrate (Gao et al., 2017). This conversion is dependent on SMAD4, a signalling transducer required for TGFβ signalling, which also drove NK cells to acquire an ILC1-like phenotype and impaired protection against tumour development (Cortez et al., 2017). In line with this, absence of TNFα reduced tumour formation in both colon and skin cancer (Popivanova et al., 2008, Scott et al., 2003). Notably, an ILC1 subset ($CD56^+CD3^-$) was shown to directly suppress infiltration of both $CD4^+$ and $CD8^+$ T cells as well as supressing T cell production of IFNγ. A dramatic increase in survival was noted in ovarian cancer patients who lacked regulatory $CD56^+CD3^-$ compared with when those cells were present within the TME (Crome et al., 2017). TNFα blockade in a rat model of colon cancer resulted in increased tumour formation and demonstrated absence of TNFα was able to promote dendritic cell infiltration and T cell production of IFNγ (Larmonier et al., 2007). In colorectal cancer, however, ILC1s were shown to be significantly reduced in late stage disease and demonstrated diminished ability to produce IFNγ (Wang et al., 2020). This suggests that ILC1s, in contradiction to Gao et al and Crome et al, drive anti-tumour responses. These data highlight the inconsistency in the current research and the lack of understanding of the contribution of group 1 ILCs to cancer progression.

1.4.2. Group 2 ILCs

The role of ILC2s in tumour development remains ambiguous. ILC2s have been shown to be present in many human cancers including mesothelioma, lung, breast and gastrointestinal cancers (Tumino et al., 2019, Salimi et al., 2018). ILC2s are increased in the peripheral blood of patients with acute promyelocytic leukaemia (APL) and gastric cancer (Trabanelli et al., 2017, Bie et al., 2014). However low numbers of ILC2s within the TME means that the role of ILC2s is more problematic to identify. In gastric cancer, increased circulating ILC2s has been associated with skewing Th2 response and poor clinical outcome (Bie et al., 2014). In murine breast cancer models, activation of ILC2s through the IL-33 axis drives tumour progression through increase tumour infiltration of Tregs and immunosuppressive macrophages coupled with a decrease in cytotoxic NK cells (Jovanovic et al., 2014). Decrease in NK cells and the

ability of NK cells to produce granzyme and IFNγ is specifically driven by IL-33 activated ILC2s and results in an increase in tumour development and metastasis (Schuijs et al., 2020). NK cell function is suppressed through IL-33 driving increased expression of ectoenzyme CD73 on ILC2s; whereby in the absence of CD73, NK cell frequency and function is sufficiently increased (Long et al., 2018). This highlights the capability of ILC2s to skew the immune response to favour type 2; which is detrimental for anti-tumour responses. In addition to suppressing NK cells, ILC2s can also drive tumour progression through the production of type 2 cytokines. IL-13, produced by ILC2s, specifically drives tumour infiltration of M2 macrophages as well as myeloid derived suppressor cells (MDSCs); both key immunosuppressive innate immune cells. MDSCs express IL-13Rα1. Prostaglandin D2 is produced by tumour cells and binds to CRTH2 receptor on human ILC2s. Cytotoxicity receptor Nkp30 is activated by tumour bound B7H6. Activation of both CRTH2 and Nkp30 drives ILC2 production of IL-13. This activates the IL-13Rα1, increasing MDSC proliferation and tumour progression; a process which can be prevented in the absence of prostaglandin D2 and αNKp30. Patients with non-muscle invasive bladder cancer demonstrated decreased reoccurrence rate with low MDSC:T cell ration; potentially suggesting a predictive biomarker in the future (Trabanelli et al., 2017) (Chevalier et al., 2017).

Amphiregulin, another product of ILC2s, is also capable of inhibiting anti-tumour responses by increasing Treg presence within the TME (Zaiss et al., 2015). Type 2 cytokines, such as IL-4, may further contribute to tumour progression by skewing T cell responses as to favour a Th2 response over a Th1 response, and as Th1 cells are associated with an anti-tumour response this results in an increase in tumour formation (van Beek et al., 2016).

Although there is data showing ILC2s can drive tumour development, there are still several studies demonstrating a protective role of ILC2s against tumour development. IL-33 driven IL-5 was shown to drive eosinophil infiltration into the TME, which was then associated with decrease tumour progression and reduced metastasis in a murine model of lung cancer (Ikuntani et al 2012). This increase in eosinophil infiltration was replicated in a murine model of lymphoma which was coupled with an increase in ILC2s and a decrease in tumour growth (Kim et al., 2016). Furthermore, IL-33 induced ILC2s were also shown to provide protection against pancreatic cancer development. Here, ILC2s produced CCL5 which was able to promote $CD103^+$ dendritic cells which then stimulated $CD8^+$ T cells leading to a robust anti-tumour response (Moral et al., 2020). As with ILC1s and TGFβ, tumour cells limit ILC2s anti-tumour response through the production of lactic acid which reduced ILC2 tumour infiltration and high

levels were associated to rapid increase in tumour development (Wagner et al., 2020). In colorectal cancer, PD-1 expression on ILC2s is increased in late stage disease which directly drives an increase in tumour cell proliferation (Wang et al., 2020).

1.4.3. Group 3 ILCs

As with ILC1 and ILC2, ILC3s also have a role in cancer development, however the role of ILC3s in cancer development has almost exclusively been described within the intestine. Particularly, there has been a large focus on tumour formation in response to chronic intestinal inflammation from pathologies such as colitis and Crohn's disease (Geremia et al., 2011). The role of ILC3 in cancer was first described in 2013, whereby IL-22 production from ILC3s was shown to drive colitis induced colon cancer (Kirchberger et al., 2013). Furthermore, in the absence of IL-22, there is a significant decrease in cancer formation within the colon. NCR^+ ILC3s were shown to accumulate within human non-small cell lung carcinoma (NSCLC), with a significant increase seen in patients at stage III of disease; a phenomenon which occurs through the recognition of tumour cells through the NKp44 receptor (Carrega et al 2015). In human breast cancer, the presence of ILC3s within tumour tissue is directly correlated with increased tumour metastasis within the lymph nodes. NCR^- ILC3s are recruited to the tumour via chemokine CCL21. CXCL13 instigates the clustering of ILC3s around meschymal stromal cells within the tumour tissue. Together, this promotes tumour metastasis to distal sites such as the lymph nodes (Irshad et al., 2017). ILC3s can interact directly with T cells through MHC II and this renders T cells anergic. Dysregulation of this interaction is associated with chronic inflammation and increased Th17 cells infiltration. As chronic intestinal inflammation is a key driver of colon cancer, an Th17 cells produce both IL-17 and IL-22, ILC3s could be driving initial tumour development (Hepworth et al., 2015). However, Th17 cells do have the capacity to produce IFNγ, and have been shown to drive anti-tumour responses (Kryczek et al., 2009). ILC3:T cell interaction in the gut has demonstrated to be sufficient to stimulate type 1 immunity within the gut and enhance anti-tumour response. In patients, dysregulation of ILC3s is associated with poor clinical outcome. This is as a result of alter microbiota which can drive tumour progression and immunotherapy resistance (Goc et al., 2021). To what extent MHC II:TCR interaction between ILC3s and T cells drives or prevents tumour development still required further investigation. Further evidence has suggested that ILC3s convert to a regulatory phenotype through increased production of anti-inflammatory cytokines throughout cancer progression. Depletion of these ILCregs showed a significant decrease in tumour growth (Wang et al., 2020).

In contrast, patients with acute myeloid leukeamia demonstrated a significant reduction in ILC3s in PBMCs within patients and was increased to healthy donor levels following successful chemotherapy (Trabanelli et al., 2015); the contribution of ILC3s to this disease remains unclear. As with other ILC subsets, there is data associated with ILC associated cytokines, for example IL-23 has been shown to significantly decrease tumour formation in colorectal cancer (Chan et al., 2014). It remains, however, unclear at this point whether tumour response to IL-23 is driven by the innate or adaptive immune system. Similarly, in $Rag^{-/-}$ mice, in the absence of IL-17 mice are resistant to tumour development, however no difference was noted between wildtype and $Rag^{-/-}$ mice, suggesting that ILC3s could drive this response (Chan et al., 2014).

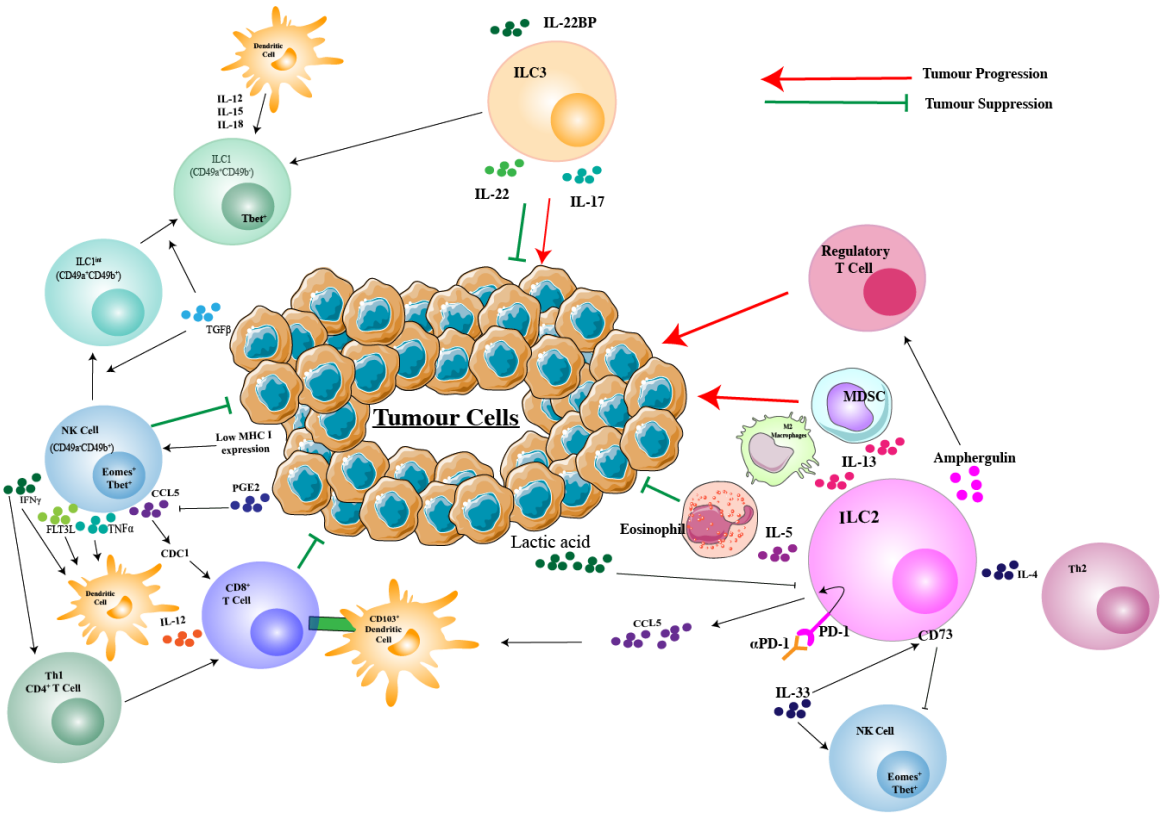

Figure 1.5. Innate lymphoid cells and cancer. Natural Killer (NK) cells produce IFNγ, granzyme and perforins which can drive anti-tumour responses. Though these cytokines or production of chemokines such as CCL5, NK cells can induce dendritic cell cytokine production and induce Th1 polarisation culminating in $CD8^+$ T cell activation and anti-tumour responses. TGFβ, produced in the tumour microenvironment (TME) drives the conversion of NK cells to a non-cytotoxic ILC1 phenotype and suppress anti-tumour defences. ILC2s can both promote and inhibit anti-tumour defences. IL-5 drives the recruitment of eosinophils which provides tumour defence. ILC2s can also produce CCL5 which upregulates $CD8^+$ T cell response through $CD103^+$ Dendritic cells. Conversely, ILC2s produce IL-13 which drives immunosuppressive M2 macrophages and amphiregulin which induces Treg infiltration. All of which support tumour progression. IL-33 activates both NK cells and ILC2s. However, on ILC2s, IL-33 upregulates CD73 which inhibits NK cells and therefore prevents anti-tumour responses. ILC3s may provide anti-tumour responses through the production of IL-17 and IL-22, however can inhibit $CD4^+$ T cells through MHC II TCR interaction. ILC3s are also capable of converting into ILC1s which may also dampen anti-tumour responses.

Hypothesis

There is clear evidence to demonstrate that ILC2s are negatively regulated by PD-1 and there is further evidence showing that ILCs are capable of expressing PD-1 within the TME within humans. It remains unclear however whether ILCs are responding to PD-1 regulation within the TME and whether they are driving anti-tumour responses or whether they are aiding in tumour progression. This is important to consider when exploring anti-tumour therapies. The main hypothesis of this project is that ILCs are negatively regulated by PD-1 within the TME and that by blocking PD-1 the anti-tumorigenic properties of ILCs are enhanced.

Aims

- Identify which ILC subsets are present within the TME and the capability of them to express PD-1
- Assess whether PD-1 may regulate any of the ILC subsets within cancer using murine models of cancer and how lack of PD-1 signalling, either through genetic ablation or therapeutic blockade, can alter ILC populations through proliferative capacity and expression of cytokines.
- Examination of human cells to establish whether findings in murine models are conserved across species.

Chapter 2: Methods

2.1. Animals

B6. *Pdcd1*$^{-/-}$ and *B6.TbetZsGreen* were bred and maintained at Newcastle University. *B6. Rag1*$^{-/-}$ mice and *B6.C57* wildtype mice were sourced from Jackson Laboratories and Charles River (respectively) and were then housed and maintained at Newcastle University. *B6.Pdcd1*$^{-/-}$ *TbetZsGreen* mice were generated and bred at Newcastle University. All mice were housed in specific pathogen free conditions in individually ventilated cages at an ambient temperature (20-24ºC) and maintained on a 12 hour light/12 hours dark cycle with free access to food and water. All experimental mice were 8-12 weeks old unless stated otherwise. All procedures were carried out under a Home Office approved project licence held by Dr Shoba Amarnath (PPL: 7008838) and personal licence held by Grace Mallett. Use of all animals was approved by the Animal Ethics Committee at Newcastle University. All experiments have been designed and carried out in accordance with the 3Rs and data are presented according to the ARRIVE guidelines. Mice were culled in accordance with Schedule 1 of the Home Office regulations using cervical dislocation. All routine animal husbandary was undertaken by the staff at Newcastle University.

2.2. Human Cells

Human peripheral blood mononuclear cells (PBMCs) from healthy donors were kindly provided by Professor John Simpson's group from Newcastle University as part of "The role of inflammation in human immunity" study. Ethical approval was obtained from the relevant research ethics committee and all donors provides written and informed consent. All donors were aged 18 and above and were both male and female participants. Unless otherwise stated, PBMCs were kindly isolated by Dr Jonathon Scott.

2.3. Murine Strain Acquisition

2.3.1.Breeding Strategy

In order to isolate the role of PD-1 signalling in Tbet^{+} ILCs, this project sort to create a novel mouse strain, namely B6.*Pdcd1*$^{-/-}$*TbetZsGreen (PD-1*$^{-/-}$ *TbetZsGreen).* B6.*Pdcd1*$^{-/-}$ mice,

created by Professor Tasuku Honjo, have a global knockout of the *Pdcd1* gene whereby both the cytoplasmic and transmembrane regions are globally deleted (previously described (Nishimura and Honjo, 2001)). B6.TbetZsGreen mice, first generated by Zhu et al 2012, were generated by inserting the ZsGreen at the starting fragment which encodes Tbet in a bacterial artificial chromosome (BAC) clone. Following injection into ooctyes, the resulting Tbet continued to be expressed from the endogenous *Tbx21* thus ZsGreen would not interfere with endoengous Tbet expression (Zhu et al., 2012). In order to achieve the novel strain, B6.*Pdcd1*$^{-/-}$ mice were crossed with B6.TbetZsGreen mice (Figure 2.1.) to acquire a heterogeneous population. Heterogenous offspring were then bred to create the resulting homozygous strain. In order to confirm the correct strain, mice were genotyped for ZsGreen by flow cytometry analysis and PD-1 genotype was confirmed by polymerase chain reaction (PCR).

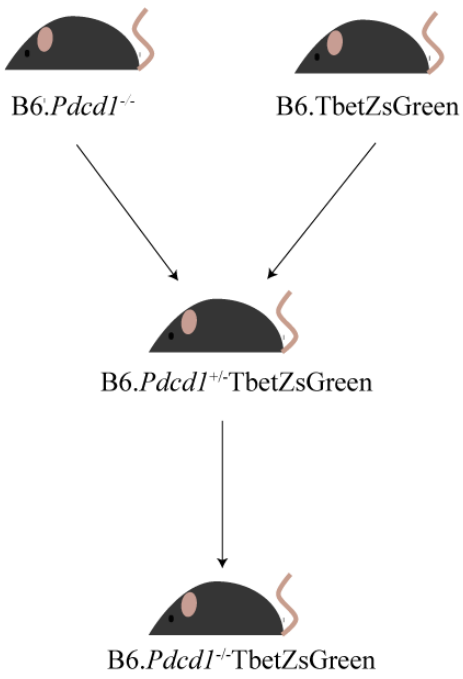

Figure 2.1.: Breeding Strategy for the generation of B6.*Pcdcd1*$^{-/-}$TbetZsGreen. B6.*Pdcd1*$^{-/-}$ were bred with B6.TbetZsGreen mice in order to generate B6.*Pdcd1*$^{+/-}$ TbetZsGreen mice. This generation was then bred together to generate B6.*Pdcd1*$^{-/-}$ TbetZsGreen. Mice were genotype was confirmed by flow cytometry and PCR in order to confirm genotype.

2.3.2. Genotyping by Flow cytometry

To confirm the presence of ZsGreen, blood samples were analysed by flow cytometry. A 50µl blood sample was acquired from the tail vein and collected in a heparin coated capillary collection tube (Sarstedt, Germany). Blood samples were diluted with PBS and then incubated with red blood cell (RBC) lysis buffer (Biolegend, CA) for 5 minutes at room temperature. Samples were then washed with FACs (Fluorescence activated cell sorting) buffer (PBS containing 0.5% sodium azide and 2.5% BSA). Samples were analysed for Tbet expression using FACSCanto II (BD Bioscience) (Figure 2.2.)

2.3.3. Genotyping by Polymerase Chain Reaction (PCR)

In order to confirm that the resulting strain was *Pdcd1*$^{-/-}$, gene expression was measured by PCR. Ear notch samples were obtained, and DNA was extracted using Tissue Extraction kit following the manufacturer's protocols (REDExtract-N-Amp^{TM} Tissue PCR Kit; Sigma-Aldrich). Briefly, samples were incubated in Tissue Extraction solution and Tissue Preparation solution at room temperature for 10 minutes in order to release DNA. Samples were then incubated at 95^{o}C for 3 minutes before being mixed with Neutralisation Buffer at room temperature. PCR reaction was carried out as described (Table 1) using primers previously described by Sharpe et al (Table 2) . Samples were then run on a 1.5% Agarose gel (UltraPure Agarose Gel; Sigma) made with TAE Buffer (0.04M Tris base, 1mM EDTA and 0.02M Acetic Acid; Sigma Aldrich) containing ethidium bromide (0.3µg/ml; Sigma) and ran at 110V for 1 hour 30 minutes. Gels were then analysed using Licor Odyssey and analysed using Image Studio.

	Temperature (°C)	Time (seconds)	Cycles
Initial Denaturation	95	240	1
Denaturation	95	20	38
Amplification	60	40	
Extension	72	60	
Final Extension	72	300	1

Table 1: Polymerase Chain Reaction (PCR) for PD-1 expression used for genotyping mice

Primer	Primer Sequence
PD1 Wildtype	5’ GCCAGCTAAGAGGCCACAGCTA 3’
PD1 Knockout	5’ GAACCTGCGTGCAATCCATCTTGTTCAATG 3’
PD9070R	5’ CGGTGCTCTCTGTGGAGGGTCTG 3’

Table 2: Primer sequences for genotyping

A.

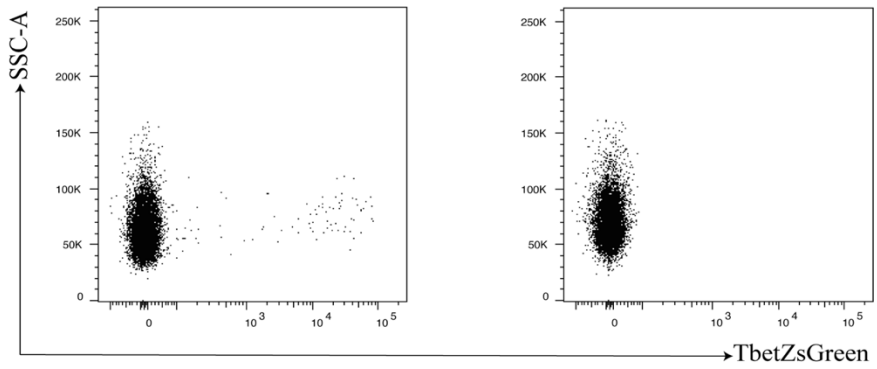

B.

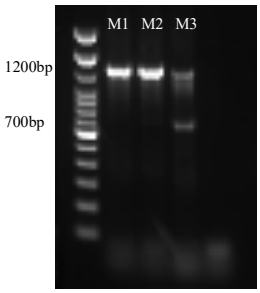

Figure 2.2.: Genotyping for *Pdcd1*$^{-/-}$TbetZsGreen. Blood samples were acquired from the tail vein and incubated with RBC lysis buffer. Samples were washed with FACs buffer and analysed on the FACSCanto II. Representative plots of TbetZsGreen positive (left panel; A) and negative mouse (right panel; A) shown. *Pdcd1*$^{-/-}$ was confirmed by polymerase chain reaction (PCR) (Wildtype = 1246bp; *Pdcd1*$^{-/-}$ =700bp). Representative gel shown in B showing wildtype mice (M1 and M2) and *Pdcd1*$^{+/-}$ mouse (M3).

2.4. Tumour Cell line Culture

2.4.1. Murine Tumour Cell Lines

For murine tumour cell line, under sterile conditions, B16 F10 Melanoma or MC38 colon carcinoma (kindly provided by Dr Gangaplara, NIH, USA) were thawed and washed with tumour media (Dulbecco's Modified Eagles Media (DMEM) (Gibco^{TM}) containing 10% fetal bovine serum (FBS) (Labtech), penicillin/streptomycin (100 units/ml of penicillin; 100µg/ml of streptomycin (Gibco^{TM}) and sodium pyruvate (1mM; Sigma Aldrich). All cells were cultured for 2-3 days prior to experiments. Cells were cultured in conical tissue culture flasks and incubated at 37^{o}C (5% CO_2). Once cells were 70% confluent, cells were harvested and expanded into multiple flasks. To harvest cells, cells were washed with warmed sterile PBS in order to remove any traces of media which may inactivate the trypsinisation process. PBS was removed and cells were incubated at 37^{o}C for 3-5 minutes with trypsin (Sigma) to allow adequate time for cells to detach from the flask. Equal volume of tumour media was added to the flask in order to inactivate trypsin and prevent cell death. Cells were transferred to falcon tubes and centrifuged at 400g for 5 minutes. Cells were re-suspended in tumour media at a concentration of 0.5 x 10^6 per ml. 0.5 x 10^6 cells were transferred to T175 for further expansion. Alternatively, cells were frozen for long term storage. To freeze cells, cells were re-suspended in tumour media with 10% DMSO. Cells are stored at -80^{o}C overnight before being transferred to liquid nitrogen for long term storage.

2.4.2. Human Tumour Cell Lines

For human tumour cell lines, C8161 human melanoma cell line and MET1 human squamous cell carcinoma cell (cSCC) line were kindly provided by Professor Penny Lovat (Newcastle University). C8161 cells were cultured in tumour media (DMEM, 10% FBS and 1% Penicillin/Streptomycin). MET4 cells were cultured in DMEM:F12 media (Gibco) with 10% FBS, 1% Penicilin streptomycin, Hydrocortisone (0.4µg/ml; Sigma), Chlorea toxin (8.5ng/ml; Sigma), Triiodo-L-Thyronine (20pM; Sigma), Adenine (180µM; Sigma), Insulin (5µg/ml; Sigma), Epithilial growth factor (EGF; 2pg/ml; Sigma) and Transferrin (5µg/ml; Sigma). As with the murine tumour cell lines, cells were cultured 2-3 days prior to experiments. Cells were cultured as described in 2.4.1.

2.5. In vivo Models

All animal *in vivo* studies were ethically reviewed and carried out in accordance with Aniamls (Scientific Procedure) Act 1986. Regulations were set by Newcastle University and the UK Home Office

2.5.1. Subcutaneous Tumour Model

B16 F10 melanoma cells or MC38 colon carcinoma cells were harvested as described above. Cells were re-suspended at a concentration of 1 x 10^6 per ml in sterile PBS. Initial mouse weight was recorded prior to starting the experiment to allow murine health to be monitored throughout the experiment. Mice were shaved at injection site (right flank) before being inoculated with 2 x 10^5 cells via a 200µl subcutaneous injection. Mice were weighed on alternate days throughout the course of the experiment. Once tumours were established, approximately day 5-7 post inoculation, tumour volume was measured daily. Tumour length (L) and width (W) were measured using electronic callipers (Draper, UK) and volume was calculated using the following equation:

$$\text{Tumour volume} = (\pi/6) \times 0.5 \times L \times W^2 \text{ (Schatton et al., 2008)}$$

For experiments where mice were treated with therapeutics, mice were injected with antibodies via intraperitoneal injection. Mice were administered with either αPD-1 blocking antibody (200µg per mouse; clone: RMP1-14) or isotype rat IgG2a (200µg per mouse; clone:2A3). For the blockade of NK cells, mice were administered with αNK1.1 (200µg per mouse; clone: PK136) or isotype mouse IgG1a control (200µg per mouse; clone: C1.18.4). For blockade of ILCs, mice received 100µg of αCD90.2 4 days prior to tumour inoculation. From day 7 onwards, mice either αCD90.2 (200µg per mouse unless otherwise stated; clone: 30H12) or isotype Rat IgG2b (200µg per mouse; clone:). All antibodies and isotype controls were purchased from BioXCell, OX, UK. For blockade of ILCs, mice were administered with 100µg of αCD90.2 on day -4 prior to tumour inoculation. For all studies, mice were administered with therapeutics on alternate days from day 7 onwards until mice reach humane endpoints. For tissue collect, mice were euthanised on day 12 post inoculation (unless otherwise stated) provided they did not exceed the humane endpoints outlined in the project licence (Tumour mean diameter exceed 1.5cm ($(^{L}/_{2}) + (^{W}/_{2})$) or weight loss exceeded more than 20% of initial

weight). Mice were euthanised via cervical dislocation and tissues were collect and processed immediately for the presence of ILCs as described below (Section 4).

2.5.2. Metastatic Tumour Model

B16 F10 melanoma cells were cultured and harvested as described above. Cells were re-suspended at a concentration of 1 x 10^6 per ml in sterile PBS. *B6.Pdcd1*$^{-/-}$ mice or wildtype littermate control animals were placed in a heated cabinet for 30 minutes prior to injection in order to increase vasodilation. Mice were inoculated with either 0.5 x 10^5 or 2 x 10^5 cells via intravenous tail vein injection; injections were performed by Ms Brigid Griffin. Mice were monitored throughout the study for signs of poor health through weight loss and clinical score. Mice were euthanised at the end of the experiment via cervical dislocation and tissues were harvested as described below (Section 2.6.).

2.5.3. AOM/DSS colon cancer model

Pdcd1$^{-/-}$TbetZsGreen mice or TbetZsGreen mice were administered with Azoxymethane (AOM; Sigma-Aldrich) via intraperitoneal (i.p.) injection at a dose of 12.5mg/kg (unless otherwise stated). 3 days post injection, mice were given 3% Dextran Sodium Sulfate (DSS) within the drinking water for 5 days, followed by a 16 day recovery period. Cycles 2 and 3 consisted of 3 days with DSS followed by 16 day recovery period as indicated (Adapted from (Parang et al., 2016); Figure 2.3). Throughout the experiment animal weight and clinical score was recorded throughout the experiment in order monitor animal health and disease progression. Stool samples were also monitored during the treatment period and scored as follows: normal stool = 0 points; loose stools = 1 point; diarrhoea = 2 points and presence of blood = 2 points (adapted from Mcdonough et al 2017; JCI). Mice were euthanised 16 days after the final treatment; whereby tumour burden and average tumour size was monitored and recorded prior to tissue harvest.

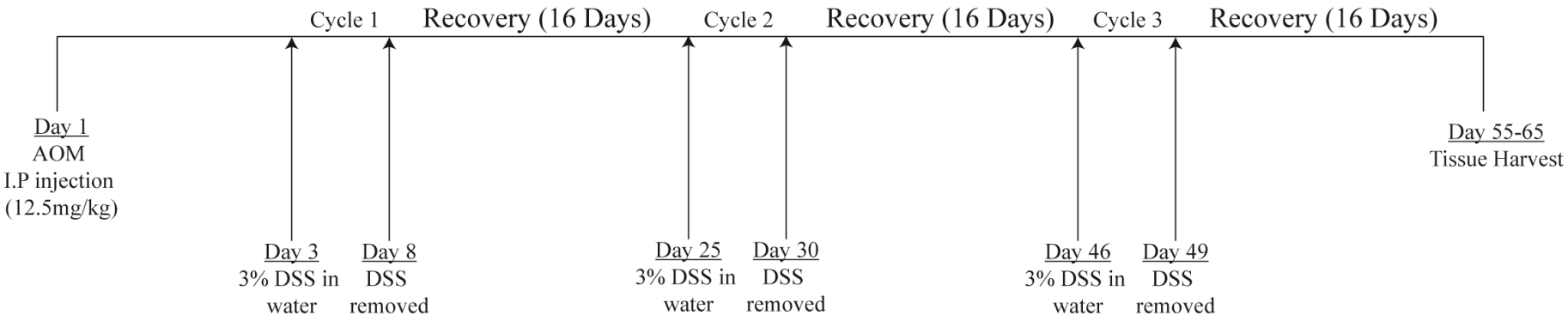

Figure 2.3. Inducible colon cancer model. Mice were treated with AOM (12.5mg/kg) via I.P injection. Mice were then treated with 3% Dextran Sodium Sulfate (DSS) in the drinking water in 3 cycles, followed by 16 day recovery period. Tissue was harvested from animals at day 65 post initial AOM injection.

2.5.4. BODIPY and 2-NBDG In vivo treatment

Mice were inoculated via subcutaneous injection with B16 melanoma tumour cells as described above (2.5.1.). Mice were injected via intraperitoneal injection with 50µg Bodipy FL C_{16} (Thermofisher Scientific) in 50µl DMSO. Mice were sacrificed 60 minutes after injection and tissue was processed immediately. Alternatively, mice were injected via intravenous injection (performed by Mr Chris Huggins) with 200µg 2-NDBG (ThermoFisher Scientific) in 100µl of PBS. Mice were sacrificed 15 minutes after injection and tissue was processed immediately.

2.6. Tissue harvesting

ILC subsets were characterised in B6.C57 Wildtype mice and B6.*Rag*$^{-/-}$ mice. Tissues characterised include spleen, lung, liver, small intestine and large intestine. For the subcutaneous tumour models, tumour infiltrating lymphocytes (TIL), spleen and tumour draining lymph nodes (TDLN) were harvested. For the metastatic tumour model, TIL, lung and TDLN were isolated. All organs were isolated into 5ml of complete mouse media (Dulbecco's Modified Eagles Media (DMEM) (Gibco^{TM}, Loughborough, UK) containing 10% fetal bovine serum (FBS) (Labtech), penicillin/streptomycin (100 units/ml of penicillin; 100µg/ml of streptomycin (Gibco^{TM}), sodium pyruvate (1mM; Sigma, Darmstadt, Germany), non-essential amino acids (0.1mM; Sigma,), L-glutamine (1mM; Sigma) and 2-mercaptoethanol (50µM; Sigma)) and stored on ice, with the exception of small and large intestine which were harvested into 5ml of PBS and stored on ice.

2.6.1. Lung

Lungs were perfused with PBS via the pulmonary artery *in situ* prior to being harvested into media in order to remove blood from the tissue. Lung tissue was washed with PBS in order to remove any traces of media, and were then incubate at 37ºC in FBS-free media containing 0.25mg/ml Liberase™ TL (Roche) and 0.5mg/ml DNAse I (Roche) for 15 minutes. Lung tissue was then mechanically pushed through a 100 micron cell strainer into a 50ml falcon tube containing 5ml of FBS with 15ml of media added. Samples were washed twice with 10ml of media before being re-suspended in 5ml of 40% percoll (Percoll (Sigma), DNase media and PBS). Samples were centrifuged at 400g for 20 minutes then the supernatant was removed. Cells were washed with media before being counted.

2.6.2. Liver

Livers were perfused with sterile PBS *in situ* via the hepatic artery prior to being harvested into complete media and stored on ice. Liver tissue was then washed with PBS to remove any traces of media, and was then incubated at 37°C in FBS-free media containing 0.25mg/ml Liberase™ TL (Roche) and 0.5mg/ml DNAse I (Roche) for 15 minutes. Tissue was then mechanically pushed through a 100 micron cell strainer into a 50ml falcon tube containing 5ml of FBS with 15ml of media added. Samples were washed twice with 10ml of media before being re-suspended in 5ml of 40% percoll (Percoll, DNase media and PBS). Samples were centrifuged at 400g for 20 minutes, supernatant was removed and cells were washed with media before being counted.

2.6.3. Intestine (Small and Large)

Small intestine and large intestine were washed in harvest buffer (2% FBS, 10mM HEPES (Sigma) and 50μM 2-Mercaptoethanol (Sigma)). Intestines were dissected longitudinally and cut into small segments in order to aid tissue digestion. Tissue was washed twice with harvest buffer in order to remove any traces of faecal matter and finally washed in PBS to remove any traces of FBS which may inactivate the digestion process. Tissue was incubated at 37°C in FBS-free media containing 0.25mg/ml Liberase™ TL (Roche) and 0.5mg/ml DNAse I (Roche) for 15 minutes. Intestine tissue was then mechanically pushed through a 100 micron cell strainer into a 50ml falcon tube containing 5ml of FBS with 15ml of media added. Samples were washed twice with 10ml of media before being re-suspended in 5ml of 40% percoll (Percoll, DNase media and 10 x PBS). Samples were centrifuged at 400g for 20 minutes, supernatant was removed and cells were washed with media before being counted.

2.6.4. Tumour Draining Lymph Nodes (TDLN)

TDLN were mechanically crushed through a 40 micron cell strainer into 5ml of complete mouse media. Cells were then transferred to falcon tubes where they were centrifuged at 400g for 5 minutes. Cells were re-suspended in 2ml of media and counted.

2.6.5. Tumour Infiltrating Lymphocytes (TILs)

TILs were removed with an excess of 2-3mm in order to ensure all tissue is collected. Tumour tissue was briefly washed in PBS to remove any traces of media and excess surrounding tissue was removed. Tumour tissue was then transferred to Liberase^{TM} TL (0.25mg/ml; Roche) DNase I (0.5mg/ml; Roche) FBS-Free media, finely chopped and incubated at 37^{o}C for 30 minutes. Tissue solution was then transferred to 5ml of FBS through 100 micron cell strainer (Corning) in order to inactivate the digestion process. Cells are then washed in 20ml of complete media and re-suspended in 10ml of media. Cell suspension was then added to 5ml of lymphocyte separation media at a ratio of 2:1 and centrifuged at 400g for 20 minutes with the brake off. The lymphocyte interphase is then transferred to a new falcon tube and washed with complete media and then counted.

2.6.6. Skin

Dorsal skin is taken from non-involved skin on the left flank. Skin was finely chopped and incubated with Liberase^{TM} TL (0.25mg/ml; Roche) DNase I (0.5mg/ml; Roche) FBS-Free media at 37^{o}C for 2 hours. Tissue solution was then transferred to 5ml FBS with 20ml of media through 100μm cell strainer (Corning) in order to inactivate the digestion process. Cells were then further strained through 70micron and 40micron strainer and counted with trypan blue.

2.6.7. Spleen

Spleen tissue was mechanically crushed through a 40 micron cell strainer into 5ml of complete mouse media. Cells were then centrifuged at 400g for 5 minutes. The supernatant was removed and cells were re-suspended in 1ml of red blood cell (RBC) lysis buffer (Biolegend, USA). Cells were incubated for 3 minutes at room temperature in RBC before 10ml of complete media was added. Cells were centrifuged and re-suspended in 5ml of media and counted.

2.7. Cell Counting

In order to count cells, a sample of cells was diluted at a 1:1 ratio with Trypan blue (Invitrogen), with the exception of spleenocytes which were diluted at a 1:10 ratio. Cells were then counted using a Haemocytometer (Corning).

2.8. Human PBMCs

Human PBMCs were isolated by Dr Jonathon Scott. PBMC cell suspensions were washed with sterile PBS and were then counted with trypan blue. Cells were re-suspended at a concentration of 2 x 10^6 per ml.

2.9. Transwell Experiments

For murine transwell experiments, spleenocytes were isolated as described above (2.6.7.) and re-suspended at a concentration 2 x 10^6 per ml. B16 melanoma tumour cell line was harvested as described above (2.4.i). 2 x 10^5 B16 melanoma cells were added to each of the 40 micron pore transwell filters (Thermofisher Scientific). Spleen cells were added at 1:1, 1:10 or 1:100 ratio with the tumour cells as indicated for 4 hours or cells were cultured at a 1:1 ratio for 2, 4, 6 or 24 hours as indicated at 37ºC (5% CO_2). Cells were then stained for flow cytometry analysis.

For human transwell experiments, PBMCs were re-suspended at a concentration of 1 x 10^6 cells per ml in human complete media (RPMI containing 10% FBS (Labtech), penicillin/streptomycin (100 units/ml of penicillin; 100µg/ml of streptomycin (Gibco^{TM}), sodium pyruvate (1mM; Sigma, Darmstadt, Germany), non-essential amino acids (0.1mM; Sigma,), L-glutamine (1mM; Sigma) and 2-mercaptoethanol (50µM; Sigma)). C8161 melanoma tumour cells and MET1 sSCC human cells were harvested as described previously (2.4.ii). 0.5 x10^6 PBMCs were added to each well of the transwell plate. Tumour cells were added at a ratio of 1:1 either in direct contact with the PBMCs or added into the transwell as indicated. Cells were cultured for 2, 4, 6 hours or overnight at 37ºC (5% CO_2) before being stained and analysed by flow cytometry.

2.10. Cell Proliferation Assay

For murine cell proliferation assays, spleenocytes were harvested as described above. Cells were incubated at 37ºC for 20 minutes with Cell Trace Violet dye (5µM; Invitrogen) as per manufactuer's instruction. 10ml of media was then added in order to absorb any unbound dye; cells were incubated for 15 minutes at 37ºC before being centrifuged at 400g x 5 minutes. Cells were then counted and re-suspended at a concentration of 1 x 10^6 cells per ml. 1 x 10^6 cells were added to each well of a plate and cells were incubated with recombinant mouse IL-2

(40ng/ml), recombinant mouse IL-7 (40ng/ml) and either αPD-1 blocking antibody (20mg/ml; Biolegend) or isotype control (20mg/ml; Biolegend) for 5 or 7 days; cytokines were re-added at day 3 and day 5. Cells were harvested on day 5 and day 7 and stained for flow cytometry analysis as described below. For human ILC proliferation assays, PBMCs were re-suspended in PBS at a concentration of 10 x 10^6 and stained with Cell Trace Violet dye (5μM; Invitrogen) as described above. PBMCs were plated at a concentration of 0.5 x 10^6 per well with recombinant mouse IL-2 (40ng/ml), recombinant mouse IL-7 (40ng/ml) and either αPD-1 blocking antibody (20mg/ml; Biolegend) or isotype control (20mg/ml; Biolegend) for 5 or 7 days. Human PBMCs were incubated with transwells seeded with C8161 melanoma cell line or MET1 SCC cell line. Transwells were removed after 16 hours. Cells were harvested and prepared for analysis by flow cytometry.

2.11. Cell Stimulation

To assess ILC function, cytokine production was analysed by flow cytometry analysis in all animal models and in human PBMCs. For both murine and human cells, 1 x 10^6 cells were added to a 48 well cell culture plate. Cells were then incubated with cell stimulation cocktail (1 in 500 dilution, Invitrogen) for 4 hours at 37°C. The stimulation cocktail contains phorbol myristate acetate (PMA) and ionomycin which promote cytokine production through the activation of Protein Kinase C (PKC) and induction of intracellular calcium signalling respectively. The stimulation cocktail also contained protein transport inhibitors Brefeldin A and monensin which prevent cytokine release from the golgi apparatus and the endoplasmic reticulum respectively. This allowed for cytokines to be retained within cells and thus allowing the intracellular measurement of cytokines. Cells were then fixed and stained for flow cytometry analysis.

2.12. Flow Cytometry Analysis

In order to analyse the presence and function of both murine and human ILCs in response to tumour, ILCs were analysed by multi-parameter flow cytometry. Flow cytometry is a technique widely used throughout immunology to phenotype cellular populations. Prior to analysis, cells are stained with antibodies for the target of interest (i.e. surface proteins such as CD3) which are conjugated to fluorophores. Fluorophores consist of a number of different molecules such as florescent proteins derived from microorganisms including phycoerythrin (PE), allophycocyan (APC) or polymer dyes created from polymer chains which respond to light

which include the brilliant violet fluorophores (BV). In order to increase the range of colours available, tandem dyes can be used which are produced when dyes such as APC or PE are chemically combined with small organic molecular dyes such as Cy5 or Cy7 (e.g. PE Cy7).

For analysis, cells are suspended in a "sheath fluid" which is pressurised to drive cells through the instrument past a series of lasers. As the laser hits the cells, it initially gives two measurements namely forward scatter area (FCS-A) and side scatter area (SSC-A). FSC refers to the light scattered by the cell in a forward direction which gives information regarding the size of the cells. SSC refers to the light scattered to the side at an angle which is dictated by the granularity and complexity of the cells i.e. cell such as lymphocytes with a low granularity would have a much lower SSC than highly granular cells such as neutrophils. Together, these measurements can be used to identified cellular populations.

Throughout this project, samples have been analysed using the BD LSR- Fortessa X20 (BD Biosciences) which consists of up to 5 different lasers. Each of the lasers function at a different wavelength and activate compatible fluorophores. Once activated, the fluorophores emit light which is detected and converted into a digital signal for analysis. The intensity of the signal provided gives information regards the expression levels of the target of interest.

Forward scatter height (FSC-H) can also be utilised for analysis. FSC-H measures the height of the cells and is used in conjunction with FSC-A for analysis. Although doublets cells, or two cells clumped together, will have a similar height to single cells, they will have approximately double the area. As the ratio of height to area is altered, this means doublets can be excluded from subsequent analysis.

Fluorophores emit light at specific wavelengths which are detected by the cytometer. Light is emitted at a higher wavelength then the excitation due energy release from the excitation. Lasers will detect any light within their wavelength, and this means that in some instances there is a "spillover" whereby one fluorophore can be detected in multiple channels. When one is only using one colour, this does not pose an issue. However, problems arise when analysing a multitude of complex immune cells which requires multiple markers and functional readouts. In order to prevent false positive data, compensation must be calculated in order to address these signals in multiple channels.

"Gating" process is applied to flow cytometry plots in order to identify and analyse specific cell populations. Controls are required in order to determine where the gates should be placed in order to exclude negative cell populations. Fluorescent minus one (FMO) controls are used in order to situate the gates. An example of the use of FMOs for identifying human ILCs is shown (Figure 2.5). FMOs contain all antibodies except for the antibody of interest thus identify where the negative population lies. FMOs, for this study in particular, are favoured over isotype control because they contain the remaining antibodies in the panel and therefore can incorporate any changes in fluorescence due to compensation. Isotypes controls contain a single fluorophore, and although can control for any autofluorescence from the cell populations, do not account for other fluorophores present so are likely to give an inaccurate representation of the negative population of cells.

2.12.1. Antibody Optimisation

Prior to running cellular analysis, antibody concentrations were optimised in order to determine the correct concentration for accurate analysis. Murine splenocytes or human PBMCs were used during antibody optimisation. 1 x 10^6 cells were washed with PBS (for Live/Dead Stain optimisation) or FACs buffer (PBS containing 2.5% Bovine serum albumin (BSA) and 0.05% sodium azide) for antibody optimisation. Cells were then incubated with varying concentrations of antibodies as stated and incubated for 30 minutes at 4^{o}C. Cells were then washed and analysed by LSR BD Fortessa X20 and optimal concentrations were determined (Figure 2.4). The negative gate was based on the unstained sample containing none of the antibody of choice which will determine where negative populations lie and will also account for any auto fluorescence produced by the cells. The optimal antibody was chosen as the minimum amount of antibody required which did not result in loss of receptor identification. In this instance, the optimal amount of CD5 required for adequate staining was 0.01μg

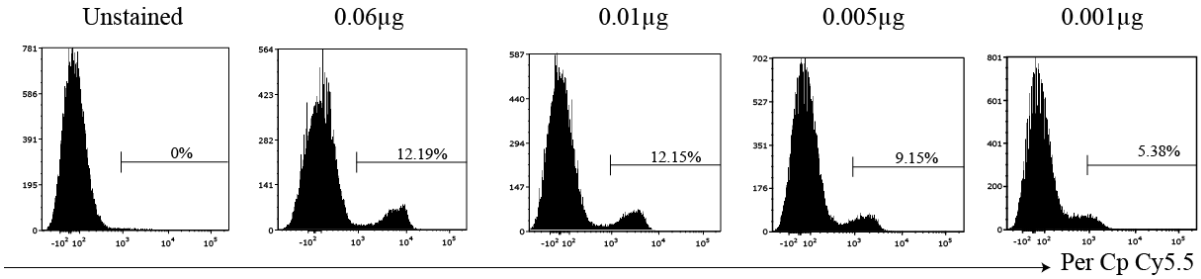

Figure 2. 4 Optimisation of CD5 Biotin Antibody Spleenocytes were isolated from Wildtype mice and incubated with red blood cell lysis buffer. Spleenocytes were washed with FACs buffer and incubated with varying with the recommended quantity of antibody (0.06µg) and varying other dosages to identify the optimum amount required.

2.12.2. Murine Flow cytometry

1 x 10^6 cells were washed in PBS in order to remove any traces of media. Cells were then incubated for 30 minutes at 4ºC with Live/Dead viability stain (Invitrogen) at a previously optimised concentration (Figure 2). Cells were then washed in PBS before being re-suspended in Biotin labelled lineage cocktail in FACs buffer (Table 3) and incubated at 4ºC for 30 minutes. Cells were washed with FACs buffer and incubated with Streptavidin Per Cp Cy5.5 (1µg/ml; Biolegend) for 20 minutes at 4ºC. Cells were washed with FACs buffer and re-suspended in 100µl of extracellular antibody cocktail (Table 4) for 30 minutes at 4ºC. Cells were washed with FACs buffer. In order to identify ILC subsets and to assess ILC function, staining for intracellular components such as transcription factors and cytokines was carried out. In order to achieve this, cell are required to be fixed. Cells were incubated with Fixation Permeabilisation solution for 30 minutes at 4ºC as per manufacturer's instructions. Cells were then washed twice with permabilisation buffer (BD Bioscience, 10x solution diluted in dH_2O) and were then incubated overnight with 100µl of intracellular antibody cocktail (Table 5). Cells were then washed the next day and re-suspended in FACs buffer and were then analysed on BD LSR Fortessa X20.

Antibody	**Clone**
CD3	145C11
CD5	53-7.3
CD8	53-6.7
CD11b	M1/70
CD11c	N418
CD19	1D3/CD19
CD49b	HMα2
Ter119	TER-119
F4/80	BM8
Gr1	RB6-8C5
NK1.1	PK136
B220	RA3-6B2

Table 3: Murine Lineage Antibodies

Antibody	Fluorochrome	Clone	Concentration
CD90.2	AF700	30-H12	1.25µg/ml
CD45	APC Cy7	30-F11	2.5µg/ml
CD45	AF700	30-F11	2.5µg/ml
CD127	BV510	A7R34	1.3µg/ml
CD25	PE Cy7	PC61	1µg/ml
CD25	BV711	PC61	1µg/ml
KLRG1	BV421	2F1/KLRG1	1µg/ml
ST2	FITC	DJ8	1µg/m;
ST2	PE	DJ8	1µg/ml
CD4	AF700	GK1.5	2.5µg/ml
Nkp46	APC	29A1.4	1.3µg/ml
Nkp46	BV711	29A1.4	1.3µg/ml
PD-1	BV605	29F.1A12	1.3µg/ml
F4/80	FITC	BM8	1µg/ml
Gr1	APC Cy7	RB6-8C5	1µg/ml
CD11b	APC	M1/70	1µg/ml
CD11c	BV605	N418	1µg/ml
NK1.1	BV510	PK136	1µg/ml
CD49a	APC	HMα1	1µg/ml
CD49b	APC Cy7	HMα2	1µg/ml

Table 4: Murine Extracellular Antibodies for Innate Lymphoid Cell Straining

Antibodies	**Fluorochrome**	**Clone**	**Concentration**
Tbet	FITC	4B10	2µg/ml
Tbet	BV711	4B10	2µg/ml
RORγt	PE	B2D	1.3µg/ml
IFNγ	PE Cy7	XMG1.2	1µg/ml
IFNγ	BV510	XMG1.2	1µg/ml
IL-10	BV605	JES5-16E3	1µg/ml
TNFα	BV785	MAb11	1µg/ml
IL-17	APC	eBio17B7	1µg/ml
IL-17	PE Cy7	eBio17B7	1µg/ml
IL-22	APC	IL22JOP	1µg/ml
IL-5	BV421	TRFK5	1µg/ml
IL-13	PE	eBio13A	1µg/ml

Table 5: Murine Intracellular Antibodies for Innate Lymphoid Cell Staining

2.12.3. Human Flow Cytometry

1 x 10^6 PBMCs were washed with PBS. Cells were then incubated for 30 minutes at 4°C with Fixable Cell Viability dye (Invitrogen). Cells were then washed with PBS before being incubated with cell surface antibodies (Table 7) which contained a lineage cocktail (Table 6) diluted in FACs buffer for 30 minutes at 4°C. Cells were washed with FACs buffer and then incubated with fixation/permeablisation solution (BD Bioscience) as per the manufacturer's instruction. Cells were then washed twice with permeablisation buffer (BD Bioscience) and incubated with intracellular antibodies overnight (Table 8). The following day cells were washed once with permeabilization buffer before being re-suspended in FACs buffer and analysed on the Fortessa X20.

Antibody	**Clone**
CD3	OKT3
CD5	L1F12
CD8	M5E2
CD11b	ICRF44
CD11c	3.9
CD14	3G8
CD19	H1B19
CD20	2H7
CD56	HCD56
TCRαβ	IP26

Table 6: Human Lineage Antibodies

Antibodies	Fluorochrome	Clone	Concentration
CD45	APC Cy 7	H130	1μg/ml
CD45	FITC	H130	1μg/ml
CD127	BV785	A019D5	1μg/ml
CD161	Per CP Cy5.5	HP-3G10	1μg/ml
CRTH2	BV421	BM16	1μg/ml
cKit	BV605	104D2	1μg/ml
NKp44	AF647	P44-8	1μg/ml
PD-1	PE Cy7	EH12.2H7	1μg/ml

Table 7: Human Extracellular Antibodies for Innate Lymphoid Cell Staining

Antibodies	Fluorochromes	Clone	Concentration
Tbet	BV711	B310	1μg/ml
RORγt	PE	B2D	1μg/ml
IFNγ	PE Cy7	XGM1.2	1μg/ml

Table 8: Human Intracellular Antibodies for Innate Lymphoid Cell Staining

ILCs were defined by the following gating strategies: Murine ILCs were defined as $Lin^-CD45^+Thy1^+$. In initial studies, ILC1s were identified as $Nkp46^+ROR\gamma t^-$. With use of TbetZsGreen mice and transcriptional staining, they were further described as $NKp46^+ROR\gamma t^-Tbet^+Eomes^-$ (definitions have been clarified in relevant results sections). ILC2s were defined as $CD127^+CD25^+KLRG1^{+/-}ST2^{+/-}$ (nILC2s $ST2^+$; iILC2s $KLRG1^+$ and mILC2s $KLRG1^+ST2^+$); NCR^+ ILC3s were defined as $ROR\gamma t^+NKp46^+$ and NCR^- ILC3s were defined as $ROR\gamma t^+Nkp46^-$. Human ILCs were defined as follows: $Lin^-CD45^+CD161^+CD127^+$. ILC1s were further defined as $CRTH2^-CD117^-Tbet^+Nkp44^{+/-}$; ILC2s were defined as $CRTH2^+CD117^-$; NCR^+ ILC3s were defined as $CRTH2^-CD117^+ROR\gamma t^+Nkp44^+$; NCR^- ILC3s were defined as $CRTH2^-CD117^+ROR\gamma t^+Nkp44^-$ and ex-ILC3s were defined as $CRTH2^-CD117^-Tbet^+Nkp44^+$. Single colour controls were established with One Comp Beads (Ebioscience) and were used to set up compensation. All gating analysis was based on FMO controls (Figure 2.5.). Cells were analysed using BD LSR Fortessa X20 with FACs DIVA software (BD Bioscience) and analysis was performed with FCS Express (De Novo) or FlowJo 10.1 software (Tree Star).

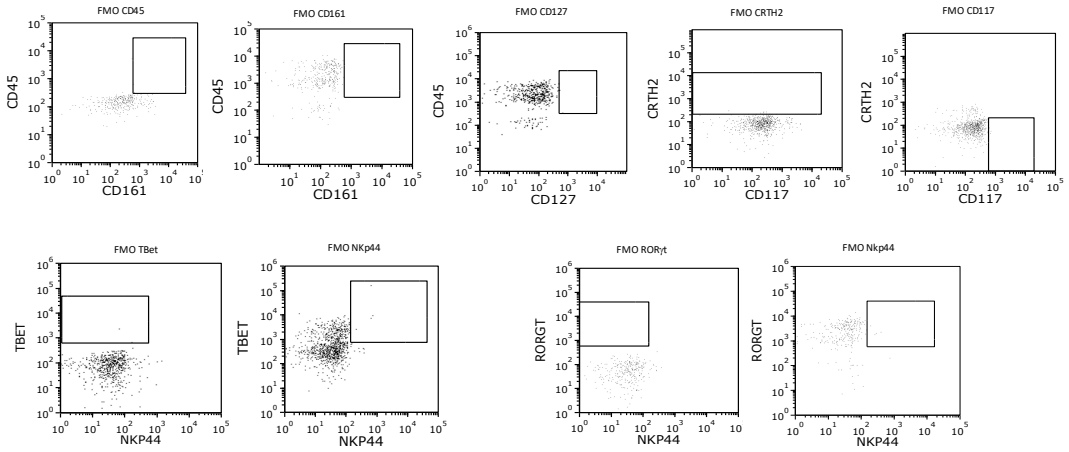

Figure 2.5. Fluorescent minus one Controls for Human PBMC analysis. Fluorescent minus one controls (FMO) were used throughout the project in order to discriminate between positive populations and background fluorescence. Representative FMO controls for the analysis of human PBMCs shown.

2.13. Statistical Analysis

Statistical analysis was carried out using GraphPad Prism (GraphPad Software Inc). Unless otherwise stated, statistical significance was determined by either an unpaired or paired t-test. For larger experiments where multiple groups were analysed, One-Way ANOVA was used to determine statistical significance. Histogram summary analysis was shown by mean values for the experiments (±SEM). P values less than 0.05 were classed as statistically significant (*$p<0.05$, **$p<0.01$, ***$p<0.001$).

Chapter 3: Innate Lymphoid Cells upregulate PD-1 expression in the TME

3.1 Introduction

ILCs have been shown to be capable of expressing PD-1 in human tissues, with studies showing PD-1 being expressed within human malignant pleural effusions, breast cancer, gastrointestinal tumours and human decidua tissue (Vacca et al., 2019, Tumino et al., 2019, Salimi et al., 2018). In murine models, PD-1 expression on ILCs thus far been shown to be limited to ILC2s, and has been shown to negatively regulate them in the context of helminth infection, obesity and cancer (Moral et al., 2020, Taylor et al., 2017, Oldenhove et al., 2018). The full extent to which other ILC subsets are capable of expressing PD-1 and whether PD-1 may regulate ILC1s and ILC3s is yet to be determined. In human decidua tissue, PD-1 expression reduces from the first trimester of pregnancy to third in ILC3s, conversely, NK cell expression of PD-1 in human decidua increases throughout pregnancy (Vacca et al., 2019). This is indicative that PD-1 expression in ILC subsets may be driven by components in the tissue microenvironment in a subset specific manner. Consistent with this, murine expression of PD-1 on ILC2s is upregulated upon IL-33 stimulation (Helou et al., 2020, Moral et al., 2020), however endogenous expression in the absence of stimulation is yet to be determined in all ILC subsets. This chapter sought to assess PD-1 expression in across ILC subsets. It was first required to characterise the mice used within the project in order to ensure ILCs distribution is consistent with what has previously been reported in the literature in strains used throughout the study. PD-1 expression was then assessed across all ILC subsets in various tissues. The project focuses on whether PD-1 on ILC subsets maybe a desirable target in order to enhance anti-cancer therapies therefore determining which subsets and in which tissues PD-1 expression occurs is critical for correctly targeting therapies.

3.2 Aims

To determine the importance of PD-1 regulation of ILCs in tumour, it was first important to establish the breadth of PD-1 expression in ILCs. Here, it was important to address whether, in the absence of stimulation, all ILCs are capable of expressing PD-1. It was also important to determine whether ILC expression is consistent in all tissues, or whether PD-1 expression is tissue and subset specific. This chapter had a particular focus on how the TME may affect PD-1 expression in ILCs.

The aims of this chapter were to:

1. Characterise ILCs in the murine strains and models used throughout this project
2. Identify PD-1 expression in all ILC subsets at mucosal tissues and secondary lymphoid organ.
3. Characterise the TME for the presence of ILC subsets
4. Assess PD-1 expression on the ILCs present within the TME

3.3 Results

3.3.1. Characterisation of Innate lymphoid cell subsets in mucosal tissue

To study ILC biology, ILCs were first characterised in both wildtype and *Rag*$^{-/-}$ mice; two strains which will be used throughout the project. Characterisation of these strains will ensure all subsets are identifiable and ILC distribution is consistent with previously reported data. Discrepancies in ILC subsets have been reported in *Rag*$^{-/-}$ mice, whereby in the absence of an adaptive immune system, there was a significant increase in ILC2 and ILC3s, which was also coupled within an increase in cytokine production (Sawa et al., 2011, Roediger et al., 2013, Korn et al., 2014, Van Gool et al., 2014). *Rag*$^{-/-}$ mice were characterised here to ensure the same results were being reported in this study and to ensure this is addressed in future data (Figure 3.1).

ILCs are a tissue resident subset of cells which are primarily located at mucosal barrier surfaces. ILC1 are enriched in the intestine and liver, whereas ILC2s are primarily associated with the lung. ILC3s play an important role in intestinal homeostasis and therefore are predominantly located within intestinal tissue (Dutton et al., 2017, Robinette et al., 2015). In light of this, liver, lung, small intestine and large intestine were isolated from wildtype mice, in addition to spleen as a secondary lymphoid organ. Single cell suspensions were created and ILC subsets were identified using flow cytometry analysis. Live cells were first identified with the use of Live/Dead stain which stains amine groups. In dead cells where cell membrane is not intact, the stain is able to target free amines within the cell and produces an intense fluorescent stain. In live cells, although cell surface amines are still stained but at a much lower intensity, thus live cells can be separated from dead cells. ILCs were identified by the lack of lineage markers which include markers for T cells, B cells, monocytes, macrophages and other immune subsets. ILC1 and ILC3 were distinguished based on the expression of RORγt and NKp46. ILC1s were defined as RORγt^{-}Nkp46^{+}. In order to exclude NK cells, the lineage cocktail also included NK1.1 and CD49b, meaning that ILC1s were ultimately defined as Nkp46^{+}RORγt^{-}NK1.1^{-} CD49b^{-}. ILC3s were defined as RORγt^{+} and were then sub divided into NCR^{+} (Nkp46^{+}) and NCR^{-} (Nkp46^{-}). ILC2s were defined as CD25^{+}CD127^{+} and then further subdivided based on their expression of KLRG1 and IL-33 receptor ST2 into nILC2s (ST2^{+}), iILC2s (KLRG1^{+}) and mature ILC2s (ST2^{+}KLRG1^{+}) (Figure 3.1A-C). Consistent with previously reported data, all ILC subsets were identified in all isolated tissues. ILC2s were predominantly located in the lung and intestine, as were ILC3s (Figure 3.1D-F). Group 1 ILCs were predominantly present

within the liver. In summary, all subsets were able to be identified in all of the mucosal tissues, and subset distribution replicated previously reported literature within the barrier tissues (Dutton et al., 2017).

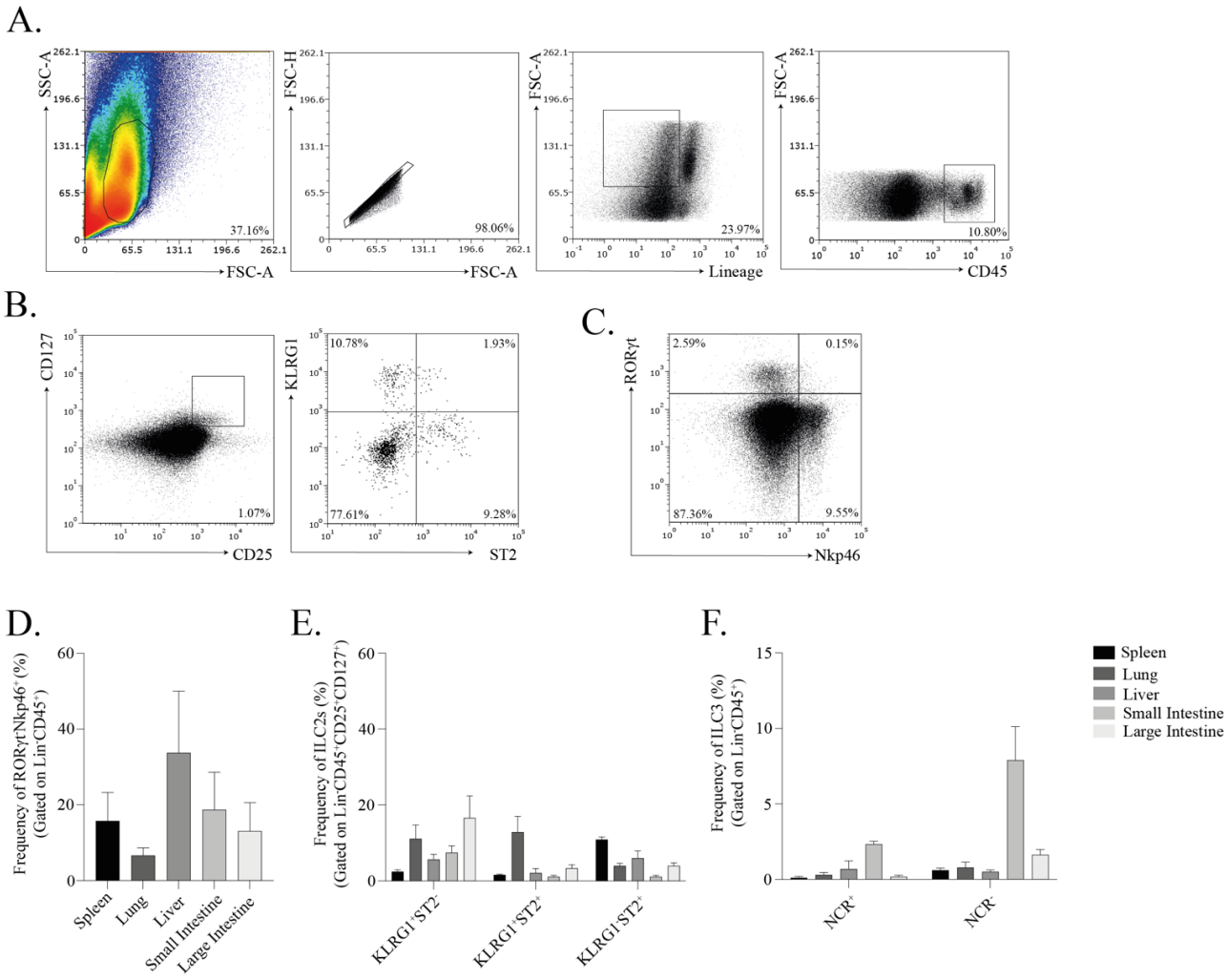

Figure 3.1: **ILC Characterization in Wildtype Mice:**Innate lymphoid cells (ILCs) were isolated from spleen, lung, liver, small intestine and large intestine. Cells were then analysed by flow cytometry in order to identify ILC populations. ILC's were defined as: $Lin^{-}CD45^{+}$. Representative analysis of small intestine shown (A). ILC2s were defined as $CD25^{+}CD127^{+}$ and identified as 3 separate subsets: nILC2 ($ST2^{+}$); mILC2s ($KLRG1^{+}ST2^{+}$) and iILC2 ($KLRG1^{+}$) (representative plots from small intestine shown in B. ILC1s were defined as $ROR\gamma t^{-}NKp46^{+}$ (C). ILC3s were sub divided into NCR^{+} ($NKp46^{+}ROR\gamma t^{+}$) and NCR^{-} ($NKp46^{-}ROR\gamma t^{+}$) (C). Summary of ILC frequencies in all organs of ILC1s (D), ILC2 subsets (E) and ILC3 subsets (F). N=5. Data shown as Mean ± SEM.

ILCs are a key component in the innate immune system and play a role as the first responders to infection however as they mirror T cells subsets so closely, it can be difficult to isolate the role that ILCs play from the role of T cells and the adaptive immune system. In order to address this, *Rag*$^{-/-}$ mice, which lack an adaptive immune system, were used in order to eliminate the contribution of T and B cells in later experiments. ILC subsets were characterised within the barrier tissues of the *Rag*$^{-/-}$ mice in order to identify any phenotypic differences in ILC distribution which may arise in the absence of T and B cells, and which may need to be considered with future data when comparing models.

As with the wildtype mice, spleen, liver, lung, small intestine and large intestine were isolated from *Rag*$^{-/-}$ mice and evaluated as before by flow cytometry (Figure 3.2A-F). Although ILC subsets followed the same patterns as they did in the wildtype mice in tissue distribution, there was a significant increase in KLRG1^{+} iILC2s within the lung in *Rag*$^{-/-}$ compared with wildtype mice ($p=0.03$; Figure 3.2h). An increase was also noted in the liver with KLRG1^{+}ST2^{+} mILC2s ($p=0.0007$; Figure 3.2i) and within the liver, small intestine and large intestine in ST2^{+} nILC2s ($p<0.0001$, $p=0.025$ and $p=0.004$ respectively; Figure 3.2j). Similarly, there was a trend to suggest an increase was observed within NCR^{+} ILC3s however this was not shown to be significant (Figure 3.2k and 3.2l).

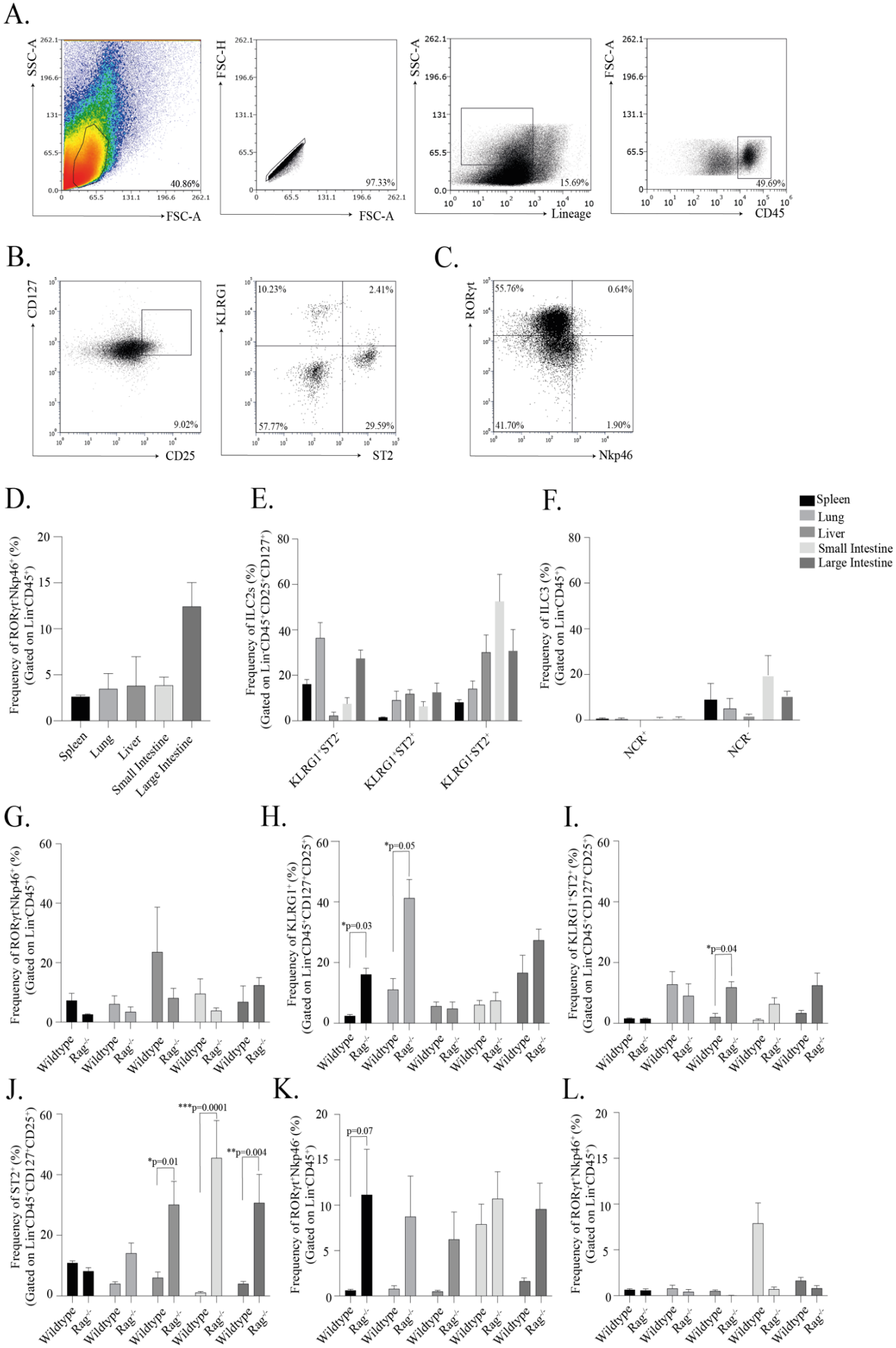
A.
SSC-A
FSC-A
40.86%
FSC-H
97.33%
15.69%
Lineage
49.69%
CD45
B.
CD127
CD25
9.02%
KLRG1
ST2
10.23%
2.41%
57.77%
29.59%
C.
RORγt
Nkp46
55.76%
0.64%
41.70%
1.90%
D.
Frequency of RORγt+Nkp46+ (%) (Gated on Lin-CD45+)
Spleen
Lung
Liver
Small Intestine
Large Intestine
E.
Frequency of ILC2s (%) (Gated on Lin-CD45+CD25+CD127+)
KLRG1+ST2-
KLRG1+ST2+
KLRG1-ST2+
F.
Frequency of ILC3 (%) (Gated on Lin-CD45+)
NCR+
NCR-
Spleen
Lung
Liver
Small Intestine
Large Intestine
G.
Frequency of RORγt+Nkp46+ (%) (Gated on Lin-CD45+)
H.
Frequency of KLRG1+ (%) (Gated on Lin-CD45+CD127+CD25+)
*p=0.03
*p=0.05
I.
Frequency of KLRG1+ST2+ (%) (Gated on Lin-CD45+CD127+CD25+)
*p=0.04
J.
Frequency of ST2+ (%) (Gated on Lin-CD45+CD127+CD25+)
*p=0.01
***p=0.0001
**p=0.004
K.
Frequency of RORγt+Nkp46- (%) (Gated on Lin-CD45+)
p=0.07
L.
Frequency of RORγt+Nkp46+ (%) (Gated on Lin-CD45+)
Wildtype
Rag-/-

Figure 3.2: **ILC Characterisation in Rag$^{-/-}$ Mice.** Innate lymphoid cells (ILCs) were isolated from spleen, lung, liver, small intestine and large intestine. Cells were then analysed by flow cytometry in order to identify ILC populations. ILC's were defined as: Lin^{-}CD45^{+}. Representative analysis of small intestine shown (A). ILC2s were defined as CD25^{+}CD127^{+} and identified as 3 separate subsets: nILC2s (ST2^{+}); mILC2 (KLRG1^{+}ST2^{+}) and iILC2 (KLRG1^{+}) (representative plots from small intestine shown in B). ILC1s were defined as RORγt^{-}Nkp46^{+} (C). ILC3s were sub divided into NCR^{+} (Nkp46^{+}RORγt^{+}) and NCR^{-} (Nkp46^{-} RORγt^{+}) (C). Summary of ILC1 (D), ILC2 subsets (E) and ILC3 subsets (F) shown. Comparison of ILC subset frequency in wildtype versus Rag$^{-/-}$ mice in ILC1 (G), iILC2s (KLRG1^{+}) (H), mILC2s (KLRG1^{+}ST2^{+}) (I), nILC2s (ST2^{+}) (J), NCR^{-} ILC3s (K) and NCR^{+} ILC3s (L). Data shown as Mean ± SEM; N=5.

3.3.2. ILCs express PD-1 in a tissue dependent manner

In human decidua tissue, PD-1 expression in ILC3s is significantly reduced throughout pregnancy suggesting that specific tissue environmental factors may influence PD-1 expression (Vacca et al., 2019). ILCs have been shown to be present in mucosal tissue therefore PD-1 expression was next assessed. There were two questions that needed to be addressed: a) are all ILC subsets capable of expressing PD-1 and b) is PD-1 expression influenced by the tissue microenvironment. To determine this, PD-1 expression was evaluated in ILCs in wildtype mice at the barrier surfaces shown before. All ILC subsets were shown to be capable of expressing PD-1 in the absence of external stimulation (Figure 3.3A-G). Of note, in Nkp46^{+}RORγt^{-} ILC1 cells, PD-1 expression was significantly increased in the liver when compared with the lung ($p=0.03$) and the spleen ($p=0.04$; Figure 3.3B). Within the ILC2s subsets, there was a significant increase in PD-1 expression in KLRG1^{+} iILC2s within the large intestine compared with spleen ($p=0.001$), lung ($p=0.01$), liver ($p=0.004$) and small intestine ($p=0.02$) (Figure 3.3C). Other ILC2 subsets, however, did not show the same variation, with only KLRG1^{+}ST2^{+} mILC2s showing an increase in PD-1 expression in the large intestine when compared with the spleen ($p=0.03$; Figure 3.3D) with no significant changes observed in ST2^{+}KLRG1^{-} nILC2s (Figure 3.3E). Within the ILC3 subsets, although cells were shown to express PD-1 in all tissues, no significant difference was noted in expression in different tissues within the ILC3 subsets (Figure 3.3F and 3.3G). This suggests that PD-1 expression is not only tissue specific, but also varied by subset and tissue induction. This is consistent with human data shown by Tumino et al who demonstrated diminished PD-1 expression in PBMCs compared with human breast cancer tumour tissues in group 2 ILCS (Tumino et al., 2019).

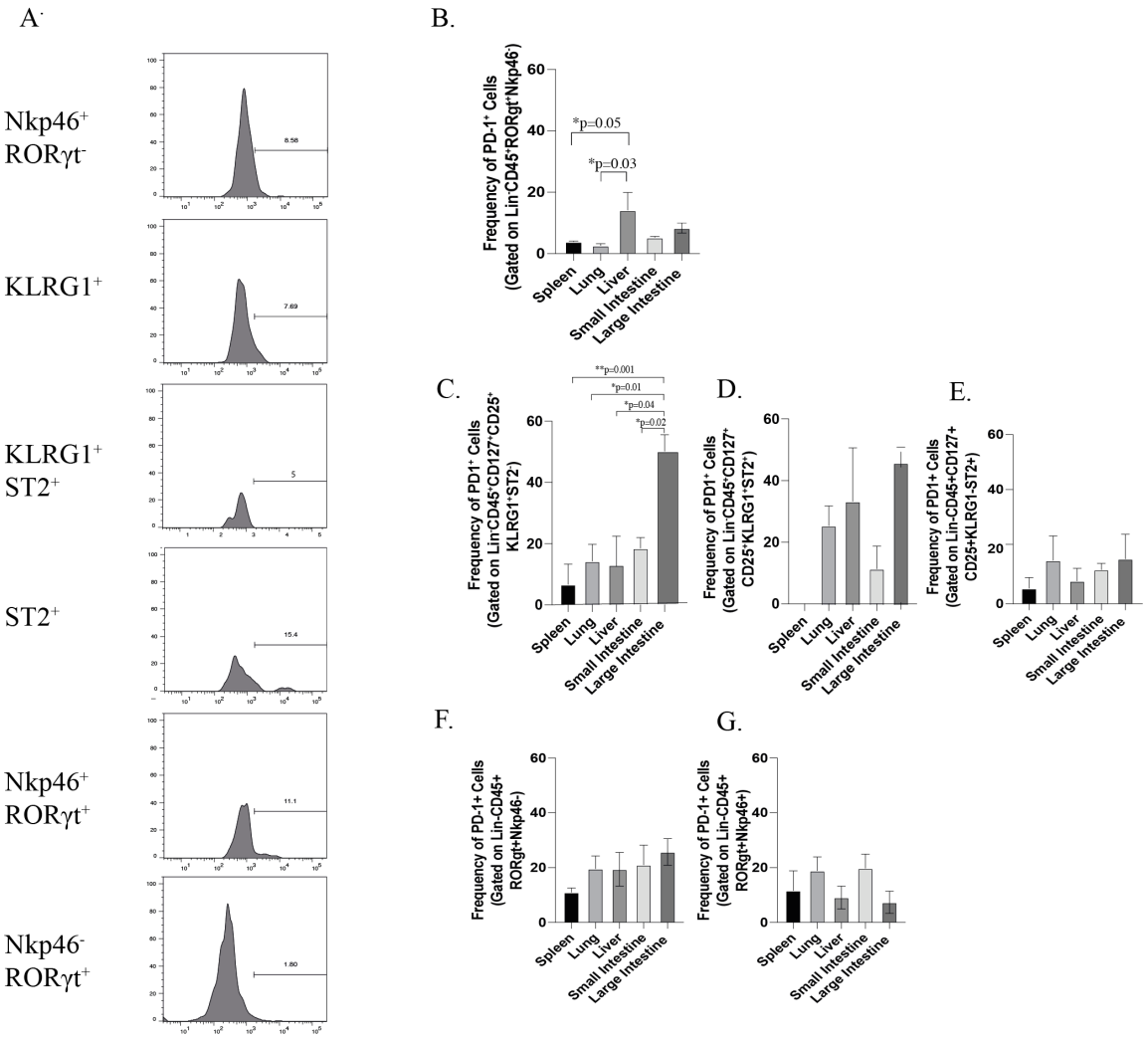

Figure 3.3: PD-1 expression in ILCs is tissue specific. Spleen, lung, liver, small intestine and large intestine were harvested from C57 Bl6 wildtype mice. ILCs were isolated from organs and identified by flow cytometry. ILCs were defined as: Lin^- (Lineage consists of CD3, CD5, CD8, CD11b, CD11c, CD19, CD49b, Gr1, Ter119, NK1.1, B220 and F4/80) $CD45^+$. Representative flow plots showing PD-1 expression in ILC subsets (A). Summary of PD-1 expression in ILC1 ($Nkp46^+ROR\gamma t^-$) (B), ILC2 subsets: iILC2s ($KLRG1^+$)(C), mILC2s ($KLRG1^+ST2^+$) (D) and nILC2 ($ST2^+$) (E) and ILC3 subsets; NCR^+ (F) and NCR^- (G). Data shown as mean +/- SEM; N=4-5

It was previously shown that *Rag*$^{-/-}$ show increases in some ILC subsets in comparison with the wildtype mice (Figure 3.2). As a result of having an increase in ILCs subsets, *Rag*$^{-/-}$ have shown to have an increase in type 2 and 3 cytokines (Sawa et al., 2011, Roediger et al., 2013, Korn et al., 2014, Van Gool et al., 2014). Figure 3.3 suggests that PD-1 is tissue specific and therefore maybe driven by the tissue microenvironment. It was, therefore, important to determine whether PD-1 expression was affected by the absence of an adaptive immune system and subsequent changes in the tissue microenvironment which is particularly important to determine as it could be important when interpreting the results when *Rag*$^{-/-}$ are treated with αPD-1 therapy. However, no significant differences in PD-1 expression were observed in *Rag*$^{-/-}$ compared with wildtype mice (Figure 3.4). PD-1 expression in ILCs does not appear to be driven by the adaptive immune system and is, instead, driven by environmental factors within the tissue. Varying levels of PD-1 expression indicates that ILCs may be responsive to αPD-1 therapies at different efficacies in different tissues. In light of this, it is important to understand how the distinct environment of the TME may drive PD-1 expression in ILCs.

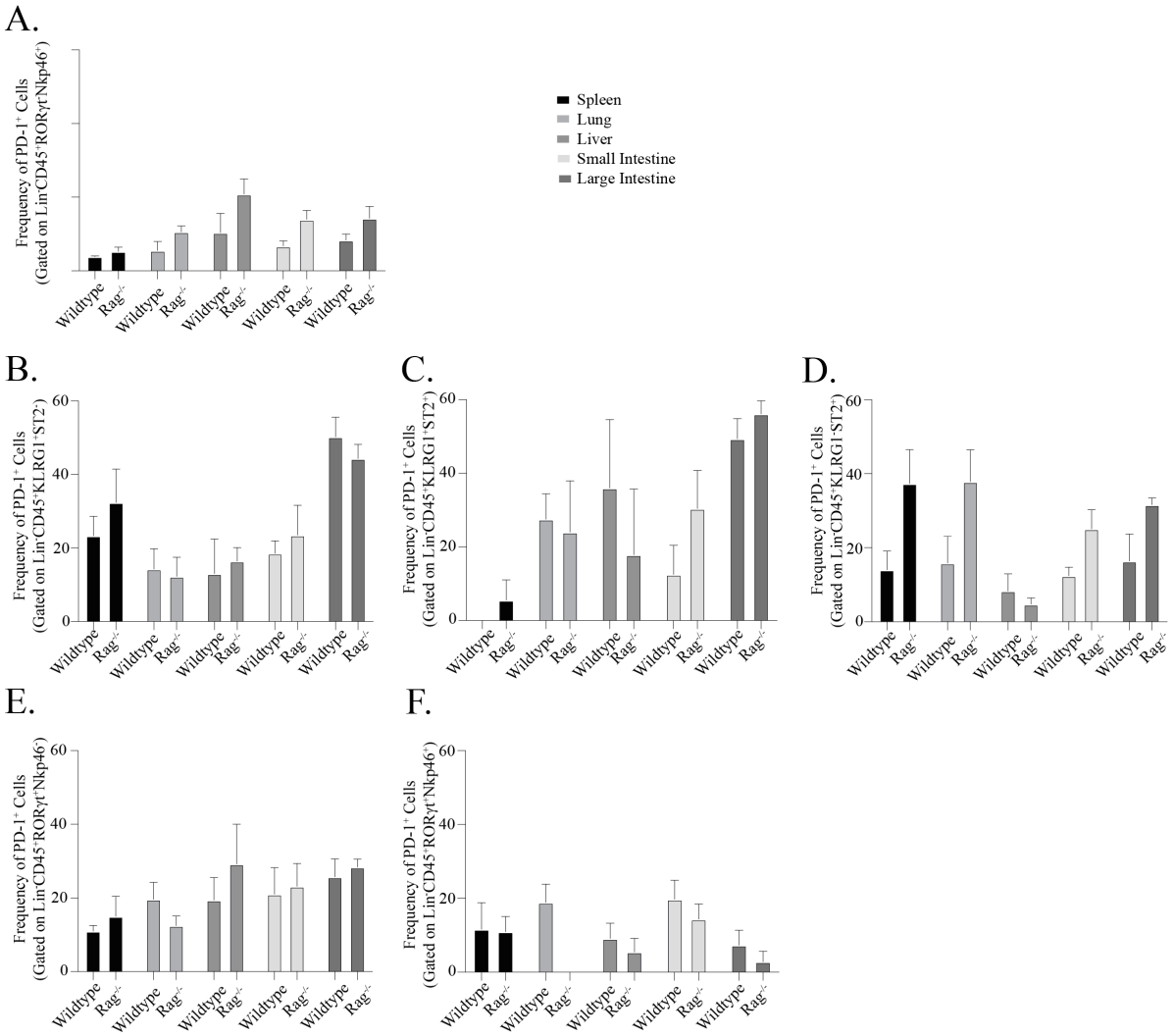

Figure 3.4: PD-1 expression does not differ in the absence of an adaptive immune system. Spleen, lung, liver, small intestine and large intestine were harvested from C57 Bl6 wildtype mice and $Rag^{-/-}$ mice. ILCs were isolated from organs and identified by flow cytometry. ILC's were defined as: Lin^{-} $CD45^{+}$. Summary of PD-1 expression in wildtype and $Rag^{-/-}$ mice shown in ILC1 ($ROR\gamma t^{-}NKp46^{+}$) (A), iILC2 ($CD127^{+}CD25^{+}KLRG1^{+}$) (B), mILC2 ($CD127^{+}CD25^{+}KLRG1^{+}ST2^{+}$)(C), nILC2 ($CD127^{+}CD25^{+}ST2^{+}$) (D), NCR^{-} ILC3s ($ROR\gamma t^{+}NKp46^{-}$; E) and NCR^{+} ILC3s ($ROR\gamma t^{+}NKp46^{+}$; F). Data shown as Mean ± SEM. N=4-5.

3.3.3. Characterisation of ILCs within the melanoma TME

To determine if and how PD-1 drives ILCs in within the TME, it was first important to determine which ILC subsets were present within the TME in our model of B16 melanoma. All ILC subtypes have been shown to be present in human breast and gastrointestinal cancer tissues (Salimi et al., 2018), therefore to ensure that the model used in this project was viable, ILC subsets needed to be identified within the TME. To assess this, wildtype mice were inoculated with B16 F10 melanoma via subcutaneous injection. Tumour tissue was harvested on day 12 post inoculation and tumour infiltrating lymphocytes (TILs) were isolated. ILCs were identified by flow cytometry as described in wildtype (Figure 3.5.A). Characterisation showed that all ILC subsets were present within the TME in the murine melanoma model. TbetZsGreen reported mice were used for this experiment and therefore ILC1 subset could be identified by their expression of Tbet ($Tbet^{+}Nkp46^{+}ROR\gamma t^{-}$). ILC2s were grouped into a single population ($CD127^{+}CD25^{+}$) due to low frequency of individual subsets. The predominant subset of the TME was an ILC subset of this microenvironment was identified as $Tbet^{+}ROR\gamma t^{-}Nkp46^{+}$ ILC1s ($CD127^{+}CD25^{+}$ $p=0.01$; NCR^{+} $p<0.0001$; NCR^{-} $p= 0.0001$) (Figure 3.5.A and B).

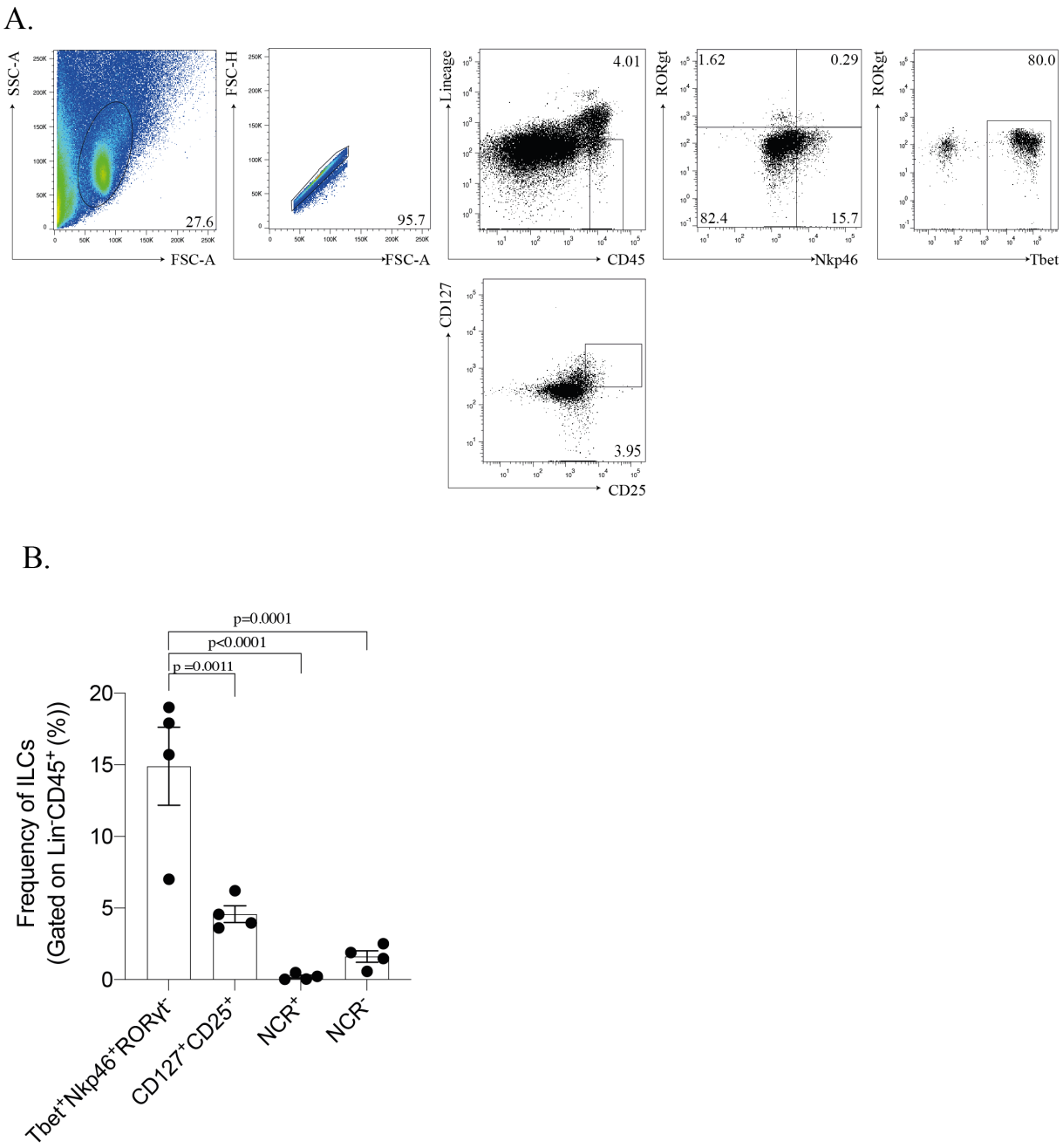

Figure 3.5: ILC Characterisation in the TME. TbetZsGreen mice were inoculated with B16 F10 melanoma via subcutaneous injection into the right flank. 12 days post inoculation, tumor tissue and non-involved skin was harvested, and cells were isolated. ILCs were identified by flow cytometry as $Lin^{-}CD45^{+}$ where Lineage is defined as CD3, CD5, CD8, CD11b, CD11c, CD19, CD49b, Ter119, F4/80, B220, NK1.1 and Gr1. Representative gating strategy of ILCs in the TME (A). Summary of ILC subsets within the tumor microenvironment (B), Data shown as Mean +/- SEM; n=4.

3.3.4 PD-1 expression in ILCs is induced in the TME.

PD-1 expression on ILCs is variable between tissue and microenvironments. The TME is a niche environment which is extremely inflammatory and, therefore, if PD-1 expression in ILCs is driven by the microenvironment, it is important to establish how this environment may alter PD-1 expression on ILC subsets as this could indicate potential targetability of ILCs within the TME. As before, mice were inoculated with B16 melanoma cells via subcutaneous injection and tumour tissue and non-involved skin was harvested as a comparison on day 12 post inoculation. ILC subsets and PD-1 expression were evaluated by flow cytometry. ILC1 ($Tbet^+Nkp46^+ROR\gamma t^-$) cells had significantly increased levels of PD-1 expression in the tumour when compared with non-involved skin (p=0.003; Figure 3.6B). An increase in PD-1 expression in ILC2s was also noted within the tumour (p=0.004; Figure 3.6C). Neither NCR^+ nor NCR^- ILC3s demonstrated any changes in PD-1 expression within the tumour (Figure 3.6D and E).

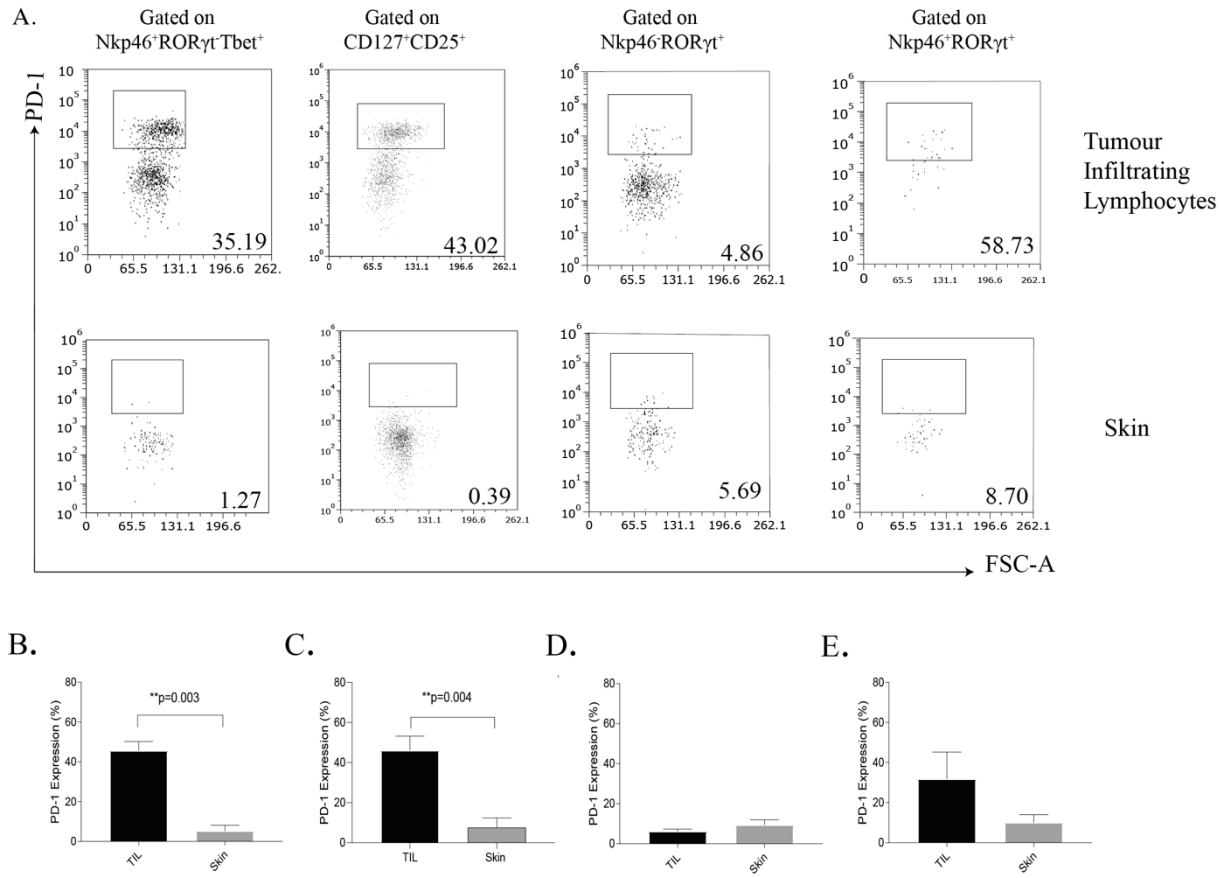

Figure 3.6: PD-1 expression is increased in the TME. TbetZsGreen mice were inoculated with B16 F10 melanoma via subcutaneous injection into the right flank. 12 days post inoculation, tumor tissue and non-involved skin was harvested, and cells were isolated. ILCs were identified by flow cytometry and PD-1 expression was evaluated into each of the subsets. ILCs were defined as Lineage$^-$CD45$^+$ where Lineage was defined as CD3, DC5, CD8, CD11b, CD11c, CD19, CD49b, F4/80, Ter119, Gr1 and NK1.1. Representative flow plots showing PD-1 expression in ILC subsets in skin and TILs (A) and summary of PD-1 expression shown in ILC1s (Tbet$^+$Nkp46$^+$RORγt$^-$) (B), ILC2s (CD127$^+$CD25$^+$) (C), NCR$^+$ ILC3s (Nkp46$^+$RORγt$^+$) (D) and NCR$^-$ (Nkp46$^-$RORγt$^+$) (E) ILC subsets. Data shown as Mean +/- SEM; N=4.

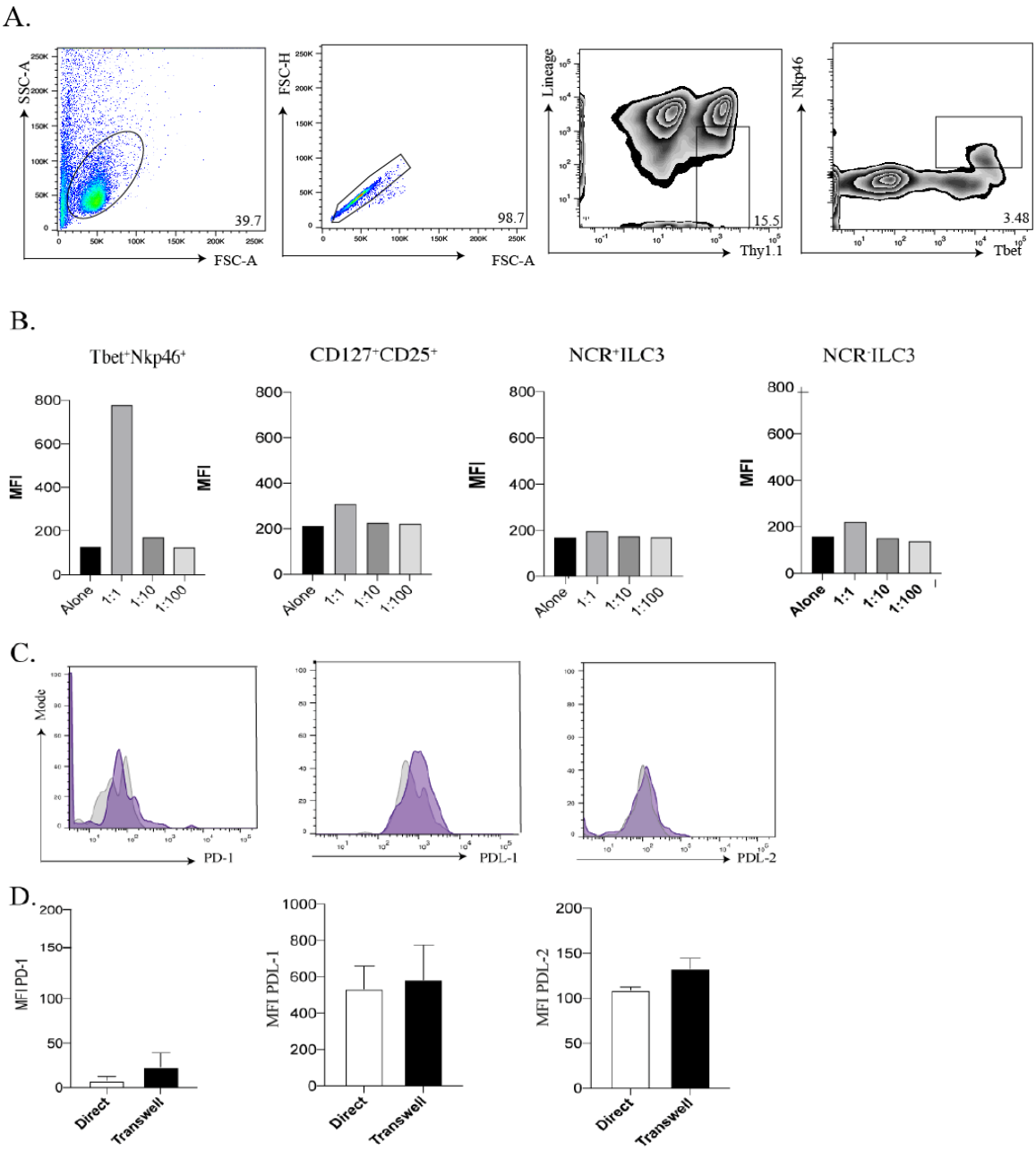

Figure 3.7: PD-1 expression is induced by the tumour secretome. Wildtype spleen cells were isolated and incubated with RBC lysis buffer as per methods. B16F10 melanoma cells were seeded in transwells and incubated for 4 hours at the indicated ratios. PD-1 expression was assessed by flow cytometry analysis. ILCs were gated on Lin$^-$CD45$^+$. Flow cytometry plots shown (A) and summary of PD-1 mean fluorescent intensity (MFI) shown in ILC1 (Tbet$^+$NKp46$^+$), ILC2 (CD127$^+$CD25$^+$), NCR$^+$ ILC3s (RORγt$^+$NKp46$^+$) and NCR$^-$ ILC3s (RORγt$^+$Nkp46$^-$) n=1.Wildtype splenocytes were incubated with B16 melanoma cells in in transwell or direct contact at a 1:1 ratio for 4hours for 37^{o}C. PD-1 expression was evaluated on Tbet$^+$NKp46$^+$ cells. Representative plots showing PD-1, PDL-1 and PDL-2 expression (C) and summary of expression shown (D). Data shown as mean +/- SEM; n=2

3.3.5 Tumour secretome drives PD-1 expression in ILCs

Moral et al demonstrated PD-1 expression in ILC2s is driven by IL-33 in the TME (Moral et al., 2020). This suggests that maybe PD-1 expression, like in T cells, is upregulated in response to activation in ILCs. Transwell cultures were used to determine whether tumour cells need to be in direct contact with ILCs in order to induce PD-1 expression. Spleens were harvested from TbetZsGreen mice. Splenocytes were isolated and then cultured with transwells seeded with B16 melanoma cells. Tumour cells were first seeded at various ratios to determine the optimum ratio for maximal PD-1 expression (Figure 3.7A and B). This, not only showed that PD-1 expression was induced in the absence of direct contact with B16 melanoma cells, it also demonstrated that 1:1 ratio with splenocytes was optimal for PD-1 expression in all ILC subsets. In line with this, splenocytes were then cultured at a 1:1 ratio with melanoma cells, either alone or in transwells at 37ºC for 4 hours. PD-1 expression was shown to increase with transwell incubation and upon stimulation with tumour secretome (Figure 3.7 C and D). Data also suggests that PDL-2 expression may also be increased by the tumour secretome however data suggests no changes in PDL-1 expression (Figure 3.7C and D).

3.4.Discussion

This chapter was focused on characterising the murine strains which would be used throughout the rest of the project. Furthermore, this chapter sought to determine PD-1 expression on ILC subsets both in mucosal tissues and within the TME. Within our mouse model it was important to ensure that ILC subset distribution was consistent with previously reported literature. As shown here, ILC distribution was consistent to that report by Dutton et al., whereby ILC2s were predominantly located within the lung and intestine (Dutton et al., 2017). Here it was also demonstrated that group 1 like ILCs were also predominantly located in the liver in comparison with other tissues, which has previously been demonstrated by Robinette *et al*.(Robinette et al., 2017). In the *Rag*$^{-/-}$ there was an observed increase in ILC subsets in tissue when compared with the wildtype mice shown in ILC2s. *Rag*$^{-/-}$ mice have increase serum circulating levels of IL-7 due to the absence of T cells which normally limit the availability of IL-7 (Guimond et al., 2009). IL-7 is important for ILC development and fate decision, therefore an increase in serum IL-7 in the absence of an adaptive immune system has been shown to specifically increases ILC2 and ILC3 subsets (Korn et al., 2014, Van Gool et al., 2014, Roediger et al., 2013, Sawa et al., 2011). Here, only an increase in ILC2 subsets were noted in the *Rag*$^{-/-}$. The discrepancy in results here compared with the literature could be due to differences in the cell markers used for identifying ILC3s in humans. Previously they were described as RORγt^{+} whereas here individual subsets have been identified. Although there is a trend to suggest an increase in NCR^{-} cells within all tissues, it is likely that due to the biological variation between some samples that this was not noted to be significant. Specifically, an increase in KLRG1^{+} cells was seen within the lung tissue The literature has previously focused purely on an increase in GATA3^{+}ILC2s whereas here, as with the ILC3 subsets, ILC2s have been further divided into individual subsets. The differences between *Rag*$^{-/-}$ and wildtype mice were important to note, as alterations in ILC subsets result in changes in cytokine levels within the tissue microenvironment which may be important to consider in subsequent experiments. Data within this chapter, and throughout the project, from the tumour tissue has been represented as frequency and data regarding cell number in the tumour tissue has not been demonstrated. For analysis of spleen and lymph nodes, whole tissues were isolated and analysed so there was an assumption of consistency between tissues. One downside of analysing tumour tissue, is that tumour development is irregular and can vary vastly between animals. As a result of this, quantification of cell counts would be inconsistent and therefore may show inaccurate trends.

PD-1 expression was identified in all ILC subsets. Previously, in mouse, expression has only been identified on ILC2s with Taylor et al showing no significant difference in PD-1 expression in KLRG1$^+$ ILC2s within the skin, small intestine and lung (Taylor et al., 2017). These results were replicated here, however here it was also shown that PD-1 expression in KLRG1$^+$ ILC2s was significantly increased in large intestine compared with the other organs. There was also a significant increase noted in ILC1 subset within the liver. This suggests that PD-1 expression is strongly influenced by the tissue microenvironment which is consistent with the previous study by Vacca et al (Vacca et al., 2019).

It was then demonstrated that the TME specifically drives PD-1 expression in Tbet$^+$RORγt$^-$ Nkp46$^+$ ILC1s and ILC2s when compared with the same subsets from non-involved skin. Tbet$^+$Nkp46$^+$RORγt$^-$ ILC1s were identified as the predominant ILC subset within our model of melanoma, and since this is the subset identified to have the biggest increase in PD-1 expression, it is a positive indication that these cells may adequately respond to αPD-1 therapy. By demonstrating that PD-1 is upregulated on Tbet$^+$RORγt$^-$Nkp46$^+$ILC1s and ILC2s, it suggests that regulation of PD-1 in each tissue is specific to each ILC subset which may be dependent on the cytokines or stimuli available at the time. This replicated what was shown in human breast cancer, whereby PD-1 expression was increased in ILC2s in breast cancer tumours when compared with ILC2s derived from patient PBMCs (Salimi et al., 2018). In both this project and the study by Salimi et al, PD-1 expression was induced in the absence of exogenous stimuli. This is in contrast to Moral et al, who showed in a murine model of pancreatic cancer, IL-33 was needed to induce PD-1 expression within the TME. Here, I have demonstrated that in the absence of exogenous stimuli, ILC subsets are still able to upregulate PD-1 expression within the TME when compared with other tissues. Upon further examination using transwell experiments, PD-1 expression was able to be induced in Tbet$^+$Nkp46$^+$RORγt$^-$ ILC1s by the tumour secretome alone, and there was no requirement for direct contact between the tumour cells and the ILCs.

The data in the chapter has demonstrated that all ILCs are capable of expressing PD-1, which appears to be in a tissue dependent manner. Of note, all ILCs have been identified within the TME within our murine model of melanoma, with the predominant subset being Tbet$^+$RORγt$^-$ NKp46$^+$ ILC1s. PD-1 expression was significantly increased within the TME in this subset which suggests that this subset may be responsive to therapeutic blockade of PD-1 and provides the basis for investigation in subsequent chapters.

3.5. Conclusions

In conclusion this chapter showed that:

- All ILC subsets were present in all tissues and distribution in mice strains used in this study were consistent with previously shown literature.
- All ILC subsets were able to express PD-1 in the absence of any exogenous additionally stimuli and this expression was shown, in NKp46^{+}RORγt^{-} ILC1s and KLRG1^{+} iILC2s to occur in a tissue dependent manner.
- ILCs were still able to express the same levels of PD-1 in the absence of an adaptive immune system suggesting that the main driver of PD-1 expression on ILCs is environmental factors within selective tissues.
- All ILC subsets were shown to be present within the TME in the murine model of melanoma.
- Specifically, Tbet^{+}Nkp46^{+}RORγt^{-} ILC1s and ILC2s had significantly increased PD-1 expression within the TME.
- The tumour secretome alone was capable of inducing PD-1 expression in ILCs, particularly in Tbet^{+}Nkp46^{+} ILC1s.

Chapter 4: Deficiency in PD-1 increases RORγt^{-}NK1.1^{-}Nkp46^{+} ILC1s within the TME

4.1. Introduction

ILCs are present within the TME in several human cancers including breast cancer and gastrointestinal cancer (Salimi et al., 2018, Tumino et al., 2019). The role of ILCs within mouse are ambiguous with studies showing a role for ILCs in both promoting tumour development but also providing tumour defence (Gao et al., 2017, Trabanelli et al., 2017, Moral et al., 2020, Wang et al., 2020). In this study it has been demonstrated that all ILC subsets are capable of expressing PD-1 within the TME, and also showing that PD-1, is upregulated within the TME in ILC1 subsets and ILC2s. It is known that ILC2s are negatively regulated by PD-1 in the case of helminth infection however whether the other ILC subsets are capable of being regulated is yet to be determined. Since therapy is only successful in a certain number of patients it highlights lack of knowledge in PD-1 modulation of the immune system. It is important to define how PD-1 may modulate ILCs to better understand why some patients may not respond to anti-PD-1 immunotherapy in the clinic. If PD-1 does in fact negatively regulate ILCs within the TME, and therefore blockade would increase ILC subsets, it is unclear whether this would in fact be beneficial or detrimental.

4.2. Aims:

The aims of this chapter are to:

1. Determine whether, in the absence of PD-1, ILCs are able to provide anti-tumour protection
2. Assess whether the absence of PD-1 affects ILC frequency within the TME and secondary lymphoid tissues and whether this affects a specific ILC subset.
3. Determine whether the absence of PD-1 modulates ILC function within the TME
4. Determine whether this modulation is specific to the melanoma model or whether it is replicated within multiple murine models.

4.3. Results

4.3.1. Absence of PD-1 leads to an increase in survival in murine tumour models.

To determine whether PD-1 may regulate ILCs in the context of tumour, it was first required to determine how PD-1 deficiency may affect tumour growth. Wildtype and *Pdcd1*$^{-/-}$ mice were inoculated with B16 melanoma via subcutaneous injection and tumours were allowed to develop. Tumour size was determined based on calculations by Schatton et al (Schatton et al., 2008). Mice were euthanised when they exceeded the maximal size of 1200mm^3. *Pdcd1*$^{-/-}$ showed a significant increase in survival (p=0.01; Figure 4.1A) and a significant decrease in tumour growth (p=0.03; Figure 4.1B-C). To ensure this is not a tumour specific response, wildtype and *Pdcd1*$^{-/-}$ mice were inoculated with 2 x 10^5 MC38 colon cancer cell line. As in the melanoma model, *Pdcd1*$^{-/-}$ mice had significantly increased survival (p=0.05; Figure 4.1D along with a trend to suggest a decrease in tumour growth in the *Pdcd1*$^{-/-}$ mice (p=0.08; Figure 4.1E and F).

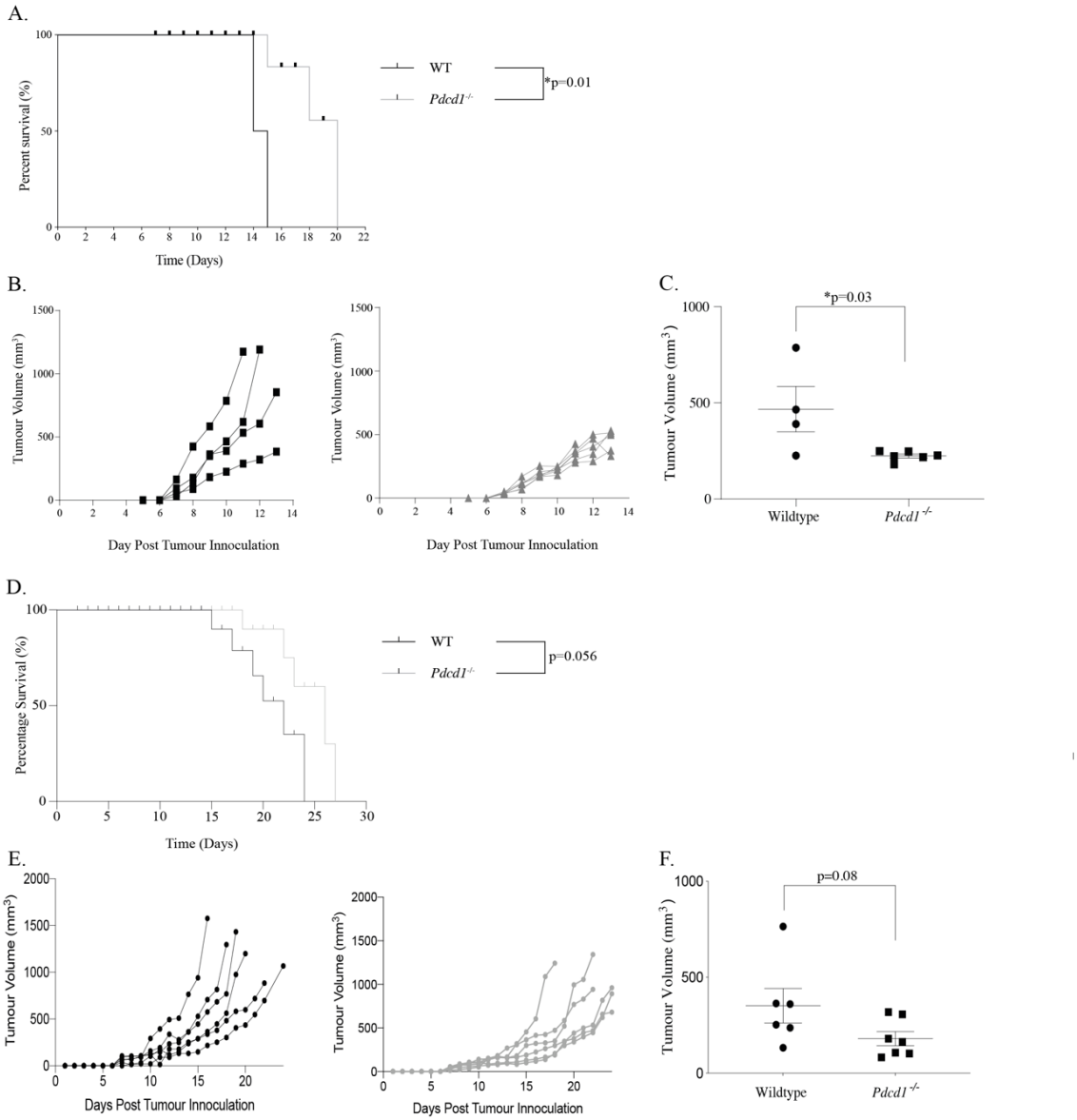

Figure 4.1: Absence of PD-1 protects against tumour growth. Wildtype and *Pdcd1*$^{-/-}$ mice were inoculated with 2 x 10^5 B16F10 Melanoma cells via subcutaneous injection. Mice were euthanised when they reached a maximal tumour volume of 1200m^3. Mouse survival shown (A). Tumour volume was calculated using the following equation: (π/6) x 0.5 x Length x Width^2 (Schatton et al). Tumour volume shown in wildtype mice (B;Left panel) and *Pdcd1*$^{-/-}$ mice (B; right panel). Summary of tumour volume on Day 10 post inoculation shown (C). Wildtype and *Pdcd1*$^{-/-}$ were inoculated with 2 x 10^5 MC38 colon cancer cells via subcutaneous injection. Mice were euthanised when the reached a maximum tumor volume of 1200m^3. Mouse survival shown (D). Tumour volume shown in wildtype mice (E; left panel) and in *Pdcd1*$^{-/-}$ (E; right panel). Tumour volume at day 14 post inoculation (F). N=4-6; An unpaired T test was used to determine significance. Data shown as Mean ± SEM

PD-1 is widely known to negatively regulate T and B cells. To ascertain determine whether this protective effect was due to T cells or innate immune cells, *Rag*$^{-/-}$ were inoculated with 2 x 10^5 B16 F10 Melanoma cells via subcutaneous injection. From day 7 post inoculation mice were treated with either αNK1.1 and/or αPD-1 or isotype control on alternate days until mice reached the humane endpoints. No significant difference was noted between the αPD-1 therapy group and αNK1.1 + αPD-1 therapy group (p=0.897; Figure 4.2B) suggesting that NK cells are not required for effective αPD-1 therapy. To ensure that therapy was effective in blocking NK cells and that they were not driving responses, TILs were isolated on day 12 post inoculation and the effectiveness of αNK blockade was assessed (Figure 4.3). Here it showed that NK cells were sufficiently diminished when treated with αNK1.1 blockade showing that they are unable to drive the protection provided in the absence of PD-1 signalling in the mice (Figure 4.3).

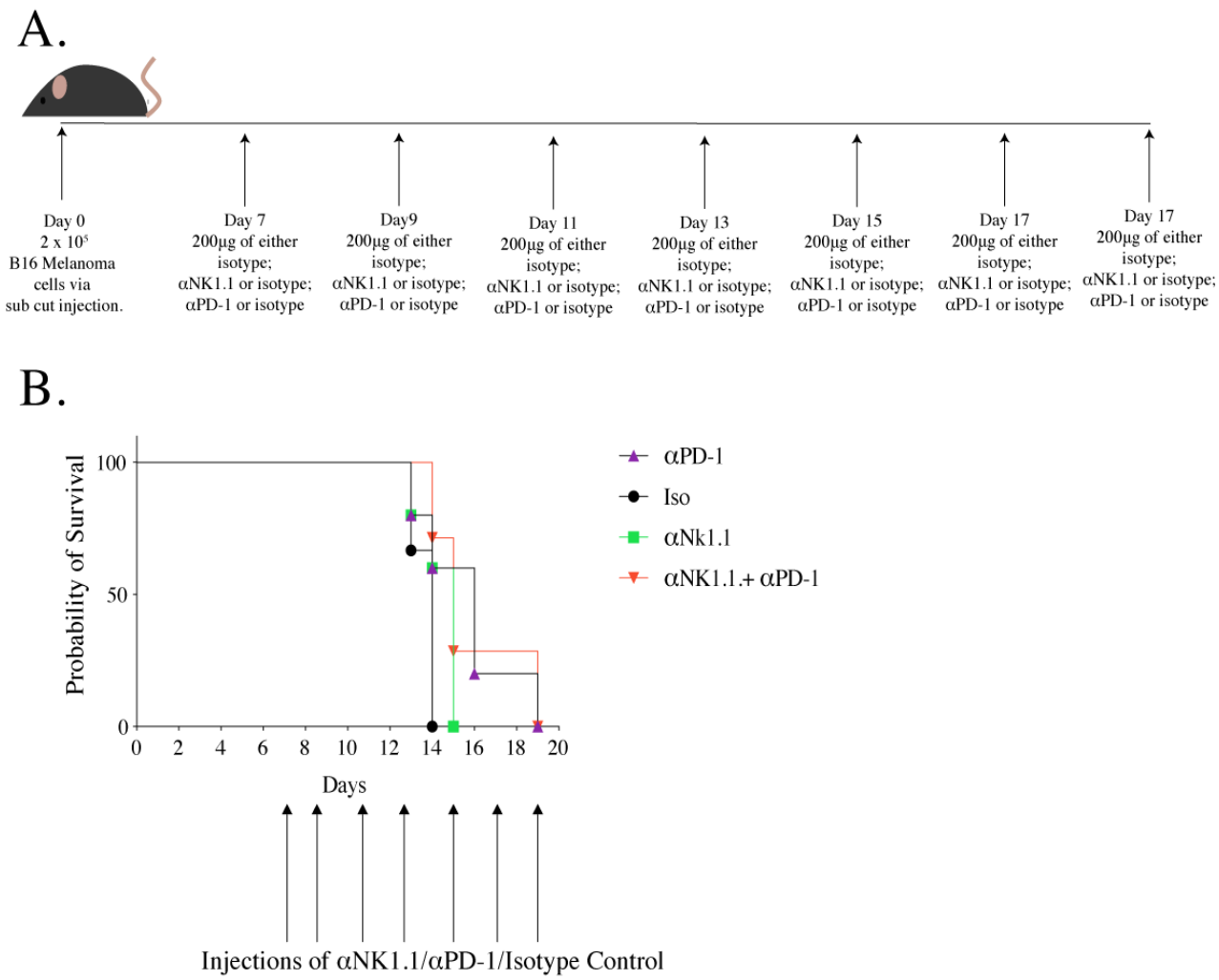

Figure 4.2: Blockade of PD-1 reduces tumour growth in the absence of NK cells and an adaptive immune system. $Rag^{-/-}$ mice were inoculated with 2 x 10^5 B16 F10 melanoma cells via subcutaneous injection. Mice were administered with 200µg of αPD-1 (clone:RPM1-4) or Isotype control (Rat IgG2a; clone: 2A3) and 200µg of αNK1.1 (clone:PK136) or isotype control (mouse IgG1a; clone: C1.18.4) on alternate days from day 7 onwards (A). Mice were euthanised when they reach the humane endpoint of tumour volume of 1200m^3. Mouse survival shown (B).

A.

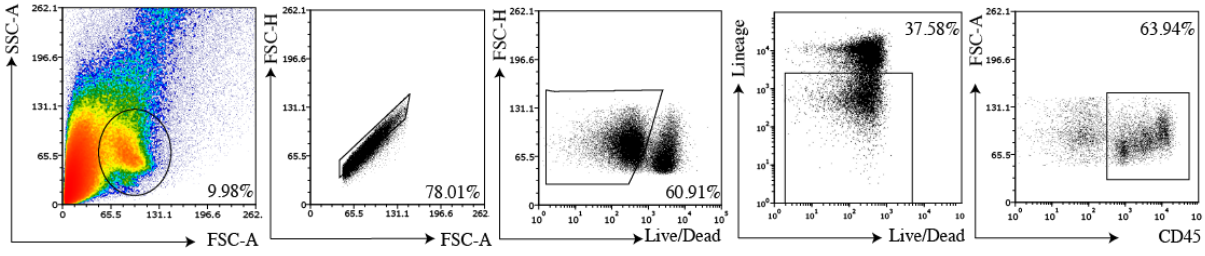

B.

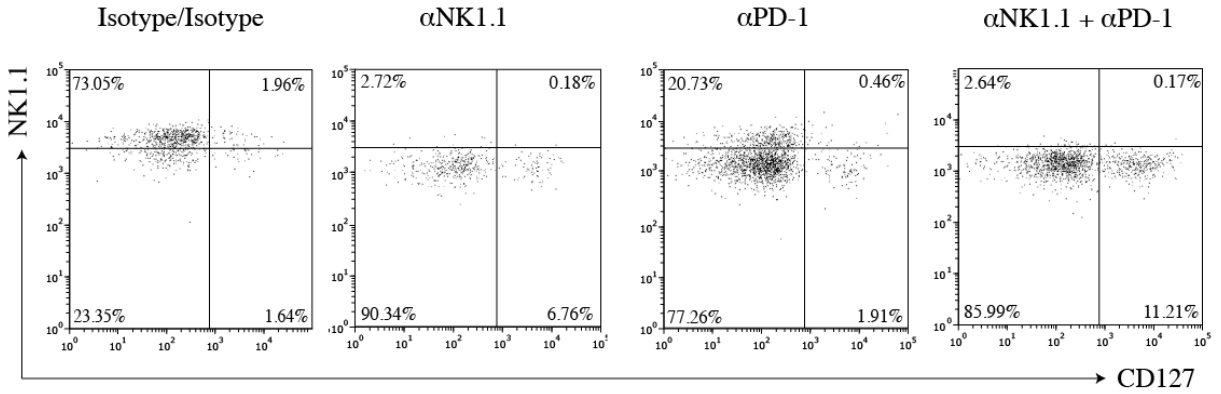

Figure 4. 3. Anti-NK1.1 therapy blocks NK cells. Rag$^{-/-}$ mice were inoculated with 2 x 10^{5} B16 F10 melanoma cells via subcutaneous injection. Mice were administered with 200µg of αPD-1 (clone:RPM1-4) or Isotype control (Rat IgG2a; clone: 2A3) and 200µg of αNK1.1 (clone: PK136) or isotype control (mouse IgG1a; cloneC1.18.4) on alternate days from day 7 onwards. Mice were euthanised on day 12 inoculation and tumour infiltrating lymphocytes were isolated. ILCs were defined as Lin^{-}CD45^{+}. Representative gating strategy shown (A). Representative flow plots showing NK cell populations in mice treated with isotype, αNK1.1, αPD-1 or αNK1.1 and αPD-1 therapy (B).

This suggests that the protective effect of αPD-1 is not driven by NK cells and is in fact driven by other cells of the innate immune system. To establish whether this was specifically driven by ILCs rather than the other immune cells present within the tissue a further experiment was carried out wherein *Rag*$^{-/-}$ mice were administered with 100µg or αCD90.2 in order to deplete ILCs or they were treated with isotype control. Four days later, mice were inoculated with 2 x 10^{5} B16 melanoma via subcutaneous injection. Mice were then administered with αCD90.2 (200µg) and αNK1.1 (200µg) or isotype controls. Mice were euthanised when mice reach the humane endpoints (Figure 4.4A). This treatment regime was altered during the experiment, due to decline in mouse health after initial injection with αCD90.2. Absence of ILCs was still confirmed via flow cytometry. There was no difference in survival noted between any of the

therapy groups (Figure 4.4B) nor was any significant difference noted in tumour growth between the experimental groups (Figure 4.4C).

There was no significant change noted between any of the therapy groups in the absence of ILCs. This suggested that αPD-1 therapy is producing an anti-tumour response through the modulation of ILCs rather than NK cells or other innate immune cells present within the tumour tissue. In order to further determine how the absence of an adaptive immune system, NK cells and PD-1 might affect ILCs, *Rag*$^{-/-}$ were inoculated with B16 F10 melanoma as before and then mice were treated with either αNK1.1 and/or αPD-1 or isotype control (Figure 4.5A). Mice were euthanised on day 12 post inoculation and tumour infiltrating lymphocytes (TILs) were isolated and innate subsets were analysed via flow cytometry. FMO controls were used to identify cells (Figure 4.5B-F). There were no differences observed in DCs (Figure 4.5H), monocytes (Figure 4.5I), granulocytes (Figure 4.5J) and macrophages (Figure 4.5K). There was however a significant increase noted in the ILCs ($p=0.03$ and $p=0.005$; Figure 4.5G). This suggests that the αPD-1 therapy is exclusively targeting the ILC subsets of the innate immune system and not targeting the other cells of the innate immune system.

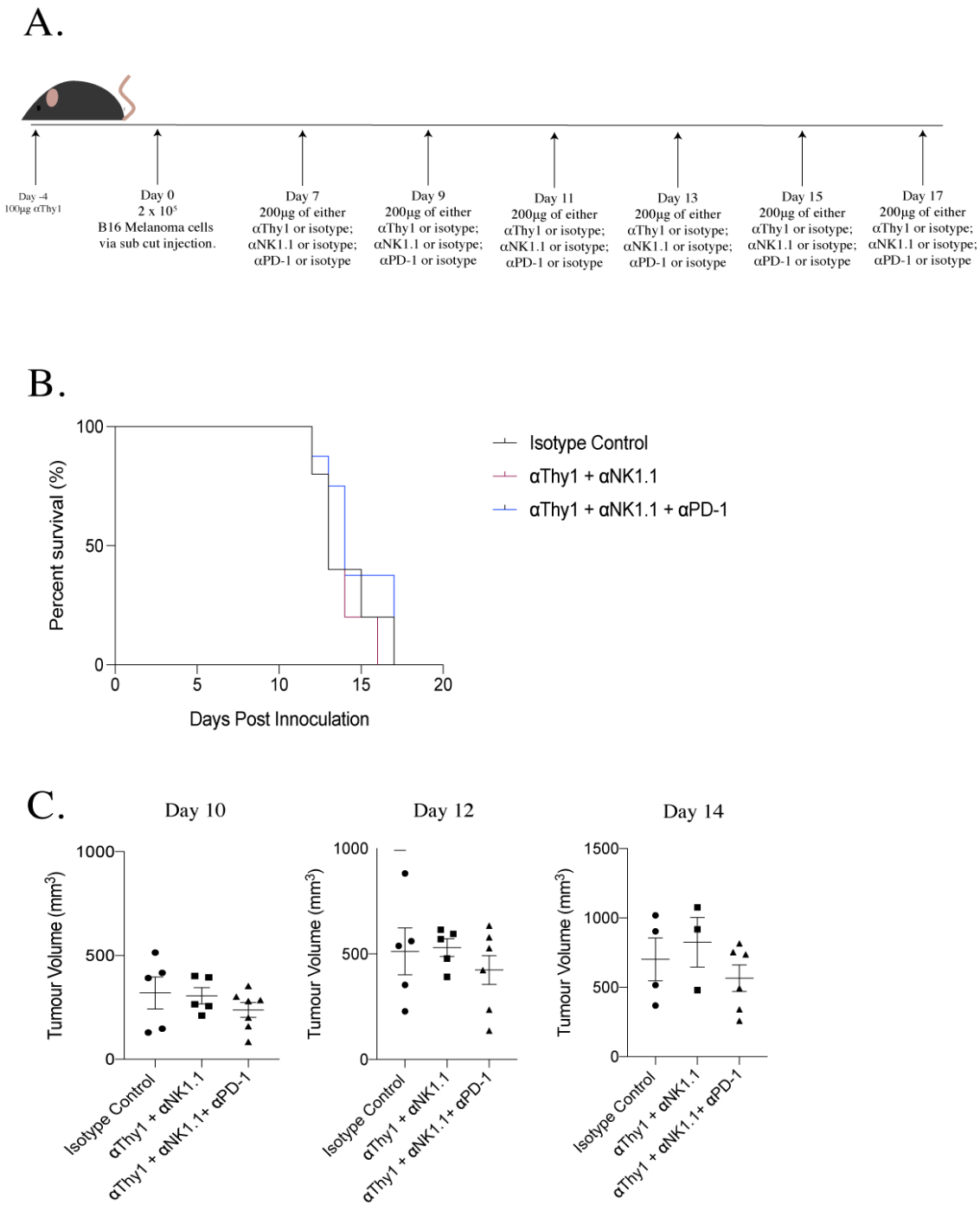

Figure 4.4.: ILCs drive protection against tumour growth in the absence of PD-1. Rag$^{-/-}$ mice were treated with 100µg of αCD90.2 (clone:30H12) or isotype control (rat IgG2b; clone: LTF2) via intraperitoneal injection 4 days prior to inoculation with tumour cells. On day 0, mice were inoculated via subcutaneous injection with 2 x 10^5 B16 F10 melanoma cells. Mice were administered with 200µg of αCD90.2 or isotype control; 200µg of αPD-1 (clone: RPM1-4) or isotype control (Rat IgG2a; clone: 2A3) and 200µg of αNK1.1 (clone: PK136) or isotype control (mouse IgG1a; clone: C1.18.4) on alternate days from day 7 onwards for the duration of the experiment (A). Mice were euthanised when they reached the humane endpoint of 1.5cm mean diameter. Mouse survival curve shown (B). Tumour volume was calculated and is shown on day 10 (C; left panel, day 12 (C; middle panel) and day 14 post inoculation (C; right panel). N=5-7; Data = Mean +- SEM.

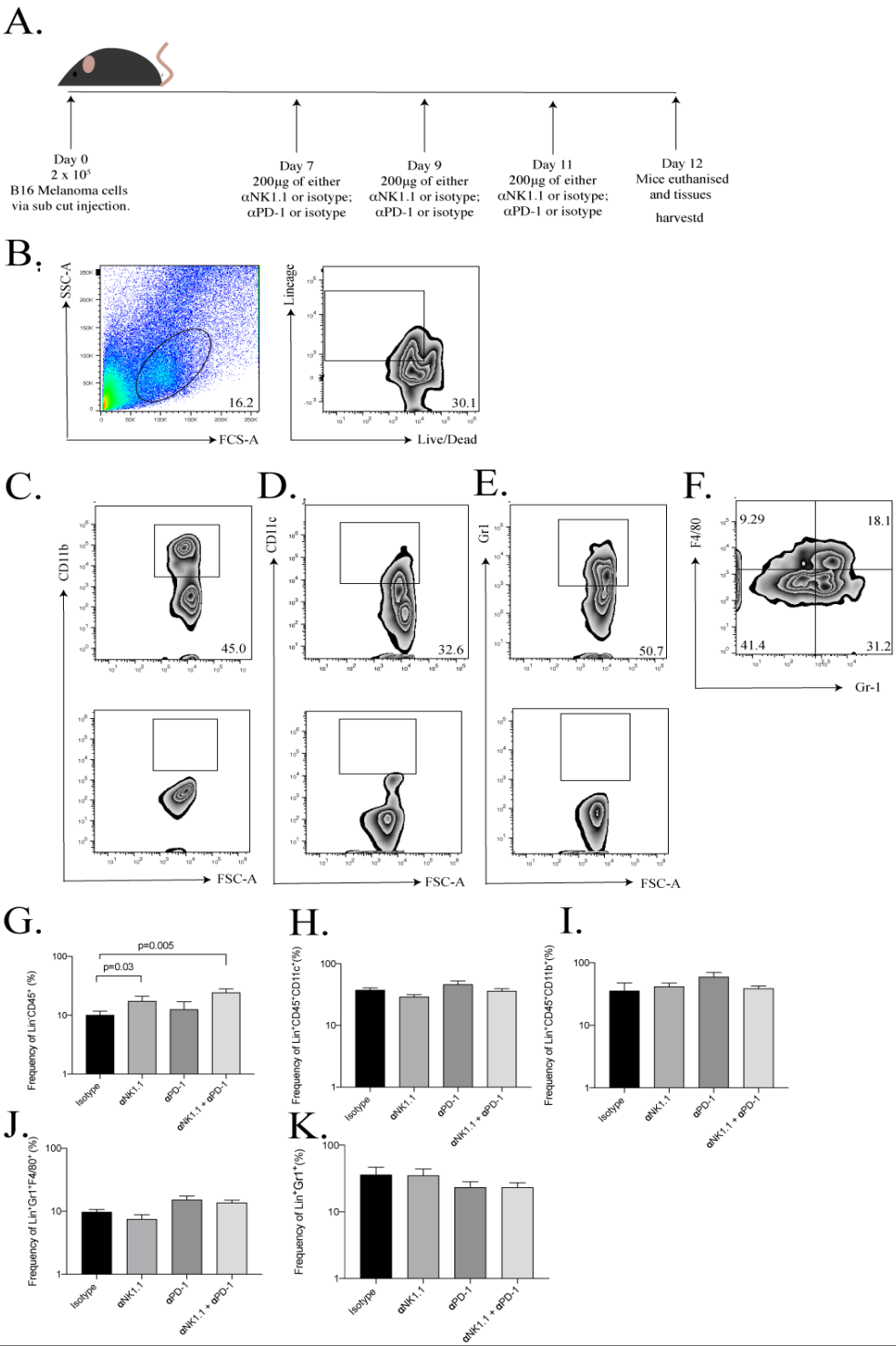

Figure 4.5. Blockade of PD-1 specifically increases ILCs in the TME but no other innate immune subsets. Rag$^{-/-}$ mice were inoculated with 2 x 10^5 tumour cells via subcutaneous injection. Day 7 post inoculation, mice were treated with 200µg of αPD-1 (clone: RPM1-4) or isotype control (Rat IgG2a; clone:2A3) and 200µg of αNK1.1 (clone:PK136) or isotype control (mouse IgG1a; clone: C1.18.4) on alternate days from day 7. Mice were euthanised on day 14 and tumour infiltrating lymphocytes (TILs) were isolated and immune subsets were quantified and analysed (A). Representative gating strategy of immune cell analysis (B). Representative graph of macrophages (C) dendritic cells (D), granulocytes (E) and monocytes (F) with corresponding FMO controls below. Summary of ILCs (G), Dendritic cells (D), macrophages (E), monocytes (F) and granulocytes (G). N=3-5; Data shown as Mean ± SEM.

4.3.2. Absence of PD-1 significantly increases Nkp46^{+}RORγt^{-} ILC1s within the TME

In this study, ILCs were shown to be the only cell of the adaptive immune system to be responsive to αPD-1 therapy within the TME in mouse. The literature has demonstrated that all ILC subsets are capable of showing varied responses to tumour progression. They have all, however, demonstrated that they are capable of providing anti-tumour responses. It was therefore critical to identify which specific ILC subsets are responding to the blockade of PD-1 signalling as this is important when assessing whether they are detrimental or beneficial to tumour development and progression. In order to do this, wildtype and *Pdcd1*$^{-/-}$ mice were inoculated with B16 F10 melanoma and mice were euthanised on day 12 post inoculation. TILs were isolated and ILC populations were identified by flow cytometry (Figure 4.6.A and B). Nkp46^{+}RORγt^{-} ILC1 subset were shown to be the only subset to be significantly increased within the *Pdcd1*$^{-/-}$ mice ($p=0.02$; Figure 4.6.C). This was shown to be the only subset which responded to a lack of PD-1 signalling (Figure 4.6.D-H). This is consistent with previous findings whereby ILC1 subset had significant increase in PD-1 expression within the TME and that they were the most abundant cell subset within the melanoma TME.

To determine whether this was tissue specific, ILCs were also characterised in the tumour draining lymph nodes (TDLN) (Figure 4.7.A-D). There was a significant increase noted in the total cell number of ST2^{+} nILC2s, whereas no difference was noticed in the NKp46^{+}RORγt^{-} ILC1 subset (Figure 4.7.G). This suggests a tissue specific regulation of ILC subsets with group 2 subsets being increased in the TDLN but with ILC1 subset cells being increased within the TME. ILC subsets within the spleen showed no differences between the wildtype mice and the *Pdcd1*$^{-/-}$ in any of the subsets (Figure 4.8.A-D).

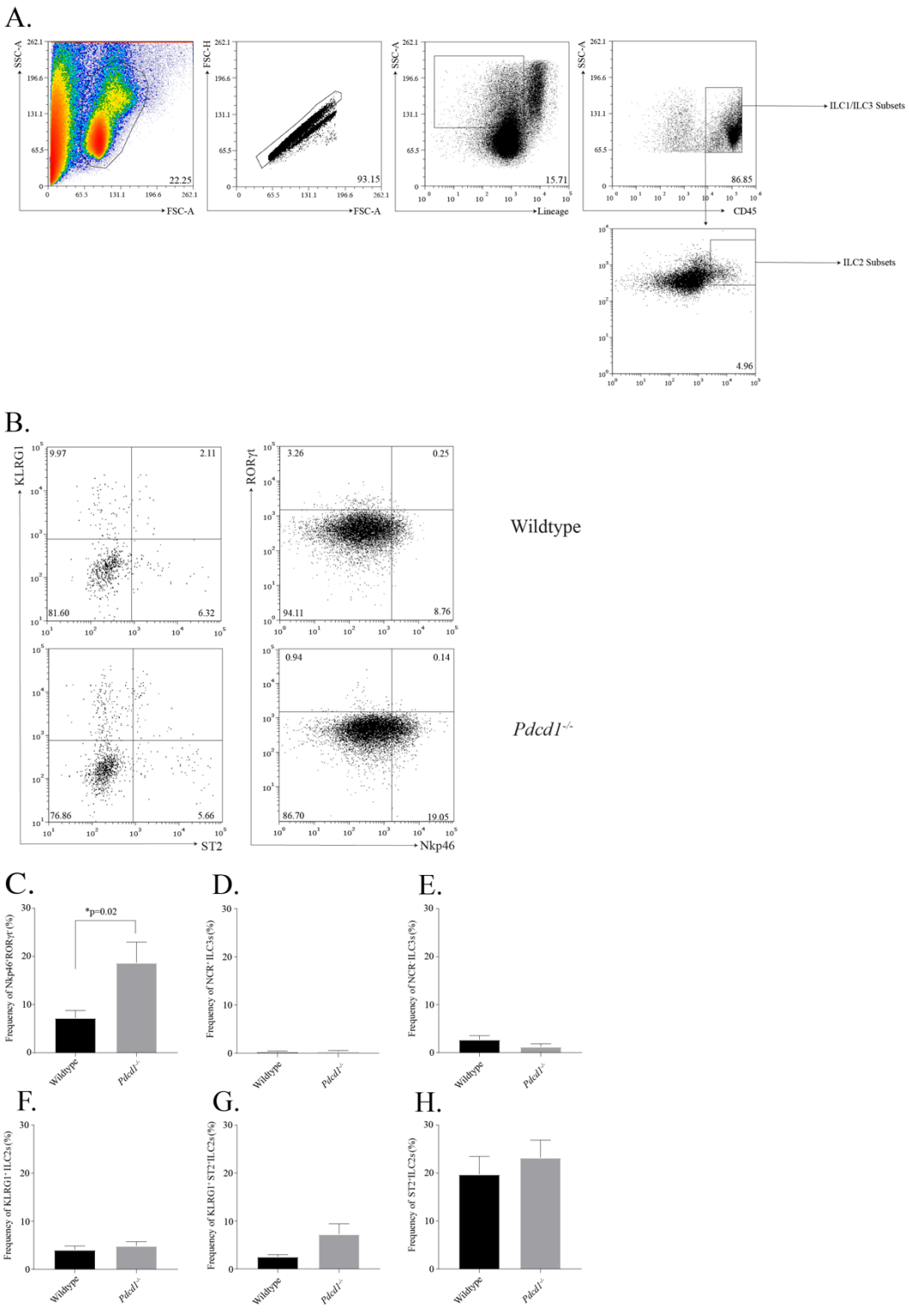

Figure 4.6: Deficiency of PD-1 increases the frequency of Nkp46^{+}RORγt^{-}NK1.1^{-} ILC1s within the TME. Wildtype and *Pdcd1*$^{-/-}$ mice were inoculated with 2 x 10^5 B16 F10 melanoma cells via subcutaneous injection. Mice were euthanised on day 12 post tumour inoculation and tumour infiltrating lymphocytes were isolated and ILC populations were analysed (A). Representative plots of ILC populations from wildtype (B; top panels) and *Pdcd1*$^{-/-}$ mice (B; bottoms panels). Summary of RORγt^{-} NKp46^{+}NK1.1^{-} ILC1s (C), NCR^{+} ILC3s(D), NCR^{-} ILC3s (E), KLRG1^{+} iILC2s (F), KLRG1^{+}ST2^{+} mILC2s (G) and ST2^{+} nILC2s (H) N= 5; Data shown as Mean±SEM

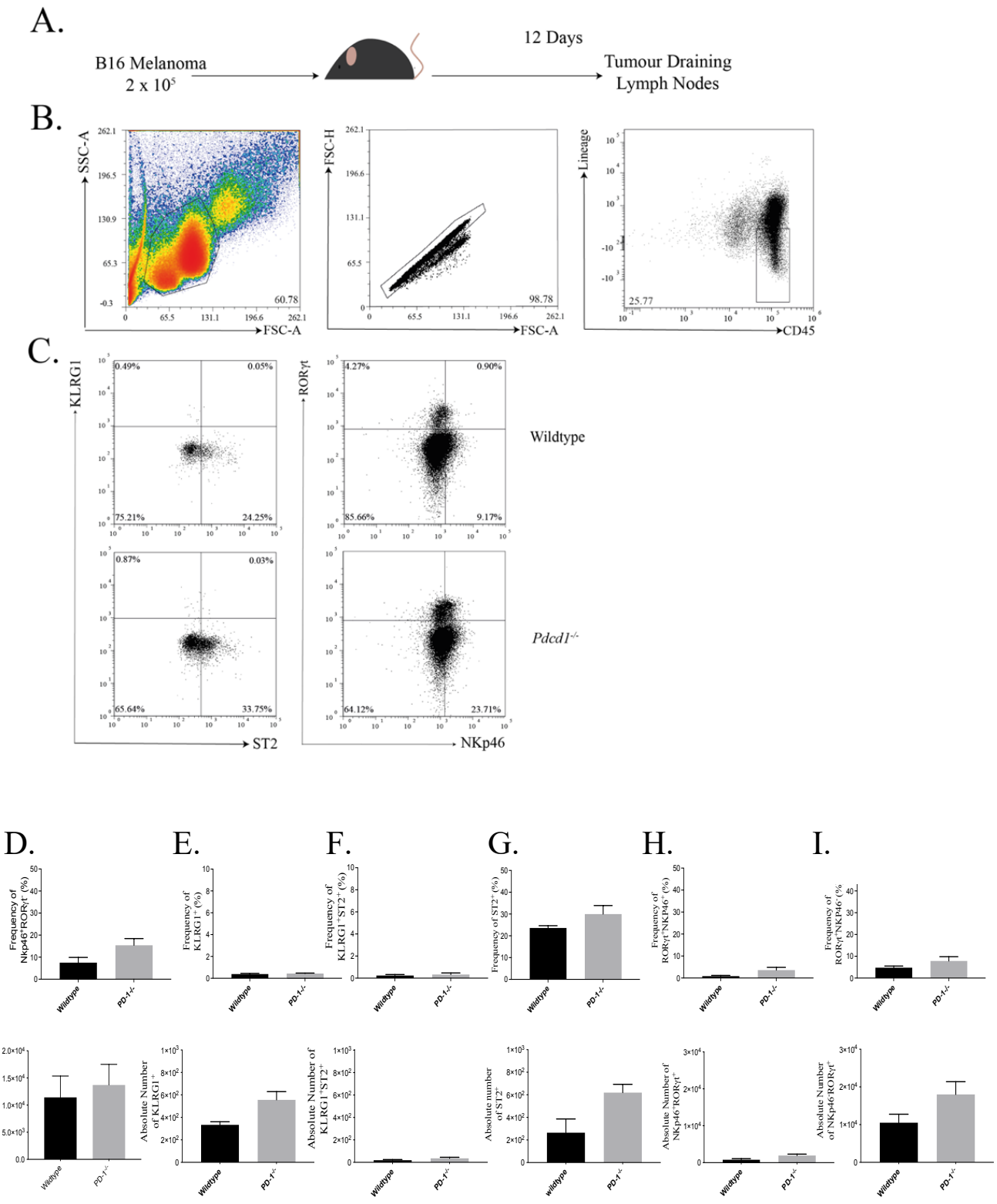
A.
B16 Melanoma
2 x 10^5
12 Days
Tumour Draining
Lymph Nodes
B.
SSC-A
FSC-A
60.78
FSC-H
FSC-A
98.78
Lineage
CD45
25.77
C.
KLRG1
ST2
RORγt
NKp46
0.49%
0.05%
75.21%
24.25%
4.27%
0.90%
85.66%
9.17%
Wildtype
0.87%
0.03%
65.64%
33.75%
64.12%
23.71%
Pdcd1-/-
D.
E.
F.
G.
H.
I.
Wildtype
PD-1-/-

Figure 4.7.: Deficiency of PD-1 increase ST2$^+$ nILC2s within the TDLN in murine melanoma. Wildtype and *Pdcd1*$^{-/-}$ mice were inoculated with 2 x 10^5 B16 F10 melanoma cells via subcutaneous injection. Mice were euthanised on day 12 post tumour inoculation. Lymphocytes from tumour draining lymph nodes (TDLN) were isolated and ILC populations were analysed (A). Representative plots of ILC populations from wildtype (B; top panels) and *Pdcd1*$^{-/-}$ mice (B; bottoms panels). Summary of frequency (top panels) and absolute cell count (lower panels) in NKp46$^+$RORγt$^-$ ILC1s (D) KLRG1$^+$ iILC2s(E), KLRG1$^+$ST2$^+$ mILC2s(F), ST2$^+$nILC2s(G), NCR$^+$ ILC3s (H) and NCR$^-$ILC3s(I) shown. N= 5; Data shown as Mean±SEM

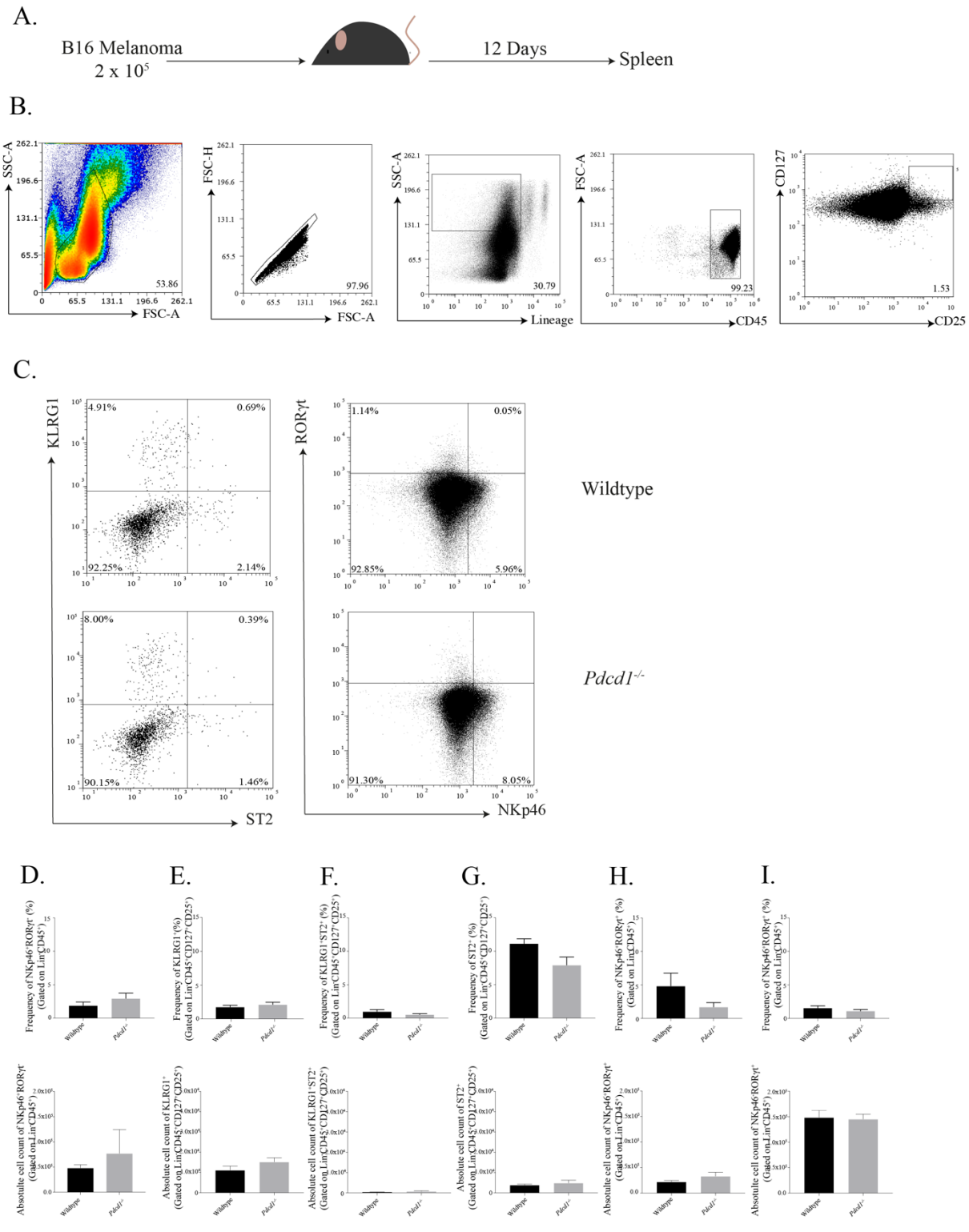

Figure 4.8.: Deficiency of PD-1 does not alter ILC subsets within the spleen in murine melanoma. Wildtype and *Pdcd1*$^{-/-}$ mice were inoculated with 2 x 10^5 B16 F10 melanoma cells via subcutaneous injection. Mice were euthanised on day 12 post tumour inoculation and spleenocytes were isolated and ILC populations were analysed (A). Representative plots of ILC populations from wildtype (B; top panels) and *Pdcd1*$^{-/-}$ mice (B; bottoms panels). Summary of frequency (top panels) and absolute cell count (lower panels) in NKp46$^+$RORγt$^-$ ILC1s (D) KLRG1$^+$ ILC2s(E), KLRG1$^+$ST2$^+$ILC2s(F), ST2$^+$ILC2s(G), NCR$^+$ ILC3s (H) and NCR$^-$ ILC3s(I) shown. N= 5; Data shown as Mean±SEM

4.3.3. Absence of PD-1 increases type 1 cytokine expression in ILCs within the TME.

Absence of PD-1 significantly increases ILCs within the TME (Figure 4.5.G). In order to elucidate whether PD-1 deletion may impact the function of ILCs, the cytokine production of ILCs in the TME was assessed. Wildtype and *Pdcd1*$^{-/-}$ mice were inoculated with 2 x10^5 B16 F10 melanoma cells via subcutaneous injection. Mice were euthanised 12 days post inoculation and TILs were isolated. TILs were stimulated for 4 hours at 37ºC with cell stimulation cocktail containing phorbol myristate acetate (PMA), ionomycin, brefeldin A and monensin. Cells were then analysed by flow cytometry and cytokine production was assessed in Lin$^-$CD45$^+$ ILCs (Figure 4.9.A). ILCs showed no significant changes in the expression of the group 2 cytokines namely IL-5 and IL-13 (Figure 4.9.C) or in the group 3 cytokines namely IL-17 and IL-22 (Figure 4.9.G). Data did however show a significant increase in cells that expressed multiple cytokines namely IL-13$^+$IL5$^+$IFNγ$^+$ (p=0.05; Figure 4.9.D). There was also a trend to suggest an increase in IFNγ expression (Figure 4.9.E and F) however this was not shown to be significant (p=0.08). There is no evidence to suggest a significant increase in cells which express both group 3 cytokines and IFNγ$^+$, with this phenomenon is only seen in the cells which express both group 2 and group 1 cytokines.

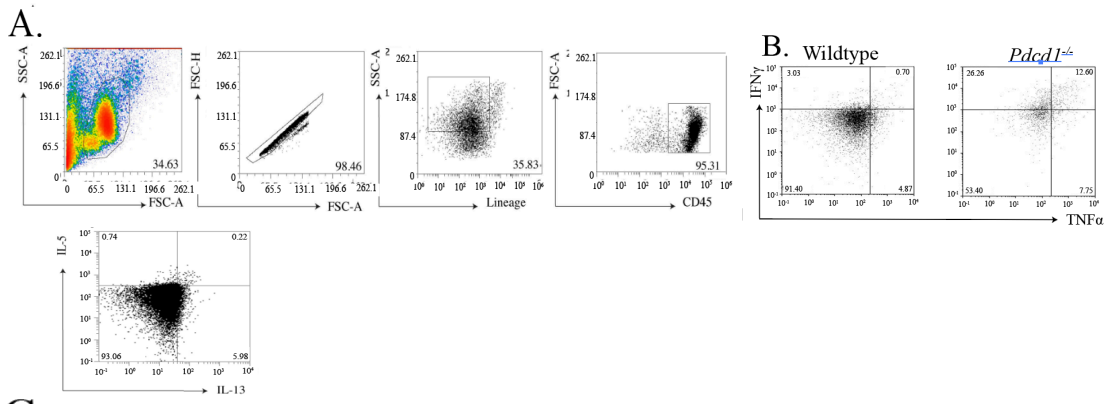
A.
SSC-A
FSC-A
34.63
FSC-H
98.46
Lineage
35.83
CD45
95.31
B.
Wildtype
Pdcd1-/-
IFNγ
TNFα
3.03
0.70
91.40
4.87
26.26
12.60
53.40
7.75
IL-5
IL-13
0.74
0.22
93.06
5.98

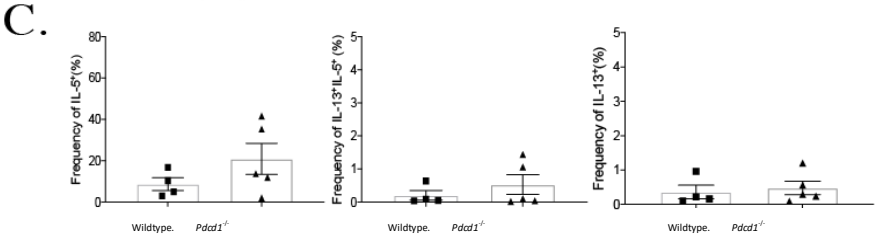
C.
Frequency of IL-5+(%)
Frequency of IL-13+IL-5+ (%)
Frequency of IL-13+(%)
Wildtype.
Pdcd1-/-

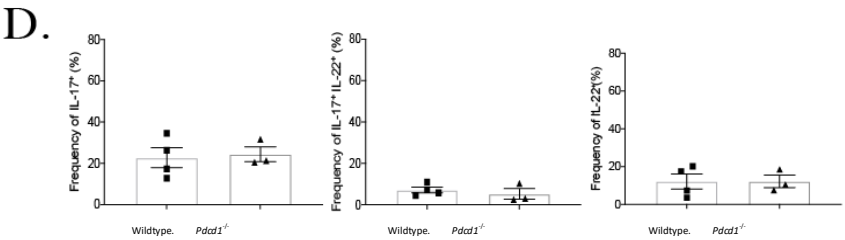
D.
Frequency of IL-17+ (%)
Frequency of IL-17+ IL-22+ (%)
Frequency of IL-22+(%)
Wildtype.
Pdcd1-/-

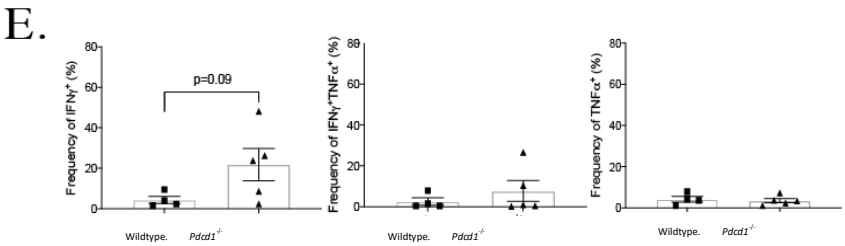
E.
Frequency of IFNγ+ (%)
p=0.09
Frequency of IFNγ+TNFα+ (%)
Frequency of TNFα+ (%)
Wildtype.
Pdcd1-/-

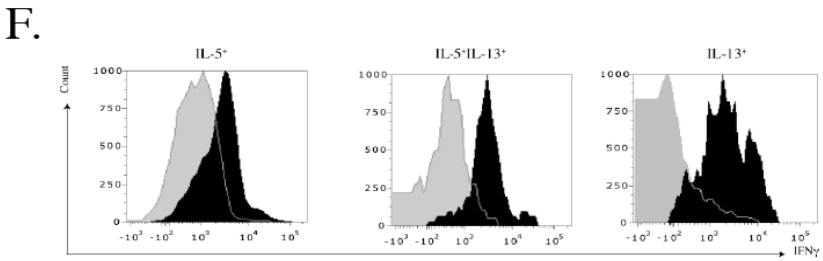
F.
IL-5+
IL-5+IL-13+
IL-13+
Count
IFNγ

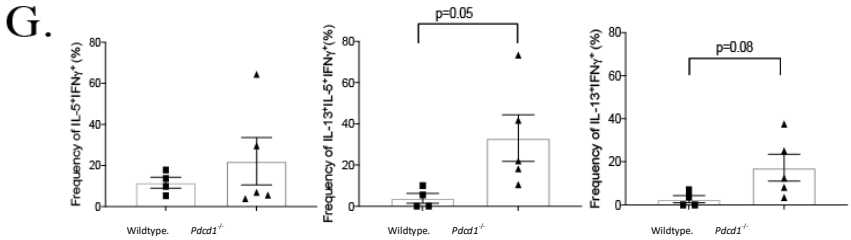
G.
Frequency of IL-5+IFNγ+ (%)
Frequency of IL-13+IL-5+IFNγ+(%)
p=0.05
Frequency of IL-13+IFNγ+ (%)
p=0.08
Wildtype.
Pdcd1-/-

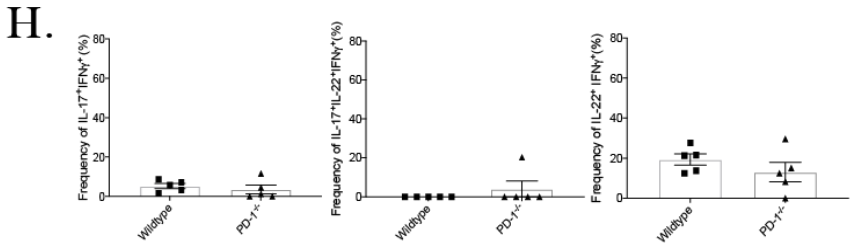
H.
Frequency of IL-17+IFNγ+ (%)
Frequency of IL-17+IL-22+IFNγ+(%)
Frequency of IL-22+ IFNγ+(%)
Wildtype
PD-1+/-

Figure 4.9.: Absence of PD-1 increases type 1 cytokine expression. Wildtype and *Pdcd1*$^{-/-}$ mice were inoculated with 2 x 10^5 B16 F10 melanoma cells via subcutaneous injection. Mice were euthanised on day 12 post tumour infiltrating lymphocytes (TILs) were isolated. Cells were stimulated with PMA, ionomycin, brefeldin A and monensin at 37^{o}C for 4 hours. ILCs were then analysed were by flow cytometry and cytokine production was analysed. Representative flow cytometry plots shown (A). Representative flow plot showing IFNγ production in TILS (B). Summary of type 2 cytokine expression (IL-5 and IL-13; C), type 3 cytokine expression (IL-17 and IL22; D) and type 1 cytokine expression (IFNγ and TNFα; D). Representative histograms showing IFNγ production in IL-5$^+$, IL-5$^+$ and IL-13$^+$ and IL-13$^+$ ILCs in wildtype (grey) and *Pdcd1*$^{-/-}$ (F). Summary of ILCs expression of type 2 cytokines and IFNγ (G). Summary of ILC expression of type 3 cytokines and IFNγ (H). N=5; Data shown as Mean ± SEM

4.3.4. PD-1 drives the changes in Tbet$^+$NKp46$^+$RORγt$^-$Eomes$^-$NK1.1$^-$ ILC1s within the TME.

It has been demonstrated that NKp46$^+$RORγt$^-$ ILC1s are present and response to PD-1 signalling within the TME. Within the previous chapter it was demonstrated that PD-1 expression was significantly increased within Tbet$^+$NKp46$^+$RORγt$^-$ ILC1s within the TME. In order to further investigate this cell type further, Eomes and Tbet expression was further investigated within these ILC1s. NK cells are distinguished from ILC1s through the expression of Eomes, being defined as Eomes$^+$Tbet$^+$, whereas ILC1s are associated as being Eomes$^-$. Therefore, Eomes expression was assessed on these cells in order to confirm they were ILC1s and not NK cells. A novel strain of mice was then utilised to determine whether these cells were significantly modulated in the absence of PD-1 signalling. The novel strain, namely *Pdcd1*$^{-/-}$TbetZsGreen, both lack PD-1 and also have fluorescently labelled Tbet in order for these cells to be easily identifiable. TbetZsGreen mice and *Pdcd1*$^{-/-}$TbetZsGreen were inoculated with B16 F10 melanoma cells and tumours were allowed to establish. Mice were euthanised on day 12 post inoculation and TILs were isolated and ILCs were assessed. Here, it was demonstrated that in the absence of PD-1, there was a significant increase in Tbet$^+$Eomes$^-$ NKp46$^+$RORγt$^-$ ILC1s within the TME (Figure 4.10.A-C). Of note, there was no significant difference noted in Eomes$^+$ subset of cells within the TME (Figure 4.10.B and C). In order to further determine how lack of PD-1 may affect ILC function, proliferation was assessed within the Tbet$^+$Nkp46$^+$ ILC1s and demonstrated that there was as significant increase in Ki67 staining

(Figure 4.10.D). In conclusion, PD-1 deficiency significantly increases ILC1 function through cytokine expression and cellular proliferation.

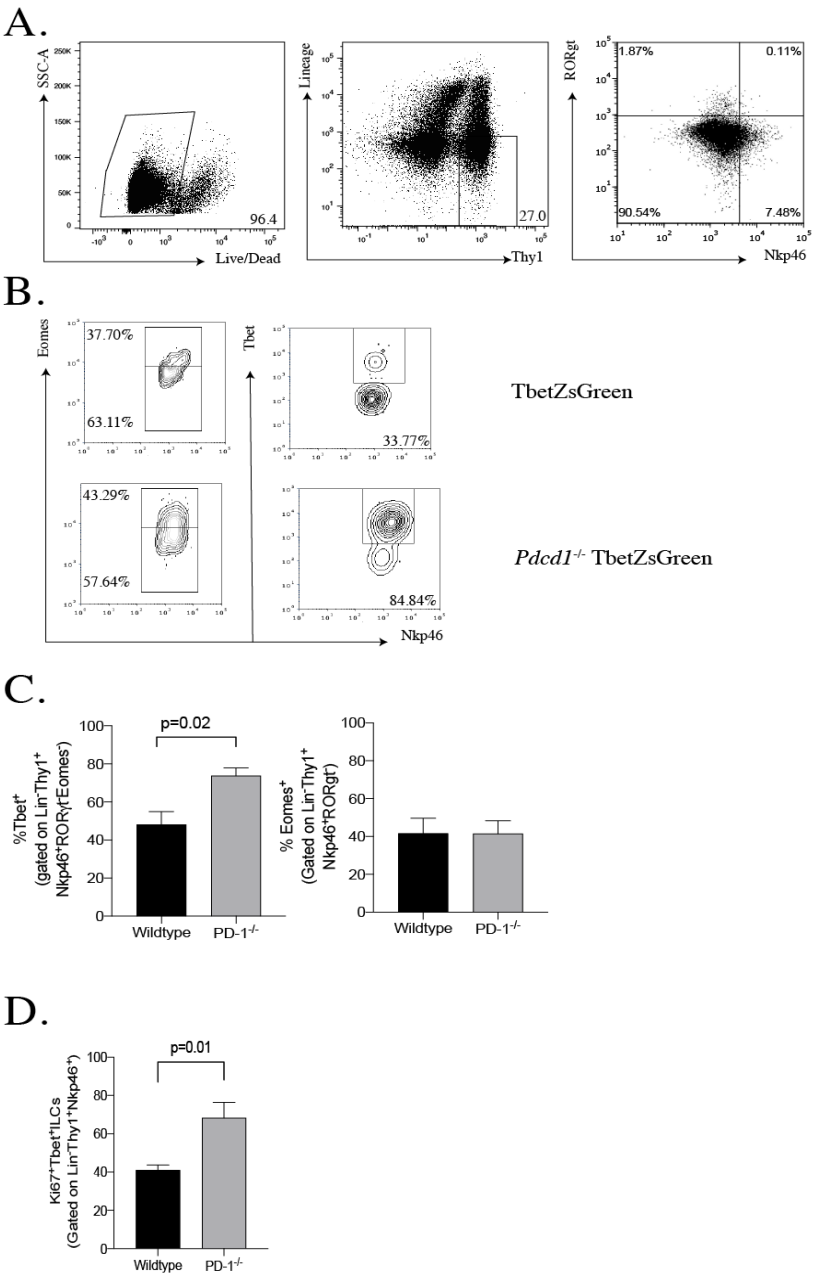

Figure 4.10.: Absence of PD-1 specifically increases Tbet^{+}Eomes^{-} Nkp46^{+}RORγt^{-} ILC1s within the TME. TbetZsGreen and *Pdcd1*$^{-/-}$ TbetZsGreen mice were inoculated with 2 x 10^{5} B16 melanoma cells via sub cutaneous injections. On Day 12 post inoculation, tumour infiltrating lymphocytes (TILs) were isolated and analysed by flow cytometry. Representative flow cytometry plots showing ILC gating shown (A). Eomes expression (left panels) and Tbet expression (right panels) shown in TbetZsGreen (top panels) and *Pdcd1*$^{-/-}$ TbetZsGreen mice (bottom panels). Summary of Tbet^{+}Eomes^{-} Nkp46^{+}RORγt^{-} (C; left panel) and Eomes+ ILCs (C; right panel). Proliferation was assessed in Tbet^{+}RORγt^{-} Nkp46^{+} cells within the tumour microenvironment. Summary of Ki67 expression shown (D). Data shown as Mean+- SEM.

4.3.5. Nkp46^{+}RORγt^{-} ILC1s are significantly increased in the TME upon PD-1 blockade

Global deletion of PD-1 results in alterations in ILCs within the TME (Figure 4.5). Data has demonstrated that lack of PD-1 results in a decrease in tumour growth and enhances specific ILC subsets in various tissues (Figure 4.1 and Figure 4.6 respectively). This data has not, however, demonstrated whether ablation of PD-1 signalling prevents initial tumour engraftment or whether it enhances anti-tumour defences in developed tumours. Anti-PD-1 therapy is used to treat a number of cancers (Callahan et al., 2016, Topalian et al., 2012); a treatment which is administered post tumour development following presentation within the clinic. For ILCs to be a viable target for anti-PD-1 therapy, the melanoma model was adapted to make it more clinically relevant. Wildtype mice were inoculated with B16 F10 melanoma via subcutaneous injection. On day 7 post inoculation, when the tumour become visible, mice were injected with either αPD-1 therapy (200μg per mouse) or isotype control. Mice were treated on days 7, 9 and 11 post tumour inoculation and mice were euthanised on day 12. TILs, spleen and TDLN were harvested and ILC populations were analysed. Administration of PD-1 blocking antibody showed that there was a significant increase in Nkp46^{+}RORγt^{-} ILC1s within the TME (p=0.02; Figure 4.11A-C). This mirrored what was seen in the *Pdcd1*$^{-/-}$ mice, whereby there was also no difference noted in the other ILC subsets (Figure 4.11C). In the TDLN, however, there was no significant changes in ST2^{+} nILC2 numbers following αPd-1 therapy which is in contrast to the findings in *Pdcd1*$^{-/-}$ *mice* (Figure 4.12 A-C). The ILC subsets within the spleen mirrored what was seen within the *Pdcd1*$^{-/-}$ mice whereby there were no significant changes in ILC subsets between mice treated with αPD-1 therapy and mice treated with isotype control (Figure 4.13 A-C). This suggests that therapeutic blockade of PD-1 signalling in driving ILCs following tumour development and suggests that ILCs, particularly Nkp46^{+}RORγt^{-} ILC1s, could be targeted within the TME with therapy as these cells appear to respond to αPD-1 therapy. In order to ensure that findings were not tumour specific, the experiments were repeated in a subcutaneous model of colon cancer using MC38 tumour cell line. As with the melanoma model, mice were inoculated with 2 x 10^5 MC38 cells via subcutaneous injection. Mice were administered with αPD-1 therapy (or isotype control) on day 7, 9 and 11 and TILs were harvested on day 12. This mirrored findings seen within the melanoma model whereby, exclusively, there was an increase in NKp46^{+}RORγt^{-} ILC1s within the TILs (p=0.03;Figure 4.13 A-C).

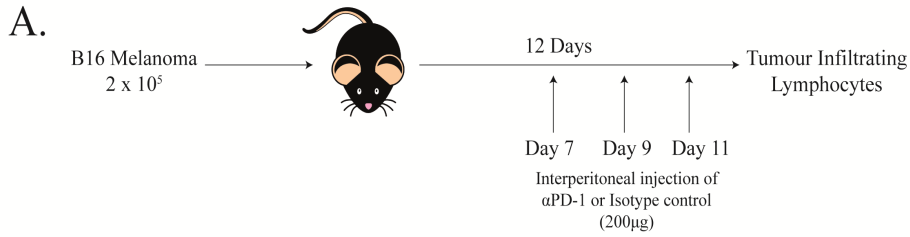
A.
B16 Melanoma
2 x 10^5
12 Days
Tumour Infiltrating Lymphocytes
Day 7
Day 9
Day 11
Interperitoneal injection of αPD-1 or Isotype control (200µg)

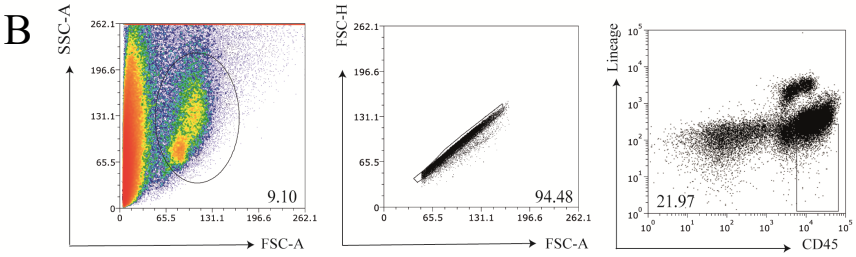
B
SSC-A
FSC-A
9.10
FSC-H
FSC-A
94.48
Lineage
CD45
21.97

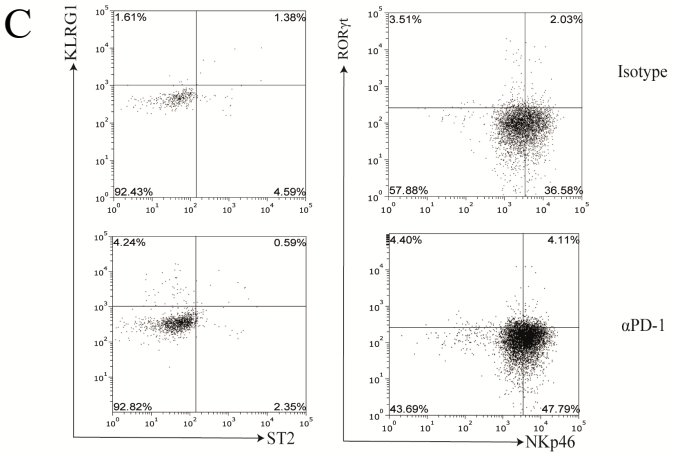
C
KLRG1
ST2
1.61%
1.38%
92.43%
4.59%
4.24%
0.59%
92.82%
2.35%
RORγt
NKp46
3.51%
2.03%
57.88%
36.58%
4.40%
4.11%
43.69%
47.79%
Isotype
αPD-1

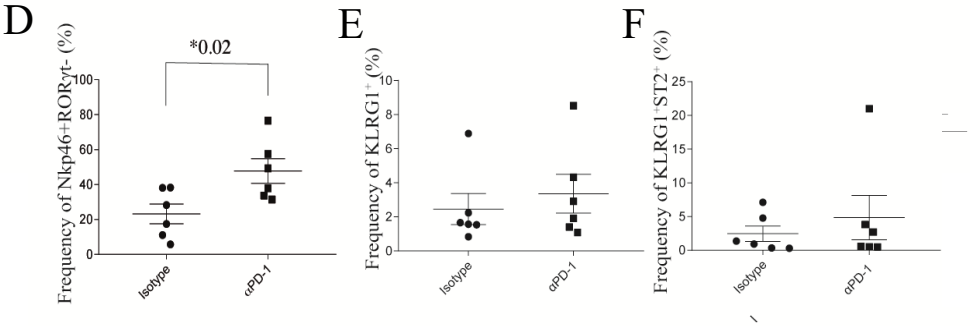
D
Frequency of Nkp46+RORγt- (%)
*0.02
Isotype
αPD-1
E
Frequency of KLRG1+ (%)
F
Frequency of KLRG1+ST2+ (%)

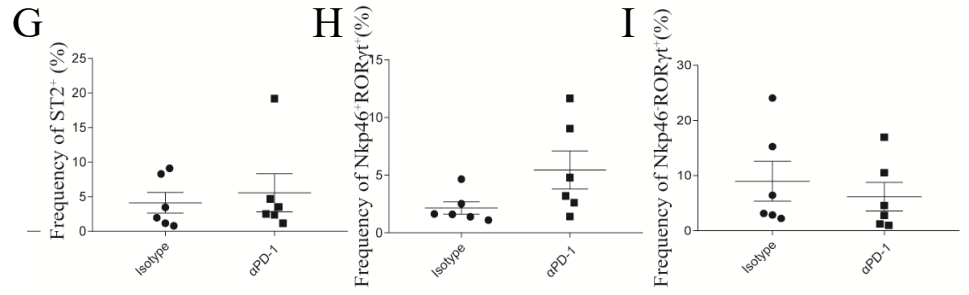
G
Frequency of ST2+ (%)
H
Frequency of Nkp46+RORγt+ (%)
I
Frequency of Nkp46 RORγt+(%)
Isotype
αPD-1

Figure 4.11.: Nkp46^{+}RORγt^{-} ILC1s increase in response to PD-1 blockade within the TME. Wildtype mice were administered with 2 x 10^{5} B16 F10 melanoma cells via subcutaneous injection. Tumor growth was monitored throughout the study. On day 7, 9 and 11 post inoculation mice were administered with aPD-1 therapy (200ug) or isotype control. Mice were euthanized on day 12 post inoculation and tumor infiltrating lymphocytes were isolated (A). ILC were characterized as Lin^{-}CD45^{+}. Representative flow plots of the gating strategy from wildtype mice (B). ILC2s were defined into three individual subsets KLRG1^{+}iILC2s, KLRG1^{+}ST2^{+}mILC2s, ST2^{+}nILC2s. ILC1s were defined as Nkp46^{+}RORγt^{-}. ILC3s were split into 2 subsets; NCR^{+}: Nkp46^{+}RORγt^{+} and NCR^{-}; Nkp46^{-}RORγt^{+}. Representative flow plots from mice treated with isotype (top panel) and αPD-1 therapy (bottom panel) (C). Summary of ILC subset frequency; NKp46^{+}RORγt^{-}(D) KLRG1^{+} ILC2s(E), KLRG1^{+}ST2^{+}ILC2s(F), ST2^{+}ILC2s(G), NCR^{+} ILC3s (H) and NCR^{-}ILC3s(I). N=8 mice. Data represents 2 repeated experiments. Data shown as mean ± SEM.

A.

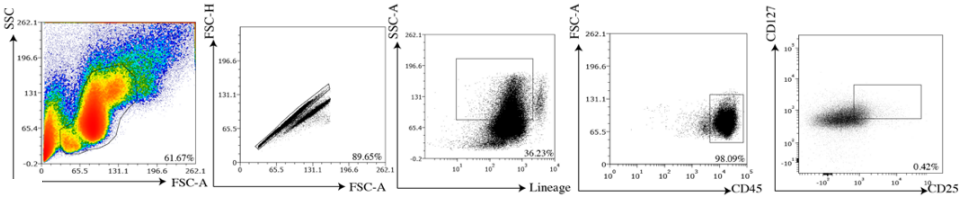
SSC
FSC-A
61.67%
FSC-H
FSC-A
89.65%
SSC-A
Lineage
36.23%
FSC-A
CD45
98.09%
CD127
CD25
0.42%

B.

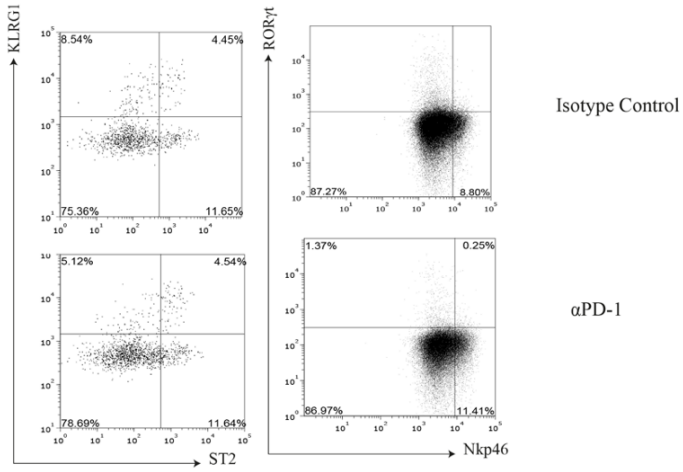
KLRG1
ST2
8.54%
4.45%
75.36%
11.65%
5.12%
4.54%
78.69%
11.64%
RORγt
Nkp46
87.27%
8.80%
1.37%
0.25%
86.97%
11.41%
Isotype Control
αPD-1

C.

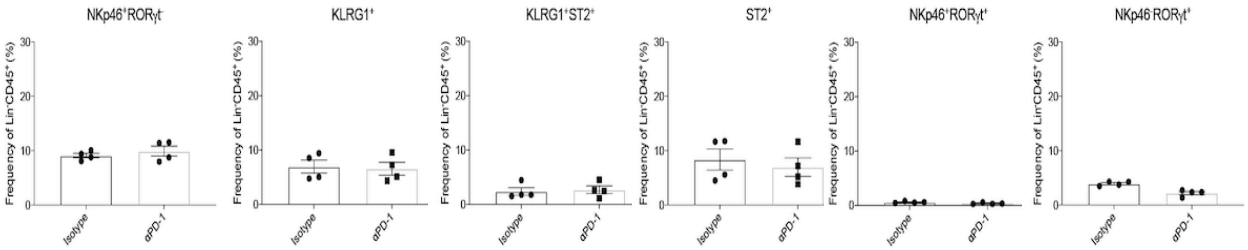
NKp46+RORγt-
KLRG1+
KLRG1+ST2+
ST2+
NKp46+RORγt+
NKp46-RORγt+
Frequency of Lin-CD45+ (%)
Isotype
αPD-1

D.

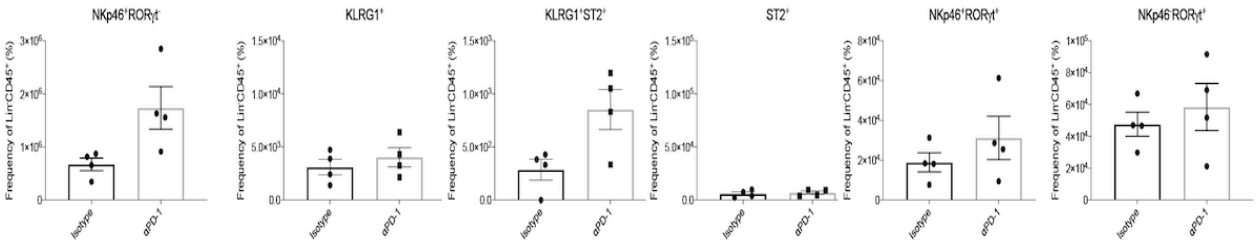
NKp46+RORγt-
KLRG1+
KLRG1+ST2+
ST2+
NKp46+RORγt+
NKp46-RORγt+
Frequency of Lin-CD45+ (%)
Isotype
αPD-1

E.

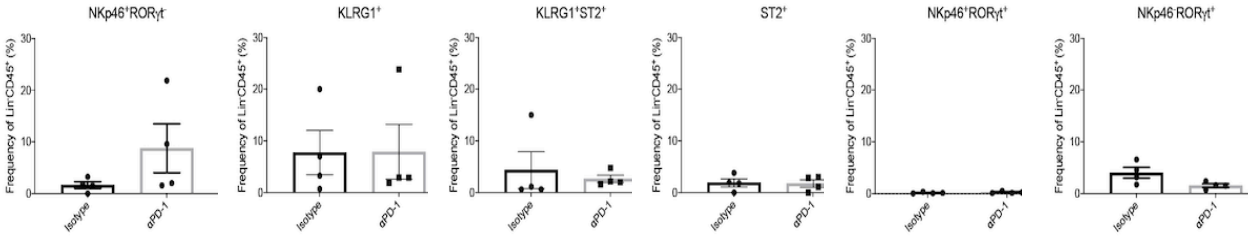
NKp46+RORγt-
KLRG1+
KLRG1+ST2+
ST2+
NKp46+RORγt+
NKp46-RORγt+
Frequency of Lin-CD45+ (%)
Isotype
αPD-1

Figure 4.12: ILC subsets remain unaffected by αPD-1 therapy within the TDLN nor the spleen. Wildtype mice were administered with 2 x 10^5 B16 F10 melanoma cells via subcutaneous injection. Tumor growth was monitored throughout the study. On day 7, 9 and 11 post inoculation mice were administered with aPD-1 therapy (200ug) or isotype control. Mice were euthanized on day 12 post inoculation and tumor infiltrating lymphocytes were isolated. ILC were characterized as Lin^-CD45^+. Representative flow plots of the gating strategy from spleen from wildtype mice (A). ILC2s were defined into three individual subsets $KLRG1^+$iILC2s, $KLRG1^+ST2^+$mILC2s, $ST2^+$ nILC2s. ILC1s were defined as $Nkp46^+ROR\gamma t^-$. ILC3s were split into 2 subsets; NCR^+: $Nkp46^+ROR\gamma t^+$ and NCR^-; $Nkp46^-ROR\gamma t^+$. Representative flow plots from mice treated with isotype (top panel) and αPD-1 therapy (bottom panel) (B). Summary of ILC subset frequency in TDLN (C) and total cell count (D). Summary of ILC subset frequency (E) spleen. N=4 mice. Data shown as mean ± SEM.

A.

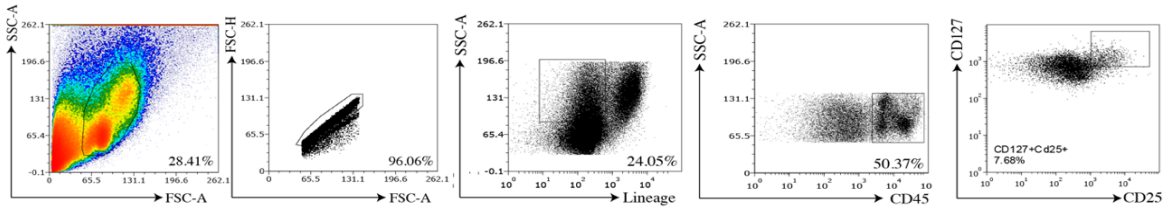

B.

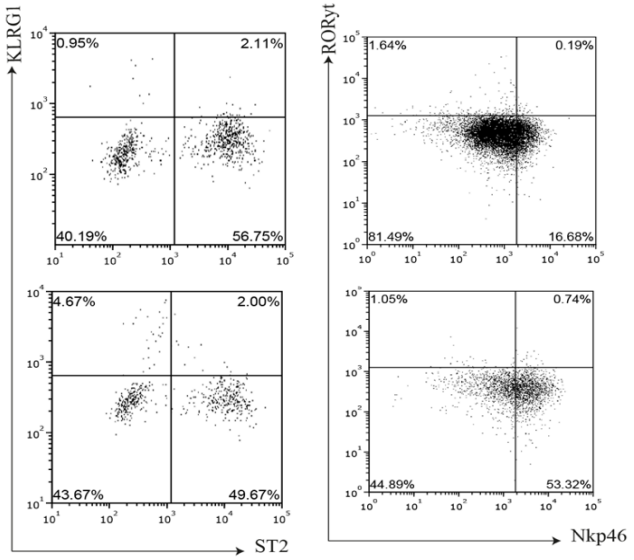

Isotype Control

αPD-1 therapy

C.

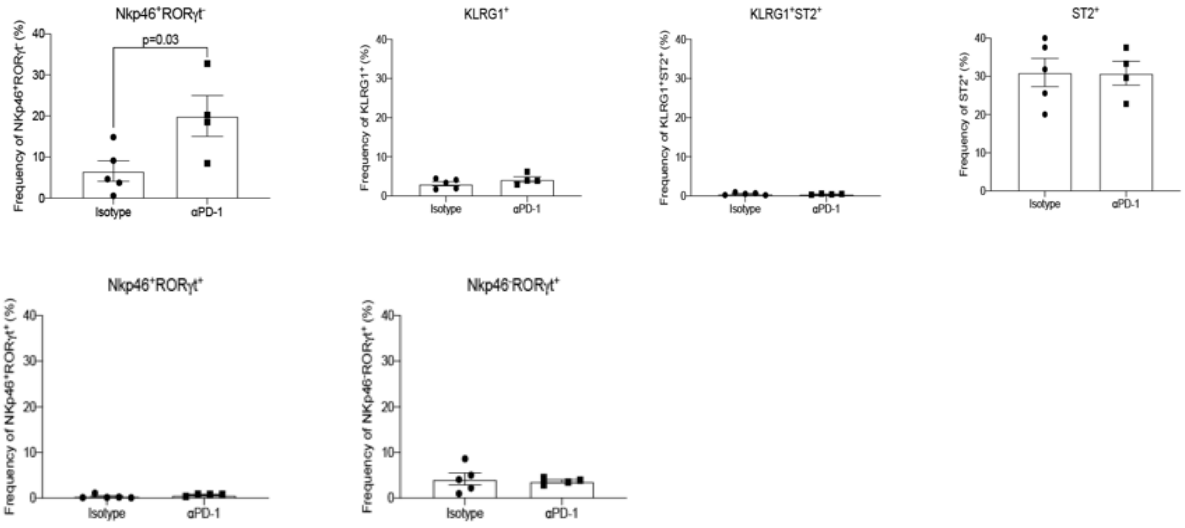

Figure 4.13: Nkp46^{+}RORγt^{-} ILC1s increase in response to PD-1 blockade in the MC38 colon cancer. Wildtype mice were administered with 2 x 10^5 MC38 cells via subcutaneous injection. Tumor growth was monitored throughout the study. On day 7, 9 and 11 post inoculation mice were administered with aPD-1 therapy (200ug) or isotype control. Mice were euthanized on day 12 post inoculation and tumor infiltrating lymphocytes (TILs) were isolated. ILC were characterized as Lin^{-}CD45^{+}. Representative flow plots of the gating strategy from spleen from wildtype mice (A). ILC2s were defined into three individual subsets: KLRG1^{+}iILC2s, KLRG1^{+}ST2^{+}mILC2s and ST2^{+} nILC2s. ILC1s were defined as Nkp46^{+}RORγt^{-}. ILC3s were split into 2 subsets; NCR^{+}: Nkp46^{+}RORγt^{+} and NCR^{-}; Nkp46^{-}RORγt^{+}. Representative flow plots from mice treated with isotype (top panel) and αPD-1 therapy (bottom panel) (B). Summary of ILC subset frequency in TIL (C). N= 4-5 mice. Data shown as mean ± SEM.

4.3.6. PD-1 blockade does not alter ILC subsets within the TME in the absence of an adaptive immune system

PD-1 therapy was shown to significantly increase Nkp46^{+}RORγt^{-} ILC1s within the wildtype mice (Figure 4.11 and Figure 4.13). It was then important to investigate to what extent this was driven and influence by the adaptive immune system. In order to test this, *Rag*$^{-/-}$ mice were inoculated with B16 melanoma cells via subcutaneous injection. Day 7, 9 and 11 post inoculation mice were treated with αPD-1 therapy or isotype control and TIL and spleen were harvested on day 12. In *Rag*$^{-/-}$ there was no significant increase in any of the ILC subsets within the TME. There was a trend to suggest an increase but there was no significant increase noted (Figure 4.13 and 4.14).

A.

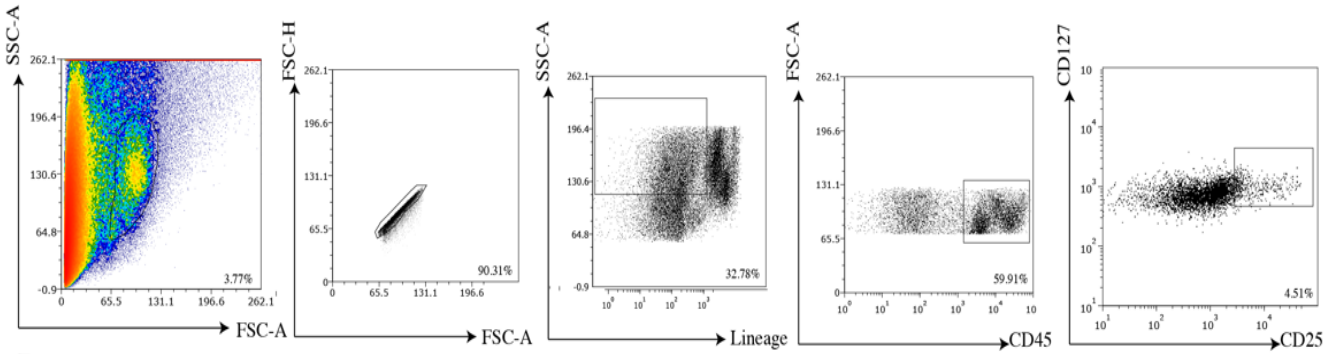
SSC-A
FSC-A
3.77%
FSC-H
FSC-A
90.31%
SSC-A
Lineage
32.78%
FSC-A
CD45
59.91%
CD127
CD25
4.51%

B.

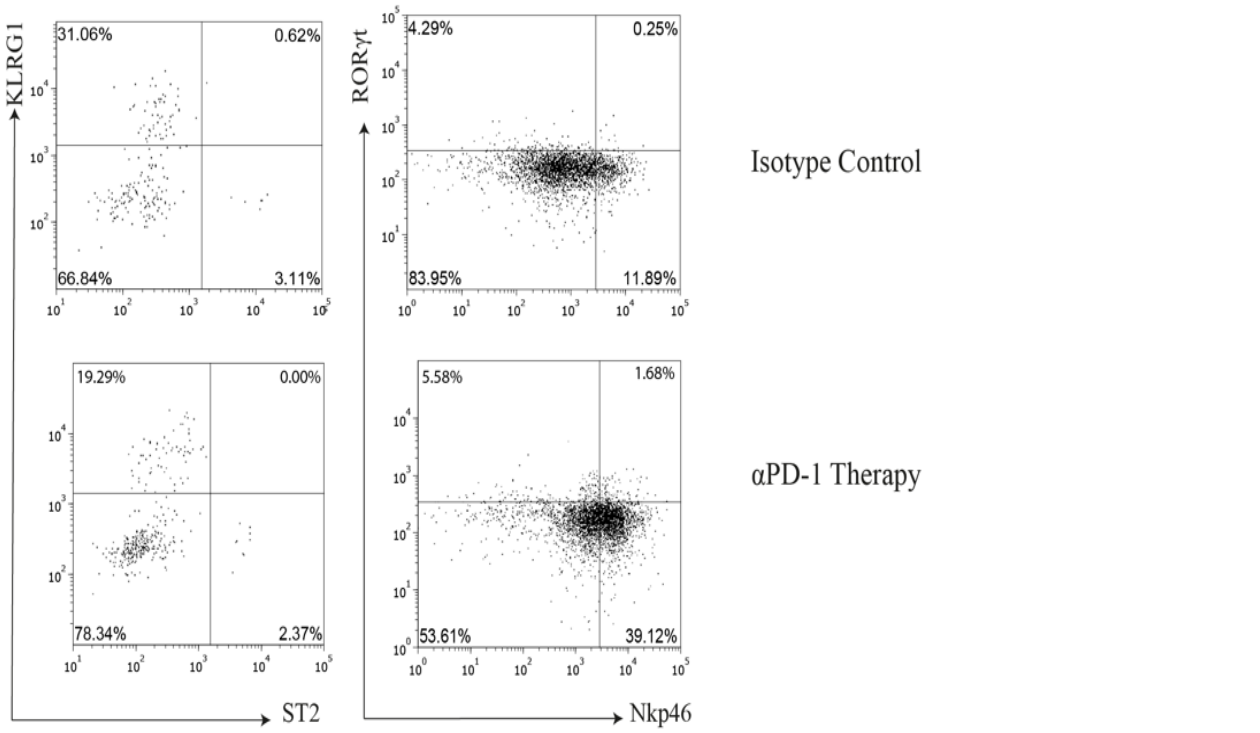
KLRG1
31.06%
0.62%
66.84%
3.11%
RORγt
4.29%
0.25%
83.95%
11.89%
Isotype Control
19.29%
0.00%
78.34%
2.37%
5.58%
1.68%
53.61%
39.12%
αPD-1 Therapy
ST2
Nkp46

C.

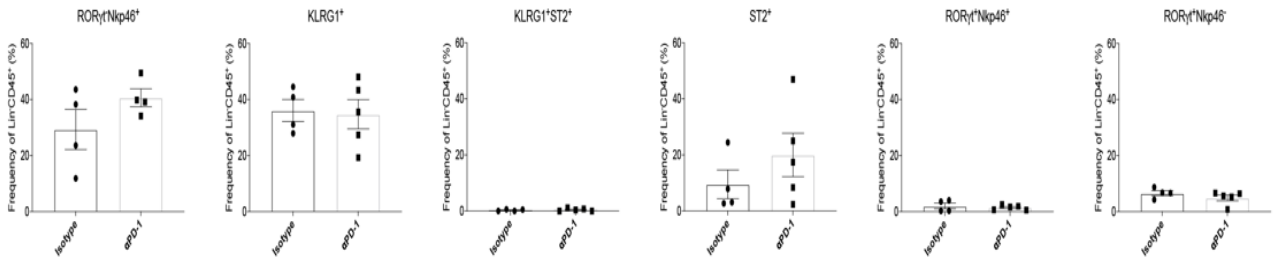
RORγt+Nkp46+
KLRG1+
KLRG1+ST2+
ST2+
RORγt+Nkp46+
RORγt+Nkp46-
Frequency of Lin-CD45+ (%)
Isotype
αPD-1

D.

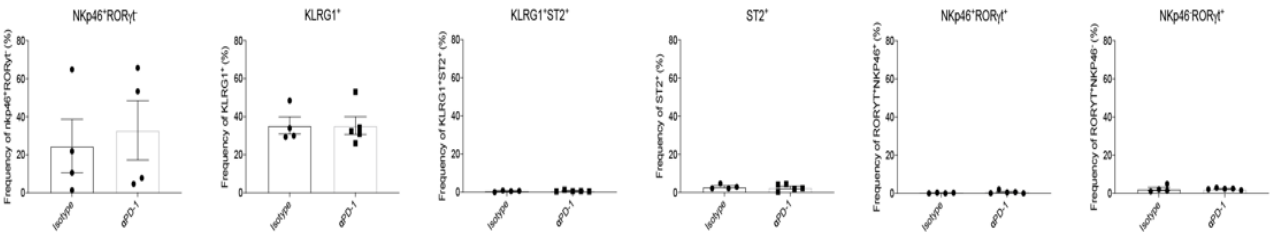
NKp46+RORγt+
KLRG1+
KLRG1+ST2+
ST2+
NKp46+RORγt+
NKp46-RORγt+
Isotype
αPD-1

Figure 4.14: PD-1 blockade does not alter ILC subsets in the TME nor the spleen in the absence of an adaptive immune system. $Rag^{-/-}$ mice were administered with 2 x 10^5 B16 melanoma colon cancer cells via subcutaneous injection. Tumor growth was monitored throughout the study. On day 7, 9 and 11 post inoculation mice were administered with aPD-1 therapy (200ug) or isotype control. Mice were euthanized on day 12 post inoculation and tumor infiltrating lymphocytes (TILs) were isolated. ILC were characterized as Lin^-CD45^+. Representative flow plots of the gating strategy from spleen from wildtype mice (A). ILC2s were defined into three individual subsets $KLRG1^+$iILC2s, $KLRG1^+ST2^+$mILC2s and $ST2^+$ nILC2s. ILC1s were defined as $Nkp46^+ROR\gamma t^-$. ILC3s were split into 2 subsets; NCR^+: $Nkp46^+ROR\gamma t^+$ and NCR^-; $Nkp46^-ROR\gamma t^+$. Representative flow plots from mice treated with isotype (top panel) and αPD-1 therapy (bottom panel) (B). Summary of ILC subset frequency in TIL (C). Summary of ILC subsets frequency (D) in spleen. N= 4-5 mice. Data shown as mean ± SEM.

4.3.7. $Tbet^+Nkp46^+ROR\gamma t^-$ ILC1s were significantly increased in a murine model of metastatic melanoma.

In an initial experiment assessing tumour growth in a murine model of subcutaneous model using wildtype mice, it was observed that wildtype mice appeared to have reduced metastasis when treated with αPD-1 antibody in comparison to treatment with isotype control (Figure 4.15). To further evaluate this, a metastatic model of melanoma was established. This was achieved by *Pdcd1*$^{-/-}$ and wildtype mice receiving an intravenous of B16 melanoma cells. This allowed B16 melanoma cells to establish in the lung. Mice were inoculated with 0.5 x 10^4 in order to optimise the model as it has not been established before. As tumour development occurs within the lung, mice health was monitored through changes in body weight. Consistent with the subcutaneous model, mice were euthanised on day 12 post inoculation. There were no visible tumours within the lungs, therefore no visible differences between the wildtype and *Pdcd1*$^{-/-}$ mice (Figure 4.15 A) nor was any difference observed within the lung weight. When immunobiology was assessed, however, there was a trend to show an increase in $NKp46^+ROR\gamma t^-$ ILC1s within the lung tissue ($p=0.08$; Figure 4.15 A-D). There was no differences noted within the other ILC subsets within the lung tissue; mirroring what was shown in the subcutaneous models of both melanoma and colon cancer model. Of note, no difference was noted in any of the ILC subsets within the TDLN, particularly important to note as this contrasts the finding seen in the subcutaneous model of melanoma.

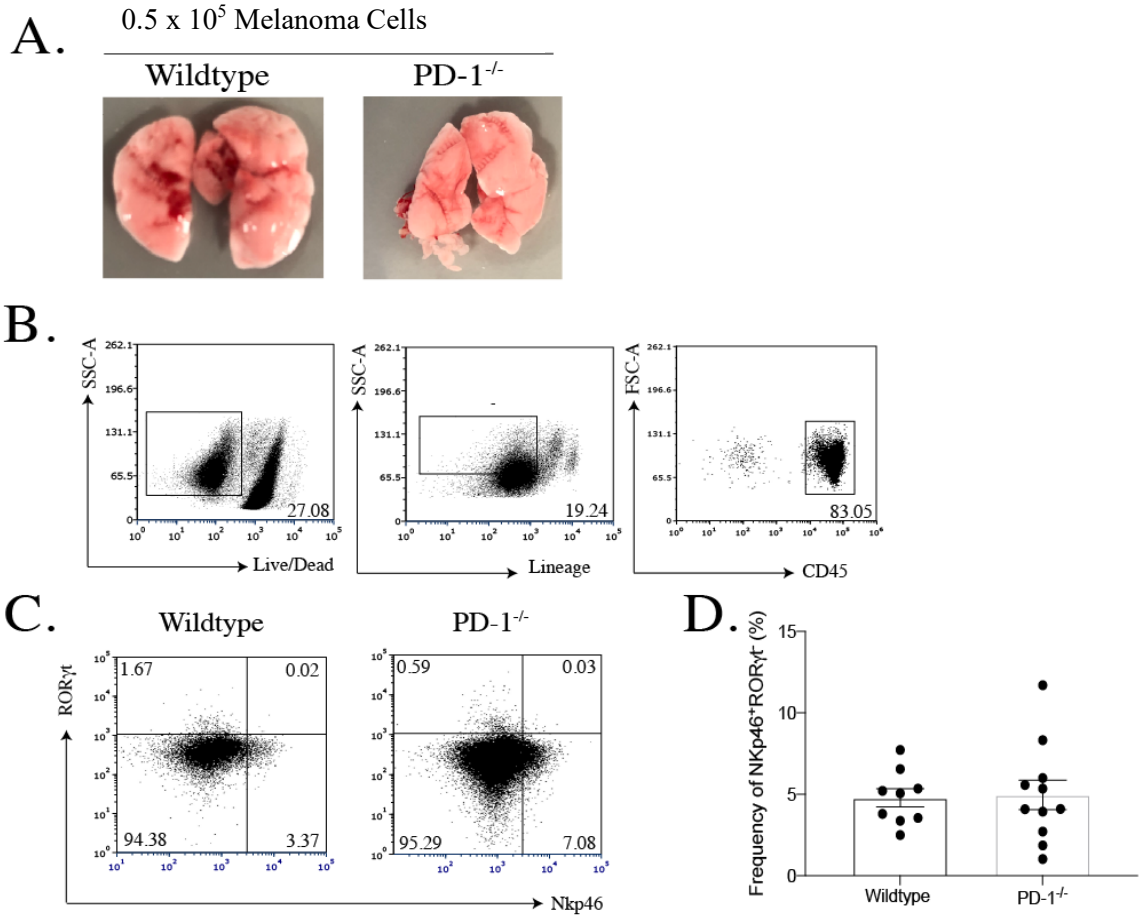
A.
0.5 x 10^5 Melanoma Cells
Wildtype
PD-1-/-
B.
SSC-A
Live/Dead
27.08
SSC-A
Lineage
19.24
FSC-A
CD45
83.05
C.
Wildtype
PD-1-/-
RORγt
Nkp46
1.67
0.02
94.38
3.37
0.59
0.03
95.29
7.08
D.
Frequency of NKp46+RORγt+ (%)
Wildtype
PD-1-/-
E.
KLRG1+
ST2+
KLRG1+ST2+
Nkp46+RORγt+
Nkp46-RORγt+
F.
Nkp46+RORγt-
KLRG1+
KLRG1+ST2+
ST2+
Nkp46+RORγt+
Nkp46-RORγt+
G.
Nkp46+RORγt-
KLRG1+
KLRG1+ST2+
ST2+
Nkp46+RORγt+
Nkp46-RORγt+

Figure 4.15: PD-1 blockade does not alter ILC subsets in the lung in a murine model of metastatic melanoma. Wildtype and PD-$1^{-/-}$ mice were administered with 0.5 x 10^4 B16 melanoma cells via intravenous injection. Mice were euthanized on day 14 post inoculation. Lung tissue and tumour draining lymph nodes (TDLN) were isolated. Representative images of lungs shown (A). ILC were characterized as Lin^-CD45^+. Representative flow plots of the gating strategy from lung from wildtype mice (B). Representative flow plots of NKp46 and RORγt$^-$ expression from wildtype and PD-$1^{-/-}$ mice shown (C). Summary of $NKp46^+ROR\gamma t^-$ ILCs within the lung tissue shown (D). ILC2s were defined into three individual subsets $KLRG1^+$iILC2s, $KLRG1^+ST2^+$mILC2s and $ST2^+$ nILC2s. ILC1s were defined as $Nkp46^+ROR\gamma t^-$. ILC3s were split into 2 subsets; NCR^+: $Nkp46^+ROR\gamma t^+$ and NCR^-; $Nkp46^-ROR\gamma t^+$. Summary of ILC subset frequency in TIL (E). Summary of ILC subsets frequency (F) and absolute cell count (G) in TDLN. N= 9-11 mice. Data represents 2 experiments. Data shown as mean ± SEM.

4.3.8. Absence of PD-1 protects mice against induced colorectal cancer

In order to further elucidate the role of PD-1 in the development of tumours and the function of ILCs, an inducible model of colorectal cancer was established. Mice were treated with a single dose of AOM (12.5mg/kg) and then received 3 cycles of DSS treatment (3% in drinking water). The first cycle lasted for 5 days and then due to rapid decline in murine health, cycles 2 and 3 were reduced to 3 days period. Clinical weight was used as a measured of clinical inflammation within the mice. In the absence of PD-1 there was a significant increase in weight loss which is linked with clinical weight loss (Figure 4.16A). Although absence of PD-1 was able to protect against tumour burden there was as significant increase in intestinal inflammation as shown by a decrease in intestinal length in *Pdcd1*$^{-/-}$ mice (Figure 4.16B-D). In order to assess the contribution of ILCs, large intestine and mesenteric lymph nodes (MLN) were isolated and lymphocytes from these tissues were analysed within the tissue. In the intestinal tissue there was no significant differences noted in either $Nkp46^+ROR\gamma t^-$ or in $Tbet^+Eomes^-Nkp46^+ROR\gamma t^-$ ILC subsets (Figure 14.16E). There was a trend to suggest an increase in $Nkp46^+ROR\gamma t^-$ cells within the MLN (p=0.09; Figure 4.16F) but no significance was reached. Colitis and intestinal inflammation have been suggested to be driven by ILC3 subsets (Geremia et al., 2011). Although again no significance was reached, there was a trend to suggest an increase in NCR^+ ILC3s within the intestine (p=0.09; Figure 17G) and a trend to suggest a decrease in NCR^- ILC3s within the MLN (p=0.07; Figure 17H). This could be an indication that ILC3s are indeed driving the inflammatory response seen in the absence of PD-1, and could be an indication that, as with human ILC3s, PD-1 may be regulating ILC3s within the tissue.

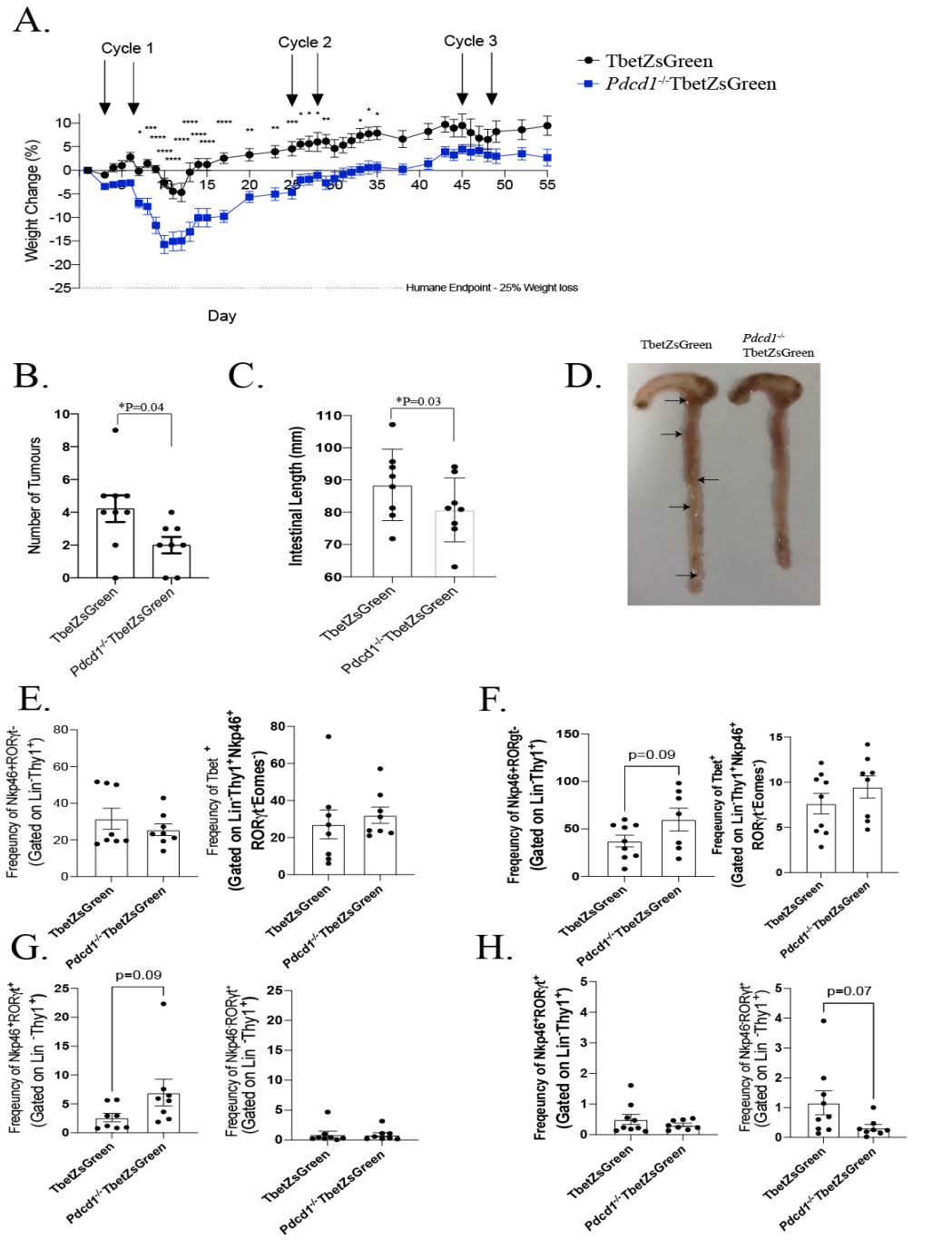

Figure 4.16: Absence of PD-1 protects against tumour burden in DSS induced colitis. TbetZsGreen and *Pdcd1*$^{-/-}$TbetZsGreen mice were treated with a single dose of AOM followed by 3 cycles of DSS. Weight loss was monitored throughout the experiment as a measure of clinical inflammation (A). Mice euthanised on day 55 and tissues were harvested. Tumour burden was assessed (B) and intestinal length was recorded (C). Representative image of large intestine within the experimental mice; arrows indicate tumour burden (D). Large intestine and mesenteric lymph node (MLN) were isolated and ILC components were analysed. ILCs were identified as Lineage^{-} (CD3, CD5, CD8, CD11b, CD11c, CD19, CD49b, Gr1, Nk1.1, F4/80 and Ter119) Thy1^{+}. Summary of Nkp46^{+}RORγt^{-} cells and Tbet^{+}Nkp46^{+}RORγt^{-}Nkp46^{+} within the large intestine (E) and within the MLN (F) and ILC3 subsets within the large intestine (G) and MLN (H). N=8-9. Data shown as Mean±SEM. *p<0.05, **p<0.005, ***p=0.0001 and ****p<0.00001

4.3.9. PD-1 signalling inhibits glycolysis in Tbet^{+}Nkp46^{+}Eomes^{-}RORγt^{-} ILC1s within the TME.

It has been demonstrated that PD-1 specifically regulates ILCs within the TME. In T cells, PD-1 signalling prevents glycolysis and increases fatty acid oxidation (Patsoukis et al., 2015). In T cells, metabolic profile is associated with T cell function with glycolysis being associated with an effector phenotype. Fatty acid oxidation on the other hand, is associated with T regulatory cells and a senescence phenotype. In order to determine whether PD-1 signalling modulated the metabolic profile of ILCs, ILC metabolism was assessed within ILCs within the TME. Prior to euthanisation, mice were treated with either fluorescently labelled BODIPY or 2-NBDG. BODIPY is a fluorophore which is conjugated to palmitate, a fatty acid which is up taken by the cell which means fatty acid oxidation can be measured by flow cytometry. Similarly, 2-NBDG is a fluorescent glucose analogue, which, through flow cytometry, can be used to measure cellular uptake of glucose. As this is a novel assay for our laboratory, the experiment was first optimised using wildtype mice.

In order to adequately assess metabolism, mice were treated with IL-33 (100ng/mouse) to stimulate ILC subsets. Mice were inoculated with either BODIPY (50ng/mouse) 60 minutes prior to euthanisation or 2-NBDG (100ug/mouse) 15 minutes prior to euthanisation. Splenocytes were isolated and ILCs were analysed by flow cytometry (Figure 4.17 A-C). Here it was demonstrated that, within Tbet^{+}Nkp46^{+}Eomes^{-}RORγt^{-} ILC1s, BODIPY fluorescence was able to be identified within the splenocytes. Equally there was an increase in 2-NBDG however as this was not as significant as previously reported literature, therefore in subsequent experiments 2-NBDG was administered by intravenous injection. For the tumour experiments, a subcutaneous model of B16 F10 melanoma was established in *Pdcd1*$^{-/-}$ and wildtype mice. Mice were treated with BODIPY or 2NBDG prior to euthanisation as previously described. There was a significant decrease in BODIPY signalling in the absence of PD-1 signalling, similarly there was a significant increase in 2-NBDG signalling in the *Pdcd1*$^{-/-}$ mice when compared with the wildtype mice (Figure 4.17 D-E). This suggests that with the lack of PD-1 signalling, there is a metabolic shift whereby there is an increase glucose uptake and a decrease with fatty acid oxidation.

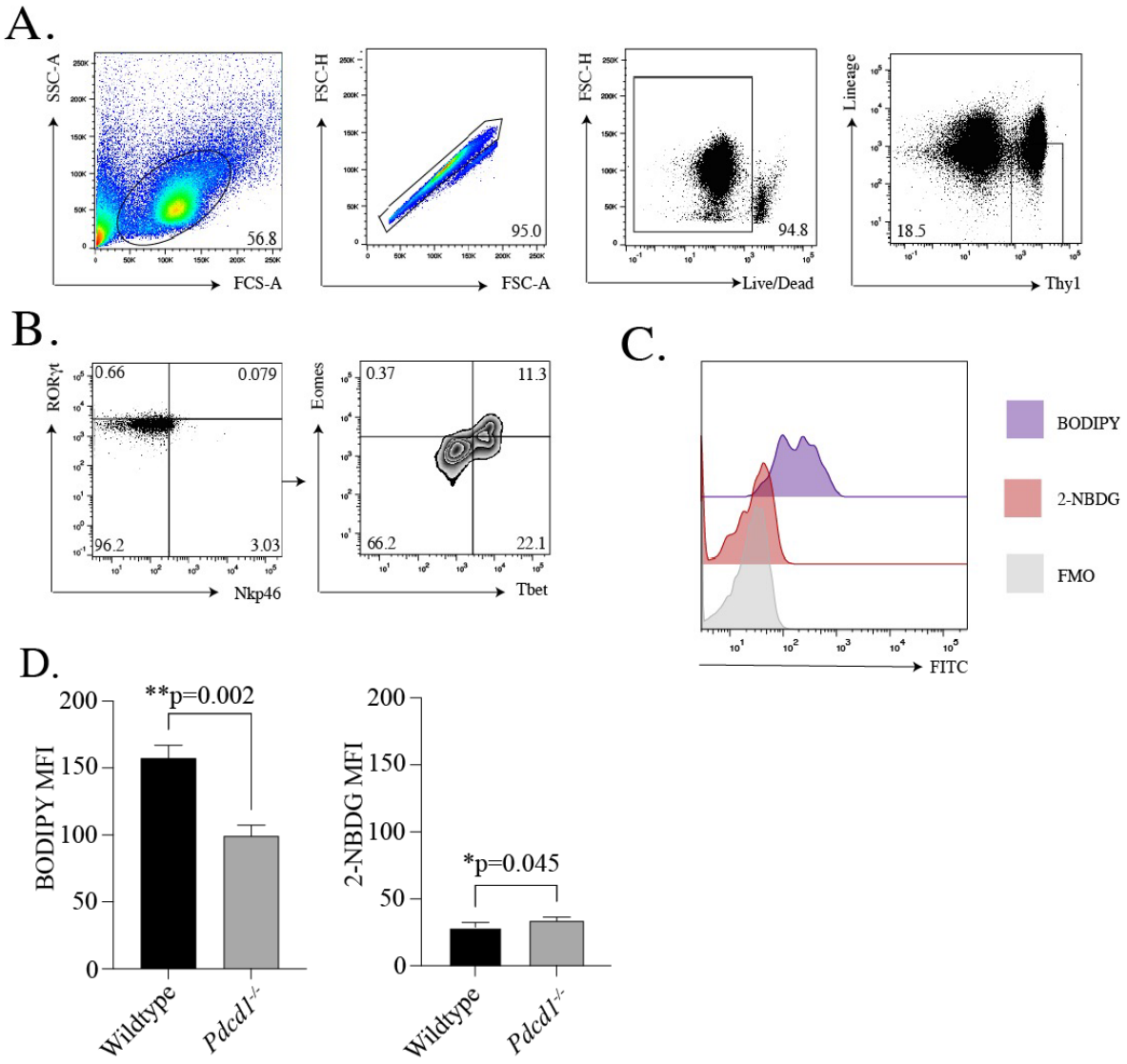

Figure 4.17: PD-1 regulates cellular metabolism in Tbet^{+}Nkp46^{+}RORγt^{-}Eomes^{-} ILC1s within the TME. Wildtype and *Pdcd1*$^{-/-}$ mice were inoculated with 2 x 10^5 B16 F10 melanoma cells via subcutaneous injection. Tumours were allowed to develop until a tumour size of 800-1000mm^3 and mice were euthanised. Prior to euthanisation mice were treated with either BODIPY or 2-NBDG for 60 minutes or 15 minutes respectively. TILs were then isolated and analysed by flow cytometry. Representative flow gating showing identification of ILCs (A) and Tbet^{+}RORγt^{-} Nkp46^{+}Eomes^{-} ILC1s. Flow data demonstrating optimisation experiment (C). Representative flow analysis of BODIPY staining in TbetZsGreen (Grey) and *Pdcd1*$^{-/-}$ TbetZsGreen (purple) mice. Summary of BODIPY and 2-NBDG staining (E). N=10, Data representative of 2 experiments; shown as mean +- SEM.

4.4. Discussion

PD-1 regulates Tbet^{+}Nkp46^{+}Eomes^{-}RORγt^{-} ILC1s within the TME by regulating cytokine production and cellular proliferation; an observation which was conserved in a subcutaneous and metastatic model of melanoma, subcutaneous model of colon cancer and inducible AOM model of colon cancer.

It was first established that in the absence of PD-1, there is a significant decrease in tumour growth and increased survival (Figure 4.1). As these mice are immune competent and have fully functioning immune system it was unclear what was driving this immune protection as PD-1 is known to regulate both the adaptive and innate immune system. In order to assess the contribution of the innate immune system in protecting against tumour development, this model was established in *Rag*$^{-/-}$ whereby there was a significant decrease in tumour development observed in the absence of both an adaptive immune system and NK cells. In this experiment, it was observed that the was an increase in survival within the mice treated with αPD-1 therapy and combined αPD-1 and αNK1.1 therapy (Figure 4.2). Since no difference was noted between these groups, it suggests that NK cells are not contributing to the protective effect and so it appears to be driven by other innate immune cells. Since tumour associated macrophages have also been shown to aid in tumour protection in the absence of PD-1, it was then important to determine whether ILCs were indeed contributing to this phenotype. When the innate immune cells were assessed within the TME, no differences were noted within any of the other innate immune cells, namely monocytes, macrophages and dendritic cells (Figure 4.5). There was a difference noted in Lin^{-}CD45^{+} cells, whereby in the absence of NK cells and in the absence of both NK cells and PD-1, there was an increase in ILCs suggesting that, in the absence of NK cells, there is an increase in ILCs. Here, ILCs were gated on Lin^{-}CD45^{+} and not sub-divided into subsets, which could explain why no increase was seen in αPD-1 treatment alone as in subsequent studies only a single subset was shown to be upregulated by αPD-1 therapy. However, in *Rag*$^{-/-}$ mice, αPD-1 therapy was unable to induce an increase in Nkp46^{+}RORγt^{-} ILC1s which was seen in other strains, this could be due to large variation between mice, or as a result of inability of therapy to sufficient provide PD-1 blockade. However, it is unlikely to be as a result of poor therapy blockade as immune competent mice responded well to therapy. Although a difference wasn't observed, ILC blocking experiment demonstrating that in the absence of NK cells and ILCs, there is no protective effect from αPD1 therapy confirming that ILCs are driving the protective effect from αPD1 therapy.

Moral et al demonstrated that ILC2s were regulated by PD-1 following stimulation from IL-33 (Moral et al., 2020). Here, it has been shown that in the absence of any additional stimuli, and in response to the TME alone, $Tbet^{+}Nkp46^{+}ROR\gamma t^{-}$ ILC1s were significantly increased and increased cytokine production and proliferation. Data supports the idea that PD-1 expression and therefore activation in ILCs is driven by ILC activation from stimuli within the TME driving specific subsets. This maybe explain why, within our study, in the absence of exogenous stimuli such as IL-33, there was no observed increase in ILC2s.

Of note, although there were no differences in ILC subsets noted within the spleen, there was a significant increase in $ST2^{+}$ ILC2s within the TDLN, with no changes noted in the $NKp46^{+}ROR\gamma t^{-}$ population. One possible explanation for this could be that the ILC2s are migrating from the lymph nodes to the TME where they are converting into ILC1 subset. Intracellular cytokine staining demonstrated an increase in ILCs expressing both type 2 cytokines and IFNγ in the absence of PD-1 (Figure 4.9), suggesting that the TME could be driving ILC plasticity. If this resulting in increase IFNγ excretion into the TME, this would drive ILCs towards a favourable type one phenotype however further analysis on ILC migration would be required to determine this.

Group 1 ILCs include both NK cells and ILC1s. Both express Tbet but can be distinguished from each other based on the expression of Eomes which is not expressed by ILC1s. Of note, cells can also be distinguished based on their expression of CD49a and CD49b. CD49a is expressed by ILC1s which is associated with tissue resident cells, however NK cells circulating marker CD49b; which is including in the lineage panel. $Eomes^{+}Tbet^{+}$ cells have shown cytotoxicity, and reduction in expression of Eomes and CD49b were associated with non-cytotoxic ILC1s which were unable to mount an anti-tumour response (Gao et al., 2017). However, here although there is an increase in $Tbet^{+}Nkp46^{+}ROR\gamma t^{-}Eomes^{-}CD49b^{-}$ ILC1s, this is associated with an increase in IFNγ producing cells suggesting that this subset that has been identified here is in fact a beneficial to anti-tumour defence.

A murine model of inducible colon cancer was established to further evaluate ILC contribution to tumour development. As this model is inducible it provides a more accurate TME as the tumour cells have developed within the tissue as opposed to being engrafted. Here, it was demonstrated that in the absence of PD-1, mice succumbed to increased intestinal inflammation however were protected against tumour burden. Although there was no significant difference noted in ILC components there was trends to indicate changes in ILC3 components. There is a

trend to suggest a decrease in NCR^- cells within the MLN however an increase in NCR^+ cells within the intestinal tissue. As NCR^+ cells are associated with inflammation it is possible that they are driving this inflammation. Of notes, analysis of the TILs (carried out by Dr Amarnath) noted an increase in $Tbet^+Nkp46^+$ ILC1s specifically within the TME, which highlights the high tissue specificity of PD-1 regulation of ILCs. This could also be the first indication in mouse that ILC3s may be regulated by PD-1 in intestinal inflammation and interesting to note, that although it is driving excessive inflammation, there is still protection against tumour development.

In T cells it has been demonstrated that PD-1 alters the cells metabolic profile by preventing glycolysis and promoting fatty acid oxidation (Patsoukis et al., 2015). ILC2s were shown to respond to PD-1 signalling in a similar way whereby in an airway inflammation model, PD-1 prevented cellular glycolysis and this results in decreased cellular activation. It was plausible, therefore, that this might be the case within the TME and here we were able to show that that was the case, with an increase in glycolysis and decrease in fatty acid oxidation *Pdcd1*$^{-/-}$ ILCs. This shift of metabolic profile in T Cells alters the T cells phenotype whereby fatty oxidation and oxidative phosphorylation is associated with senescence and a regulatory phenotype, showing that PD-1 signalling drives this phenotype and therefore reduces the effector phenotype. As ILC subsets mirror T cell subsets it is reasonable to speculated that this shift in metabolism by PD-1 activation and would similarly drive a regulatory phenotype within ILCs and cause a reduction in ILC function.

4.5. Conclusions:

In this chapter I have shown that:

- Absence of PD-1 protects against tumour growth in immune competent mice, *Rag*$^{-/-}$ and in the absence of NK cells
- The only innate immune subset which is affected by the absence of PD-1 are ILCs
- Absence of PD-1 significantly increases NKp46^{+}RORγt^{-} ILC1s both in response to genetic ablation and in response to therapy; an observation unique to the TME.
- Specifically, these cells do not express Eomes.
- Absence of PD-1 regulates these ILCs through reducing cellular cytokine expression and proliferation.
- Observations have been repeated in several models including MC38 colon cancer and metastatic melanoma
- PD-1 drives fatty acid oxidation within Tbet^{+}NKp46^{+}Eomes^{-}RORγt^{-} ILC1s and reduces glycolysis; thus altering cellular metabolic profile.

Chapter 5: Human Tbet^{+}Nkp44^{+}RORγt^{-} ILC1s are regulated by PD-1

5.1. Introduction

In human, ILCs have been shown to express PD-1 in several cancers (Salimi et al., 2018, Tumino et al., 2019). In human decidua tissue, ILC3s not only express PD-1, but also adapt during pregnancy and down regulate PD-1 expression as pregnancy advances. Furthermore, ILC3s cultured with αPD-1 were also shown to have reduced capacity to produce cytokines (Tumino et al., 2019). PD-1^{+} ILC2s isolated from human PBMCs also showed reduced cytokine production (Taylor et al., 2017). Although PD-1^{+} ILCs from all subsets have been identified within the TME, whether ILCs directly respond to anti-PD-1 cancer therapy in human tumour tissue remains unknown. This project, thus far, has demonstrated in mouse, that Tbet^{+}Nkp46^{+}RORγt^{-} ILCs were regulated by PD-1 signalling exclusively within the TME. PD-1 specifically regulated the cytokine production and proliferation of these cells within the TME. Here, it was sort to determine if the same regulation occurs within human ILCs.

5.2. Aims

The aims of this chapter were to determine whether the PD-1 regulation was shown within the mouse models were able to be replicated within human cells. Specifically, the aims were:

- Determine whether all ILC subsets can be identified within human and identify whether they are capable of expressing PD-1.
- Assess whether human tumour cell lines induce PD-1 expression within ILCs
- Determine whether PD-1 can regulate human ILC function through modulation of cellular proliferation

5.3. Results

5.3.1. ILC subsets are presents within healthy donor human PBMCs

To establish the role of PD-1 in regulating human ILCs, it was first important to establish a robust method of identifying ILCs within human PBMCs. Healthy donor PBMCs were kindly isolated by Jonathon Scott. Cells were then stained and analysed by flow cytometry in order to identify ILC subsets. As with the mice, all ILCs were defined as lineage negative (CD3, CD8, CD14, CD20, CD56, CD5, CD11b, CD11c, TCRα/β). Human ILCs are then further defined as $CD45^{+}CD161^{+}CD127^{+}$. ILC2s were defined as positive for prostaglandin D2 receptor; $CRTH2^{+}$. ILC3s were defined as $CRTH2^{-}CD117^{+}ROR\gamma t^{+}$ and then subdivided into $NKp44^{+}$ (NCR^{+}) and $NKp44^{-}$ (NCR^{-}). ILC1s in the literature have been previously defined as $CRTH2^{-}CD117^{-}$. Here we also identified ILC1s as $Tbet^{+}$ and through expression of Nkp44. All ILC subsets were capable of being identified within human PBMCs (Figure 5.1.A). During this assessment PD-1 expression was also examined on the ILCs subsets within the healthy donors in the absence of stimulation (Figure 5.1.B). The highest PD-1 expression was noted within the ILC2s subset when compared with ILC1 and ILC3s, consistent with previously reported data (Salimi et al., 2018).

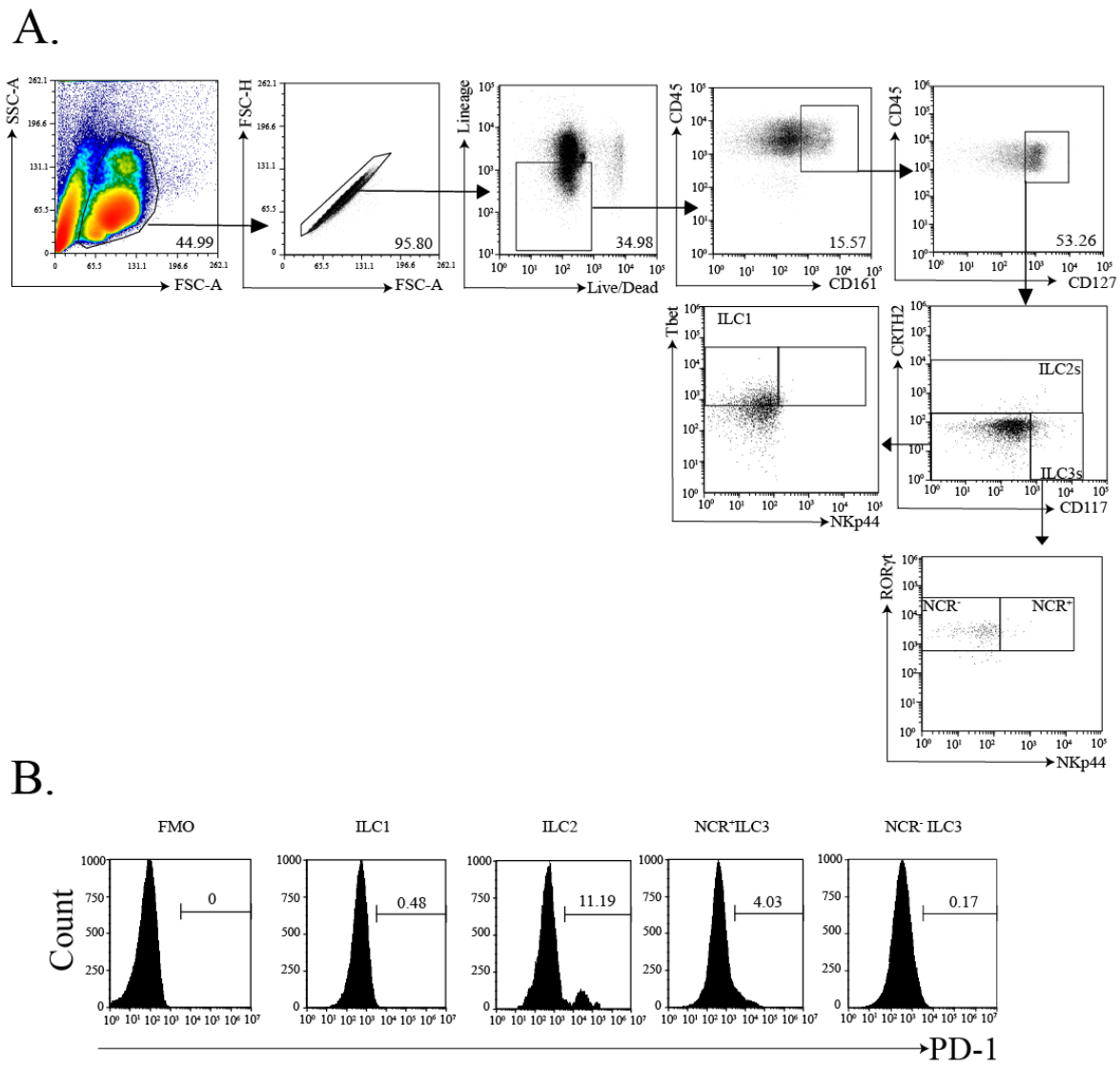

Figure 5.1: ILC Characterisation in human PBMCs. PBMCs were donated by healthy human donors. ILCs were stained by flow cytometry in order to analyse ILC subsets within the PBMCs. Representative flow plots of ILCs in human PBMCs. ILCs were defined as $Lin^{-}CD45^{+}CD161^{+}CD127^{+}$. ILC2s were described as $CRTH2^{+}$. ILC3s were described as $CRTH2^{-}CD117^{+}$ and then further distinguished into NCR^{+} and NCR^{-} based on the expression of Nkp44. ILC1s were defined as $CRTH2^{-}CD117^{-}Tbet^{+}$. Subsequently they were defined as ILC1s ($Nkp44^{-}$) and ex-ILC3s ($Nkp44^{-}$) (A). Representative plots showing PD-1 expression in human ILC subsets. Representative sample shown. N=1.

5.3.2. Tumour secretome upregulates PD-1 expression in Tbet^{+}Nkp44^{+}RORγt^{-} ILCs

PD-1 expression in human ILC3s correlates with tissue expression of PDL-1 (Vacca et al., 2019) demonstrating that, as with murine ILCs, PD-1 expression is driven by the tissue environment. In mouse it was demonstrated that the tumour secretome from a murine melanoma cell line was sufficient to induce PD-1 expression in ILCs and therefore it was sought to determine whether this mirrored in human ILCs. Healthy donor PBMCs were isolated and cultured overnight with transwells containing human tumour cell lines C8161 and MET1. C8161 is a human metastatic melanoma cell line which was used to ensure consistency with the murine data. MET1 is a cutaneous squamous cell carcinoma (cSCC) cell line. A recent clinical study has shown that patients with metastatic (cSCC) treated with cemiplimab (an anti-PD-1 therapy) showed 50% progression free survival (Migden et al., 2018). cSCC is an aggressive skin cancer and has a significant increase in risk with patients undergoing immunosuppressive treatment suggesting a strong immune contribution to protection against disease progression. As it is unclear the mechanism as to how PD-1 functions in cSCC, MET1 cell line was utilised here to establish whether ILCs may contribute to any of the immunobiology. Previous experiments within the laboratory carried out by BSc Student Amy Towler identified C8161 and MET1 cell lines to both express substantial levels of PDL-1 and therefore were most likely to evoke a response in the PBMCs (Data not shown). PBMCs were incubated at a 1:1 ratio with tumour cell lines overnight. Cells were then analysed by flow cytometry in order to identify ILC populations and assessed PD-1 expression was assessed (Figure 5.3.). cSCC cell line MET1 significantly increased the expression of PD-1 on Tbet^{+}Nkp44^{+} cells from PBMCs ($p=0.03$) as did the melanoma cell line ($p=0.01$).

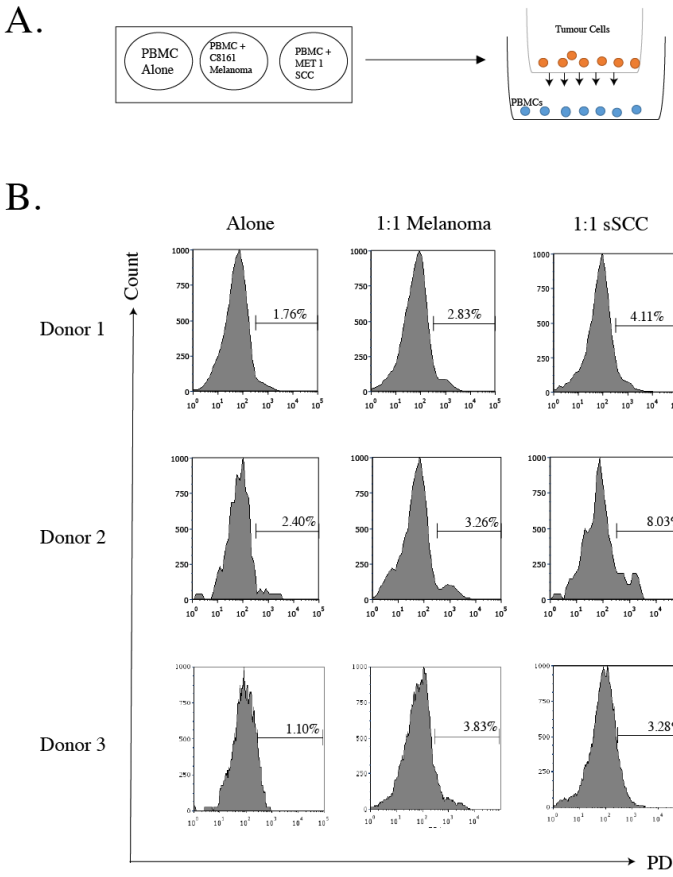

Figure 5.2. PD-1 is induced by the human tumour secretome in human Tbet^{+}Nkp44^{+} ILC1s. PBMCs were isolated from healthy donors. Cells were cultured with transwells containing either human melanoma cell line C8161 or human cSCC cell line MET1. Cells were cultured overnight before being harvested and analysed by flow cytometry (A). ILCs were gated on Lin^{-} CD45^{+}Tbet^{+}Nkp44^{+} ILC1s and PD-1 expression was assessed (B). Summary of PD-1 expression was shown (C). N=3. Data is shown as Mean ±SEM.

5.3.3. PD-1^{+}Tbet^{+}Nkp44^{+}RORγt^{-} ILC1 subset identified within the TME of cSCC patients

The cSCC cell line secretome induced significant levels of PD-1 expression within ILCs in PBMCs. Although the immune component of the TME in cSCC patients has recently been described (Migden et al., 2018), whether ILC subsets are present is still unknown. As cSCC cell lines can significantly upregulate PD-1 expression on Tbet^{+}Nkp44^{+} ILC1s, if ILCs are indeed present within the TME, this could provide an insight and a possible mechanism into how these cancers may be responding to cancer therapy. Primary cSCC tumours were kindly acquired and processed by Dr Chester Lai. Flow cytometry files were then transferred from Southampton to Newcastle for analysis. Here, I carried out t-distributed stochastic neighbour embedding (tSNE) analysis on TILs and PBMCs from patients. tSNE is a statistical tool which creates a two-dimensional map of complex data sets based on the probability of the relationship between each of the data points. Data points closely related to each other are most likely to neighbour each other and form "clusters". These clusters are then identified as specific cell populations based on the expression of markers such as transcription factors or cell surface proteins, as they would be in flow cytometry. It is key to note, that the distance between each population cluster is not a representation of how closely related the clusters are. Prior to identifying the clusters, tSNE plots were created to visualise the populations. Plots showing individual donors are shown to ensure that the clustering of populations is based on cell type and data points are not clustering based on differences between samples. Clusters are identified manually with the aid of the density plots for clarification and colour coded for subsequent analysis of marker expression (Figure 5.3 A). Expression of proteins of interest (i.e. Tbet, NKp44, RORγt and PD-1) were then visualised based on the level on MFI, which was then quantified for each cluster and plotted on a heatmap in order to identify populations (Figure 5.3. B). tSNE analysis identified a cell population PD-1^{+}Tbet^{+}Nkp44^{+}RORγt^{-} which was only found to be present within the TME and was absent from the PBMCs (Figure 5.3). Notably, several other cell types identified, also appeared to express markers associated with multiple subsets, suggesting that cells may be unstable and may be converting between subsets within the TME. Subsequent analysis of healthy donor PBMCs also showed an inability to identify the PD-1^{+}Tbet^{+}Nkp44^{+}RORγt^{-} population suggesting, this population is exclusive to the TME in cSCC patients.

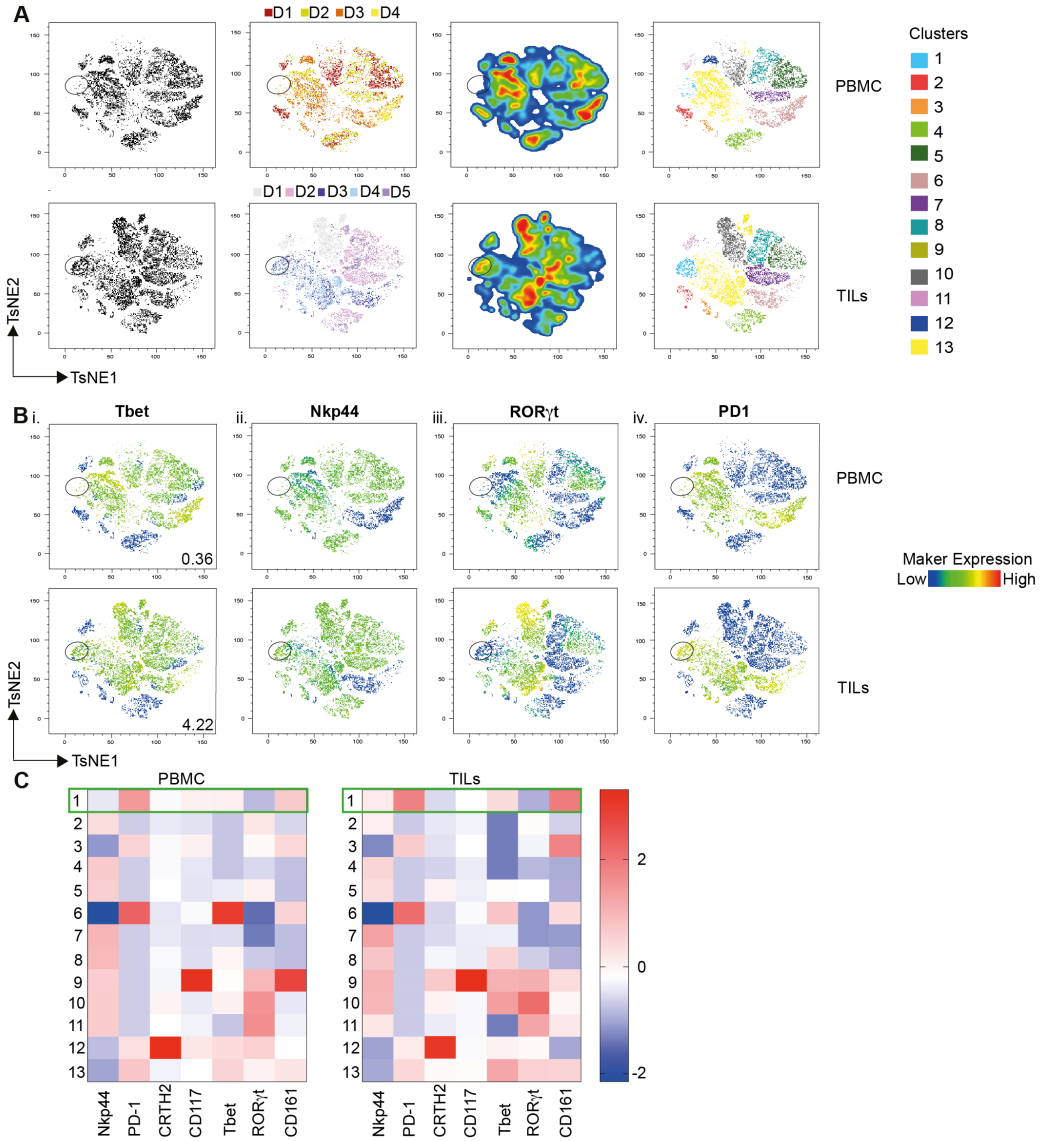

Figure 5.3. PD-1 is expression by Tbet^{+}Nkp44^{+}RORγt^{-} ILC1s within the cSCC Tumour. Blood and tumour tissue were obtained from cutaneous squamous cell carcinoma (cSCC) patients and ILCs were characterised using flow cytometry. ILCs were characterised as Lin^{-}CD45^{+}CD127^{+}CD161^{+}. TsNE analysis of ILC populations on samples from 5 cSCC donors and 4 matched blood donors are shown as population plot, individual donors, population density and individual clusters(A). Expression levels of Tbet (Bi), Nkp44 (Bii), RORγt (Biii) and PD-1 (Biv) shown in PBMCs (top panel) and TILs (bottom panel) (B). Heatmap summary of marker expression in PBMCs (Left panel) and TILs (Right panel). N=4-5.

5.3.4. PD-1 drives proliferation in Tbet^{+}Nkp44^{+}RORγt^{-} cells

PD-1 regulates cellular function in T cells. In our murine model, it was demonstrated that PD-1 regulates the cellular function of Tbet^{+}Nkp46^{+}RORγt^{-} ILC1s through downregulation of cellular proliferation and cytokine production. The question therefore remained whether the same was possible in human Tbet^{+}Nkp44^{+}RORγt^{-} ILC1s. To do this, human PBMCs were isolated from healthy donors by Dr Jonathan Scott. PBMCs were then stained with cell trace violet which is a "dilution" dye, whereby the dye intensity is reduced on every proliferation. Cells were then cultured for 5 days with IL-2 (40ng/ml) and IL-7 (40ng/ml) in the presence of either αPD-1 antibody (10mg/ml) or isotype control (10mg/ml). Cells were then harvested and analysed by flow cytometry. Here, it was demonstrated that there was an increase in the proliferative capacity of Tbet^{+}Nkp44^{+}RORγt^{-} ILC1s from healthy donors when PD-1 signalling was blocked by αPD-1 antibody (Figure 5.5) suggesting that PD-1 signalling can indeed control proliferation in these cells as was shown previously in mouse.

A.

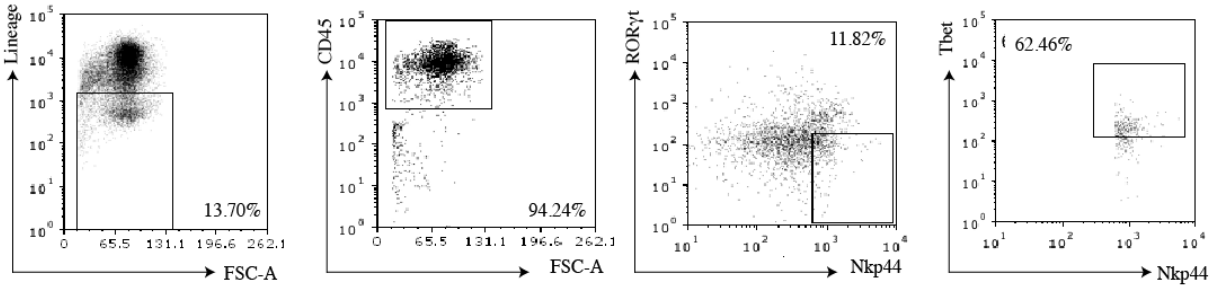

B.

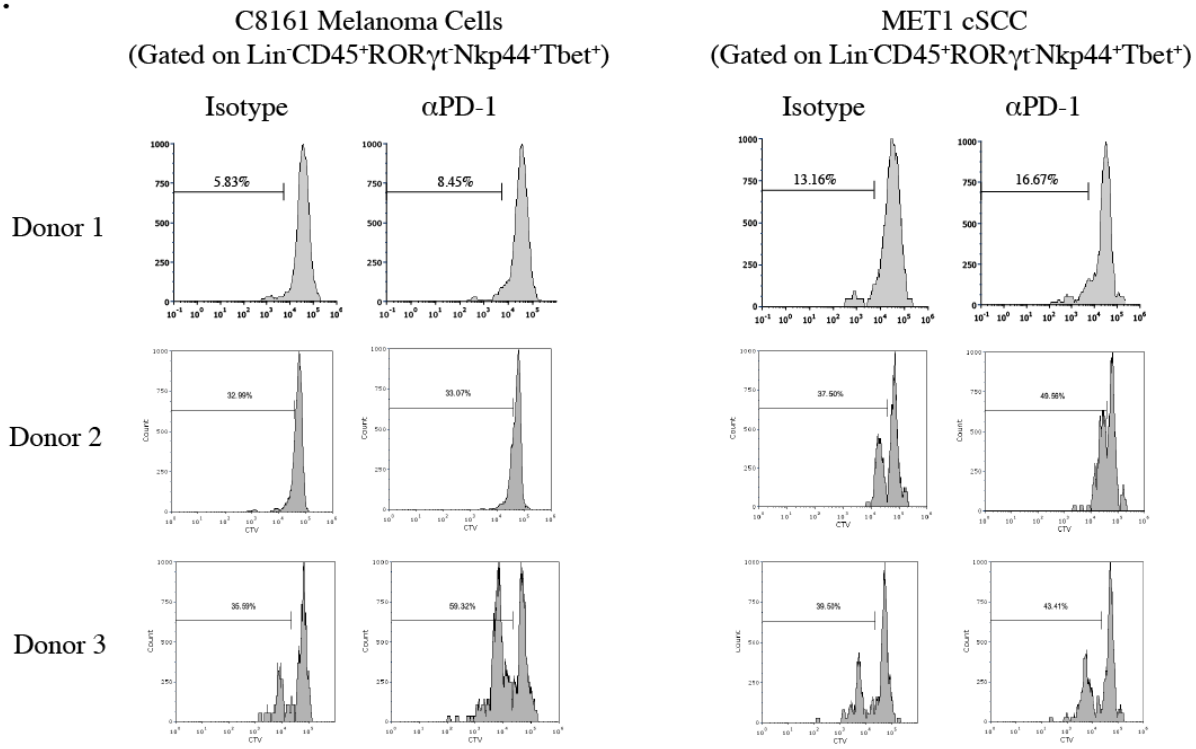

Figure 5.5. PD-1 blockade drives the proliferation of Tbet$^+$Nkp44$^+$RORγt$^-$ cells. PBMCs were isolated from healthy donors. Cells were stained with Cell trace violet and then cultured for 7 days in the presence of IL-2, IL-7 and in the presence or absence of αPD-1 antibody or isotype control. ILCs were then harvested and isolated and identified by flow cytometry. ILCs were defined as Lineage$^-$CD45$^+$RORγt$^-$ Nkp44$^+$Tbet$^+$ ILC1s (A). Cell trace violet was then examined via flow cytometry as analysis of cellular proliferation (B). N=3.

5.4. Discussion

ILC populations within PBMCs expressed PD-1 in healthy donors in the absence of exogenous stimulation (Figure 5.1). As with mice, all ILC subsets were shown to be capable of expressing PD-1 however expression levels varied between subsets, with the most expression being shown in ILC2s, consistent with (Salimi et al., 2018). Consistent with the murine data, PD-1 expression was able to be induced by the tumour secretome and did not require direct contact with the tumour cells (Figure 5.2). However, as with the splenocytes in the mouse experiment, transwell experiments were conducted in the presence of PBMCs so it is unknown at this time whether PD-1 expression is driven by activation from other immune cells or from the tumour secretome directly.

Within the cSCC patient samples, PD-1$^+$ Tbet$^+$Nkp44$^+$ RORγt$^-$ ILC1s were identified almost exclusively within the TME (Figure 5.3). This mirrors the data which has been shown within mice, which demonstrate a stringent tissue specific regulation of these cells. This could be particularly important as it could aid in reducing off target adverse effects of immunotherapy treatment. Cell proliferation was further shown to be increased in the presence of tumour cells in this human subset and cytokine production was also shown to be increased. Here there was no significant differences overall due to large variation between patients, however in each case there is consistently an increase in cellular proliferation in response to anti-PD-1 therapy in every patient. This is in line with the murine data that has been acquired suggesting that PD-1 regulation is conserved between murine and human. This provides promising indications that PD-1 therapy maybe be able to regulate specific ILC subsets within the TME.

5.5. Conclusion

In conclusion human data and analysis has demonstrated that:

- All human ILC subsets can express PD-1 in PBMCs in the absence of stimulation
- PD-1 expression on human Tbet$^+$Nkp44$^+$RORγt$^-$ cells is induced by the tumour secretome and direct contact with the tumour is not required.
- PD-1 expression on Tbet$^+$Nkp44$^+$RORγt$^-$ cells is significantly upregulated within the TME in patients when compared with PBMCs.
- Absence of PD-1 drives the proliferation of Tbet$^+$Nkp44$^+$RORγt$^-$ ILC1s.

Chapter 6: Discussion

Therapies targeting PD-1 have had significant success within the clinic in treating numerous cancers including melanoma, colorectal and ovarian cancer (Zhang et al., 2020, Krempski et al., 2011). However, as PD-1 therapies are associated with severe adverse effects, and have a limited success rate (~50%), a full understanding of the role of PD-1 in the regulation of immune cells within the TME is needed in order to improve patient responses. This project focused on a specific subset of innate immune cells, namely ILCs. PD-1 regulation of ILCs had previously been shown in alternative murine models; obesity and helminth infection (Taylor et al., 2017, Gordon et al., 2017). Although all ILC subset had been shown to express PD-1 within patients with gastrointestinal and breast cancer (Tumino et al., 2019), the role of PD-1 in ILC regulation in cancer remained undetermined. Additionally, the role of ILCs in tumour progression was also yet to be elucidated.

This project aimed to address three major questions:

1) Are ILCs regulated by PD-1 within the TME?
2) Do ILCs respond to αPD-1 therapy within the TME?
3) Does blockade of PD-1 on ILC subset enhance pro-tumorigenic or anti-tumorigenic properties?

This project determined that PD-1 negatively regulated group 1 ILC subset ($Tbet^{+}NKp46^{+}NK1.1^{-}ROR\gamma t^{-}$). In the absence of PD-1 signalling, these ILC1s were increased exclusively within the TME, and demonstrated an increase in type 1 cytokine expression. The equivalent population was also identified within human cSCC tumours and increased cellular proliferation in response to PD-1 blockade. Due to their critical role in anti-tumour responses, $CD8^{+}$ T cells have been widely studied for their response to CPI therapy. Here, the ILC1 subset has been described for the first time to respond exclusively within the tumour tissue to anti-PD-1 therapy and in doing so enhances anti-tumour responses.

In this project, the role of PD-1 regulation of ILC1s has been demonstrated in three different tumour models using two different cell lines. This has been performed in order to determine whether any differences seen are exclusive to specific tumour or tissue environments, however, it has been demonstrated that these findings are conserved across tumour models. This is particularly beneficial when contemplating future therapeutics as it suggests that targeting ILC1s is not restricted to a single cancer setting. In all models, ILC1s were exclusively

upregulated within the TME. These observations were coupled with an increase in the expression of IFNγ. IFNγ drives anti-tumour responses through MHC I upregulation in tumours and its absence is associated with increased tumour progression (Martini et al., 2010). This suggests that ILC response to PD-1 therapy could be beneficial in promoting anti-tumour responses. This project has not only identified a potential new therapeutic target within cancer immunotherapy, but has also raised a multitude of new questions and considerations, which unfortunately, were not possible to address within the time frame of this project. These considerations include the role of the adaptive immune system, the origins and location of ILC1s and the role of PD-1 on ILC1 metabolism.

Adaptive immune System

One of the key benefits of ILCs as an anti-cancer target, highlighted throughout the project, is their tissue residency and the implications that they may already be present in non-immunogenic "cold" tumours. Cold tumours, with poor immune infiltration, could benefit most from the increase in ILC1s and their ability to drive an anti-tumorigenic microenvironment. The hope would be that the increase in ILC1s could drive infiltration of cytotoxic cells such as $CD8^+$ T cells into the TME to aid in tumour elimination. Similarly, through increasing production of IFNγ, if this is proven to be secreted by the ILC1s, this creates a favourable TME for anti-tumour responses which can influence macrophage polarisation, $CD4^+$ T cell polarisation and increased elimination of tumour cell (Nathan et al., 1983, Song et al., 2019).

It has been shown here that ILCs respond to PD-1 therapy in $Rag^{-/-}$ mice, in the absence of T cells. However, in an immune competent mouse, it is likely they respond synergistically and interact with each other. ILC2s can drive naïve T cells to a Th2 phenotype also demonstrating that ILC2s can behave as APCs by presenting antigen through MHC II (Mirchandani et al., 2014). In contrast, ILC3s are capable of rendering Th17 anergic through MHC II (Hepworth et al., 2015). There is currently no evidence to suggest ILC1s express MHC II, so whether they would also be capable of inducing Th1 and $CD8^+$ is unclear but this would be important to fully elucidate in the future. The evidence here shows ILC1s associated with enhanced anti-tumour responses so it would be assumed that if MHC II was confirmed, ILC1s would enhance effector T cell responses.

There is also limited evidence to determine ILC1s capability of killing tumour cells directly. As they are shown to provide anti-tumour defence in the absence of adaptive immune cells,

ILCs must be pivotal in anti-tumour responses; but how is still yet to be determined. The caveat here may be that in $Rag^{-/-}$ mice there may be an alteration in the TME due to lack of adaptive immune cells - whether this is a factor that can influence ILCs remains undetermined. NK cells are known to produce substances such as granzyme and perforin which can directly kill tumour cells. $Rag^{-/-}$ mice treated with αNK1.1 demonstrated that ILC subsets are able to directly reduce tumour growth in the absence of NK cells. Gao *et al* demonstrated that NK cells within the tumour convert to a non-cytotoxic, immune suppressive ILC1 phenotype in the presence of TGFβ (Gao et al., 2017), however, here an ILC1 subset has been shown to enhance tumour elimination.

This project has demonstrated that ILCs, in the absence of an adaptive immune system, are capable of driving anti-tumour responses, however due to their low cell number, it is unlikely that they drive anti-tumour mechanisms in isolation. It is well documented that cytotoxic cells such as $CD8^+$ T cells play a critical role in tumour elimination and respond well to CPI therapy both in murine models and within the clinic. The question that this project raises, is the importance of ILCs in boosting this response. Future work would be required to decipher the exact interaction between the cell subsets. This could be done in a multitude of ways. One such method could adoptively transfer ILCs and $CD8^+$ cells into tumour bearing $Rag^{-/-}\gamma c^{-/-}$ mice which lack both an adaptive and innate immune system. This would then highlight whether combination of ILC1s and $CD8^+$ can provide more potent anti-tumour response than $CD8^+$ T cells or ILC1s alone.

Different Tumour Types

ILC1s were first shown to respond to blockade of PD-1 signalling in a subcutaneous murine model of melanoma. In addition, the use of several other models, including a metastatic melanoma model, a subcutaneous model of colon cancer and an inducible model of colon cancer were used. The B16 melanoma model is an aggressive fast growing, metastatic tumour line which is associated with poor immune cell infiltration which could really benefit from ILC presence within the TME to help boost immune cell infiltration. On the contrary, with the MC38 cell line, tumours have immune infiltration but are slower growing and respond to therapy. Both these contrasting models demonstrated an increase in ILC1s within the TME. Although ILC1s respond specifically in the TME compared with other tissues including TDLN and spleen, these experiments have demonstrated that this is consistent across tumour models. There are benefits of using engrafted tumour models as they are rapid models which can be used to easily monitor

tumour growth and immunology, however there are also limitations with these models. An inducible colon cancer model was utilised within this project in order to provide a model with a more translatable TME. The inducible model allows the tumours to develop in the relevant tissue in the relevant microenvironment. This is a particularly important tool when considering tissue resident subset of cells such as ILCs. It provides a more realistic TME. As the tumours have developed in the relevant tissue, it provided with the opportunity to study the surrounding tissue where it was shown that there was an increase in NCR^+ ILC3s and a decrease in non-inflammatory NCR^- ILC3s.

Of note, observations of an increase in $Nkp46^+ROR\gamma t^-$ ILC1s in wildtype mice were not shown to be increased in *Rag*$^{-/-}$ mice. This could be as a result of several factors including 1) efficacy of αPD-1 therapy and the ability for the therapy to sufficiently reach the tumour 2) requirement of adaptive immune systems to interact with ILCs to direct the anti-tumour response 3) $Nkp46^+ROR\gamma t^-$ does not provide sufficient identification of the ILC1 cellular subsets. Although drug delivery may have played a factor in the inability of ILCs to respond, it is unlikely there is insufficient blockade as immune competent mice showed significant response to therapy. The adaptive immune system has also been demonstrated not to be required for murine survival in melanoma. Therefore, it is likely that this lack of response to therapy in our model could be due to an inability to detect $Tbet^+$ ILCs within these early experiments. To further elucidate this, it would be required to generate *Rag*$^{-/-}$*TbetZsGreen* which would enable more specific identification of ILC1s in the absence of an adaptive immune system.

PD-1 Expression and Regulation

Pdcd1$^{-/-}$ mice demonstrated an increase in murine survival in subcutaneous tumour models using both melanoma and colon cancer cell lines. Experiments in $Rag^{-/-}$ where NK cells were blocked still demonstrated protection against tumour development with αPD-1 therapy, however when ILCs were blocked this protection was lost. This demonstrates a pivotal role for ILCs in protecting against tumour development. In the inducible model of colon cancer, mice not only demonstrated a decrease in tumour burden, but also an increase in intestinal inflammation. These experiments were carried out in immune competent mice, however, an increase in NCR^+ ILC3s was indicated within the intestine surround the tumour tissue. This data provides evidence that ILC3s are regulated by PD-1 within the intestinal tissue. ILC3s were not observed to change within the tumour tissue, further confirming the tissue specific regulation of ILCs by PD-1.

In T cells, PD-1 is upregulated in response to T cell activation in order to maintain immune tolerance. Here, it has been shown that PD-1 expression in both ILC1s and ILC2s was increased within the TME compared with non-involved skin and ILC3s were significantly increased in the absence to PD-1 within intestinal tissue. These data strongly suggests that, like with T cells, PD-1 expression on ILCs is upregulated in response to cellular activation. This was mirrored in human experiments, where PD-1^{+} ILC1s were present within the tumour tissue but not within patient PBMCs. It is likely that proteins present within the TME driving this cellular activation, as transwell experiments in both human and murine cells demonstrated that the tumour secretome can sufficient stimulation to upregulate PD-1 expression on ILC1s.

It should be noted that, within the transwell experiments, ILCs were not isolated and were either cultured as splenocytes or as human PBMCs. This means that it is still not determined whether the tumour secretome is activating ILCs directly or whether it is driving other immune subsets (such as dendritic cells) to induce PD-1 expression. Transwell cultures with isolated ILC1s would determine whether this PD-1 expression was due to other immune cells or the direct impact of tumour secretome. These sorting experiments, however, are particularly challenging due to limited cell numbers. Traditionally, to isolate ILCs, exogenous cytokines are administered *in vivo* in order to retrieve adequate cell numbers for analysis. As these experiments would be designed to determine if PD-1 expression is driven by cell activation, pre-activation of cells would mask any results seen from the tumour cells and would be undesirable. The use of reporter mice in order to isolate naïve ILCs, as reported by Constantides et al would provide a possible solution , although whether these would truly represent ILC phenotype when isolated from tissue microenvironment would be brought into question (Constantinides et al., 2014). Nevertheless, the environment created by the tumour is sufficient to induce PD-1 expression in ILC1 and ILC2 subsets. Of note, here it was also demonstrated that ILC3s subsets did not respond with the increased PD-1 expression, suggesting that factors within the TME are specifically providing stimulation for ILC1 and ILC2 subsets. This is consistent with data from the inducible colon cancer model where ILC3s appear to be regulated specifically within the intestine where they encounter ILC3s stimulating factor but not within the TME.

Metabolism

One avenue which was addressed within this project was the notion of metabolic conversion of ILCs in response to aPD-1 therapy. Here it was shown that absence of PD-1 signalling drove ILC1s towards an effector glycolytic phenotype through the increased uptake of glucose derivative 2-NBDG and decreased uptake of the fatty acid derivative, palmitate. PD-1 regulation of ILCs has only previous been described in the case of ILC2s. This is the first current evidence that PD-1 can also drive metabolic changed in ILC1 subsets. Helou *et al* provided evidence that in the absence of PD-1, stimulated ILC2s upregulated a number of glycolytic genes and downregulated a series of genes associated with fatty acid oxidation (Helou et al., 2020). It is conceivable that this would also be the case within this model, however several limitations may arise. Due to the low cell numbers, sorting this ILC1 population from tumour tissue poses a much higher challenge than the isolation of stimulated ILC2s from ILC2-rich lung tissue. It is critical that the ILC1s are sorted from tumour tissue, as shown they respond to PD-1 signalling in a very tissue specific manner. It is also critical that this is carried out in the absence of exogenous stimuli as this may drastically alter cellular phenotype; particularly as it remains unclear which stimuli ILC1s are responding to within the tumour tissue. Whether it is practical or ethical to generate enough tumour bearing to provide sufficient quantities of ILC1s to be sorted in the absence of additional stimuli, remains unclear. If possible, this would provide a wealth of opportunities to fully explore the regulation of ILC1s by PD-1. Recent technologies have been developed which could address this problem. Hartmann *et al* describe the use of single-cell metabolic regulome profiling (scMEP) whereby proteins associated with metabolic pathway regulation can be quantified within single cells (Hartmann et al., 2021). This initial research has been carried out on tumour tissue from patients with colorectal cancer and been used to assess the metabolic profile within $CD8^+$ T cells. This could provide an exciting opportunity in the future metabolic assessment of ILC1s.

Location

A further point worth discussing, would be where the ILCs might be located within the tumour tissue itself. If ILCs are purely located within the centre of the tumour it may make it difficult for cytokines excreted from cytokines to reach $CD8^+$ T cells and recruit them. Equally, if they remain located on the tumour periphery, they may not enhance $CD8^+$ infiltration into the tumour core where anti-tumour responses are required. This may have been an impossible question to address with traditional methods such as immunofluorescent staining, as these techniques are typically limited to small numbers of markers which would not be sufficient to identify individual ILC populations. One critical issue with ILCs is that they do not possess any ILC

specific markers and are primarily identified by negative gating through their lack of markers for other cell subsets such as CD3, CD19 etc. and hence require large flow panels for analysis. New technologies, however, such as Hyperion, maybe be able to give a novel insight into the locations of ILCs within tissues, specifically tumour tissue. Hyperion is an imaging mass spectrometry system which recognises metal tagged antibodies on tissue sections and can image in excess of 40 markers at a time. As this also images tissue sections, it would mean it might be possible to determine ILC location within the tumour tissue, and localisation of ILCs with other cell types including adaptive cells i.e., $CD8^+$ T cells or innate cells such as macrophages and dendritic cells.

Human

This project has been predominantly carried out in murine models, however, the initial human experiments have shown that this same ILC1 subset is present exclusively in human tissue and not within the blood of cSCC patients. Similarly, within healthy donors, these ILC1s mirrored responses to PD-1 blockade seen in the mouse, whereby there was an increase in cellular proliferation. These experiments were preliminary, and more work is required to truly show the clinically targetability of ILCs within cancer. Blood samples from the patients were taken at the time of the tumour resection prior to any further treatment. Future analysis of patients pre-treatment, during treatment, and post treatment with anti-PD-1 therapies would be exceptional advantageous for a thorough understanding. *In vitro* experiments have shown that PD-1 blockade can increase cellular proliferation within this subset. The limitations of this data is that these cells are grown in culture and therefore may not give a full representation of how these cells would behave within patients. It has been reported that patients which high levels of PD-1^+ILC2s have significant increased survival compared with low levels of PD-1 expression (Moral et al 2021). There is no data, however, investigating the levels of ILCs, particularly how ILC1s change in patients who receive αPD-1 therapy, both during and post treatment. Future experiments examining patients samples before treatment, and during treatment would help to confirm findings reported within the mouse models demonstrating blockade of PD-1 can increase ILC1s. The primary treatment for skin cancers such as melanoma and cSCC is resection of the tumour, so this may be limited in whether subsequent tumour analysis throughout treatment is available. Blood samples from different cancers, however, may be able to show the desired population. Tumio *et al* showed all ILC subsets were present within the blood in a number of cancers including gastrointestinal cancers and breast cancers (Tumino et al., 2019). By comparing $Tbet^+Nkp46^+$ ILC1s prior to treatment and during treatment will show

how these cells behave in disease and whether they are targetable in the clinic. In murine models, ILC1s were increased in all models, assessment in patients with both “hot” and “cold” tumours would show whether these findings are conserved from mouse to human. Correlation of patients with high or low levels ILC1s with responsiveness to treatment may would suggest that increased levels of ILC1s would enhance patient responsiveness to treatment and improve patient care however this is yet to be determined.

Overall, human data has replicated findings demonstrated in murine models. Although cytokine expression was briefly addressed, levels of IFNγ were undetermined due to low cell numbers and high patient variation. Other methods of assessing ILC1 production of IFNγ should be explored to fully elucidate how PD-1 regulates ILC1s in humans.

Within ILC biology, ILC2s are by far the best studied subset due to their definitive markers which makes them an easier target to identify. Limitations arise in ILC1 and 3 where the defining markers are much less definitive and are often interchangeable. Furthermore, ILCs account for less than 1% of lymphocytes making functional experiments particularly challenging. Much of the literature has relied of exogenous stimuli, in order to boost ILC subsets prior to analysis or observed clinical action. Here, however, it has been demonstrated that ILC1s are capable of driving anti-tumour responses in the absence of this exogenous stimuli. This could make ILC1s a more favourable target, as if it is possible for this cell population to be boosted in the absence of exogenous stimuli, it reduces the requirement for additional treatments, such as cytokines, within the clinic which would inevitably increase patients side effects. It is known in the literature that ILC1s are driven by IL-12 and IL-18, similarly that ILC2s are driven by IL-33. This therefore constitutes the exogenous stimuli seen in research papers. Here, however, by carrying out these experiments in the absence of exogenous stimuli, it leaves a question remaining whether there could be a missed opportunity of a cytokine or molecule present within the TME which is specifically driving these cells. It has been shown here that this cell subset is exclusively upregulated within the TME, which therefore indicates that the TME possesses a tissue specific stimulus for these cells.

The origins of this subset however are yet to be explored. The 3 main possibilities to consider would be a) the migration of these cells from other tissues b) direct activation of ILC1 subsets present within the skin or c) increased conversion of ILC3s to ILC1s in the presence of IL-12. ILCs are generally regarded as a tissue resident population of cells, however, emerging data has demonstrated that they have the capacity to migrate in the case of helminth infection where

ILC2s migrate from intestinal to the site of infection in the lung (Huang et al., 2018). There is currently no data, however, to demonstrate ILC migration into the tumour tissue. As there is an increase in ILC2s within the lymph nodes, it could be proposed that the cells are indeed migrating from the lymph nodes and converting to ILC1s within the TME. Furthermore, in the inducible tumour model, an increase in ILC3s was noted in the intestine and an increase in ILC1s noted within the tumour tissue. This suggests a similar mechanism within the colon cancer where ILC3s may be converting into ILC1s within the TME. One way to analyse this could be the use of Kaede mice (Tomura and Kabashima, 2013). These mice have photoconvertible cells which, when exposed to UV light, cells convert from green fluorescence to red fluorescence. Dutton *et al* previously demonstrated migration of ILCs from tissues by assessing frequency of red cells in non-exposed tissue (Dutton et al., 2017). This could be used to determine whether cells are indeed migrating into the tumour or there is a boost in the cells that are tissue residents.

Overall, the data here has demonstrated that PD-1 can regulates $Tbet^{+}Nkp46^{+}$-ILC1s within the mouse; an observation which has been replicated within human whereby it was demonstrated that PD-1 regulation is conserved. This data further shows that this PD-1 regulation down regulates cellular proliferation and cytokine production.

Chapter 7: Conclusions

In conclusion, here we have demonstrated that within the TME, PD-1 can specifically dampen $Tbet^+$ ILC1s proliferation and cytokine expression in a tissue specific manner. Following PD-1 blockade in murine cancer models $Tbet^+NKp46^+ROR\gamma t^-$ ILCls showed higher frequency and specifically protected against tumour development. Furthermore, in human cSCC patients, $PD\text{-}1^+Tbet^+$ILC1s are upregulated within the TME when compared with PBMCs from patients and healthy donors suggesting tissue specific ILC tumour responses. Whether these ILCs respond to therapy within humans is still to be determined however murine data showed specific increase in ILC subsets within the TME in response to PD-1 blockade in the absence of exogenous stimuli. By boosting ILCs within the TME, this may be able to enhance patient responses to therapy in the clinic.

Chapter 8: Future Work

This project has identified as an ILC subset which is specifically modulated by PD-1 within the TME, with a huge potential for these cells to be targeted to enhance therapeutic responses in the future. There are, however, many questions which have arisen as a result of the data presented. A thorough understanding of how these cells behave within the TME and their response to checkpoint inhibitors is essential for harnessing their therapeutic potential.

8.1. Determine tissue residency of Tbet^{+}Nkp46^{+}RORγt^{-} ILC1s within the TME

It is widely accepted that ILCs are a tissue resident innate immune subset. It is this attribute which could favour ILCs as a therapeutic target for tumours with poor immune cell infiltration. However, their true tissue residency remains undetermined as published data has identified CCR7 dependent migration of ILC2s critical for defence against helminth infection. ILC2s were shown to migrate from the lamina propria to the site of infection. (Huang et al., 2018). Sphingosine 1-phosphate (S1P) was required from ILC egress from the lymph nodes. All three ILC subsets were shown to express $S1P_1$, and when treated with an S1P inhibitor, ILCs pooled in the lymph nodes; unable to egress (Dutton et al 2019). Within my model, an increase in Tbet^{+}Nkp46^{+}RORγt^{-} ILCls was specifically seen within the TME which was coupled with an increase in Ki67 expression which suggests an increase in proliferation in the resident ILCs, however whether cells were initially in the TME or migrated from the TDLN is yet to be determined. In human, ILCs are present within PBMCs suggesting circulatory ILCs (Salimi et al., 2018). The true tissue residency could be determined by inhibiting migratory factors such as S1P within the tumour model and assessing any ILC pooling within the TDLN.

8.2.ILC Plasticity

In my data, I have shown increase in Tbet^{+}Nkp46^{+}RORγt^{-} ILC1s specifically within the TME. However, increases in ILC2s were shown in TDLN and a trend showing an increase in ILC3s within the intestinal tissue was observed in the colon cancer model in the absence of PD-1. Whether ILC2s migrate from TDLN and convert into Tbet^{+}Nkp46^{+}RORγt^{-} ILC1s within the TME in response to stimuli produced by the tumour. ILCs have a noted plasticity between other subsets. Similar to the increase in TDLN, an observation of possible increase ILC3s within the intestine and there is clear evidence that ILC3s have the ability to convert into ILC1s with the

correct stimulation. A combination of understanding ILC migration and plasticity and whether this may be influenced by PD-1 therapy could be particularly vital in fully elucidating the role and importance of PD-1 in these cell subsets. This would determine the source of the ILCs responding to PD-1 therapy and to decipher whether ILC2 or ILC3s are migrating and converting or Tbet^{+} ILCs are specifically responding to PD-1 within TME.

8.3.Immune Cell Recruitment

In the TME, in response to activation, ILC2s produce CCL5 which stimulates CD103^{+}dendritic cells to drive CD8^{+} T cell recruitment and anti-tumour responses (Moral et al., 2020). As a novel subset, Tbet^{+}Nkp46^{+}Eomes^{-}RORγt^{-} cells, are regulated by PD-1 within the TME, it would be important to note how they are driving an anti-tumour response. Although they have been shown to increase IFNγ production in the absence of PD-1 and ILCs alone are capable of providing protection against tumour development, it would be important to determine to what extent these specific ILCs drive T cells recruitment and anti-tumour response in order to examine how effective additional ILC boosting cytokine may be. It would also be worth assessing levels of chemokines, such as CCL5, which may be produced by ILCs in order to induce other immune responses.

8.4.PD-1 Signalling in ILCs

It also remains to be identified the exact mechanism by which PD-1 is driving ILC response. In ILC2s, PD-1 inhibits phosphorylation of STAT5 which inhibits cellular proliferation and cytokine production (Taylor et al., 2017). As Tbet^{+}Nkp46^{+}RORγ^{-} ILC1s have a ILC1-like phenotype, it is possible the are driven by type 1 cytokines such as IL-12. Similar to IL-33 activation in ILC2s, IL-12 drives the phosphorylation of STAT4 and the production of IFNγ in ILC1 and ILC3s (Dulson et al., 2019). It is yet to be determined, however, whether the cells identified within this project respond in the same way. As STAT4 drives IFNγ production in ILC1s whether PD-1 inhibits STAT4 phosphorylation within our ILC1 subset is yet to be determined. Alternatively, as data has indicated that the absence of PD-1 drives a glycolytic phenotype in Tbet^{+}Nkp46^{+}RORγt^{-} ILC1s. It could therefore be understandable that PD-1 may be regulating glycolytic pathways. Assessment of the mtor signalling pathway may also show a specific metabolic regulation of ILCs by PD-1. A more in depth analysis of ILC metabolic profile can be achieved through seahorse analysis.

Finally, to fully confirm and elucidate the effect of anti-PD-1 therapy in patients, ILC composition should be assessed in the TME of patients receiving αPD-1 therapy in the clinic. Although cSCC patients have sufficient PD-1^{+} ILCs present within the TME and it is likely that they respond, there is currently not data to demonstrate that, in the clinic, ILCs within the TME respond to αPD-1 therapy. This information would be a critical indicator as it would be a good indication as to whether ILC boosting cytokines would be beneficial as a supplement to patients undergoing anti-PD-1 therapy.

This project has demonstrated that ILCs exhibit tightly regulated tissue specific PD-1 expression. By fully understanding how this occurs and the subsequent consequences of this would hopefully enhance patient responses to therapy within the clinic.

References

ABT, M. C., LEWIS, B. B., CABALLERO, S., XIONG, H., CARTER, R. A., SUSAC, B., LING, L., LEINER, I. & PAMER, E. G. 2015. Innate Immune Defenses Mediated by Two ILC Subsets Are Critical for Protection against Acute Clostridium difficile Infection. *Cell Host Microbe,* 18**,** 27-37.

AGATA, Y., KAWASAKI, A., NISHIMURA, H., ISHIDA, Y., TSUBATA, T., YAGITA, H. & HONJO, T. 1996. Expression of the PD-1 antigen on the surface of stimulated mouse T and B lymphocytes. *Int Immunol,* 8**,** 765-72.

AKIRA, S., UEMATSU, S. & TAKEUCHI, O. 2006. Pathogen recognition and innate immunity. *Cell,* 124**,** 783-801.

ALIAHMAD, P., DE LA TORRE, B. & KAYE, J. 2010. Shared dependence on the DNA-binding factor TOX for the development of lymphoid tissue-inducer cell and NK cell lineages. *Nat Immunol,* 11**,** 945-52.

ALMEIDA, F. F., TOGNARELLI, S., MARCAIS, A., KUEH, A. J., FRIEDE, M. E., LIAO, Y., WILLIS, S. N., LUONG, K., FAURE, F., MERCIER, F. E., GALLUSO, J., FIRTH, M., NARNI-MANCINELLI, E., RAIS, B., SCADDEN, D. T., SPALLOTTA, F., WEIL, S., GIANNATTASIO, A., KALENSEE, F., ZOLLER, T., HUNTINGTON, N. D., SCHLEICHER, U., CHIOCCHETTI, A. G., UGOLINI, S., HEROLD, M. J., SHI, W., KOCH, J., STEINLE, A., VIVIER, E., WALZER, T., BELZ, G. T. & ULLRICH, E. 2018. A point mutation in the Ncr1 signal peptide impairs the development of innate lymphoid cell subsets. *Oncoimmunology,* 7**,** e1475875.

ANSARI, M. J., SALAMA, A. D., CHITNIS, T., SMITH, R. N., YAGITA, H., AKIBA, H., YAMAZAKI, T., AZUMA, M., IWAI, H., KHOURY, S. J., AUCHINCLOSS, H., JR. & SAYEGH, M. H. 2003. The programmed death-1 (PD-1) pathway regulates autoimmune diabetes in nonobese diabetic (NOD) mice. *J Exp Med,* 198**,** 63-9.

ASPESLAGH, S., POSTEL-VINAY, S., RUSAKIEWICZ, S., SORIA, J. C., ZITVOGEL, L. & MARABELLE, A. 2016. Rationale for anti-OX40 cancer immunotherapy. *Eur J Cancer,* 52**,** 50-66.

AZUMA, M., ITO, D., YAGITA, H., OKUMURA, K., PHILLIPS, J. H., LANIER, L. L. & SOMOZA, C. 1993. B70 antigen is a second ligand for CTLA-4 and CD28. *Nature,* 366**,** 76-9.

BANDO, J. K., GILFILLAN, S., DI LUCCIA, B., FACHI, J. L., SECCA, C., CELLA, M. & COLONNA, M. 2020. ILC2s are the predominant source of intestinal ILC-derived IL-10. *J Exp Med,* 217.

BEATTY, G. & PATERSON, Y. 2001. IFN-gamma-dependent inhibition of tumor angiogenesis by tumor-infiltrating CD4+ T cells requires tumor responsiveness to IFN-gamma. *J Immunol,* 166**,** 2276-82.

BENEZRA, R., DAVIS, R. L., LOCKSHON, D., TURNER, D. L. & WEINTRAUB, H. 1990. The protein Id: a negative regulator of helix-loop-helix DNA binding proteins. *Cell,* 61**,** 49-59.

BERNINK, J. H., KRABBENDAM, L., GERMAR, K., DE JONG, E., GRONKE, K., KOFOED-NIELSEN, M., MUNNEKE, J. M., HAZENBERG, M. D., VILLAUDY, J., BUSKENS, C. J., BEMELMAN, W. A., DIEFENBACH, A., BLOM, B. & SPITS, H. 2015. Interleukin-12 and -23 Control Plasticity of CD127(+) Group 1 and Group 3 Innate Lymphoid Cells in the Intestinal Lamina Propria. *Immunity,* 43**,** 146-60.

BIE, Q., ZHANG, P., SU, Z., ZHENG, D., YING, X., WU, Y., YANG, H., CHEN, D., WANG, S. & XU, H. 2014. Polarization of ILC2s in peripheral blood might contribute to immunosuppressive microenvironment in patients with gastric cancer. *J Immunol Res,* 2014**,** 923135.

BITTNER, S., KNOLL, G. & EHRENSCHWENDER, M. 2017. Death receptor 3 signaling enhances proliferation of human regulatory T cells. *FEBS Lett,* 591**,** 1187-1195.

BOISE, L. H., MINN, A. J., NOEL, P. J., JUNE, C. H., ACCAVITTI, M. A., LINDSTEN, T. & THOMPSON, C. B. 1995. CD28 costimulation can promote T cell survival by enhancing the expression of Bcl-XL. *Immunity,* 3**,** 87-98.

BOOS, M. D., YOKOTA, Y., EBERL, G. & KEE, B. L. 2007. Mature natural killer cell and lymphoid tissue-inducing cell development requires Id2-mediated suppression of E protein activity. *J Exp Med,* 204**,** 1119-30.

BOTTCHER, J. P., BONAVITA, E., CHAKRAVARTY, P., BLEES, H., CABEZA-CABRERIZO, M., SAMMICHELI, S., ROGERS, N. C., SAHAI, E., ZELENAY, S. & REIS, E. S. C. 2018. NK Cells Stimulate Recruitment of cDC1 into the Tumor Microenvironment Promoting Cancer Immune Control. *Cell,* 172**,** 1022-1037 e14.

BOULENOUAR, S., MICHELET, X., DUQUETTE, D., ALVAREZ, D., HOGAN, A. E., DOLD, C., O'CONNOR, D., STUTTE, S., TAVAKKOLI, A., WINTERS, D., EXLEY, M. A., O'SHEA, D., BRENNER, M. B., VON ANDRIAN, U. & LYNCH, L. 2017. Adipose Type One Innate Lymphoid Cells Regulate Macrophage Homeostasis through Targeted Cytotoxicity. *Immunity,* 46**,** 273-286.

BRESTOFF, J. R., KIM, B. S., SAENZ, S. A., STINE, R. R., MONTICELLI, L. A., SONNENBERG, G. F., THOME, J. J., FARBER, D. L., LUTFY, K., SEALE, P. & ARTIS, D. 2015. Group 2 innate lymphoid cells promote beiging of white adipose tissue and limit obesity. *Nature,* 519**,** 242-6.

BUCK, M. D., O'SULLIVAN, D. & PEARCE, E. L. 2015. T cell metabolism drives immunity. *J Exp Med,* 212**,** 1345-60.

BUETTNER, M. & LOCHNER, M. 2016. Development and Function of Secondary and Tertiary Lymphoid Organs in the Small Intestine and the Colon. *Front Immunol,* 7**,** 342.

BUONOCORE, S., AHERN, P. P., UHLIG, H. H., IVANOV, II, LITTMAN, D. R., MALOY, K. J. & POWRIE, F. 2010. Innate lymphoid cells drive interleukin-23-dependent innate intestinal pathology. *Nature,* 464**,** 1371-5.

CALLAHAN, M. K., POSTOW, M. A. & WOLCHOK, J. D. 2016. Targeting T Cell Co-receptors for Cancer Therapy. *Immunity,* 44**,** 1069-78.

CARDOSO, V., CHESNE, J., RIBEIRO, H., GARCIA-CASSANI, B., CARVALHO, T., BOUCHERY, T., SHAH, K., BARBOSA-MORAIS, N. L., HARRIS, N. & VEIGA-FERNANDES, H. 2017. Neuronal regulation of type 2 innate lymphoid cells via neuromedin U. *Nature,* 549**,** 277-281.

CHAN, I. H., JAIN, R., TESSMER, M. S., GORMAN, D., MANGADU, R., SATHE, M., VIVES, F., MOON, C., PENAFLOR, E., TURNER, S., AYANOGLU, G., CHANG, C., BASHAM, B., MUMM, J. B., PIERCE, R. H., YEARLEY, J. H., MCCLANAHAN, T. K., PHILLIPS, J. H., CUA, D. J., BOWMAN, E. P., KASTELEIN, R. A. & LAFACE, D. 2014. Interleukin-23 is sufficient to induce rapid de novo gut tumorigenesis, independent of carcinogens, through activation of innate lymphoid cells. *Mucosal Immunol,* 7**,** 842-56.

CHEMNITZ, J. M., PARRY, R. V., NICHOLS, K. E., JUNE, C. H. & RILEY, J. L. 2004. SHP-1 and SHP-2 associate with immunoreceptor tyrosine-based switch motif of programmed death 1 upon primary human T cell stimulation, but only receptor ligation prevents T cell activation. *J Immunol,* 173**,** 945-54.

CHEUNG, T. C., OBORNE, L. M., STEINBERG, M. W., MACAULEY, M. G., FUKUYAMA, S., SANJO, H., D'SOUZA, C., NORRIS, P. S., PFEFFER, K., MURPHY, K. M., KRONENBERG, M., SPEAR, P. G. & WARE, C. F. 2009. T cell intrinsic heterodimeric complexes between HVEM and BTLA determine receptivity to the surrounding microenvironment. *J Immunol,* 183**,** 7286-96.

CHEVALIER, M. F., TRABANELLI, S., RACLE, J., SALOME, B., CESSON, V., GHARBI, D., BOHNER, P., DOMINGOS-PEREIRA, S., DARTIGUENAVE, F., FRITSCHI, A. S., SPEISER, D. E.,

RENTSCH, C. A., GFELLER, D., JICHLINSKI, P., NARDELLI-HAEFLIGER, D., JANDUS, C. & DERRE, L. 2017. ILC2-modulated T cell-to-MDSC balance is associated with bladder cancer recurrence. *J Clin Invest,* 127**,** 2916-2929.

CHOWDHURY, F. Z., RAMOS, H. J., DAVIS, L. S., FORMAN, J. & FARRAR, J. D. 2011. IL-12 selectively programs effector pathways that are stably expressed in human CD8+ effector memory T cells in vivo. *Blood,* 118**,** 3890-900.

CONLON, K. C., MILJKOVIC, M. D. & WALDMANN, T. A. 2019. Cytokines in the Treatment of Cancer. *J Interferon Cytokine Res,* 39**,** 6-21.

CONSTANTINIDES, M. G., MCDONALD, B. D., VERHOEF, P. A. & BENDELAC, A. 2014. A committed precursor to innate lymphoid cells. *Nature,* 508**,** 397-401.

CORTEZ, V. S., ULLAND, T. K., CERVANTES-BARRAGAN, L., BANDO, J. K., ROBINETTE, M. L., WANG, Q., WHITE, A. J., GILFILLAN, S., CELLA, M. & COLONNA, M. 2017. SMAD4 impedes the conversion of NK cells into ILC1-like cells by curtailing non-canonical TGF-beta signaling. *Nat Immunol,* 18**,** 995-1003.

CROME, S. Q., NGUYEN, L. T., LOPEZ-VERGES, S., YANG, S. Y., MARTIN, B., YAM, J. Y., JOHNSON, D. J., NIE, J., PNIAK, M., YEN, P. H., MILEA, A., SOWAMBER, R., KATZ, S. R., BERNARDINI, M. Q., CLARKE, B. A., SHAW, P. A., LANG, P. A., BERMAN, H. K., PUGH, T. J., LANIER, L. L. & OHASHI, P. S. 2017. A distinct innate lymphoid cell population regulates tumor-associated T cells. *Nat Med,* 23**,** 368-375.

CUFF, A. O., SILLITO, F., DERTSCHNIG, S., HALL, A., LUONG, T. V., CHAKRAVERTY, R. & MALE, V. 2019. The Obese Liver Environment Mediates Conversion of NK Cells to a Less Cytotoxic ILC1-Like Phenotype. *Front Immunol,* 10**,** 2180.

DADI, S., CHHANGAWALA, S., WHITLOCK, B. M., FRANKLIN, R. A., LUO, C. T., OH, S. A., TOURE, A., PRITYKIN, Y., HUSE, M., LESLIE, C. S. & LI, M. O. 2016. Cancer Immunosurveillance by Tissue-Resident Innate Lymphoid Cells and Innate-like T Cells. *Cell,* 164**,** 365-77.

DAUSSY, C., FAURE, F., MAYOL, K., VIEL, S., GASTEIGER, G., CHARRIER, E., BIENVENU, J., HENRY, T., DEBIEN, E., HASAN, U. A., MARVEL, J., YOH, K., TAKAHASHI, S., PRINZ, I., DE BERNARD, S., BUFFAT, L. & WALZER, T. 2014. T-bet and Eomes instruct the development of two distinct natural killer cell lineages in the liver and in the bone marrow. *J Exp Med,* 211**,** 563-77.

DE WEERDT, I., VAN HOEVEN, V., MUNNEKE, J. M., ENDSTRA, S., HOFLAND, T., HAZENBERG, M. D. & KATER, A. P. 2016. Innate lymphoid cells are expanded and functionally altered in chronic lymphocytic leukemia. *Haematologica,* 101**,** e461-e464.

DENG, T., SUO, C., CHANG, J., YANG, R., LI, J., CAI, T. & QIU, J. 2020. ILC3-derived OX40L is essential for homeostasis of intestinal Tregs in immunodeficient mice. *Cell Mol Immunol,* 17**,** 163-177.

DIEFENBACH, A., COLONNA, M. & KOYASU, S. 2014. Development, differentiation, and diversity of innate lymphoid cells. *Immunity,* 41**,** 354-365.

DONG, C., JUEDES, A. E., TEMANN, U. A., SHRESTA, S., ALLISON, J. P., RUDDLE, N. H. & FLAVELL, R. A. 2001. ICOS co-stimulatory receptor is essential for T-cell activation and function. *Nature,* 409**,** 97-101.

DONG, Y., SUN, Q. & ZHANG, X. 2017. PD-1 and its ligands are important immune checkpoints in cancer. *Oncotarget,* 8**,** 2171-2186.

DRAKE, L. Y., IIJIMA, K. & KITA, H. 2014. Group 2 innate lymphoid cells and CD4+ T cells cooperate to mediate type 2 immune response in mice. *Allergy,* 69**,** 1300-7.

DULSON, S. J., WATKINS, E. E., CROSSMAN, D. K. & HARRINGTON, L. E. 2019. STAT4 Directs a Protective Innate Lymphoid Cell Response to Gastrointestinal Infection. *J Immunol,* 203**,** 2472-2484.

DUTTON, E. E., CAMELO, A., SLEEMAN, M., HERBST, R., CARLESSO, G., BELZ, G. T. & WITHERS, D. R. 2017. Characterisation of innate lymphoid cell populations at different sites in mice with defective T cell immunity. *Wellcome Open Res,* 2**,** 117.

EBIHARA, T., SONG, C., RYU, S. H., PLOUGASTEL-DOUGLAS, B., YANG, L., LEVANON, D., GRONER, Y., BERN, M. D., STAPPENBECK, T. S., COLONNA, M., EGAWA, T. & YOKOYAMA, W. M. 2015. Runx3 specifies lineage commitment of innate lymphoid cells. *Nat Immunol,* 16**,** 1124-33.

FIFE, B. T., PAUKEN, K. E., EAGAR, T. N., OBU, T., WU, J., TANG, Q., AZUMA, M., KRUMMEL, M. F. & BLUESTONE, J. A. 2009. Interactions between PD-1 and PD-L1 promote tolerance by blocking the TCR-induced stop signal. *Nat Immunol,* 10**,** 1185-92.

FILIPOVIC, I., CHIOSSONE, L., VACCA, P., HAMILTON, R. S., INGEGNERE, T., DOISNE, J. M., HAWKES, D. A., MINGARI, M. C., SHARKEY, A. M., MORETTA, L. & COLUCCI, F. 2018. Molecular definition of group 1 innate lymphoid cells in the mouse uterus. *Nat Commun,* 9**,** 4492.

FOS, C., SALLES, A., LANG, V., CARRETTE, F., AUDEBERT, S., PASTOR, S., GHIOTTO, M., OLIVE, D., BISMUTH, G. & NUNES, J. A. 2008. ICOS ligation recruits the p50alpha PI3K regulatory subunit to the immunological synapse. *J Immunol,* 181**,** 1969-77.

FUCHS, A. 2016. ILC1s in Tissue Inflammation and Infection. *Front Immunol,* 7**,** 104.

GALLE-TREGER, L., SANKARANARAYANAN, I., HURRELL, B. P., HOWARD, E., LO, R., MAAZI, H., LEWIS, G., BANIE, H., EPSTEIN, A. L., HU, P., REHAN, V. K., GILLILAND, F. D., ALLAYEE, H., SOROOSH, P., SHARPE, A. H. & AKBARI, O. 2019. Costimulation of type-2 innate lymphoid cells by GITR promotes effector function and ameliorates type 2 diabetes. *Nat Commun,* 10**,** 713.

GAO, Y., SOUZA-FONSECA-GUIMARAES, F., BALD, T., NG, S. S., YOUNG, A., NGIOW, S. F., RAUTELA, J., STRAUBE, J., WADDELL, N., BLAKE, S. J., YAN, J., BARTHOLIN, L., LEE, J. S., VIVIER, E., TAKEDA, K., MESSAOUDENE, M., ZITVOGEL, L., TENG, M. W. L., BELZ, G. T., ENGWERDA, C. R., HUNTINGTON, N. D., NAKAMURA, K., HOLZEL, M. & SMYTH, M. J. 2017. Tumor immunoevasion by the conversion of effector NK cells into type 1 innate lymphoid cells. *Nat Immunol,* 18**,** 1004-1015.

GEIGER, T. L., ABT, M. C., GASTEIGER, G., FIRTH, M. A., O'CONNOR, M. H., GEARY, C. D., O'SULLIVAN, T. E., VAN DEN BRINK, M. R., PAMER, E. G., HANASH, A. M. & SUN, J. C. 2014. Nfil3 is crucial for development of innate lymphoid cells and host protection against intestinal pathogens. *J Exp Med,* 211**,** 1723-31.

GEREMIA, A., ARANCIBIA-CARCAMO, C. V., FLEMING, M. P., RUST, N., SINGH, B., MORTENSEN, N. J., TRAVIS, S. P. & POWRIE, F. 2011. IL-23-responsive innate lymphoid cells are increased in inflammatory bowel disease. *J Exp Med,* 208**,** 1127-33.

GIL-CRUZ, C., PEREZ-SHIBAYAMA, C., ONDER, L., CHAI, Q., CUPOVIC, J., CHENG, H. W., NOVKOVIC, M., LANG, P. A., GEUKING, M. B., MCCOY, K. D., ABE, S., CUI, G., IKUTA, K., SCANDELLA, E. & LUDEWIG, B. 2016. Fibroblastic reticular cells regulate intestinal inflammation via IL-15-mediated control of group 1 ILCs. *Nat Immunol,* 17**,** 1388-1396.

GOC, J., LV, M., BESSMAN, N. J., FLAMAR, A. L., SAHOTA, S., SUZUKI, H., TENG, F., PUTZEL, G. G., BANK, J. R. I. L. C., EBERL, G., WITHERS, D. R., ARTHUR, J. C., SHAH, M. A. & SONNENBERG, G. F. 2021. Dysregulation of ILC3s unleashes progression and immunotherapy resistance in colon cancer. *Cell,* 184**,** 5015-5030 e16.

GOPALAKRISHNAN, V., SPENCER, C. N., NEZI, L., REUBEN, A., ANDREWS, M. C., KARPINETS, T. V., PRIETO, P. A., VICENTE, D., HOFFMAN, K., WEI, S. C., COGDILL, A. P., ZHAO, L., HUDGENS, C. W., HUTCHINSON, D. S., MANZO, T., PETACCIA DE MACEDO, M.,

COTECHINI, T., KUMAR, T., CHEN, W. S., REDDY, S. M., SZCZEPANIAK SLOANE, R., GALLOWAY-PENA, J., JIANG, H., CHEN, P. L., SHPALL, E. J., REZVANI, K., ALOUSI, A. M., CHEMALY, R. F., SHELBURNE, S., VENCE, L. M., OKHUYSEN, P. C., JENSEN, V. B., SWENNES, A. G., MCALLISTER, F., MARCELO RIQUELME SANCHEZ, E., ZHANG, Y., LE CHATELIER, E., ZITVOGEL, L., PONS, N., AUSTIN-BRENEMAN, J. L., HAYDU, L. E., BURTON, E. M., GARDNER, J. M., SIRMANS, E., HU, J., LAZAR, A. J., TSUJIKAWA, T., DIAB, A., TAWBI, H., GLITZA, I. C., HWU, W. J., PATEL, S. P., WOODMAN, S. E., AMARIA, R. N., DAVIES, M. A., GERSHENWALD, J. E., HWU, P., LEE, J. E., ZHANG, J., COUSSENS, L. M., COOPER, Z. A., FUTREAL, P. A., DANIEL, C. R., AJAMI, N. J., PETROSINO, J. F., TETZLAFF, M. T., SHARMA, P., ALLISON, J. P., JENQ, R. R. & WARGO, J. A. 2018. Gut microbiome modulates response to anti-PD-1 immunotherapy in melanoma patients. *Science,* 359**,** 97-103.

GORDON, S. M., CHAIX, J., RUPP, L. J., WU, J., MADERA, S., SUN, J. C., LINDSTEN, T. & REINER, S. L. 2012. The transcription factors T-bet and Eomes control key checkpoints of natural killer cell maturation. *Immunity,* 36**,** 55-67.

GORDON, S. R., MAUTE, R. L., DULKEN, B. W., HUTTER, G., GEORGE, B. M., MCCRACKEN, M. N., GUPTA, R., TSAI, J. M., SINHA, R., COREY, D., RING, A. M., CONNOLLY, A. J. & WEISSMAN, I. L. 2017. PD-1 expression by tumour-associated macrophages inhibits phagocytosis and tumour immunity. *Nature,* 545**,** 495-499.

GREEN, J. M., KARPITSKIY, V., KIMZEY, S. L. & SHAW, A. S. 2000. Coordinate regulation of T cell activation by CD2 and CD28. *J Immunol,* 164**,** 3591-5.

GUIMOND, M., VEENSTRA, R. G., GRINDLER, D. J., ZHANG, H., CUI, Y., MURPHY, R. D., KIM, S. Y., NA, R., HENNIGHAUSEN, L., KURTULUS, S., ERMAN, B., MATZINGER, P., MERCHANT, M. S. & MACKALL, C. L. 2009. Interleukin 7 signaling in dendritic cells regulates the homeostatic proliferation and niche size of CD4+ T cells. *Nat Immunol,* 10**,** 149-57.

HALIM, T. Y. F., RANA, B. M. J., WALKER, J. A., KERSCHER, B., KNOLLE, M. D., JOLIN, H. E., SERRAO, E. M., HAIM-VILMOVSKY, L., TEICHMANN, S. A., RODEWALD, H. R., BOTTO, M., VYSE, T. J., FALLON, P. G., LI, Z., WITHERS, D. R. & MCKENZIE, A. N. J. 2018. Tissue-Restricted Adaptive Type 2 Immunity Is Orchestrated by Expression of the Costimulatory Molecule OX40L on Group 2 Innate Lymphoid Cells. *Immunity,* 48**,** 1195-1207 e6.

HAMS, E., LOCKSLEY, R. M., MCKENZIE, A. N. & FALLON, P. G. 2013. Cutting edge: IL-25 elicits innate lymphoid type 2 and type II NKT cells that regulate obesity in mice. *J Immunol,* 191**,** 5349-53.

HARTMANN, F. J., MRDJEN, D., MCCAFFREY, E., GLASS, D. R., GREENWALD, N. F., BHARADWAJ, A., KHAIR, Z., VERBERK, S. G. S., BARANSKI, A., BASKAR, R., GRAF, W., VAN VALEN, D., VAN DEN BOSSCHE, J., ANGELO, M. & BENDALL, S. C. 2021. Single-cell metabolic profiling of human cytotoxic T cells. *Nat Biotechnol,* 39**,** 186-197.

HELOU, D. G., SHAFIEI-JAHANI, P., LO, R., HOWARD, E., HURRELL, B. P., GALLE-TREGER, L., PAINTER, J. D., LEWIS, G., SOROOSH, P., SHARPE, A. H. & AKBARI, O. 2020. PD-1 pathway regulates ILC2 metabolism and PD-1 agonist treatment ameliorates airway hyperreactivity. *Nat Commun,* 11**,** 3998.

HEPWORTH, M. R., FUNG, T. C., MASUR, S. H., KELSEN, J. R., MCCONNELL, F. M., DUBROT, J., WITHERS, D. R., HUGUES, S., FARRAR, M. A., REITH, W., EBERL, G., BALDASSANO, R. N., LAUFER, T. M., ELSON, C. O. & SONNENBERG, G. F. 2015. Immune tolerance. Group 3 innate lymphoid cells mediate intestinal selection of commensal bacteria-specific CD4(+) T cells. *Science,* 348**,** 1031-5.

HEUFLER, C., KOCH, F., STANZL, U., TOPAR, G., WYSOCKA, M., TRINCHIERI, G., ENK, A., STEINMAN, R. M., ROMANI, N. & SCHULER, G. 1996. Interleukin-12 is produced by dendritic cells and mediates T helper 1 development as well as interferon-gamma production by T helper 1 cells. *Eur J Immunol,* 26**,** 659-68.

HOYLER, T., CONNOR, C. A., KISS, E. A. & DIEFENBACH, A. 2013. T-bet and Gata3 in controlling type 1 and type 2 immunity mediated by innate lymphoid cells. *Curr Opin Immunol,* 25**,** 139-47.

HOYLER, T., KLOSE, C. S., SOUABNI, A., TURQUETI-NEVES, A., PFEIFER, D., RAWLINS, E. L., VOEHRINGER, D., BUSSLINGER, M. & DIEFENBACH, A. 2012. The transcription factor GATA-3 controls cell fate and maintenance of type 2 innate lymphoid cells. *Immunity,* 37**,** 634-48.

HRUSCH, C. L., MANNS, S. T., BRYAZKA, D., CASAOS, J., BONHAM, C. A., JAFFERY, M. R., BLAINE, K. M., MILLS, K. A. M., VERHOEF, P. A., ADEGUNSOYE, A. O., WILLIAMS, J. W., TJOTA, M. Y., MOORE, T. V., STREK, M. E., NOTH, I. & SPERLING, A. I. 2018. ICOS protects against mortality from acute lung injury through activation of IL-5(+) ILC2s. *Mucosal Immunol,* 11**,** 61-70.

HUANG, Y., GUO, L., QIU, J., CHEN, X., HU-LI, J., SIEBENLIST, U., WILLIAMSON, P. R., URBAN, J. F., JR. & PAUL, W. E. 2015. IL-25-responsive, lineage-negative KLRG1(hi) cells are multipotential 'inflammatory' type 2 innate lymphoid cells. *Nat Immunol,* 16**,** 161-9.

HUANG, Y., MAO, K., CHEN, X., SUN, M. A., KAWABE, T., LI, W., USHER, N., ZHU, J., URBAN, J. F., JR., PAUL, W. E. & GERMAIN, R. N. 2018. S1P-dependent interorgan trafficking of group 2 innate lymphoid cells supports host defense. *Science,* 359**,** 114-119.

IRSHAD, S., FLORES-BORJA, F., LAWLER, K., MONYPENNY, J., EVANS, R., MALE, V., GORDON, P., CHEUNG, A., GAZINSKA, P., NOOR, F., WONG, F., GRIGORIADIS, A., FRUHWIRTH, G. O., BARBER, P. R., WOODMAN, N., PATEL, D., RODRIGUEZ-JUSTO, M., OWEN, J., MARTIN, S. G., PINDER, S. E., GILLETT, C. E., POLAND, S. P., AMEER-BEG, S., MCCAUGHAN, F., CARLIN, L. M., HASAN, U., WITHERS, D. R., LANE, P., VOJNOVIC, B., QUEZADA, S. A., ELLIS, P., TUTT, A. N. & NG, T. 2017. RORgammat(+) Innate Lymphoid Cells Promote Lymph Node Metastasis of Breast Cancers. *Cancer Res,* 77**,** 1083-1096.

ISHIDA, Y., AGATA, Y., SHIBAHARA, K. & HONJO, T. 1992. Induced expression of PD-1, a novel member of the immunoglobulin gene superfamily, upon programmed cell death. *EMBO J,* 11**,** 3887-95.

JAEGER, B. N. & VIVIER, E. 2012. Natural killer cell tolerance: control by self or self-control? *Cold Spring Harb Perspect Biol,* 4.

JIE, Z., LIANG, Y., HOU, L., DONG, C., IWAKURA, Y., SOONG, L., CONG, Y. & SUN, J. 2014. Intrahepatic innate lymphoid cells secrete IL-17A and IL-17F that are crucial for T cell priming in viral infection. *J Immunol,* 192**,** 3289-300.

JOVANOVIC, I. P., PEJNOVIC, N. N., RADOSAVLJEVIC, G. D., PANTIC, J. M., MILOVANOVIC, M. Z., ARSENIJEVIC, N. N. & LUKIC, M. L. 2014. Interleukin-33/ST2 axis promotes breast cancer growth and metastases by facilitating intratumoral accumulation of immunosuppressive and innate lymphoid cells. *Int J Cancer,* 134**,** 1669-82.

JUNEJA, V. R., MCGUIRE, K. A., MANGUSO, R. T., LAFLEUR, M. W., COLLINS, N., HAINING, W. N., FREEMAN, G. J. & SHARPE, A. H. 2017. PD-L1 on tumor cells is sufficient for immune evasion in immunogenic tumors and inhibits CD8 T cell cytotoxicity. *J Exp Med,* 214**,** 895-904.

KADKHODA, K., WANG, S., JOYEE, A. G., FAN, Y., YANG, J. & YANG, X. 2010. Th1 cytokine responses fail to effectively control Chlamydia lung infection in ICOS ligand knockout mice. *J Immunol,* 184**,** 3780-8.

KAO, C., OESTREICH, K. J., PALEY, M. A., CRAWFORD, A., ANGELOSANTO, J. M., ALI, M. A., INTLEKOFER, A. M., BOSS, J. M., REINER, S. L., WEINMANN, A. S. & WHERRY, E. J. 2011. Transcription factor T-bet represses expression of the inhibitory receptor PD-1 and sustains virus-specific CD8+ T cell responses during chronic infection. *Nat Immunol,* 12**,** 663-71.

KERKAR, S. P., MURANSKI, P., KAISER, A., BONI, A., SANCHEZ-PEREZ, L., YU, Z., PALMER, D. C., REGER, R. N., BORMAN, Z. A., ZHANG, L., MORGAN, R. A., GATTINONI, L., ROSENBERG, S. A., TRINCHIERI, G. & RESTIFO, N. P. 2010. Tumor-specific CD8+ T cells expressing interleukin-12 eradicate established cancers in lymphodepleted hosts. *Cancer Res,* 70**,** 6725-34.

KIESSLING, R., KLEIN, E. & WIGZELL, H. 1975. "Natural" killer cells in the mouse. I. Cytotoxic cells with specificity for mouse Moloney leukemia cells. Specificity and distribution according to genotype. *Eur J Immunol,* 5**,** 112-7.

KIM, H. Y., LEE, H. J., CHANG, Y. J., PICHAVANT, M., SHORE, S. A., FITZGERALD, K. A., IWAKURA, Y., ISRAEL, E., BOLGER, K., FAUL, J., DEKRUYFF, R. H. & UMETSU, D. T. 2014. Interleukin-17-producing innate lymphoid cells and the NLRP3 inflammasome facilitate obesity-associated airway hyperreactivity. *Nat Med,* 20**,** 54-61.

KIM, J., KIM, W., MOON, U. J., KIM, H. J., CHOI, H. J., SIN, J. I., PARK, N. H., CHO, H. R. & KWON, B. 2016. Intratumorally Establishing Type 2 Innate Lymphoid Cells Blocks Tumor Growth. *J Immunol,* 196**,** 2410-23.

KIM, M. H., TAPAROWSKY, E. J. & KIM, C. H. 2015. Retinoic Acid Differentially Regulates the Migration of Innate Lymphoid Cell Subsets to the Gut. *Immunity,* 43**,** 107-19.

KIRCHBERGER, S., ROYSTON, D. J., BOULARD, O., THORNTON, E., FRANCHINI, F., SZABADY, R. L., HARRISON, O. & POWRIE, F. 2013. Innate lymphoid cells sustain colon cancer through production of interleukin-22 in a mouse model. *J Exp Med,* 210**,** 917-31.

KLEFFEL, S., POSCH, C., BARTHEL, S. R., MUELLER, H., SCHLAPBACH, C., GUENOVA, E., ELCO, C. P., LEE, N., JUNEJA, V. R., ZHAN, Q., LIAN, C. G., THOMI, R., HOETZENECKER, W., COZZIO, A., DUMMER, R., MIHM, M. C., JR., FLAHERTY, K. T., FRANK, M. H., MURPHY, G. F., SHARPE, A. H., KUPPER, T. S. & SCHATTON, T. 2015. Melanoma Cell-Intrinsic PD-1 Receptor Functions Promote Tumor Growth. *Cell,* 162**,** 1242-56.

KLOSE, C. S., KISS, E. A., SCHWIERZECK, V., EBERT, K., HOYLER, T., D'HARGUES, Y., GOPPERT, N., CROXFORD, A. L., WAISMAN, A., TANRIVER, Y. & DIEFENBACH, A. 2013. A T-bet gradient controls the fate and function of CCR6-RORgammat+ innate lymphoid cells. *Nature,* 494**,** 261-5.

KLOSE, C. S. N., FLACH, M., MOHLE, L., ROGELL, L., HOYLER, T., EBERT, K., FABIUNKE, C., PFEIFER, D., SEXL, V., FONSECA-PEREIRA, D., DOMINGUES, R. G., VEIGA-FERNANDES, H., ARNOLD, S. J., BUSSLINGER, M., DUNAY, I. R., TANRIVER, Y. & DIEFENBACH, A. 2014. Differentiation of type 1 ILCs from a common progenitor to all helper-like innate lymphoid cell lineages. *Cell,* 157**,** 340-356.

KLOSE, C. S. N., MAHLAKOIV, T., MOELLER, J. B., RANKIN, L. C., FLAMAR, A. L., KABATA, H., MONTICELLI, L. A., MORIYAMA, S., PUTZEL, G. G., RAKHILIN, N., SHEN, X., KOSTENIS, E., KONIG, G. M., SENDA, T., CARPENTER, D., FARBER, D. L. & ARTIS, D. 2017. The neuropeptide neuromedin U stimulates innate lymphoid cells and type 2 inflammation. *Nature,* 549**,** 282-286.

KOGA, S., HOZUMI, K., HIRANO, K. I., YAZAWA, M., TEROOATEA, T., MINODA, A., NAGASAWA, T., KOYASU, S. & MORO, K. 2018. Peripheral PDGFRalpha(+)gp38(+) mesenchymal cells support the differentiation of fetal liver-derived ILC2. *J Exp Med,* 215**,** 1609-1626.

KOPF, M., RUEDL, C., SCHMITZ, N., GALLIMORE, A., LEFRANG, K., ECABERT, B., ODERMATT, B. & BACHMANN, M. F. 1999. OX40-deficient mice are defective in Th cell proliferation but are competent in generating B cell and CTL Responses after virus infection. *Immunity,* 11**,** 699-708.

KORN, L. L., THOMAS, H. L., HUBBELING, H. G., SPENCER, S. P., SINHA, R., SIMKINS, H. M., SALZMAN, N. H., BUSHMAN, F. D. & LAUFER, T. M. 2014. Conventional CD4+ T cells regulate IL-22-producing intestinal innate lymphoid cells. *Mucosal Immunol,* 7**,** 1045-57.

KOULOVA, L., CLARK, E. A., SHU, G. & DUPONT, B. 1991. The CD28 ligand B7/BB1 provides costimulatory signal for alloactivation of CD4+ T cells. *J Exp Med,* 173**,** 759-62.

KREMPSKI, J., KARYAMPUDI, L., BEHRENS, M. D., ERSKINE, C. L., HARTMANN, L., DONG, H., GOODE, E. L., KALLI, K. R. & KNUTSON, K. L. 2011. Tumor-infiltrating programmed death receptor-1+ dendritic cells mediate immune suppression in ovarian cancer. *J Immunol,* 186**,** 6905-13.

KRYCZEK, I., BANERJEE, M., CHENG, P., VATAN, L., SZELIGA, W., WEI, S., HUANG, E., FINLAYSON, E., SIMEONE, D., WELLING, T. H., CHANG, A., COUKOS, G., LIU, R. & ZOU, W. 2009. Phenotype, distribution, generation, and functional and clinical relevance of Th17 cells in the human tumor environments. *Blood,* 114**,** 1141-9.

KWONG, B., RUA, R., GAO, Y., FLICKINGER, J., JR., WANG, Y., KRUHLAK, M. J., ZHU, J., VIVIER, E., MCGAVERN, D. B. & LAZAREVIC, V. 2017. T-bet-dependent NKp46(+) innate lymphoid cells regulate the onset of TH17-induced neuroinflammation. *Nat Immunol,* 18**,** 1117-1127.

LARMONIER, N., CATHELIN, D., LARMONIER, C., NICOLAS, A., MERINO, D., JANIKASHVILI, N., AUDIA, S., BATEMAN, A., THOMPSON, J., KOTTKE, T., HARTUNG, T., KATSANIS, E., VILE, R. & BONNOTTE, B. 2007. The inhibition of TNF-alpha anti-tumoral properties by blocking antibodies promotes tumor growth in a rat model. *Exp Cell Res,* 313**,** 2345-55.

LAZAR-MOLNAR, E., CHEN, B., SWEENEY, K. A., WANG, E. J., LIU, W., LIN, J., PORCELLI, S. A., ALMO, S. C., NATHENSON, S. G. & JACOBS, W. R., JR. 2010. Programmed death-1 (PD-1)-deficient mice are extraordinarily sensitive to tuberculosis. *Proc Natl Acad Sci U S A,* 107**,** 13402-7.

LEACH, D. R., KRUMMEL, M. F. & ALLISON, J. P. 1996. Enhancement of antitumor immunity by CTLA-4 blockade. *Science,* 271**,** 1734-6.

LEHMANN, F. M., VON BURG, N., IVANEK, R., TEUFEL, C., HORVATH, E., PETER, A., TURCHINOVICH, G., STAEHLI, D., EICHLISBERGER, T., GOMEZ DE AGUERO, M., COTO-LLERENA, M., PRCHAL-MURPHY, M., SEXL, V., BENTIRES-ALJ, M., MUELLER, C. & FINKE, D. 2020. Microbiota-induced tissue signals regulate ILC3-mediated antigen presentation. *Nat Commun,* 11**,** 1794.

LEI, A. H., XIAO, Q., LIU, G. Y., SHI, K., YANG, Q., LI, X., LIU, Y. F., WANG, H. K., CAI, W. P., GUAN, Y. J., GABRILOVICH, D. I. & ZHOU, J. 2018. ICAM-1 controls development and function of ILC2. *J Exp Med,* 215**,** 2157-2174.

LI, J., SHI, W., SUN, H., JI, Y., CHEN, Y., GUO, X., SHENG, H., SHU, J., ZHOU, L., CAI, T. & QIU, J. 2019. Activation of DR3 signaling causes loss of ILC3s and exacerbates intestinal inflammation. *Nat Commun,* 10**,** 3371.

LIM, A. I., MENEGATTI, S., BUSTAMANTE, J., LE BOURHIS, L., ALLEZ, M., ROGGE, L., CASANOVA, J. L., YSSEL, H. & DI SANTO, J. P. 2016. IL-12 drives functional plasticity of human group 2 innate lymphoid cells. *J Exp Med,* 213**,** 569-83.

LINSLEY, P. S., GREENE, J. L., TAN, P., BRADSHAW, J., LEDBETTER, J. A., ANASETTI, C. & DAMLE, N. K. 1992. Coexpression and functional cooperation of CTLA-4 and CD28 on activated T lymphocytes. *J Exp Med,* 176**,** 1595-604.

LOH, J., CHU, D. T., O'GUIN, A. K., YOKOYAMA, W. M. & VIRGIN, H. W. T. 2005. Natural killer cells utilize both perforin and gamma interferon to regulate murine cytomegalovirus infection in the spleen and liver. *J Virol,* 79**,** 661-7.

LONG, A., DOMINGUEZ, D., QIN, L., CHEN, S., FAN, J., ZHANG, M., FANG, D., ZHANG, Y., KUZEL, T. M. & ZHANG, B. 2018. Type 2 Innate Lymphoid Cells Impede IL-33-Mediated Tumor Suppression. *J Immunol,* 201**,** 3456-3464.

LOPEZ-YGLESIAS, A. H., BURGER, E., CAMANZO, E., MARTIN, A. T., ARAUJO, A. M., KWOK, S. F. & YAROVINSKY, F. 2021. T-bet-dependent ILC1- and NK cell-derived IFN-gamma mediates cDC1-dependent host resistance against Toxoplasma gondii. *PLoS Pathog,* 17**,** e1008299.

MAAZI, H., PATEL, N., SANKARANARAYANAN, I., SUZUKI, Y., RIGAS, D., SOROOSH, P., FREEMAN, G. J., SHARPE, A. H. & AKBARI, O. 2015. ICOS:ICOS-ligand interaction is required for type 2 innate lymphoid cell function, homeostasis, and induction of airway hyperreactivity. *Immunity,* 42**,** 538-51.

MALLETT, G., LAURENCE, A. & AMARNATH, S. 2019. Programmed Cell Death-1 Receptor (PD-1)-Mediated Regulation of Innate Lymphoid Cells. *Int J Mol Sci,* 20.

MAO, Y., WANG, Y., DONG, L., ZHANG, Q., WANG, C., ZHANG, Y., LI, X. & FU, Z. 2019. Circulating exosomes from esophageal squamous cell carcinoma mediate the generation of B10 and PD-1(high) Breg cells. *Cancer Sci,* 110**,** 2700-2710.

MARSTERS, S. A., AYRES, T. M., SKUBATCH, M., GRAY, C. L., ROTHE, M. & ASHKENAZI, A. 1997. Herpesvirus entry mediator, a member of the tumor necrosis factor receptor (TNFR) family, interacts with members of the TNFR-associated factor family and activates the transcription factors NF-kappaB and AP-1. *J Biol Chem,* 272**,** 14029-32.

MARTINEZ-GONZALEZ, I., MATHA, L., STEER, C. A., GHAEDI, M., POON, G. F. & TAKEI, F. 2016. Allergen-Experienced Group 2 Innate Lymphoid Cells Acquire Memory-like Properties and Enhance Allergic Lung Inflammation. *Immunity,* 45**,** 198-208.

MARTINI, M., TESTI, M. G., PASETTO, M., PICCHIO, M. C., INNAMORATI, G., MAZZOCCO, M., UGEL, S., CINGARLINI, S., BRONTE, V., ZANOVELLO, P., KRAMPERA, M., MOSNA, F., CESTARI, T., RIVIERA, A. P., BRUTTI, N., BARBIERI, O., MATERA, L., TRIDENTE, G., COLOMBATTI, M. & SARTORIS, S. 2010. IFN-gamma-mediated upmodulation of MHC class I expression activates tumor-specific immune response in a mouse model of prostate cancer. *Vaccine,* 28**,** 3548-57.

MCADAM, A. J., CHANG, T. T., LUMELSKY, A. E., GREENFIELD, E. A., BOUSSIOTIS, V. A., DUKE-COHAN, J. S., CHERNOVA, T., MALENKOVICH, N., JABS, C., KUCHROO, V. K., LING, V., COLLINS, M., SHARPE, A. H. & FREEMAN, G. J. 2000. Mouse inducible costimulatory molecule (ICOS) expression is enhanced by CD28 costimulation and regulates differentiation of CD4+ T cells. *J Immunol,* 165**,** 5035-40.

MEBIUS, R. E., RENNERT, P. & WEISSMAN, I. L. 1997. Developing lymph nodes collect CD4+CD3- LTbeta+ cells that can differentiate to APC, NK cells, and follicular cells but not T or B cells. *Immunity,* 7**,** 493-504.

MELAIU, O., LUCARINI, V., CIFALDI, L. & FRUCI, D. 2019. Influence of the Tumor Microenvironment on NK Cell Function in Solid Tumors. *Front Immunol,* 10**,** 3038.

MEYLAN, F., RICHARD, A. C. & SIEGEL, R. M. 2011. TL1A and DR3, a TNF family ligand-receptor pair that promotes lymphocyte costimulation, mucosal hyperplasia, and autoimmune inflammation. *Immunol Rev,* 244**,** 188-96.

MIGDEN, M. R., RISCHIN, D., SCHMULTS, C. D., GUMINSKI, A., HAUSCHILD, A., LEWIS, K. D., CHUNG, C. H., HERNANDEZ-AYA, L., LIM, A. M., CHANG, A. L. S., RABINOWITS, G., THAI, A. A., DUNN, L. A., HUGHES, B. G. M., KHUSHALANI, N. I., MODI, B., SCHADENDORF, D., GAO, B., SEEBACH, F., LI, S., LI, J., MATHIAS, M., BOOTH, J., MOHAN, K., STANKEVICH, E., BABIKER, H. M., BRANA, I., GIL-MARTIN, M., HOMSI, J., JOHNSON, M. L., MORENO, V., NIU, J., OWONIKOKO, T. K., PAPADOPOULOS, K. P., YANCOPOULOS, G. D., LOWY, I. & FURY, M. G. 2018. PD-1 Blockade with Cemiplimab in Advanced Cutaneous Squamous-Cell Carcinoma. *N Engl J Med,* 379**,** 341-351.

MIRCHANDANI, A. S., BESNARD, A. G., YIP, E., SCOTT, C., BAIN, C. C., CEROVIC, V., SALMOND, R. J. & LIEW, F. Y. 2014. Type 2 innate lymphoid cells drive CD4+ Th2 cell responses. *J Immunol,* 192**,** 2442-8.

MOLOFSKY, A. B., NUSSBAUM, J. C., LIANG, H. E., VAN DYKEN, S. J., CHENG, L. E., MOHAPATRA, A., CHAWLA, A. & LOCKSLEY, R. M. 2013. Innate lymphoid type 2 cells sustain visceral adipose tissue eosinophils and alternatively activated macrophages. *J Exp Med,* 210**,** 535-49.

MONTICELLI, L. A., OSBORNE, L. C., NOTI, M., TRAN, S. V., ZAISS, D. M. & ARTIS, D. 2015. IL-33 promotes an innate immune pathway of intestinal tissue protection dependent on amphiregulin-EGFR interactions. *Proc Natl Acad Sci U S A,* 112**,** 10762-7.

MONTICELLI, L. A., SONNENBERG, G. F., ABT, M. C., ALENGHAT, T., ZIEGLER, C. G., DOERING, T. A., ANGELOSANTO, J. M., LAIDLAW, B. J., YANG, C. Y., SATHALIYAWALA, T., KUBOTA, M., TURNER, D., DIAMOND, J. M., GOLDRATH, A. W., FARBER, D. L., COLLMAN, R. G., WHERRY, E. J. & ARTIS, D. 2011. Innate lymphoid cells promote lung-tissue homeostasis after infection with influenza virus. *Nat Immunol,* 12**,** 1045-54.

MORAL, J. A., LEUNG, J., ROJAS, L. A., RUAN, J., ZHAO, J., SETHNA, Z., RAMNARAIN, A., GASMI, B., GURURAJAN, M., REDMOND, D., ASKAN, G., BHANOT, U., ELYADA, E., PARK, Y., TUVESON, D. A., GONEN, M., LEACH, S. D., WOLCHOK, J. D., DEMATTEO, R. P., MERGHOUB, T. & BALACHANDRAN, V. P. 2020. ILC2s amplify PD-1 blockade by activating tissue-specific cancer immunity. *Nature,* 579**,** 130-135.

MORO, K., YAMADA, T., TANABE, M., TAKEUCHI, T., IKAWA, T., KAWAMOTO, H., FURUSAWA, J., OHTANI, M., FUJII, H. & KOYASU, S. 2010. Innate production of T(H)2 cytokines by adipose tissue-associated c-Kit(+)Sca-1(+) lymphoid cells. *Nature,* 463**,** 540-4.

MORROW, M. A., MAYER, E. W., PEREZ, C. A., ADLAM, M. & SIU, G. 1999. Overexpression of the Helix-Loop-Helix protein Id2 blocks T cell development at multiple stages. *Mol Immunol,* 36**,** 491-503.

MORTHA, A., CHUDNOVSKIY, A., HASHIMOTO, D., BOGUNOVIC, M., SPENCER, S. P., BELKAID, Y. & MERAD, M. 2014. Microbiota-dependent crosstalk between macrophages and ILC3 promotes intestinal homeostasis. *Science,* 343**,** 1249288.

MUELLER, D. L., JENKINS, M. K. & SCHWARTZ, R. H. 1989. Clonal expansion versus functional clonal inactivation: a costimulatory signalling pathway determines the outcome of T cell antigen receptor occupancy. *Annu Rev Immunol,* 7**,** 445-80.

MUNNEKE, J. M., BJORKLUND, A. T., MJOSBERG, J. M., GARMING-LEGERT, K., BERNINK, J. H., BLOM, B., HUISMAN, C., VAN OERS, M. H., SPITS, H., MALMBERG, K. J. & HAZENBERG, M. D. 2014. Activated innate lymphoid cells are associated with a reduced susceptibility to graft-versus-host disease. *Blood,* 124**,** 812-21.

MURPHY, T. L. & MURPHY, K. M. 2010. Slow down and survive: Enigmatic immunoregulation by BTLA and HVEM. *Annu Rev Immunol,* 28**,** 389-411.

NABEKURA, T., RIGGAN, L., HILDRETH, A. D., O'SULLIVAN, T. E. & SHIBUYA, A. 2020. Type 1 Innate Lymphoid Cells Protect Mice from Acute Liver Injury via Interferon-gamma

Secretion for Upregulating Bcl-xL Expression in Hepatocytes. *Immunity,* 52**,** 96-108 e9.

NAKAJIMA, C., UEKUSA, Y., IWASAKI, M., YAMAGUCHI, N., MUKAI, T., GAO, P., TOMURA, M., ONO, S., TSUJIMURA, T., FUJIWARA, H. & HAMAOKA, T. 2001. A role of interferon-gamma (IFN-gamma) in tumor immunity: T cells with the capacity to reject tumor cells are generated but fail to migrate to tumor sites in IFN-gamma-deficient mice. *Cancer Res,* 61**,** 3399-405.

NATHAN, C. F., MURRAY, H. W., WIEBE, M. E. & RUBIN, B. Y. 1983. Identification of interferon-gamma as the lymphokine that activates human macrophage oxidative metabolism and antimicrobial activity. *J Exp Med,* 158**,** 670-89.

NEILL, D. R., WONG, S. H., BELLOSI, A., FLYNN, R. J., DALY, M., LANGFORD, T. K., BUCKS, C., KANE, C. M., FALLON, P. G., PANNELL, R., JOLIN, H. E. & MCKENZIE, A. N. 2010. Nuocytes represent a new innate effector leukocyte that mediates type-2 immunity. *Nature,* 464**,** 1367-70.

NEWLAND, S. A., MOHANTA, S., CLEMENT, M., TALEB, S., WALKER, J. A., NUS, M., SAGE, A. P., YIN, C., HU, D., KITT, L. L., FINIGAN, A. J., RODEWALD, H. R., BINDER, C. J., MCKENZIE, A. N. J., HABENICHT, A. J. & MALLAT, Z. 2017. Type-2 innate lymphoid cells control the development of atherosclerosis in mice. *Nat Commun,* 8**,** 15781.

NISHIMURA, H. & HONJO, T. 2001. PD-1: an inhibitory immunoreceptor involved in peripheral tolerance. *Trends Immunol,* 22**,** 265-8.

NISHIMURA, H., NOSE, M., HIAI, H., MINATO, N. & HONJO, T. 1999. Development of lupus-like autoimmune diseases by disruption of the PD-1 gene encoding an ITIM motif-carrying immunoreceptor. *Immunity,* 11**,** 141-51.

NISHIMURA, H., OKAZAKI, T., TANAKA, Y., NAKATANI, K., HARA, M., MATSUMORI, A., SASAYAMA, S., MIZOGUCHI, A., HIAI, H., MINATO, N. & HONJO, T. 2001. Autoimmune dilated cardiomyopathy in PD-1 receptor-deficient mice. *Science,* 291**,** 319-22.

O'SULLIVAN, T. E., RAPP, M., FAN, X., WEIZMAN, O. E., BHARDWAJ, P., ADAMS, N. M., WALZER, T., DANNENBERG, A. J. & SUN, J. C. 2016. Adipose-Resident Group 1 Innate Lymphoid Cells Promote Obesity-Associated Insulin Resistance. *Immunity,* 45**,** 428-41.

OLDENHOVE, G., BOUCQUEY, E., TAQUIN, A., ACOLTY, V., BONETTI, L., RYFFEL, B., LE BERT, M., ENGLEBERT, K., BOON, L. & MOSER, M. 2018. PD-1 Is Involved in the Dysregulation of Type 2 Innate Lymphoid Cells in a Murine Model of Obesity. *Cell Rep,* 25**,** 2053-2060 e4.

PACLIK, D., STEHLE, C., LAHMANN, A., HUTLOFF, A. & ROMAGNANI, C. 2015. ICOS regulates the pool of group 2 innate lymphoid cells under homeostatic and inflammatory conditions in mice. *Eur J Immunol,* 45**,** 2766-72.

PAINE, A., KIRCHNER, H., IMMENSCHUH, S., OELKE, M., BLASCZYK, R. & EIZ-VESPER, B. 2012. IL-2 upregulates CD86 expression on human CD4(+) and CD8(+) T cells. *J Immunol,* 188**,** 1620-9.

PAN, J., ZHANG, M., WANG, J., WANG, Q., XIA, D., SUN, W., ZHANG, L., YU, H., LIU, Y. & CAO, X. 2004. Interferon-gamma is an autocrine mediator for dendritic cell maturation. *Immunol Lett,* 94**,** 141-51.

PARANG, B., BARRETT, C. W. & WILLIAMS, C. S. 2016. AOM/DSS Model of Colitis-Associated Cancer. *Methods Mol Biol,* 1422**,** 297-307.

PARRY, R. V., CHEMNITZ, J. M., FRAUWIRTH, K. A., LANFRANCO, A. R., BRAUNSTEIN, I., KOBAYASHI, S. V., LINSLEY, P. S., THOMPSON, C. B. & RILEY, J. L. 2005. CTLA-4 and PD-1 receptors inhibit T-cell activation by distinct mechanisms. *Mol Cell Biol,* 25**,** 9543-53.

PATSOUKIS, N., BARDHAN, K., CHATTERJEE, P., SARI, D., LIU, B., BELL, L. N., KAROLY, E. D., FREEMAN, G. J., PETKOVA, V., SETH, P., LI, L. & BOUSSIOTIS, V. A. 2015. PD-1 alters T-cell metabolic reprogramming by inhibiting glycolysis and promoting lipolysis and fatty acid oxidation. *Nat Commun,* 6**,** 6692.

PEAPER, D. R. & CRESSWELL, P. 2008. Regulation of MHC class I assembly and peptide binding. *Annu Rev Cell Dev Biol,* 24**,** 343-68.

POPIVANOVA, B. K., KITAMURA, K., WU, Y., KONDO, T., KAGAYA, T., KANEKO, S., OSHIMA, M., FUJII, C. & MUKAIDA, N. 2008. Blocking TNF-alpha in mice reduces colorectal carcinogenesis associated with chronic colitis. *J Clin Invest,* 118**,** 560-70.

RAHIM, M. M., TU, M. M., MAHMOUD, A. B., WIGHT, A., ABOU-SAMRA, E., LIMA, P. D. & MAKRIGIANNIS, A. P. 2014. Ly49 receptors: innate and adaptive immune paradigms. *Front Immunol,* 5**,** 145.

RALLI, M., BOTTICELLI, A., VISCONTI, I. C., ANGELETTI, D., FIORE, M., MARCHETTI, P., LAMBIASE, A., DE VINCENTIIS, M. & GRECO, A. 2020. Immunotherapy in the Treatment of Metastatic Melanoma: Current Knowledge and Future Directions. *J Immunol Res,* 2020**,** 9235638.

RANKIN, L. C., GROOM, J. R., CHOPIN, M., HEROLD, M. J., WALKER, J. A., MIELKE, L. A., MCKENZIE, A. N., CAROTTA, S., NUTT, S. L. & BELZ, G. T. 2013. The transcription factor T-bet is essential for the development of NKp46+ innate lymphocytes via the Notch pathway. *Nat Immunol,* 14**,** 389-95.

ROBINETTE, M. L., BANDO, J. K., SONG, W., ULLAND, T. K., GILFILLAN, S. & COLONNA, M. 2017. IL-15 sustains IL-7R-independent ILC2 and ILC3 development. *Nat Commun,* 8**,** 14601.

ROBINETTE, M. L., FUCHS, A., CORTEZ, V. S., LEE, J. S., WANG, Y., DURUM, S. K., GILFILLAN, S., COLONNA, M. & IMMUNOLOGICAL GENOME, C. 2015. Transcriptional programs define molecular characteristics of innate lymphoid cell classes and subsets. *Nat Immunol,* 16**,** 306-17.

ROEDIGER, B., KYLE, R., YIP, K. H., SUMARIA, N., GUY, T. V., KIM, B. S., MITCHELL, A. J., TAY, S. S., JAIN, R., FORBES-BLOM, E., CHEN, X., TONG, P. L., BOLTON, H. A., ARTIS, D., PAUL, W. E., FAZEKAS DE ST GROTH, B., GRIMBALDESTON, M. A., LE GROS, G. & WENINGER, W. 2013. Cutaneous immunosurveillance and regulation of inflammation by group 2 innate lymphoid cells. *Nat Immunol,* 14**,** 564-73.

RUDD, C. E., TAYLOR, A. & SCHNEIDER, H. 2009. CD28 and CTLA-4 coreceptor expression and signal transduction. *Immunol Rev,* 229**,** 12-26.

RUDENSKY, A., PRESTON-HURLBURT, P., HONG, S. C., BARLOW, A. & JANEWAY, C. A., JR. 1991. Sequence analysis of peptides bound to MHC class II molecules. *Nature,* 353**,** 622-7.

RUEGG, C., POSTIGO, A. A., SIKORSKI, E. E., BUTCHER, E. C., PYTELA, R. & ERLE, D. J. 1992. Role of integrin alpha 4 beta 7/alpha 4 beta P in lymphocyte adherence to fibronectin and VCAM-1 and in homotypic cell clustering. *J Cell Biol,* 117**,** 179-89.

SABHARWAL, S. S., ROSEN, D. B., GREIN, J., TEDESCO, D., JOYCE-SHAIKH, B., UEDA, R., SEMANA, M., BAUER, M., BANG, K., STEVENSON, C., CUA, D. J. & ZUNIGA, L. A. 2018. GITR Agonism Enhances Cellular Metabolism to Support CD8(+) T-cell Proliferation and Effector Cytokine Production in a Mouse Tumor Model. *Cancer Immunol Res,* 6**,** 1199-1211.

SALIMI, M., BARLOW, J. L., SAUNDERS, S. P., XUE, L., GUTOWSKA-OWSIAK, D., WANG, X., HUANG, L. C., JOHNSON, D., SCANLON, S. T., MCKENZIE, A. N., FALLON, P. G. & OGG, G. S. 2013. A role for IL-25 and IL-33-driven type-2 innate lymphoid cells in atopic dermatitis. *J Exp Med,* 210**,** 2939-50.

SALIMI, M., WANG, R., YAO, X., LI, X., WANG, X., HU, Y., CHANG, X., FAN, P., DONG, T. & OGG, G. 2018. Activated innate lymphoid cell populations accumulate in human tumour tissues. *BMC Cancer,* 18**,** 341.

SANCHEZ-PAULETE, A. R., CUETO, F. J., MARTINEZ-LOPEZ, M., LABIANO, S., MORALES-KASTRESANA, A., RODRIGUEZ-RUIZ, M. E., JURE-KUNKEL, M., AZPILIKUETA, A., AZNAR, M. A., QUETGLAS, J. I., SANCHO, D. & MELERO, I. 2016. Cancer Immunotherapy with Immunomodulatory Anti-CD137 and Anti-PD-1 Monoclonal Antibodies Requires BATF3-Dependent Dendritic Cells. *Cancer Discov,* 6**,** 71-9.

SAWA, S., LOCHNER, M., SATOH-TAKAYAMA, N., DULAUROY, S., BERARD, M., KLEINSCHEK, M., CUA, D., DI SANTO, J. P. & EBERL, G. 2011. RORgammat+ innate lymphoid cells regulate intestinal homeostasis by integrating negative signals from the symbiotic microbiota. *Nat Immunol,* 12**,** 320-6.

SCHATTON, T., MURPHY, G. F., FRANK, N. Y., YAMAURA, K., WAAGA-GASSER, A. M., GASSER, M., ZHAN, Q., JORDAN, S., DUNCAN, L. M., WEISHAUPT, C., FUHLBRIGGE, R. C., KUPPER, T. S., SAYEGH, M. H. & FRANK, M. H. 2008. Identification of cells initiating human melanomas. *Nature,* 451**,** 345-9.

SCHNYDER-CANDRIAN, S., TOGBE, D., COUILLIN, I., MERCIER, I., BROMBACHER, F., QUESNIAUX, V., FOSSIEZ, F., RYFFEL, B. & SCHNYDER, B. 2006. Interleukin-17 is a negative regulator of established allergic asthma. *J Exp Med,* 203**,** 2715-25.

SCHUIJS, M. J., PNG, S., RICHARD, A. C., TSYBEN, A., HAMM, G., STOCKIS, J., GARCIA, C., PINAUD, S., NICHOLLS, A., ROS, X. R., SU, J., ELDRIDGE, M. D., RIEDEL, A., SERRAO, E. M., RODEWALD, H. R., MACK, M., SHIELDS, J. D., COHEN, E. S., MCKENZIE, A. N. J., GOODWIN, R. J. A., BRINDLE, K. M., MARIONI, J. C. & HALIM, T. Y. F. 2020. ILC2-driven innate immune checkpoint mechanism antagonizes NK cell antimetastatic function in the lung. *Nat Immunol,* 21**,** 998-1009.

SCHWARTZ, C., KHAN, A. R., FLOUDAS, A., SAUNDERS, S. P., HAMS, E., RODEWALD, H. R., MCKENZIE, A. N. J. & FALLON, P. G. 2017. ILC2s regulate adaptive Th2 cell functions via PD-L1 checkpoint control. *J Exp Med,* 214**,** 2507-2521.

SCHWARTZ, R. H. 2003. T cell anergy. *Annu Rev Immunol,* 21**,** 305-34.

SCOTT, K. A., MOORE, R. J., ARNOTT, C. H., EAST, N., THOMPSON, R. G., SCALLON, B. J., SHEALY, D. J. & BALKWILL, F. R. 2003. An anti-tumor necrosis factor-alpha antibody inhibits the development of experimental skin tumors. *Mol Cancer Ther,* 2**,** 445-51.

SEEHUS, C. R., ALIAHMAD, P., DE LA TORRE, B., ILIEV, I. D., SPURKA, L., FUNARI, V. A. & KAYE, J. 2015. The development of innate lymphoid cells requires TOX-dependent generation of a common innate lymphoid cell progenitor. *Nat Immunol,* 16**,** 599-608.

SEILLET, C. & BELZ, G. T. 2016. Differentiation and diversity of subsets in group 1 innate lymphoid cells. *Int Immunol,* 28**,** 3-11.

SEILLET, C., MIELKE, L. A., AMANN-ZALCENSTEIN, D. B., SU, S., GAO, J., ALMEIDA, F. F., SHI, W., RITCHIE, M. E., NAIK, S. H., HUNTINGTON, N. D., CAROTTA, S. & BELZ, G. T. 2016. Deciphering the Innate Lymphoid Cell Transcriptional Program. *Cell Rep,* 17**,** 436-447.

SEO, G. Y., SHUI, J. W., TAKAHASHI, D., SONG, C., WANG, Q., KIM, K., MIKULSKI, Z., CHANDRA, S., GILES, D. A., ZAHNER, S., KIM, P. H., CHEROUTRE, H., COLONNA, M. & KRONENBERG, M. 2018. LIGHT-HVEM Signaling in Innate Lymphoid Cell Subsets Protects Against Enteric Bacterial Infection. *Cell Host Microbe,* 24**,** 249-260 e4.

SERAFINI, N., KLEIN WOLTERINK, R. G., SATOH-TAKAYAMA, N., XU, W., VOSSHENRICH, C. A., HENDRIKS, R. W. & DI SANTO, J. P. 2014. Gata3 drives development of RORgammat+ group 3 innate lymphoid cells. *J Exp Med,* 211**,** 199-208.

SERAFINI, N., VOSSHENRICH, C. A. & DI SANTO, J. P. 2015. Transcriptional regulation of innate lymphoid cell fate. *Nat Rev Immunol,* 15**,** 415-28.

SHAFIEI-JAHANI, P., HURRELL, B. P., GALLE-TREGER, L., HELOU, D. G., HOWARD, E., PAINTER, J., LO, R., LEWIS, G., SOROOSH, P. & AKBARI, O. 2020. DR3 stimulation of adipose resident ILC2s ameliorates type 2 diabetes mellitus. *Nat Commun,* 11**,** 4718.

SHAHINIAN, A., PFEFFER, K., LEE, K. P., KUNDIG, T. M., KISHIHARA, K., WAKEHAM, A., KAWAI, K., OHASHI, P. S., THOMPSON, C. B. & MAK, T. W. 1993. Differential T cell costimulatory requirements in CD28-deficient mice. *Science,* 261**,** 609-12.

SHI, M., ROEMER, M. G., CHAPUY, B., LIAO, X., SUN, H., PINKUS, G. S., SHIPP, M. A., FREEMAN, G. J. & RODIG, S. J. 2014. Expression of programmed cell death 1 ligand 2 (PD-L2) is a distinguishing feature of primary mediastinal (thymic) large B-cell lymphoma and associated with PDCD1LG2 copy gain. *Am J Surg Pathol,* 38**,** 1715-23.

SHUI, J. W. & KRONENBERG, M. 2013. HVEM: An unusual TNF receptor family member important for mucosal innate immune responses to microbes. *Gut Microbes,* 4**,** 146-51.

SIMPSON, T. R., QUEZADA, S. A. & ALLISON, J. P. 2010. Regulation of CD4 T cell activation and effector function by inducible costimulator (ICOS). *Curr Opin Immunol,* 22**,** 326-32.

SO, T. & CROFT, M. 2007. Cutting edge: OX40 inhibits TGF-beta- and antigen-driven conversion of naive CD4 T cells into CD25+Foxp3+ T cells. *J Immunol,* 179**,** 1427-30.

SONG, M., PING, Y., ZHANG, K., YANG, L., LI, F., ZHANG, C., CHENG, S., YUE, D., MAIMELA, N. R., QU, J., LIU, S., SUN, T., LI, Z., XIA, J., ZHANG, B., WANG, L. & ZHANG, Y. 2019. Low-Dose IFNgamma Induces Tumor Cell Stemness in Tumor Microenvironment of Non-Small Cell Lung Cancer. *Cancer Res,* 79**,** 3737-3748.

SONNENBERG, G. F. & ARTIS, D. 2015. Innate lymphoid cells in the initiation, regulation and resolution of inflammation. *Nat Med,* 21**,** 698-708.

SONNENBERG, G. F., MONTICELLI, L. A., ELLOSO, M. M., FOUSER, L. A. & ARTIS, D. 2011. CD4(+) lymphoid tissue-inducer cells promote innate immunity in the gut. *Immunity,* 34**,** 122-34.

STRAUSS, L., MAHMOUD, M. A. A., WEAVER, J. D., TIJARO-OVALLE, N. M., CHRISTOFIDES, A., WANG, Q., PAL, R., YUAN, M., ASARA, J., PATSOUKIS, N. & BOUSSIOTIS, V. A. 2020. Targeted deletion of PD-1 in myeloid cells induces antitumor immunity. *Sci Immunol,* 5.

SUGIMOTO, K., OGAWA, A., MIZOGUCHI, E., SHIMOMURA, Y., ANDOH, A., BHAN, A. K., BLUMBERG, R. S., XAVIER, R. J. & MIZOGUCHI, A. 2008. IL-22 ameliorates intestinal inflammation in a mouse model of ulcerative colitis. *J Clin Invest,* 118**,** 534-44.

SUNG, H., FERLAY, J., SIEGEL, R. L., LAVERSANNE, M., SOERJOMATARAM, I., JEMAL, A. & BRAY, F. 2021. Global Cancer Statistics 2020: GLOBOCAN Estimates of Incidence and Mortality Worldwide for 36 Cancers in 185 Countries. *CA Cancer J Clin,* 71**,** 209-249.

SWALLOW, M. M., WALLIN, J. J. & SHA, W. C. 1999. B7h, a novel costimulatory homolog of B7.1 and B7.2, is induced by TNFalpha. *Immunity,* 11**,** 423-32.

TAKAHASHI, T., TAGAMI, T., YAMAZAKI, S., UEDE, T., SHIMIZU, J., SAKAGUCHI, N., MAK, T. W. & SAKAGUCHI, S. 2000. Immunologic self-tolerance maintained by CD25(+)CD4(+) regulatory T cells constitutively expressing cytotoxic T lymphocyte-associated antigen 4. *J Exp Med,* 192**,** 303-10.

TAYLOR, S., HUANG, Y., MALLETT, G., STATHOPOULOU, C., FELIZARDO, T. C., SUN, M. A., MARTIN, E. L., ZHU, N., WOODWARD, E. L., ELIAS, M. S., SCOTT, J., REYNOLDS, N. J., PAUL, W. E., FOWLER, D. H. & AMARNATH, S. 2017. PD-1 regulates KLRG1(+) group 2 innate lymphoid cells. *J Exp Med,* 214**,** 1663-1678.

TEUNISSEN, M. B. M., MUNNEKE, J. M., BERNINK, J. H., SPULS, P. I., RES, P. C. M., TE VELDE, A., CHEUK, S., BROUWER, M. W. D., MENTING, S. P., EIDSMO, L., SPITS, H.,

HAZENBERG, M. D. & MJOSBERG, J. 2014. Composition of innate lymphoid cell subsets in the human skin: enrichment of NCR(+) ILC3 in lesional skin and blood of psoriasis patients. *J Invest Dermatol,* 134**,** 2351-2360.

TIAN, J., ZHANG, B., RUI, K. & WANG, S. 2020. The Role of GITR/GITRL Interaction in Autoimmune Diseases. *Front Immunol,* 11**,** 588682.

TIVOL, E. A., BORRIELLO, F., SCHWEITZER, A. N., LYNCH, W. P., BLUESTONE, J. A. & SHARPE, A. H. 1995. Loss of CTLA-4 leads to massive lymphoproliferation and fatal multiorgan tissue destruction, revealing a critical negative regulatory role of CTLA-4. *Immunity,* 3**,** 541-7.

TOMURA, M. & KABASHIMA, K. 2013. Analysis of cell movement between skin and other anatomical sites in vivo using photoconvertible fluorescent protein "Kaede"-transgenic mice. *Methods Mol Biol,* 961**,** 279-86.

TOPALIAN, S. L., HODI, F. S., BRAHMER, J. R., GETTINGER, S. N., SMITH, D. C., MCDERMOTT, D. F., POWDERLY, J. D., CARVAJAL, R. D., SOSMAN, J. A., ATKINS, M. B., LEMING, P. D., SPIGEL, D. R., ANTONIA, S. J., HORN, L., DRAKE, C. G., PARDOLL, D. M., CHEN, L., SHARFMAN, W. H., ANDERS, R. A., TAUBE, J. M., MCMILLER, T. L., XU, H., KORMAN, A. J., JURE-KUNKEL, M., AGRAWAL, S., MCDONALD, D., KOLLIA, G. D., GUPTA, A., WIGGINTON, J. M. & SZNOL, M. 2012. Safety, activity, and immune correlates of anti-PD-1 antibody in cancer. *N Engl J Med,* 366**,** 2443-54.

TRABANELLI, S., CHEVALIER, M. F., MARTINEZ-USATORRE, A., GOMEZ-CADENA, A., SALOME, B., LECCISO, M., SALVESTRINI, V., VERDEIL, G., RACLE, J., PAPAYANNIDIS, C., MORITA, H., PIZZITOLA, I., GRANDCLEMENT, C., BOHNER, P., BRUNI, E., GIROTRA, M., PALLAVI, R., FALVO, P., LEIBUNDGUT, E. O., BAERLOCHER, G. M., CARLO-STELLA, C., TAURINO, D., SANTORO, A., SPINELLI, O., RAMBALDI, A., GIARIN, E., BASSO, G., TRESOLDI, C., CICERI, F., GFELLER, D., AKDIS, C. A., MAZZARELLA, L., MINUCCI, S., PELICCI, P. G., MARCENARO, E., MCKENZIE, A. N. J., VANHECKE, D., COUKOS, G., MAVILIO, D., CURTI, A., DERRE, L. & JANDUS, C. 2017. Tumour-derived PGD2 and NKp30-B7H6 engagement drives an immunosuppressive ILC2-MDSC axis. *Nat Commun,* 8**,** 593.

TRABANELLI, S., CURTI, A., LECCISO, M., SALOME, B., RIETHER, C., OCHSENBEIN, A., ROMERO, P. & JANDUS, C. 2015. CD127+ innate lymphoid cells are dysregulated in treatment naive acute myeloid leukemia patients at diagnosis. *Haematologica,* 100**,** e257-60.

TUMINO, N., MARTINI, S., MUNARI, E., SCORDAMAGLIA, F., BESI, F., MARIOTTI, F. R., BOGINA, G., MINGARI, M. C., VACCA, P. & MORETTA, L. 2019. Presence of innate lymphoid cells in pleural effusions of primary and metastatic tumors: Functional analysis and expression of PD-1 receptor. *Int J Cancer,* 145**,** 1660-1668.

TURCHINOVICH, G., GANTER, S., BARENWALDT, A. & FINKE, D. 2018. NKp46 Calibrates Tumoricidal Potential of Type 1 Innate Lymphocytes by Regulating TRAIL Expression. *J Immunol,* 200**,** 3762-3768.

TWOHIG, J. P., MARSDEN, M., CUFF, S. M., FERDINAND, J. R., GALLIMORE, A. M., PERKS, W. V., AL-SHAMKHANI, A., HUMPHREYS, I. R. & WANG, E. C. 2012. The death receptor 3/TL1A pathway is essential for efficient development of antiviral CD4(+) and CD8(+) T-cell immunity. *FASEB J,* 26**,** 3575-86.

URQUHART, L. 2021. Top companies and drugs by sales in 2020. *Nat Rev Drug Discov,* 20**,** 253.

VACCA, P., PESCE, S., GREPPI, M., FULCHERI, E., MUNARI, E., OLIVE, D., MINGARI, M. C., MORETTA, A., MORETTA, L. & MARCENARO, E. 2019. PD-1 is expressed by and regulates human group 3 innate lymphoid cells in human decidua. *Mucosal Immunol,* 12**,** 624-631.

VAN BEEK, J. J. P., MARTENS, A. W. J., BAKDASH, G. & DE VRIES, I. J. M. 2016. Innate Lymphoid Cells in Tumor Immunity. *Biomedicines,* 4.

VAN DE WALLE, I., DOLENS, A. C., DURINCK, K., DE MULDER, K., VAN LOOCKE, W., DAMLE, S., WAEGEMANS, E., DE MEDTS, J., VELGHE, I., DE SMEDT, M., VANDEKERCKHOVE, B., KERRE, T., PLUM, J., LECLERCQ, G., ROTHENBERG, E. V., VAN VLIERBERGHE, P., SPELEMAN, F. & TAGHON, T. 2016. GATA3 induces human T-cell commitment by restraining Notch activity and repressing NK-cell fate. *Nat Commun,* 7**,** 11171.

VAN DER BRUGGEN, P., TRAVERSARI, C., CHOMEZ, P., LURQUIN, C., DE PLAEN, E., VAN DEN EYNDE, B., KNUTH, A. & BOON, T. 1991. A gene encoding an antigen recognized by cytolytic T lymphocytes on a human melanoma. *Science,* 254**,** 1643-7.

VAN DER MERWE, P. A., BODIAN, D. L., DAENKE, S., LINSLEY, P. & DAVIS, S. J. 1997. CD80 (B7-1) binds both CD28 and CTLA-4 with a low affinity and very fast kinetics. *J Exp Med,* 185**,** 393-403.

VAN GOOL, F., MOLOFSKY, A. B., MORAR, M. M., ROSENZWAJG, M., LIANG, H. E., KLATZMANN, D., LOCKSLEY, R. M. & BLUESTONE, J. A. 2014. Interleukin-5-producing group 2 innate lymphoid cells control eosinophilia induced by interleukin-2 therapy. *Blood,* 124**,** 3572-6.

VAN OLFFEN, R. W., KONING, N., VAN GISBERGEN, K. P., WENSVEEN, F. M., HOEK, R. M., BOON, L., HAMANN, J., VAN LIER, R. A. & NOLTE, M. A. 2009. GITR triggering induces expansion of both effector and regulatory CD4+ T cells in vivo. *J Immunol,* 182**,** 7490-500.

VASHIST, N., TRITTEL, S., EBENSEN, T., CHAMBERS, B. J., GUZMAN, C. A. & RIESE, P. 2018. Influenza-Activated ILC1s Contribute to Antiviral Immunity Partially Influenced by Differential GITR Expression. *Front Immunol,* 9**,** 505.

VILLANOVA, F., FLUTTER, B., TOSI, I., GRYS, K., SREENEEBUS, H., PERERA, G. K., CHAPMAN, A., SMITH, C. H., DI MEGLIO, P. & NESTLE, F. O. 2014. Characterization of innate lymphoid cells in human skin and blood demonstrates increase of NKp44+ ILC3 in psoriasis. *J Invest Dermatol,* 134**,** 984-991.

VORON, T., COLUSSI, O., MARCHETEAU, E., PERNOT, S., NIZARD, M., POINTET, A. L., LATRECHE, S., BERGAYA, S., BENHAMOUDA, N., TANCHOT, C., STOCKMANN, C., COMBE, P., BERGER, A., ZINZINDOHOUE, F., YAGITA, H., TARTOUR, E., TAIEB, J. & TERME, M. 2015. VEGF-A modulates expression of inhibitory checkpoints on CD8+ T cells in tumors. *J Exp Med,* 212**,** 139-48.

WAGNER, M., EALEY, K. N., TETSU, H., KINIWA, T., MOTOMURA, Y., MORO, K. & KOYASU, S. 2020. Tumor-Derived Lactic Acid Contributes to the Paucity of Intratumoral ILC2s. *Cell Rep,* 30**,** 2743-2757 e5.

WALDMAN, A. D., FRITZ, J. M. & LENARDO, M. J. 2020. A guide to cancer immunotherapy: from T cell basic science to clinical practice. *Nat Rev Immunol,* 20**,** 651-668.

WALKER, J. A. & MCKENZIE, A. N. 2013. Development and function of group 2 innate lymphoid cells. *Curr Opin Immunol,* 25**,** 148-55.

WANG, S., QU, Y., XIA, P., CHEN, Y., ZHU, X., ZHANG, J., WANG, G., TIAN, Y., YING, J. & FAN, Z. 2020. Transdifferentiation of tumor infiltrating innate lymphoid cells during progression of colorectal cancer. *Cell Res,* 30**,** 610-622.

WANG, S., XIA, P., CHEN, Y., QU, Y., XIONG, Z., YE, B., DU, Y., TIAN, Y., YIN, Z., XU, Z. & FAN, Z. 2017. Regulatory Innate Lymphoid Cells Control Innate Intestinal Inflammation. *Cell,* 171**,** 201-216 e18.

WANG, X., PENG, H., CONG, J., WANG, X., LIAN, Z., WEI, H., SUN, R. & TIAN, Z. 2018. Memory formation and long-term maintenance of IL-7Ralpha(+) ILC1s via a lymph node-liver axis. *Nat Commun,* 9**,** 4854.

WANG, X., PENG, H. & TIAN, Z. 2019. Innate lymphoid cell memory. *Cell Mol Immunol,* 16**,** 423-429.

WEBER, J. S., D'ANGELO, S. P., MINOR, D., HODI, F. S., GUTZMER, R., NEYNS, B., HOELLER, C., KHUSHALANI, N. I., MILLER, W. H., JR., LAO, C. D., LINETTE, G. P., THOMAS, L., LORIGAN, P., GROSSMANN, K. F., HASSEL, J. C., MAIO, M., SZNOL, M., ASCIERTO, P. A., MOHR, P., CHMIELOWSKI, B., BRYCE, A., SVANE, I. M., GROB, J. J., KRACKHARDT, A. M., HORAK, C., LAMBERT, A., YANG, A. S. & LARKIN, J. 2015. Nivolumab versus chemotherapy in patients with advanced melanoma who progressed after anti-CTLA-4 treatment (CheckMate 037): a randomised, controlled, open-label, phase 3 trial. *Lancet Oncol,* 16**,** 375-84.

WEIZMAN, O. E., ADAMS, N. M., SCHUSTER, I. S., KRISHNA, C., PRITYKIN, Y., LAU, C., DEGLI-ESPOSTI, M. A., LESLIE, C. S., SUN, J. C. & O'SULLIVAN, T. E. 2017. ILC1 Confer Early Host Protection at Initial Sites of Viral Infection. *Cell,* 171**,** 795-808 e12.

WOHLFAHRT, T., USHERENKO, S., ENGLBRECHT, M., DEES, C., WEBER, S., BEYER, C., GELSE, K., DISTLER, O., SCHETT, G., DISTLER, J. H. & RAMMING, A. 2016. Type 2 innate lymphoid cell counts are increased in patients with systemic sclerosis and correlate with the extent of fibrosis. *Ann Rheum Dis,* 75**,** 623-6.

WONG, S. H., WALKER, J. A., JOLIN, H. E., DRYNAN, L. F., HAMS, E., CAMELO, A., BARLOW, J. L., NEILL, D. R., PANOVA, V., KOCH, U., RADTKE, F., HARDMAN, C. S., HWANG, Y. Y., FALLON, P. G. & MCKENZIE, A. N. 2012. Transcription factor RORalpha is critical for nuocyte development. *Nat Immunol,* 13**,** 229-36.

WU, J., CUI, Y., ZHU, W., BAI, S., ZHAO, N. & LIU, B. 2019. Critical role of OX40/OX40L in ILC2-mediated activation of CD4(+)T cells during respiratory syncytial virus infection in mice. *Int Immunopharmacol,* 76**,** 105784.

XIAO, X., LAO, X. M., CHEN, M. M., LIU, R. X., WEI, Y., OUYANG, F. Z., CHEN, D. P., ZHAO, X. Y., ZHAO, Q., LI, X. F., LIU, C. L., ZHENG, L. & KUANG, D. M. 2016. PD-1hi Identifies a Novel Regulatory B-cell Population in Human Hepatoma That Promotes Disease Progression. *Cancer Discov,* 6**,** 546-59.

YANG, J., YAN, J. & LIU, B. 2018. Targeting VEGF/VEGFR to Modulate Antitumor Immunity. *Front Immunol,* 9**,** 978.

YANG, Q., SAENZ, S. A., ZLOTOFF, D. A., ARTIS, D. & BHANDOOLA, A. 2011. Cutting edge: Natural helper cells derive from lymphoid progenitors. *J Immunol,* 187**,** 5505-9.

YOKOTA, Y., MANSOURI, A., MORI, S., SUGAWARA, S., ADACHI, S., NISHIKAWA, S. & GRUSS, P. 1999. Development of peripheral lymphoid organs and natural killer cells depends on the helix-loop-helix inhibitor Id2. *Nature,* 397**,** 702-6.

YOUNGBLOOD, B., OESTREICH, K. J., HA, S. J., DURAISWAMY, J., AKONDY, R. S., WEST, E. E., WEI, Z., LU, P., AUSTIN, J. W., RILEY, J. L., BOSS, J. M. & AHMED, R. 2011. Chronic virus infection enforces demethylation of the locus that encodes PD-1 in antigen-specific CD8(+) T cells. *Immunity,* 35**,** 400-12.

ZAISS, D. M. W., GAUSE, W. C., OSBORNE, L. C. & ARTIS, D. 2015. Emerging functions of amphiregulin in orchestrating immunity, inflammation, and tissue repair. *Immunity,* 42**,** 216-226.

ZHANG, J. Y., YAN, Y. Y., LI, J. J., ADHIKARI, R. & FU, L. W. 2020. PD-1/PD-L1 Based Combinational Cancer Therapy: Icing on the Cake. *Front Pharmacol,* 11**,** 722.

ZHANG, L., CONEJO-GARCIA, J. R., KATSAROS, D., GIMOTTY, P. A., MASSOBRIO, M., REGNANI, G., MAKRIGIANNAKIS, A., GRAY, H., SCHLIENGER, K., LIEBMAN, M. N., RUBIN, S. C. & COUKOS, G. 2003. Intratumoral T cells, recurrence, and survival in epithelial ovarian cancer. *N Engl J Med,* 348**,** 203-13.

ZHENG, Y., VALDEZ, P. A., DANILENKO, D. M., HU, Y., SA, S. M., GONG, Q., ABBAS, A. R., MODRUSAN, Z., GHILARDI, N., DE SAUVAGE, F. J. & OUYANG, W. 2008. Interleukin-22 mediates early host defense against attaching and effacing bacterial pathogens. *Nat Med,* 14**,** 282-9.

ZHU, J., JANKOVIC, D., OLER, A. J., WEI, G., SHARMA, S., HU, G., GUO, L., YAGI, R., YAMANE, H., PUNKOSDY, G., FEIGENBAUM, L., ZHAO, K. & PAUL, W. E. 2012. The transcription factor T-bet is induced by multiple pathways and prevents an endogenous Th2 cell program during Th1 cell responses. *Immunity,* 37**,** 660-73.

ZIMMER, L., GOLDINGER, S. M., HOFMANN, L., LOQUAI, C., UGUREL, S., THOMAS, I., SCHMIDGEN, M. I., GUTZMER, R., UTIKAL, J. S., GOPPNER, D., HASSEL, J. C., MEIER, F., TIETZE, J. K., FORSCHNER, A., WEISHAUPT, C., LEVERKUS, M., WAHL, R., DIETRICH, U., GARBE, C., KIRCHBERGER, M. C., EIGENTLER, T., BERKING, C., GESIERICH, A., KRACKHARDT, A. M., SCHADENDORF, D., SCHULER, G., DUMMER, R. & HEINZERLING, L. M. 2016. Neurological, respiratory, musculoskeletal, cardiac and ocular side-effects of anti-PD-1 therapy. *Eur J Cancer,* 60**,** 210-25.

ZOU, W. & CHEN, L. 2008. Inhibitory B7-family molecules in the tumour microenvironment. *Nat Rev Immunol,* 8**,** 467-77.